DESIGN AND SIMULATION OF AN ABS FOR AN INTEGRATED ACTIVE SAFETY SYSTEM FOR ROAD VEHICLES

A THESIS SUBMITTED TO
THE GRADUATE SCHOOL OF NATURAL AND APPLIED SCIENCES
OF
MIDDLE EAST TECHNICAL UNIVERSITY

BY

MURAT ŞAHİN

IN PARTIAL FULFILLMENT OF THE REQUIREMENTS
FOR
THE DEGREE OF MASTER OF SCIENCE
IN
MECHANICAL ENGINEERING

SEPTEMBER 2007

Approval of the thesis:

DESIGN AND SIMULATION OF AN ABS FOR AN INTEGRATED ACTIVE SAFETY SYSTEM FOR ROAD VEHICLES

submitted by **MURAT ŞAHİN** in partial fulfillment of the requirements for the degree of **Master of Science in Mechanical Engineering Department, Middle East Technical University** by,

Prof. Dr. Canan Özgen
Dean, Graduate School of **Natural and Applied Sciences** _____

Prof. Dr. Kemal İder
Head of Department, **Mechanical Engineering** _____

Prof. Dr. Y. Samim Ünlüsoy
Supervisor, **Mechanical Engineering Dept., METU** _____

Examining Committee Members:

Prof. Dr. Tuna Balkan
Mechanical Engineering Dept., METU _____

Prof. Dr. Y. Samim Ünlüsoy
Mechanical Engineering Dept., METU _____

Assist. Prof. Dr. Yiğit Yazıcıoğlu
Mechanical Engineering Dept., METU _____

Assist. Prof. Dr. E. İlhan Konukseven
Mechanical Engineering Dept., METU _____

Kutluk Bilge Arıkan
Instructor, Mechatronics Dept., Atılım University _____

Date: 07.09.2007

I hereby declare that all information in this document has been obtained and presented in accordance with academic rules and ethical conduct. I also declare that, as required by these rules and conduct, I have fully cited and referenced all material and results that are not original to this work.

Name, Last name : Murat Şahin

Signature :

ABSTRACT

DESIGN AND SIMULATION OF AN ABS FOR AN INTEGRATED ACTIVE SAFETY SYSTEM FOR ROAD VEHICLES

Şahin, Murat

M.S., Department of Mechanical Engineering

Supervisor: Prof. Dr. Y. Samim Ünlüsoy

September 2007, 159 pages

Active safety systems for road vehicles have been improved considerably in recent years along with technological advances and the increasing demand for road safety. In the development route of active safety systems which started with introduction of digital controlled ABS in the late seventies, vehicle stability control systems have been developed which today, with an integration approach, incorporate ABS and other previously developed active safety technologies. ABS, as a main part of this new structure, still maintains its importance.

In this thesis, a design methodology of an antilock braking system controller for four wheeled road vehicles is presented with a detailed simulation work. In the study, it is intended to follow a flexible approach for integration with unified control structure of an integrated active safety system. The objective of the ABS controller, as in the previous designs in literature, is basically to provide retention of vehicle directional control capability and if possible shorter braking distances by controlling the wheel slip during braking.

A hierarchical structure was adopted for the ABS controller design. A high-level controller, through vehicle longitudinal acceleration based estimation, determines reference slip values and a low-level controller attempts to track these reference slip signals by modulating braking torques. Two control alternatives were offered for the design of the low-level controller: Fuzzy Logic Control and PID Control. Performance of the ABS controller was analyzed through extensive simulations conducted in MATLAB/Simulink for different road conditions and steering maneuvers. For simulations, an 8 DOF vehicle model was constructed with nonlinear tires.

Keywords: Antilock Braking System (ABS), Active Safety Systems, Fuzzy Logic Control (FLC), Proportional-Integrative-Derivative Control (PID), Vehicle Model

ÖZ

YOL ARAÇLARINDA TÜMLEŞİK AKTİF GÜVENLİK SİSTEMİ İÇİN ABS TASARIM VE SİMULASYONU

Şahin, Murat
Yüksek Lisans, Makina Mühendisliği Bölümü
Tez Yöneticisi: Prof. Dr. Y. Samim Ünlüsoy

Eylül 2007, 159 sayfa

Yolcu araçlarında artan yol güvenliği gereksinimi ve teknolojik gelişmelerle beraber, yol araçları için tasarlanan aktif güvenlik sistemleri, yakın zamanda, önemli ölçüde iyileştirildi. 70'li yılların sonunda, sayısal kontrollü ABS'nin geliştirilmesiyle başlayan aktif güvenlik sistemlerinin gelişimi sürecinde bugün, araç denge kontrol sistemleri, entegrasyon yaklaşımıyla, önceden bağımsız tasarlanan aktif güvenlik teknolojilerini bir çatı altında toplamaktadır ve ABS, bu yeni yapının temel bir parçası olarak, hala önemini korumaktadır.

Bu tez çalışmasında, dört tekerlekli yol araçları için kilitlenme önleyici fren sistemi kontrolcüsünün tasarım metodolojisi ayrintili bir simulasyon çalışmasıyla beraber sunulmuştur. Bu çalışmada, kontrolcünün, tümleşik aktif güvenlik sisteminin kontrol yapısı ile entegrasyonu düşünülerek esnek bir yaklaşım benimsenmiştir. ABS kontrolcüsünün hedefi, literatürdeki önceki tasarımlar gibi, temel olarak, frenleme sırasında tekerleğin kaymasını kontrol ederek, aracın doğrultu kontrol kapasitesini korumak ve mümkünse daha kısa fren mesafelerine ulaşmaktır.

ABS kontrolcü tasarımı için hiyerarşik bir yapı benimsenmiştir. Tasarlanan üst seviye kontrolcü, araç ivmelenmesi temelli kestirim yardımıyla referans tekerlek kayma değerlerini belirler ve alt seviye kontrolcü, fren torklarını düzenleyerek bu referans değerlerini takip etmeye çalışır. Alt seviye kontrolcü tasarımı için iki kontrol alternatifi önerilmiştir: Bulanık Mantık Kontrolü ve PID Kontrol. ABS kontrolcüsünün performansı, MATLAB/Simulink ortamında, farklı yol koşulları ve dönüş manevraları için gerçekleştirilen simulasyonlar aracılığıyla analiz edilmiştir. Simulasyonlar için doğrusal olmayan lastik modeline sahip sekiz serbestlik dereceli bir araç modeli oluşturulmuştur.

Anahtar Kelimeler: Kilitlenme Önleyici Fren Sistemi (ABS), Aktif Güvenlik Sistemleri, Bulanık Mantık Kontrolü (FLC), PID Kontrol, Araç Modeli

To the Memory of My Father

ACKNOWLEDGEMENTS

First, I would like to express my gratitude to my supervisor Prof. Dr. Y. Samim Ünlüsoy for his guidance, encouragement, patience and practical insight throughout my thesis study.

I feel indebted to my friends Gökhan Tekin, Görkem Oktay, Hakan Temizsoy and Emir Kutluay for their moral assistance, support and help.

I am truly grateful to my family for their never-ending support, encouragement and trust during this difficult time of my life.

Financial support of TÜBİTAK is also gratefully acknowledged.

TABLE OF CONTENTS

LIST OF TABLES

TABLES

LIST OF FIGURES

FIGURES

LIST OF SYMBOLS

a	Distance of center of gravity from the front axle
a_p	Tire contact patch length
a_{p0}	Tire contact patch length at design conditions
A_f	Frontal projected area
A_i	Experimental tire parameters for stiffness characteristics
a_x	Vehicle longitudinal acceleration
a_y	Vehicle lateral acceleration
α	Tire slip angle
b	Distance of center of gravity from the rear axle
B_i	Experimental tire parameters for friction characteristics
C_Φ	Roll damping
C_i	Experimental tire parameters for saturation function
C_d	Drag coefficient
CS/FZ	Experimental coefficient for tire model
δ	Steer angle
F_x	Longitudinal tire force
F_y	Lateral tire force
F_z	Normal tire load
F_{ZT}	Tire design load
g	Gravitational acceleration
h	Height of the sprung mass center of gravity
h^*	Distance of sprung mass center of gravity from roll axis
I_w	Rotational inertia of the tire
I_{zz}	Vehicle inertia about z axis
I_{xxs}	Sprung mass inertia about x axis
K_a	Coefficient for tire patch elongation
k_c	Longitudinal stiffness coefficient
k_c'	Transition stiffness coefficient

ks	Lateral stiffness coefficient
kμ	Friction transition coefficient
K_R	Front roll stiffness ratio
K_Φ	Roll stiffness
K_{rf}	Front roll steer coefficient
K_{rr}	Rear roll steer coefficient
M	Total vehicle mass
M_b	Wheel brake moment
M_s	Sprung mass
μ	Longitudinal coefficient of friction
μ_0	Peak tire/road friction coefficient
n(k)	measurement noise
ω	Wheel angular velocity
φ	Roll angle
Q(k)	System noise covariance matrix
R	Wheel radius
R(k)	Measurement noise covariance matrix
R_a	Aerodynamic force
R_g	Gradient resistance
r	Yaw rate
ρ_a	Air density
σ	Composite slip
s	Longitudinal wheel slip ratio
S_r	Steering ratio
T	Track length
T_w	Tire width
T_p	Tire pressure
τ	Simulation time step
u	Longitudinal vehicle velocity
v	Lateral vehicle velocity
V_w	Vehicle velocity in the plane of the wheel
W	Weight of the total vehicle

w(k)	System noise
ζ	Road slope

CHAPTER 1

INTRODUCTION

Active safety concept principally has its roots in the early applications of antilock braking. The idea, however, became popular with the implementation of electronically controlled anti-lock braking systems (ABS) in luxury sedans in the late seventies. In the following years, along with technological advances and increasing demand for road safety, the systems were improved and new safety enhancement technologies such as electronic brake distribution and active yaw control systems were introduced. The need for providing these individually developed technologies together in passenger cars has resulted in the concept of integration of the active safety systems, commercially realized with the common name of ESP, Electronic Stability Program. ABS as an important part of this new structure maintains its importance and its design requires also attention in this direction.

In this chapter, an overview of ABS is presented followed by a review of previous work in literature, a brief explanation of motivation for the study and an outline of the thesis. At the beginning, it is desired to give information about the basic operation logic of antilock braking systems and thus, prepare the reader for the material in the following chapters.

1.1. OVERVIEW OF ANTI-LOCK BRAKING SYSTEM (ABS)

Anti-lock braking system (ABS) is an electronic braking technology developed to enhance braking safety by reducing tendency for wheel lock and thus improving

vehicle control. The system detects imminent wheel-lock and reacts in time by modulating brake torque independent of pedal force.

Early studies for development of ABS brakes began in Europe in 1920's. One of the first patents issued in Europe in 1932 was entitled "An Improved Safety Device for Preventing the Jamming of the Running Wheels of Automobiles when Braking" [1]. In 1936, Bosch registered a patent for a "mechanism to prevent locking of the wheels of a motor vehicle". The first practical applications of the anti-lock braking system were used in railroad trains in 1940's; however Dunlop's Maxaret system, developed for aircrafts in 1952, was recognized as the foundation of the ABS design.

The first car to include anti-lock braking system was a high-power sports car, 1966 Jensen FF, which was equipped with a Dunlop Maxaret based ABS system. In 1969, a rear-wheel-only ABS system developed by Ford and Kelsey Hayes was offered on the thunderbird. Chrysler and Bendix produced a four-wheel ABS for the 1971 Imperial [2]. However these early applications did not find acceptance from the market due to reliability issues, low public awareness and high additional cost to the buyer.

The Bosch ABS system, provided as optional equipment in Mercedes passenger cars in 1978, was a significant development. The four-wheel controlled system was the add-on type which can be installed in the existing vacuum or hydraulic boost brake system [2] and utilized digital electronic technology.

In the nineties, in order to increase the marketing range, ABS designs became lighter, smaller and more cost-effective as the multi-component structure evolved into a one-housing design. Beginning from the late '90s, focus of research changed from hardware issues into improvements in control algorithms.

Almost all road vehicles built today are fitted with anti-lock braking systems and ABS is now accepted as an essential improvement to braking safety and standard equipment in passenger cars.

1.1.1. ABS Basics

The objective of an ABS system is generally to provide retention of vehicle directional control capability and in most conditions, shorter braking distances by maintaining the maximum braking force while preventing wheel-lock.

Almost all ABS control schemes in literature are based on the control of longitudinal wheel slip. Longitudinal wheel slip or tire braking slip, λ, is defined as the difference between vehicle velocity component in the plane of the tire and wheel circumferential velocity, normalized to again component of vehicle velocity in the plane of the tire.

$$\lambda = \frac{V_w - \omega \cdot R}{V_w} \tag{1.1}$$

When sufficient braking force is applied, wheel angular speed decelerates rapidly and eventually causes the wheel lock up; by definition, longitudinal wheel slip ratio reaches 100% at this instant.

The importance of the longitudinal wheel slip can be understood from the typical longitudinal coefficient of friction μ versus slip curve provided in figure 1.1 [3]. In order to achieve directional stability, lateral forces must be considered. As can be inferred from the figure, lateral coefficient of friction and hence lateral force decreases with increasing longitudinal slip, reaching absolute zero at wheel-lock.

Longitudinal coefficient of friction vs. longitudinal slip graph may be divided into two regions. Friction process is stable in the first linearly increasing part including the peak point and at the 100% slip point [2]. Decreasing part of the curve is unstable and unless braking force is reduced in time, longitudinal wheel slip increases very rapidly and wheel lock becomes unavoidable. ABS control system acts by limiting slip values to the stable region to prevent wheel lock.

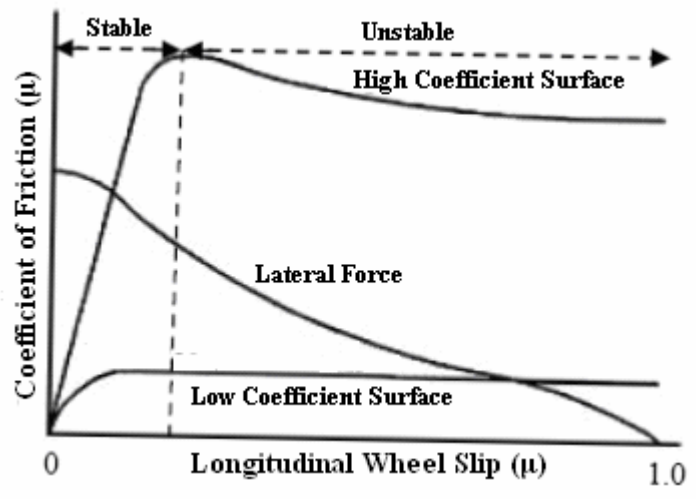

Figure 1.1. Longitudinal coefficient of friction (μ) vs. longitudinal wheel slip (λ) [3]

It is obvious from figure 1.1 that the ideal longitudinal wheel slip point for the control system is around the value corresponding to the peak longitudinal coefficient of friction point. By selecting a slip ratio in the vicinity of this particular point, maximum use of the available friction can also be achieved which results in shorter braking distance. It should also be noted that however, the wheel slip ratio, for which the peak longitudinal friction force is obtained, increases with increasing tire slip angle but lateral force generating capability of tires decreases for higher longitudinal wheel slip; therefore in the case of cornering while braking, there is certainly a compromise between braking performance and maneuverability of the vehicle.

ABS controller design is a challenging work because of the nonlinear tire behavior, time-varying characteristics of the braking system and environmental influences. Road surface condition is a serious problem for the controller as an environmental disturbance factor. ABS controller irrespectively must maintain adequate performance on different road conditions with various μ – slip curves. There exists also a high uncertainty in estimation of longitudinal wheel slip, or more correctly the vehicle velocity in the tire plane.

Conventional ABS controller utilizes a rule-based method to maintain longitudinal wheel slip in a certain range on the information provided by angular wheel speed sensors. The generic control approach is based on wheel slip and angular acceleration control [4]. The production ABS modulates hydraulic pressure in the wheel cylinder using solenoid valves with three pressure modes: increase, hold and pressure.

The principle of the algorithm implemented in conventional ABS is based on limited cycling of longitudinal wheel slip in a desired range. The algorithm sets certain bounds for wheel angular acceleration and wheel angular speed and uses a complex rule set to decide for the pressure mode of the actuator [5,6]. The control is known to be highly adaptive to uncertainities in tire force characteristics and the friction coefficient; however the oscillatory nature of the conventional ABS is undesirable due to noticeable vibrations and resulting performance limitations [4].

1.2. LITERATURE SURVEY

Antilock braking system has been the focus of substantial amount of research over the years due to its commercial value and significant benefits to vehicle safety. With the electronically controlled systems implemented in luxury cars in the late 70's, the subject became increasingly popular and since then, has attracted the attention of vehicle manufactures, automotive parts companies and countless independent academic researchers. During the time, the focus of the studies has gradually changed from hardware improvements to control algorithms.

Earlier studies, which were leaded mostly by automotive companies, presented various approaches for hardware configurations of the systems and also the proposed designs had different controller strategies.

Shinomiya, et al [7] published a study regarding the development of a new antilock braking system. The system configuration was a 4 sensors / 3 channel type. The proposed design incorporated a deboost type hydraulic unit with power source which

provided satisfactory pedal feel and easy adaptability to the addition of a traction control system.

Miyake, Yamaki and Fujita [8] proposed an ABS design for 4WD vehicles. The system had adopted a diagonal 2 channel, 4 sensor arrangement. In the design, it was aimed to provide a solution to the problems caused by the rigidly engaged drive shafts of 4WD systems.

Watanabe and Noguchi [9] developed an algorithm to compensate for degraded performance of ABS due to road-disturbances. The algorithm was based on mainly two concepts. The first was to shift the allowable minimum wheel acceleration threshold downward by the disturbance amplitude of the wheel acceleration. The second concept was to determine the proper duration for the brake pressure reduction by the road friction coefficient. The road friction coefficient was obtained from the wheel acceleration smoothed by the filters and the disturbance of the wheel acceleration was calculated by band pass filters.

Hattwig performed a study [10] to develop a system of taxonomy to classify ABS hydraulic system designs. The study also aimed to make the synthetic generation of any random assembly possible. For the analysis, a function structure was introduced with four function blocks: a cut-off/throttling element between master and wheel brake cylinder, an accumulator connected to wheel brake cylinder, a transport element for the brake fluid in the accumulator and an energy source or motor to drive the transport element.

Naito, Takeuchi,et al [11], performed a study to develop a Four Solenoid ABS. For the algorithm duty control concept was adopted. The concept was based on the ordinary four-pressure gradient control (rapid increase, rapid decrease, hold and gradual increase), where hold and gradual increase modes were created by combining pressure increase and decrease. This application required the algorithm to learn appropriate increase/decrease duty ratio values. For this purpose, a learning method was developed, which was also described in the paper.

Simulation is an efficient and cost-effective method for quick development and performance evaluation of antilock braking systems. In the literature, there exist numerous research publications in this area, including the development studies of complex simulation models, simulation environments and hardware-in-the-loop simulators.

An early simulation study, conducted for the development of a commercial ABS system was presented by Kempf, Bonderson and Slafer [12] in 1987. For the real time simulations, a specifically designed computer system was used, on which the developed simulation model was implemented in both “pure” and hardware-in-the-loop “mixed” simulation forms. In mixed simulation tests, the controller and sensor models were replaced with actual ABS controller and specialized test equipment, while vehicle dynamics and tire/road interface models, developed previously for pure simulation tests, were implemented with modification.

Lee, Jeon, et al [13] in their study, compared two performance evaluation methods for an ABS for pneumatic brake systems, namely Hardware In-the-Loop simulation and in-vehicle test. In designed HILS, the full-air brake system of a real bus and ABS components were used as hardware. The software parts were composed of a vehicle dynamics model and wheel speed simulation program. In the second part of the study, the ABS controller was equipped in a real bus for the field test.

Day and Roberts [14] described a new ABS model implemented in HVE (Human Vehicle Environment) simulation environment. The model was applicable to the design of ABS systems and to the study of loss-of-control crashes of ABS-equipped vehicles. In the paper, the HVE ABS user interface and two ABS algorithms implemented to date were described. The available algorithms were the simple Tire Slip algorithm and the HVE Bosch Version 1 algorithm which is based on the conventional Bosch ABS. Simulation results of the HVE Bosch algorithm was compared against the experimental data, and results compared favorably.

In literature, numerous control design approaches were proposed for antilock braking systems including fuzzy logic control, rule-based approaches, sliding mode control, etc.

Madau, Yuan, et al [15] conducted a study to develop and implement a fuzzy logic controller for an antilock brake system. An initial fuzzy logic controller was developed using a simple simulation model. The designed rule base was then tested on an experimental brake system. With slight modification of the initial control rules, a performance comparable to that of a conventional ABS was achieved on high μ surface.

Mauer, Gissinger and Chamaillard [16] presented a fuzzy logic controller design for ABS braking. In their study, a decision logic network accompanied the controller to identify the current road condition. The road condition estimation logic was based on current and past readings of the slip ratio and brake pressure. Simulations were conducted with both quantizing and continuous actuators on a quarter vehicle model. The simulation results showed that a fuzzy controller in combination with a road condition identifier logic is rapid and effective over a wide range of operating conditions.

Layne, Passino and Yurkovich [17] introduced a fuzzy learning control scheme to compensate for performance degradation observed on harsh road conditions. The learning algorithm was able to tune the fuzzy controller rules to adapt the system to adverse road conditions, when encountered.

Yu, Feng and Li developed a control method [18] for an ABS controller design, which calculates an optimal target wheel slip ratio based on vehicle dynamic states and prevailing road condition. In their study, a fuzzy logic approach was adopted to maintain the optimal target slip ratio which yields the best compromise between braking deceleration, stopping distance and directional stability performance.

Mirzaei, Moallem, et al [19] proposed an optimized fuzzy controller for antilock brake systems. Rules of the fuzzy system were optimized using genetic algorithms and error based optimization technique. Simulations showed that proposed controller was successful in tracking the maximum adhesion coefficient and in comparison with PI and Fuzzy logic controllers, vibrations due to torque and slip variations were much lower, and wheel slip was kept at a very small value for slow speeds.

Drakunov,Özgüner et al [20], worked on a ABS controller design by using sliding mode approach. The problem was formulated as the design of a control algorithm which provides tracking of the extremal wheel slip value during braking. A longitudinal tire force observer was developed to provide feedback information for the designed controller. In the study, contrary to similar previous "sliding mode" design approaches, optimal wheel slip value was a priori unknown.

Lee and Sin [21] proposed a slip-ratio control method for ABS using sliding mode control. For the study, a quarter vehicle model was constructed and to reduce the frequently encountered chattering problem of the simple sliding mode controller, a sigmoid-like function was used. Control performance of the proposed sliding mode controller was compared with that of a simple PID controller. The results showed that the proposed sliding mode controller has better braking performance and a decreased percent overshoot for slip ratio in comparison with the PID controller.

Buckholtz [22] investigated the use of sliding mode control for the purpose of tracking a reference input wheel slip. Continuous switching control was adopted to reduce system chattering. For the feedback information in the simulation, longitudinal tire force signals were used, which were corrupted with white noise.

Wellstead and Pettit introduced a new method [23] to analyze the dynamical behavior of an antilock brake system. The underlying basis of the approach was the idea that piecewise linear dynamical systems cannot be adequately studied using conventional simulation tools. For this purpose, a special piecewise linear analysis tool was employed to study the performance of the ABS controller. Piecewise linear

analysis principles were used to analyze an initial controller design. The controller laws were consequently redesigned according to weaknesses in the rules illustrated by the applied method.

Regardless of the control method implemented, vehicle velocity estimation is an important concern in design of an ABS system. Vehicle speed can also be measured directly with the help of specialized sensors, or calculated from other noisy sensor signals; however for a cost effective design and more accurate information, estimation methods are preferred.

Watanabe, Kobayashi and Cheok [24] used a rule-based Kalman filtering technique to estimate the absolute vehicle speed from noisy vehicle acceleration measurement and erroneous wheel speed signal. In the proposed method, a rule-based strategy was incorporated which adjusts the Kalman filter coefficients to compensate for abrupt nonstationary errors in the measurement.

Daiss and Kiencke [25] in their study, compared the Kalman filtering technique with a new developed fuzzy estimation method for vehicle speed estimation. For the study, wheel speed sensors, longitudinal acceleration sensor and a gyroscope for yaw rate measurement were necessary.

Jiang and Gao [26] proposed an approach to estimate vehicle velocity based on solely wheel speed measurement. The study had intended to eliminate the need for an additional sensor and thus making the resulting system more cost effective while also lowering system complexity and preventing possible unreliability issues associated with sensors. An adaptive nonlinear filter approach was adopted in the research.

1.3. MOTIVATION FOR THE STUDY

A review of previous work in literature on antilock braking systems design shows that the studies were concentrated on researches for development of control system

techniques which neglect a complete design approach and total vehicle response; however, probably the most critical observation is the fact that in literature there exists hardly any study concerning integration of ABS with other active vehicle safety enhancement system controllers.

Today, active safety systems design is a very active research area where vehicle stability control systems is at the focus of attention and clearly, integration of the stand-alone safety enhancement systems is the next stage of development in this area. In the published works, however, the concept of integration and its application did not take the necessary attention. Research is limited to general discussions regarding control structures and only a few studies about contributions of steering actuators and active suspensions to vehicle stability control. Incorporation of ABS in an integrated active safety system control structure definitely brings advantages; especially coordinated operation of ABS with wheel braking based vehicle stability controller offers promising performance improvement possibilities in addition to the basic expectations such as sharing hardware and reduction of complexity.

In this study, it is intended to contribute to open literature by presenting a design methodology for antilock braking system controller which adopts a flexible approach considering easy adaptability to unified control structure of an integrated active safety system. The study aims to provide a thorough design scheme and detailed analysis of response of vehicle in different conditions and for steering maneuvers which will also constitute a base to study the requirements and possible contributions of the integration.

1.4. OUTLINE

In chapter 2, mathematical modeling details of the constructed nonlinear 8-DOF vehicle dynamics model and the nonlinear tire model are described. Tire force variation plots and simulink diagram of the prepared model are given in addition to the presented mathematical formulation.

In chapter 3, ABS controller details and design procedure is explained. Following an overview of basic controller operation logic, functional details and design structures of high-level and low-level controllers are described with information concerning the development stage to give insight into the designs. Finally, state identification scheme and in particular, calculation of longitudinal wheel slip is explained. The chapter also gives mathematical formulation for the Kalman filtering technique used in the study to estimate wheel slip ratio in the presence of noise.

In chapter 4, results of the simulations tests in MATLAB/Simulink environment are presented to show the performance of the designed ABS controller. Simulation study comprises sequentially, the case without the ABS controller, straight-line test and combined braking and steering test for different road conditions ranging from dry asphalt to icy road and on a road surface with changing coefficient of friction levels. In these simulations, the results for different low-level slip controllers are compared and discussed for each case. Performance of the ABS is tested for a quantizing controller and for noisy measurement data as well. The results for these cases are also presented briefly in this chapter.

In chapter 5, a discussion over integration possibilities for the proposed antilock braking system controller is presented and expected benefits from the coordination of the systems are explained.

In chapter 6, discussion and conclusion for the study is given.

Vehicle data and parameters for the tire model are provided in Appendix A. Appendix B is the continuation of the simulation study “Road transitions test” presented in chapter 4. Appendix C presents the results of the combined braking and simulation test for PID controller.

CHAPTER 2

MODELING

In this thesis study, a vehicle model was constructed in MATLAB/Simulink software environment to replace the real vehicle for the development and performance analysis of the ABS controller. The controller was modeled also in Simulink as a separate block which receives the required signals from the vehicle model through a pre-processing block emulating sensor hardware and a state identification algorithm. ABS controller details and design procedure is explained in chapter 3.

Modeling is an important engineering means for analysis of the real systems and has a crucial role in feasible design procedures. A mathematical model describes a system by a set of equations and serves as a platform for simulation as well. In the study, a mathematical 8 degrees of freedom (DOF) nonlinear vehicle model with a nonlinear tire model was constructed in MATLAB/Simulink. Simulink software through modeling and solving the defined set of equations numerically, allows the vehicle dynamic behavior to be analyzed. In this chapter, mathematical modeling details of the constructed vehicle dynamics model are presented.

2.1. TIRE MODEL

Tire behavior has definitely a decisive role in dynamic response of the vehicle; therefore an accurate modeling of the tire is indispensable for realistic simulation of vehicle dynamics behavior. Tire force characteristics are highly nonlinear and thus, difficult to model. In literature, there exist numerous tire models developed based on

empirical approaches and analytical studies. The tire model used in this study is based on the work of Allen et al [27].

Allen tire model is a nonlinear model based on an analytical study which makes use of experimentally obtained parameters. Tire forces can be calculated from longitudinal wheel slip, *s,* lateral slip angle, α, normal tire load, F_z, velocity of the tire in wheel plane and nominal longitudinal coefficient of friction, μ_{nom}. The governing equations of the Allen tire model are presented below.

Longitudinal and lateral tire forces, for zero camber angle, are calculated from the below simple equations, where *F(σ)* is the force saturation function and k_c and k_s are respectively, corrected longitudinal stiffness and lateral stiffness coefficients.

$$\frac{F_x}{\mu \cdot F_z} = \frac{-F(\sigma) \cdot k_c' \cdot s}{\sqrt{k_s^{\,2} \cdot \tan^2 \alpha + \left(k_c'\right)^2 \cdot s^2}}, \quad \frac{F_y}{\mu \cdot F_z} = \frac{F(\sigma) \cdot k_s \cdot \tan \alpha}{\sqrt{k_s^{\,2} \cdot \tan^2 \alpha + \left(k_c'\right)^2 \cdot s^2}} \tag{2.1}$$

The force saturation function is a function of composite slip, σ and experimental coefficients.

$$F(\sigma) = \frac{C_1 \cdot \sigma^3 + C_2 \cdot \sigma^2 + 4/\pi \cdot \sigma}{C_1 \cdot \sigma^3 + C_3 \cdot \sigma^2 + C_4 \cdot \sigma + 1} \tag{2.2}$$

$$\sigma = \frac{\pi \cdot a_p^{\,2}}{8 \cdot \mu_0 \cdot F_z} \cdot \left[k_s^{\,2} \cdot \tan^2 \alpha + k_c^{\,2} \cdot \left(\frac{s}{1-s} \right)^2 \right]^{1/2} \tag{2.3}$$

Tire contact patch length, a_p can be calculated as below. T_w, T_p, k_a and F_{zt} represent respectively tread width, tire pressure, tire contact patch coefficient and designed tire load.

$$a_p = a_{p0} \cdot \left[1 - k_a \cdot \frac{F_x}{F_z} \right], \quad a_{p0} = \frac{0.0768 \cdot \sqrt{F_z \cdot F_{zt}}}{T_w \cdot \left(T_p + 5\right)} \tag{2.4}$$

Calculation of lateral and longitudinal stiffness coefficients is as following:

$$k_s = \frac{2 \cdot \left[A_0 + A_1 \cdot F_z - \frac{A_1}{A_2} \cdot {F_z}^2 \right]}{{a_{p0}}^2} \tag{2.5}$$

$$k_c = \frac{2 \cdot F_z}{{a_{p0}}^2} \cdot \left(\frac{CS}{F_z} \right) \tag{2.6}$$

A Modified form of longitudinal stiffness coefficient is used in calculation of tire forces which is defined as in the following equation.

$$k_c{}' = k_c + (k_s - k_c) \cdot \sqrt{\sin^2 \alpha + s^2 \cdot \cos^2 \alpha} \tag{2.7}$$

For calculation of μ in equation 2.1, peak tire road friction coefficient μ_0 should be first calculated.

$$\mu_0 = 1.176 \cdot \mu_{nom} \cdot \left(B_1 \cdot F_z + B_3 + B_4 \cdot {F_z}^2 \right) \tag{2.8}$$

$$\mu = \mu_0 \cdot \left[1 - k_\mu \cdot \sqrt{\left(\sin^2 \alpha + s^2 \cdot \cos^2 \alpha \right)} \right] \tag{2.9}$$

The transition parameter, k_μ, in equation 2.9 is a nonlinear function of the velocity of the tire in tire plane.

$$k_\mu = \frac{1}{11} \cdot {V_w}^{1/4} \tag{2.10}$$

Figures 2.1 and 2.2 illustrate the longitudinal and lateral tire force behavior of the model.

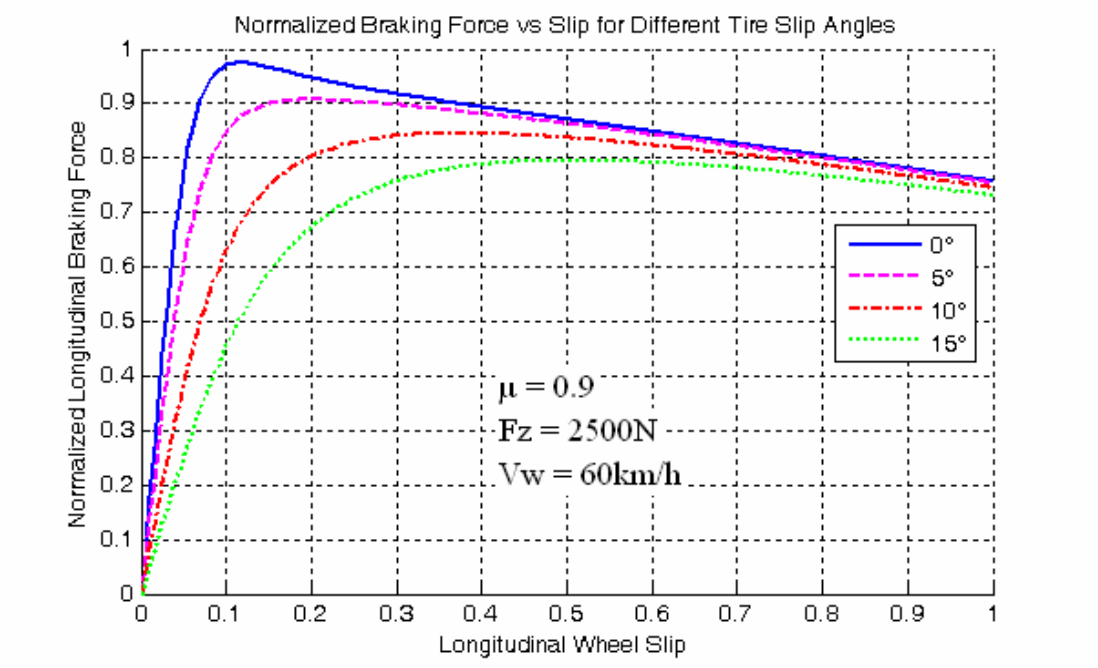

Figure 2.1. Normalized longitudinal force vs. longitudinal wheel slip

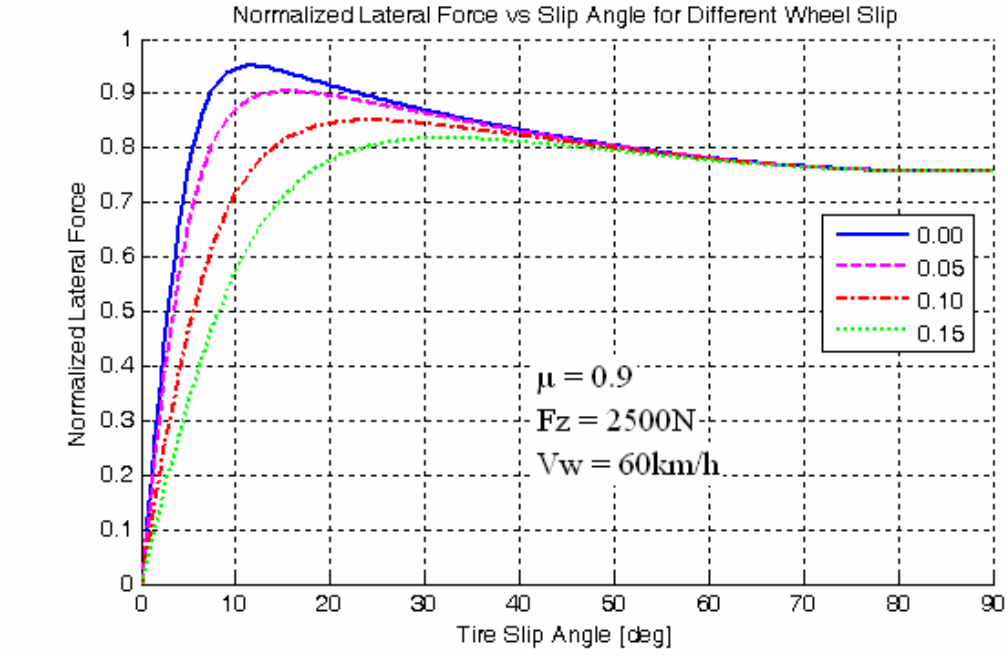

Figure 2.2. Normalized lateral force vs. tire slip angle

2.2. VEHICLE MODEL

In the present study, a nonlinear 8-DOF vehicle model is constructed which includes longitudinal, lateral, yaw and roll degrees of freedom together with motion of four independent wheels. The model allows the simulation of the vehicle motion in roll direction and takes account of lateral weight transfer. The mathematical vehicle model was not developed for pre-determined vehicle specifications; but rather it was aimed to allow the accurate simulation of any two-axle vehicle with front wheel steer (FWS), in any condition that is necessary for the design and analysis of an ABS system. From this standpoint, inclusion of roll degree of freedom and nonlinearity is important since this may contribute to the accuracy of the model considerably especially in emergency maneuvers when compared to the conventional 2-DOF 'Bicycle Model'; however in the same context, further detailing of the suspension modeling was not justified in the same amount.

The vehicle was modeled as an arrangement of three rigid bodies: the sprung mass and front and rear unsprung masses. The sprung mass interacts with unsprung masses by front and rear suspension systems. The roll stiffness and roll damping of the suspensions are assumed to be constant for the whole range of roll motion. The roll axis is defined as the line connecting roll centers, around which sprung mass rotates. The roll centre locations are assumed not to change during vehicle motion.

For the purposes of the model, the vertical motions of sprung and unsprung masses and steering system dynamics were not modeled. Effect of camber angle was not considered, thus, it was assumed that there exists no static or dynamic deviation between the central plane of the tire and vertical plane.

The effect of roll steer is included in the model. Roll steer is defined as the steering motion of the wheels with respect to the sprung mass which is due to the rolling motion of the sprung mass [28]. Roll steer effect can be incorporated by modifying the wheel steering angle input for front and rear wheels as below [29]. K_{rf} and K_{rr} are the respective front and rear roll steer coefficients.

$$\delta_{f,r} = \begin{cases} \delta + K_{rf} \cdot \phi \\ K_{rr} \cdot \phi \end{cases} \tag{2.11}$$

The governing differential equations of motion are derived for a body fixed reference frame located at the centre of gravity of the vehicle to achieve simplest set of equations. SAE convention is adopted for the definition of the moving reference frame.

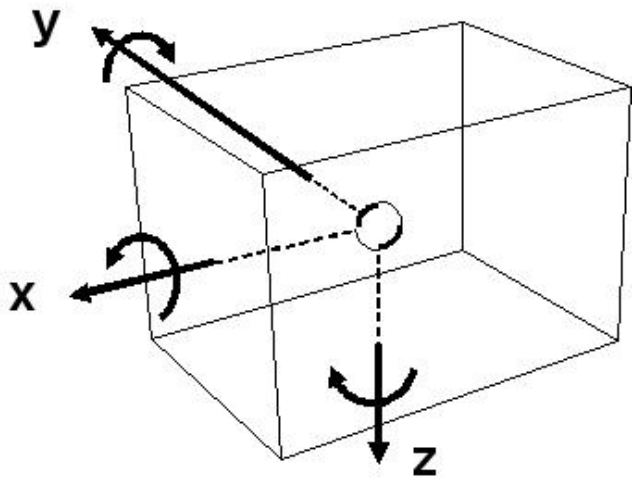

Figure 2.3. SAE reference system

The equations of motion for the non-linear 8-DOF model are presented below:

1) Longitudinal Motion:

Summing forces along the longitudinal X axis yields (see figure 2.4):

$$M \cdot a_X = \sum F_X - R_g - R_a \tag{2.12}$$

R_a is the aerodynamic force defined as $R_a = \frac{1}{2} \cdot C_d \cdot A_f \cdot \rho_a \cdot u^2$

R_g is the gradient resistance: $R_g = m \cdot g \cdot \sin \xi$

$$\sum F_X = F_{xfl} \cdot \cos\delta_{fl} + F_{xfr} \cdot \cos\delta_{fr} + F_{xrl} + F_{xrr} - F_{yfl} \cdot \sin\delta_{fl} - F_{yfr} \cdot \sin\delta_{fr}$$

The longitudinal acceleration of the vehicle center of gravity along body fixed reference frame, a_X, equals $(\dot{u} - v \cdot r)$

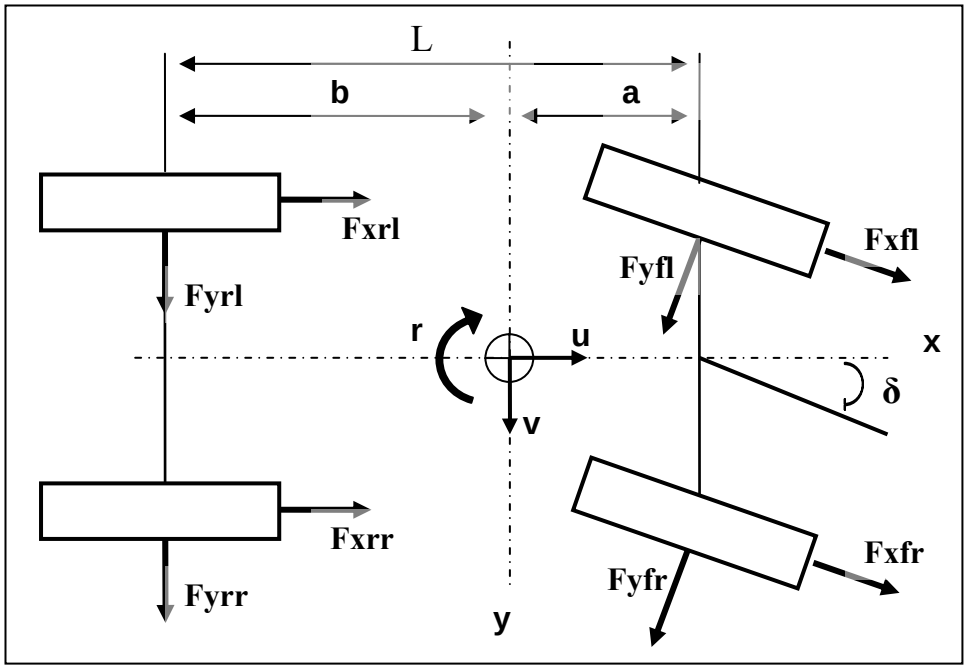

Figure 2.4. Vehicle model with tire force interactions

2) Lateral Motion:

Lateral motion is governed by the following equation:

$$M \cdot a_Y + M_S \cdot h' \cdot \ddot{\phi} \cdot \cos(\phi) - M_S \cdot h' \cdot \dot{\phi}^2 \cdot \sin(\phi) = \sum F_Y \qquad (2.13)$$

Second and third terms in left hand side of the equation are the resultant forces due to roll acceleration of the sprung mass around roll axis.

Sum of the lateral tire forces results in the following equation:

$$\sum F_Y = F_{yfl} \cdot \cos\delta_{fl} + F_{yfr} \cdot \cos\delta_{fr} + F_{yrl} + F_{yrr} + F_{xfl} \cdot \sin\delta_{fl} + F_{xfr} \cdot \sin\delta_{fr}$$

Lateral acceleration a_Y equals $(\dot{v} + u \cdot r)$

3) Yaw Motion

For yaw motion the equation of motion is as follows:

$$I_{ZZ} \cdot \dot{r} = a \cdot \left(F_{xfl} \cdot \sin\delta_{fl} + F_{yfl} \cdot \cos\delta_{fl} + F_{xfr} \cdot \sin\delta_{fr} + F_{yfr} \cdot \cos\delta_{fr}\right) - b \cdot \left(F_{yrl} + F_{yrr}\right) + \frac{t_f}{2}\left(F_{xfl} \cdot \cos\delta_{fl} - F_{yfl} \cdot \sin\delta_{fl} - F_{xfr} \cdot \cos\delta_{fr} + F_{yfr} \cdot \sin\delta_{fr}\right) + \frac{t_r}{2} \cdot \left(F_{xrl} - F_{xrr}\right) \quad (2.14)$$

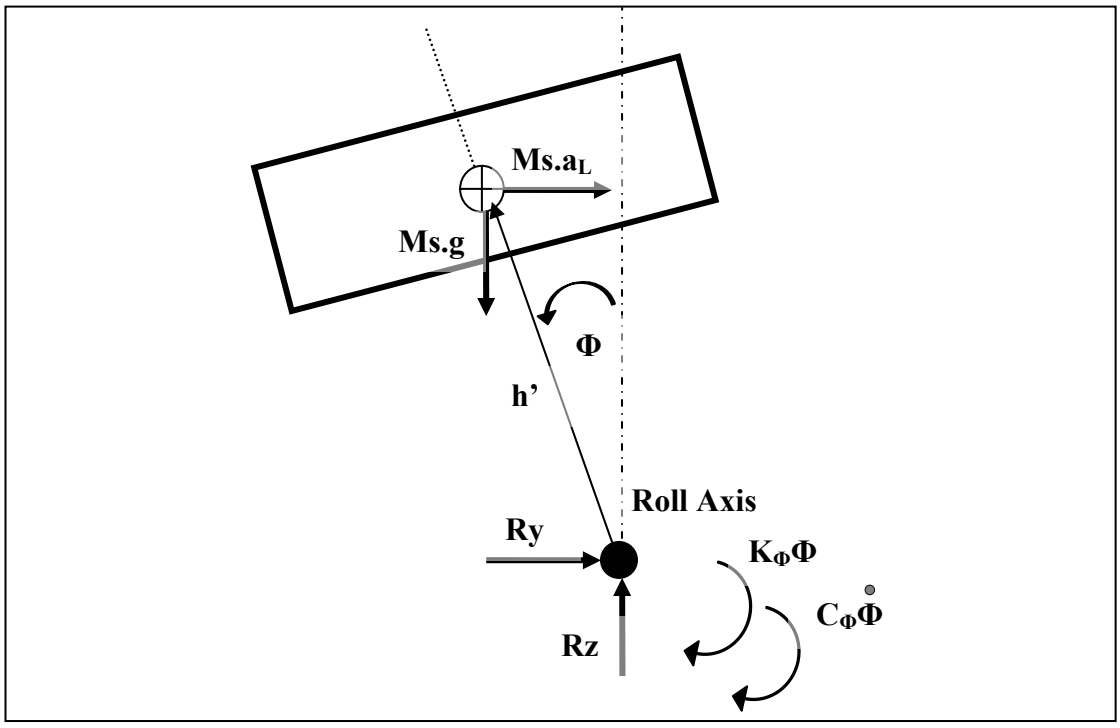

Figure 2.5. Roll model – free body diagram of sprung mass

4) Roll Motion:

For roll motion, governing equation can be obtained by summing roll moments about roll axis in the free body diagram of the sprung mass as shown in figure 2.5.

$$I_{XX} \cdot \ddot{\phi} = M_S \cdot g \cdot h' \cdot \sin\phi - M_S \cdot a_Y \cdot h' \cdot \cos\phi - K_\phi \cdot \phi - C_\phi \cdot \dot{\phi} \tag{2.15}$$

Note that for the rigid body assumption, roll angle is the same for front and rear axle; therefore contribution of front and rear restoring moments can be summed to be: $K_\phi \cdot \phi + C_\phi \cdot \dot{\phi}$ as shown in the figure 2.5 where K_ϕ is the roll stiffness term and C_ϕ represents total roll damping.

The equations of motion can be further simplified without having a significant effect on resulting state variables:

1) The nonlinear term $M_S \cdot h' \cdot \dot{\phi}^2 \cdot \sin(\phi)$ in the lateral motion equation can be neglected
2) Track length can be accepted to be same for both front and rear axles.
3) An average steering angle, "Ackermann Angle", can be assumed for both left and right tires; therefore "parallel steer" geometry is adopted for this case.

Simplified form of the equations is further modified for the effect of roll steer; the resulting equation set is as following:

$$\begin{aligned} M \cdot a_X = &\left(F_{xfl} + F_{xfr}\right) \cdot \cos\delta_f + \left(F_{xrl} + F_{xrr}\right) \cdot \cos\delta_r - \left(F_{yfl} + F_{yfr}\right) \cdot \sin\delta_f \\ &- \left(F_{yrl} + F_{yrr}\right) \cdot \sin\delta_r - R_g - R_a \end{aligned} \tag{2.16}$$

$$\begin{aligned} M \cdot a_Y + M_S \cdot h' \cdot \ddot{\phi} \cdot \cos(\phi) = &\left(F_{yfl} + F_{yfr}\right) \cdot \cos\delta_f + \left(F_{yrl} + F_{yrr}\right) \cdot \cos\delta_r \\ &+ \left(F_{xfl} + F_{xfr}\right) \cdot \sin\delta_f + \left(F_{xrl} + F_{xrr}\right) \cdot \sin\delta_r \end{aligned} \tag{2.17}$$

$$\begin{aligned} I_{ZZ} \cdot \dot{r} = &a \cdot \left[\left(F_{xfl} + F_{xfr}\right) \cdot \sin\delta_f + \left(F_{yfl} + F_{yfr}\right) \cdot \cos\delta_f\right] - b \cdot \left[\left(F_{yrl} + F_{yrr}\right) \cdot \cos\delta_r + \left(F_{xrl} + F_{xrr}\right) \cdot \sin\delta_r\right] \\ &+ \frac{t}{2} \cdot \left[\left(F_{xfl} - F_{xfr}\right) \cdot \cos\delta_f + \left(F_{yfr} - F_{yfl}\right) \cdot \sin\delta_f + \left(F_{xrl} - F_{xrr}\right) \cdot \cos\delta_r + \left(F_{yrr} - F_{rrl}\right) \cdot \sin\delta_r\right] \end{aligned} \tag{2.18}$$

$$I_{XX} \cdot \ddot{\phi} = M_S \cdot g \cdot h' \cdot \sin\phi - M_S \cdot a_Y \cdot h' \cdot \cos\phi - K_\phi \cdot \phi - C_\phi \cdot \dot{\phi} \tag{2.19}$$

Load Transfer:

Normal loads for each wheel can vary due to longitudinal and lateral load transfers. For front inner wheel, normal load expression in a turn is:

$$F_{zfi}=\frac{W}{2}\cdot b/L \;-\; 1/2\cdot M\cdot a_X\cdot h/L \;-\; K_R\cdot\left[M\cdot a_Y\cdot\frac{h}{T}+M_S\cdot h'\cdot\ddot{\phi}\cdot\frac{h}{T}-M_S\cdot g\cdot\frac{h'}{T}\cdot\sin\phi\right] \qquad (2.20)$$

First term defines the static condition. Second term $1/2\cdot M\cdot a_X\cdot h/L$ is the contribution of the longitudinal acceleration and is negative for the positive acceleration of the vehicle.

Last term is the expression for the lateral weight transfer. Load transfer is the result of the roll moment and lateral forces acting on the vehicle. The expression follows directly from the moment equation written for the whole vehicle around roll axis. The moment sum is then split front to rear by multiplying by a bias factor. Expression involves effect of the lateral force in X direction and the tilting moment of the sprung weight appearing in the equations of motion defined before.

Similarly normal loads for other wheels can be written:

$$F_{zfo}=\frac{W}{2}\cdot b/L \;-\; 1/2\cdot M\cdot a_X\cdot h/L \;+\; K_R\cdot\left[M\cdot a_Y\cdot\frac{h}{T}+M_S\cdot h'\cdot\ddot{\phi}\cdot\frac{h}{T}-M_S\cdot g\cdot\frac{h'}{T}\cdot\sin\phi\right] \qquad (2.21)$$

$$F_{zri}=\frac{W}{2}\cdot a/L \;+\; 1/2\cdot M\cdot a_X\cdot h/L \;-\; (1-K_R)\cdot\left[M\cdot a_Y\cdot\frac{h}{T}+M_S\cdot h'\cdot\ddot{\phi}\cdot\frac{h}{T}-M_S\cdot g\cdot\frac{h'}{T}\cdot\sin\phi\right] \qquad (2.22)$$

$$F_{zro}=\frac{W}{2}\cdot a/L \;+\; 1/2\cdot M\cdot a_X\cdot h/L \;+\; (1-K_R)\cdot\left[M\cdot a_Y\cdot\frac{h}{T}+M_S\cdot h'\cdot\ddot{\phi}\cdot\frac{h}{T}-M_S\cdot g\cdot\frac{h'}{T}\cdot\sin\phi\right] \qquad (2.23)$$

Braking System Dynamics

Braking system and a corresponding transport delay was not modeled for the purposes of this study. The input applied brake torque is accepted to be split 70:30

between front and rear axles. The applied torque at each axle is then divided into half for each wheel, effect of which is added to the equations of motion through the dynamical equation of the wheel below.

$$\dot{\omega}_{fl} = \frac{1}{I_w} \cdot \left(- F_{xfl} \cdot R - M_{bfl} \right) \tag{2.24}$$

$$\dot{\omega}_{fr} = \frac{1}{I_w} \cdot \left(- F_{xfr} \cdot R - M_{bfr} \right) \tag{2.25}$$

$$\dot{\omega}_{rl} = \frac{1}{I_w} \cdot \left(- F_{xrl} \cdot R - M_{brl} \right) \tag{2.26}$$

$$\dot{\omega}_{rr} = \frac{1}{I_w} \cdot \left(- F_{xrr} \cdot R - M_{brr} \right) \tag{2.27}$$

Calculations for Tire Model:

For Allen tire model, it is required to calculate also longitudinal wheel slip and lateral slip angles.

Lateral slip angle is the angle between the direction of motion and the plane of the wheel and is calculated for each wheel as below:

$$\alpha_{fl} = \delta_f - \tan^{-1}\left(\frac{v + a \cdot r}{u + r \cdot T/2}\right) \tag{2.28}$$

$$\alpha_{fr} = \delta_f - \tan^{-1}\left(\frac{v + a \cdot r}{u - r \cdot T/2}\right) \tag{2.29}$$

$$\alpha_{rl} = \tan^{-1}\left(\frac{v - b \cdot r}{u + r \cdot T/2}\right) - \delta_r \tag{2.30}$$

$$\alpha_{rr} = \tan^{-1}\left(\frac{v - b \cdot r}{u - r \cdot T/2}\right) - \delta_r \tag{2.31}$$

The velocity of the wheel in the tire plane, $v_{w,}$ is also necessary for tire model and for calculation of the longitudinal slip. The related equations are as following:

$$V_{wfl} = \sqrt{(u + r \cdot T/2)^2 + (v + a \cdot r)^2} \cdot \cos\alpha_{fl} \tag{2.32}$$

$$V_{wfr} = \sqrt{(u - r \cdot T/2)^2 + (v + a \cdot r)^2} \cdot \cos\alpha_{fr} \tag{2.33}$$

$$V_{wrl} = \sqrt{(u + r \cdot T/2)^2 + (v - b \cdot r)^2} \cdot \cos\alpha_{rl} \tag{2.34}$$

$$V_{wrr} = \sqrt{(u - r \cdot T/2)^2 + (v - b \cdot r)^2} \cdot \cos\alpha_{rr} \tag{2.35}$$

Longitudinal wheel slip is defined as the difference of wheel circumferential velocity and velocity component of the vehicle in the direction of the tire plane divided over velocity at the tire plane again. The necessary set of equations is written as:

$$s_{fl} = \frac{V_{wfl} - \omega_{fl} \cdot R}{V_{wfl}} \tag{2.36}$$

$$s_{fr} = \frac{V_{wfr} - \omega_{fr} \cdot R}{V_{wfr}} \tag{2.37}$$

$$s_{rl} = \frac{V_{wrl} - \omega_{rl} \cdot R}{V_{wrl}} \tag{2.38}$$

$$s_{rr} = \frac{V_{wrr} - \omega_{rr} \cdot R}{V_{wrr}} \tag{2.39}$$

All equations were modeled in Simulink. Allen tire model was implemented into the constructed vehicle model through an embedded MATLAB function block. Vehicle model block diagram in Simulink is depicted in figure 2.6.

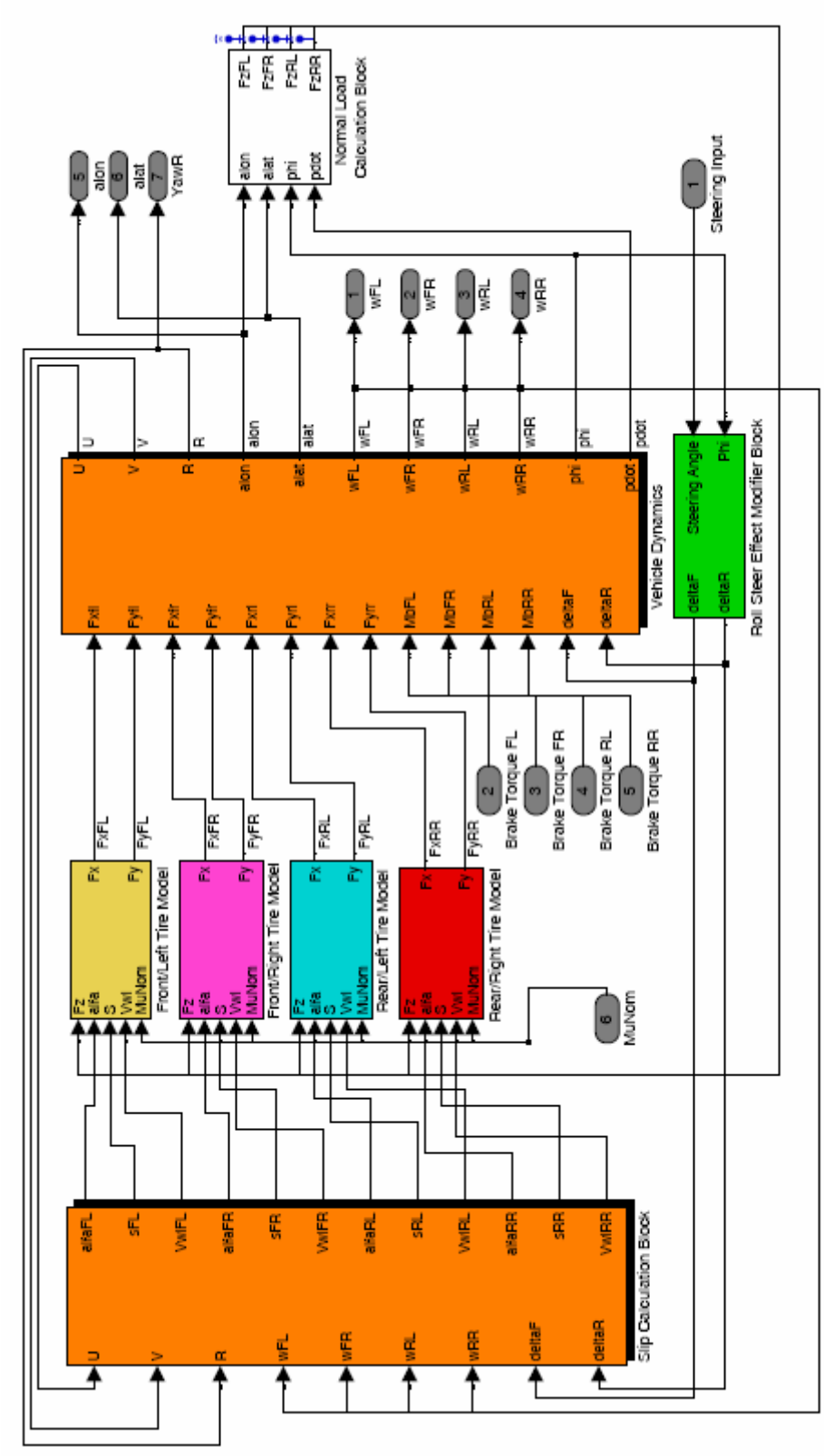

Figure 2.6. Vehicle Model - Simulink

CHAPTER 3

CONTROLLER DESIGN

The basic objective of the ABS controller proposed in this study is to reduce tendency for wheel-lock during braking and through maintaining longitudinal wheel slip at a certain setpoint, retain steerability of the vehicle and at the same time, achieve shorter stopping distances if possible. In this chapter, the development of the controller is explained in detail.

The proposed ABS controller structure is composed of two sub-controllers: A high-level controller and low-level slip controller. The hierarchical structure was adopted considering easy adaptability to integration with an ESP controller and also for the purpose of realizing a more failsafe and flexible design. ABS control is maintained individually for each wheel through independent controller modules of both sub-controllers.

The two-stage ABS controller was designed to have a single data transfer in between for each wheel. The reference slip signal as the single output of the high-level controller includes the information for the initiation of the ABS control at the corresponding wheel in addition to the reference slip data that is necessary for the low-level slip controller. Inputs to the ABS controller are vehicle longitudinal acceleration, brake pedal on/off signal, wheel angular accelerations and longitudinal slips of each wheel. Figure 3.1 shows the structure of the proposed design.

The operation of the designed ABS is basically as follows: The high-level controller sensing the impending lock at a wheel through the inherent initiation logic dispatches

a reference slip signal, which is then received by the low-level wheel slip controller. The low-level controller modulates braking torque at the corresponding wheel independently in order to track this reference signal.

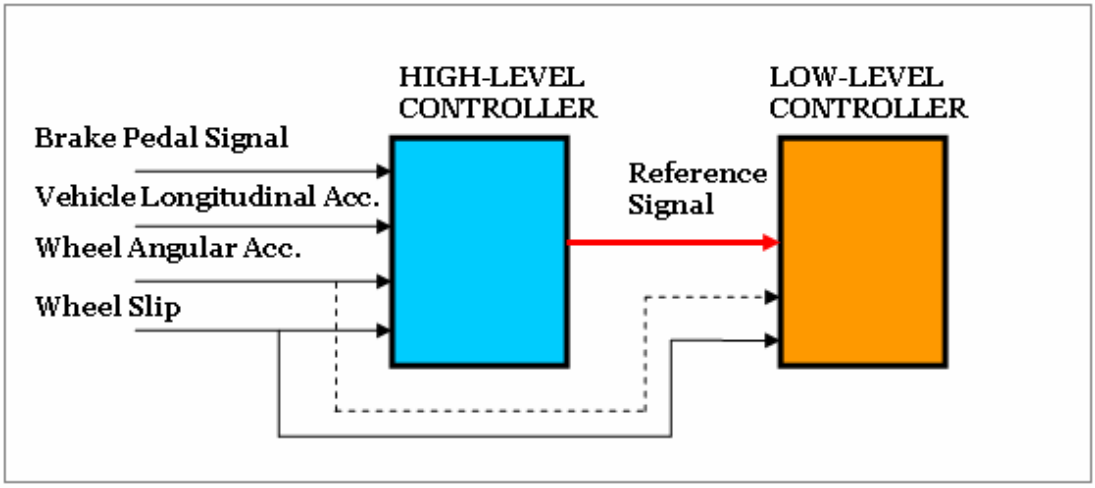

Figure 3.1. Proposed ABS controller structure

3.1. HIGH-LEVEL CONTROLLER

The duty of the high-level controller is to set the reference slip values which will be attained by the low-level slip controller.

In the design of the high-level controller, there were some points which constituted the base of the work. For the purpose of showing the approach followed for the design, these are summarized as below.

- The controller is expected to be flexible such that it can adapt to different road conditions and driver inputs and provide reliable and satisfactory information to the low-level slip controller.

- In a braking situation without steering, the priority of the controller is to maintain the longitudinal wheel slip at a point that gives the peak value of

longitudinal coefficient of friction in the μ-slip curve, in order to obtain the maximum braking force from road surface, thus the minimum stopping distance. The road condition must be taken into account to achieve the optimum longitudinal wheel slip value.

- For the case of braking with turning, the complex relationships between longitudinal brake force and side traction must be taken into account.

- The high-level controller must be designed to operate with different sub-level slip controllers and therefore is expected to work well for different performance outputs.

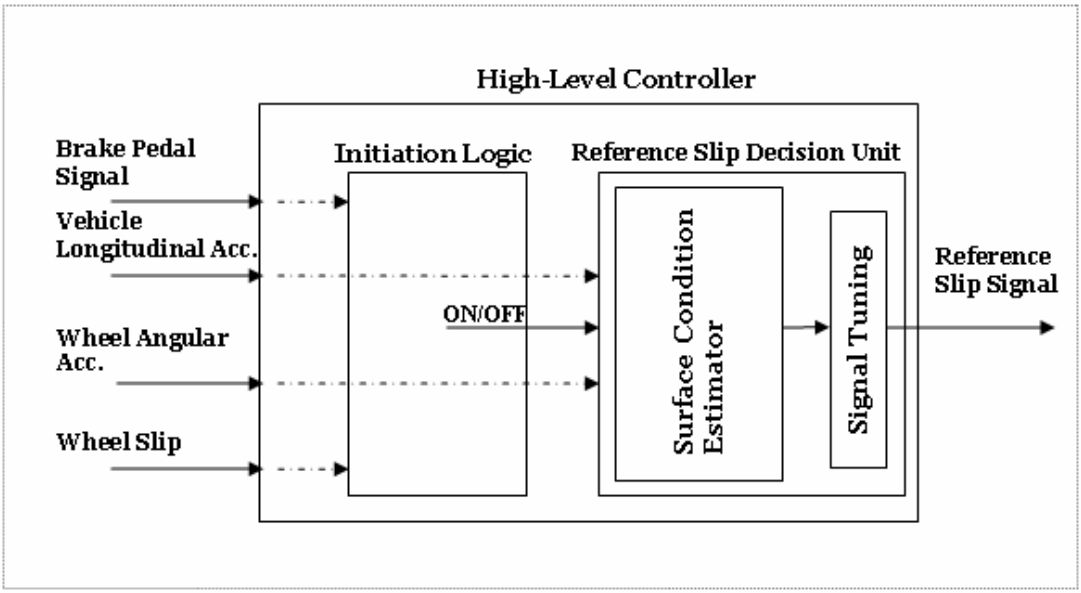

Figure 3.2. High-level controller structure

In the design of the controller, the above mentioned points were taken into account. High-level controller takes brake pedal on/off signal, longitudinal acceleration, longitudinal slip and wheel acceleration information for each wheel. The controller is composed of two function blocks: ABS initiation logic and reference slip decision

unit. Structure of the high-level controller is depicted by the representative diagram provided in figure 3.2

ABS initiation logic was realized in MATLAB/Simulink by a Stateflow® block shown in figure 3.3. ABS initializes when longitudinal slip at the corresponding wheel reaches a certain threshold and if brake pedal is pressed at the same time. Note that ABS operates only when braking is present; therefore as soon as the driver releases brake pedal, control is switched off.

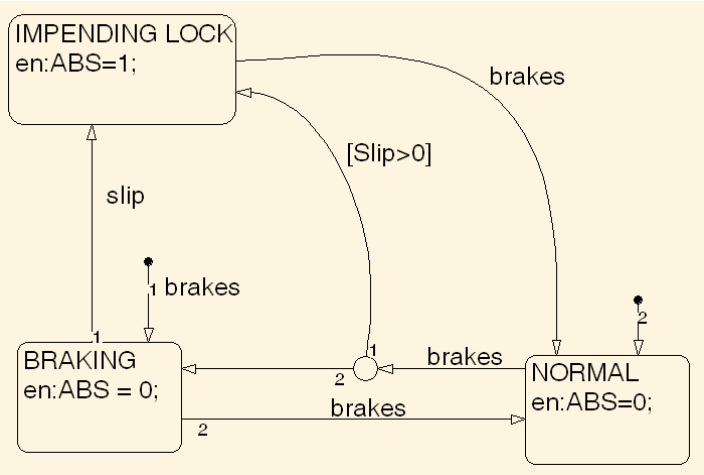

Figure 3.3. ABS initiation logic – Stateflow diagram

Reference slip decision unit takes longitudinal acceleration, output signal of the ABS initiation logic block and wheel angular acceleration signal as inputs. The block incorporates a fuzzy logic based surface condition estimator and a Stateflow block for tuning the signal according to wheel angular acceleration information. The only input of the estimator system is the longitudinal acceleration of the vehicle.

Estimation of the longitudinal coefficient of friction, μ, from vehicle longitudinal acceleration can give reasonable results in the ABS operation range. There are studies in literature which use longitudinal acceleration as a parameter in the identification of road condition [3,6,18]. Following from equations of motion,

longitudinal acceleration is basically a function of braking force. Since wheel slip can be maintained in a certain range when ABS is active and assuming effect of changes in normal load and vehicle velocity variation is negligible in tire braking force development, longitudinal acceleration can be used to predict nominal surface coefficient of friction. In the proposed design, vehicle longitudinal acceleration information is used directly as an estimate of road condition and is the input to the fuzzy logic block.

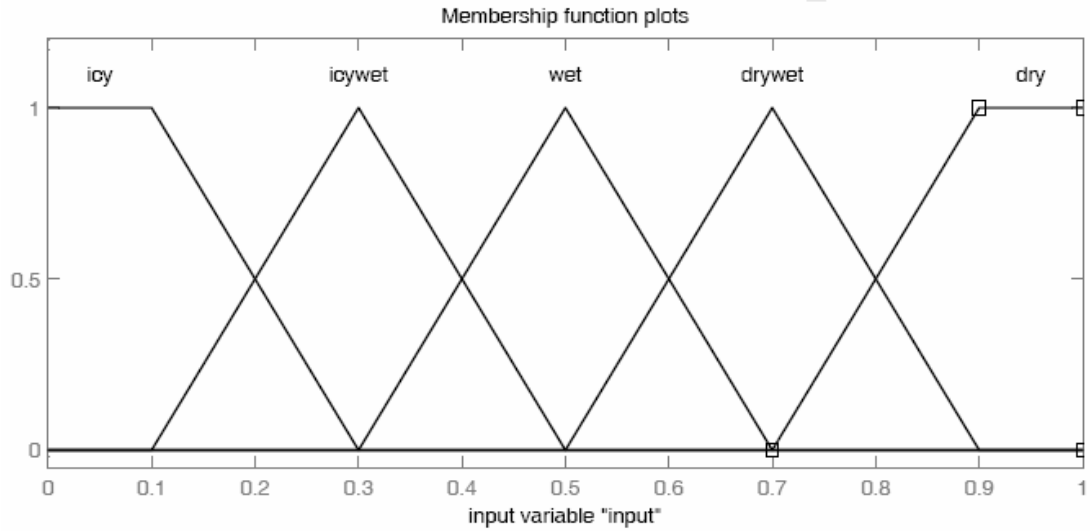

Figure 3.4. Input fuzzy set for reference slip decision logic

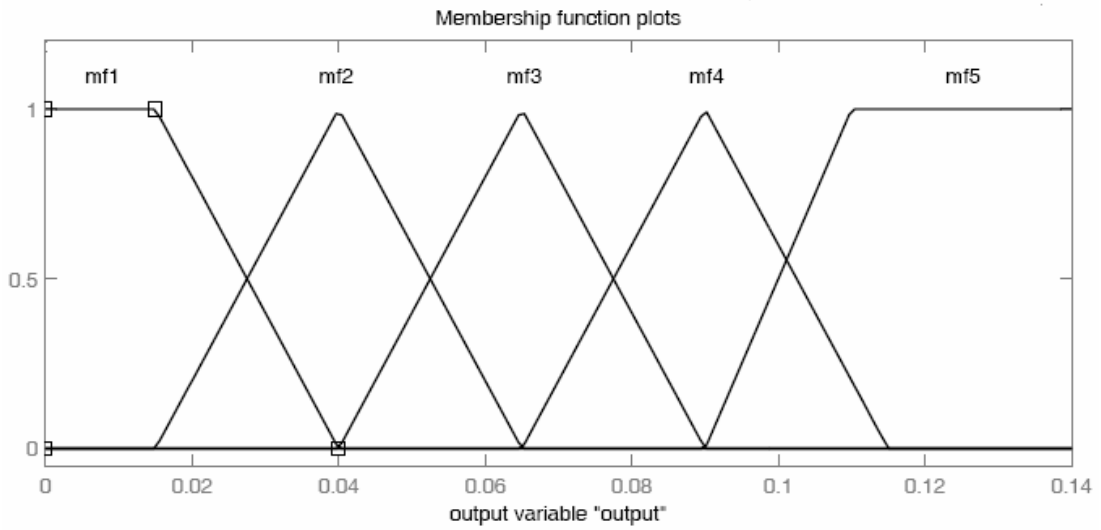

Figure 3.5. Output fuzzy set for reference slip decision logic

Fuzzy membership functions are designed to output a reference longitudinal slip value that is close to the peak of the μ-slip curve of the identified surface for zero slip angle. The design simply maps surface friction coefficient estimates to predetermined reference slip values which provide highest braking force in straight-line driving.

Input variable of the fuzzy block is a_x/g, vehicle longitudinal acceleration divided over gravitational acceleration and output is the reference slip ratio. Mamdani-type fuzzy sets are depicted in figures 3.4 and 3.5. Each fuzzy set has 5 membership functions. Strong overlapping of the membership functions provides a more sensitive and smooth reference signal output. For defuzzification, centroid method was used. Fuzzy rules are as follows:

- If input is ‘dry’ then output is ‘mf5’
- If input is ‘drywet’ then output is ‘mf4’
- If input is ‘wet’ then output is ‘mf3’
- If input is ‘icywet’ then output is ‘mf2’
- If input is ‘icy’ then output is ‘mf1’

During the development stage of the high-level controller, it was observed that dynamic reference tracking of the reference signal generated directly from the surface condition estimator may cause performance problems since the single input of the estimator is the vehicle longitudinal acceleration which is naturally subject to changes in the output of the low-level slip controller and hence surface identification is dependent on the performance of the designed controllers. Degraded performance of the slip controllers would certainly affect the reference slip decision in such a situation, and ultimately the response of the vehicle would be inferior in return. In order to handle the problem, output of surface condition estimator was bounded where the lower limit is 4 % slip and a Stateflow block was incorporated in reference slip decision unit to allow the transmission of the output signal of the estimator to the low-level controller only if the wheel angular acceleration is between certain limits.

By this way, the performance of ABS was improved especially on roads with surface friction transitions and at the initialization step. The Stateflow block is simply designed to hold reference signal constant until the wheel acceleration drops below admissible bounds and at the initialization, dispatches a constant predetermined value which was chosen as 10 % slip for the simulations.

On-line calculation of optimal slip values in combined steering and braking maneuvers was much desired; but complex relationships between longitudinal brake force and side traction make it difficult to make a decision without predicting the intention of the driver since a compromise is required. Vehicle response dependency of the surface condition estimation, mentioned above, provides actually a flexibility at this point; the mechanism itself indirectly leaves initiative to the driver. In a combined steering and braking maneuver during ABS operation, longitudinal deceleration drops off for sufficiently large steering due to limited adhesion which causes the misinterpretation of the surface condition, resulting a lower reference slip value and this improves eventually the lateral force generation capability of the tires. The situation can be observed from the results of the simulations for cornering and braking case presented in chapter 4.

Reference slip decision unit in the high-level controller was designed to output the reference slip according to same fuzzy rules and membership functions regardless of the steering maneuvers. Note that this design favors lateral performance due to the effect of sideslipping on tire force characteristics. Peak of the μ-slip curve shifts to right as slip angle increases while side friction force decreases with increasing longitudinal wheel slip; therefore by keeping the reference slip constant in steering, the proposed design preserves the lateral force generation capability of the tire.

3.2. LOW-LEVEL CONTROLLER

The task of low-level controller is basically to maintain the longitudinal slip value at a wheel close to the reference slip signal, i.e. track the reference slip, by modulating

brake torques accordingly. In this thesis, two controller designs are proposed for this purpose: Fuzzy logic controller and PID controller.

The output of the both low-level slip controller alternatives was chosen to be the rate of change of brake torque applied at wheels, as it would be proper in the case of a hydraulic actuator. Although as noted before, the brake system was not modeled in order to realize a flexible design, it was necessary to have a logical and physically realizable controller output for the application. For this reason, the output of the controller was also selected to be on the order of attainable hydraulic pressure change rates in other studies [30,31]**.** More precisely, the actuator is thought to be able to deliver braking torques at any rate continuously between -30000 N.m/s and 30000 N.m/s without time delay. Note also that, when required, the control system can be adapted to a customary hydraulic brake system by scaling the output of the controller and using these scaled values through a post-processing block to decide for the on-off times of the valves as in the study of Madau, D.P. et.al. [15]**.**

3.2.1. Low-Level Fuzzy Logic Controller

Fuzzy logic is an efficient method for quick design of control systems for high-order nonlinear, time-varying systems such as the case in this study. The approach offers highly robust control despite the absence of mathematical modeling and for these advantages, the method has been implemented successfully in a wide variety of applications since it was introduced by Zadeh in mid-60's.

Fuzzy logic controller was designed using Mamdani type fuzzy inference method which is the most commonly implemented methodology and centroid method was adopted for defuzzification. For implementation to Simulink, Fuzzy Logic Toolbox of MATLAB was used. Controller was designed to take longitudinal wheel slip error and wheel angular acceleration as inputs. The wheel slip error is defined to be the deviation of the actual longitudinal slip from the reference signal sent by the high-level controller. Input variables and output are each realized by five membership

functions as shown in figures 3.6, 3.7 and 3.8. Note that fuzzy rules and membership functions are same for all road conditions. There exist 25 rules for the fuzzy logic system. In the design of the fuzzy sets, symmetric triangular and trapezoidal membership functions were chosen. Shapes of the membership functions were designed to be sufficiently wide to compensate for possible uncertainity but also narrow enough for fine control.

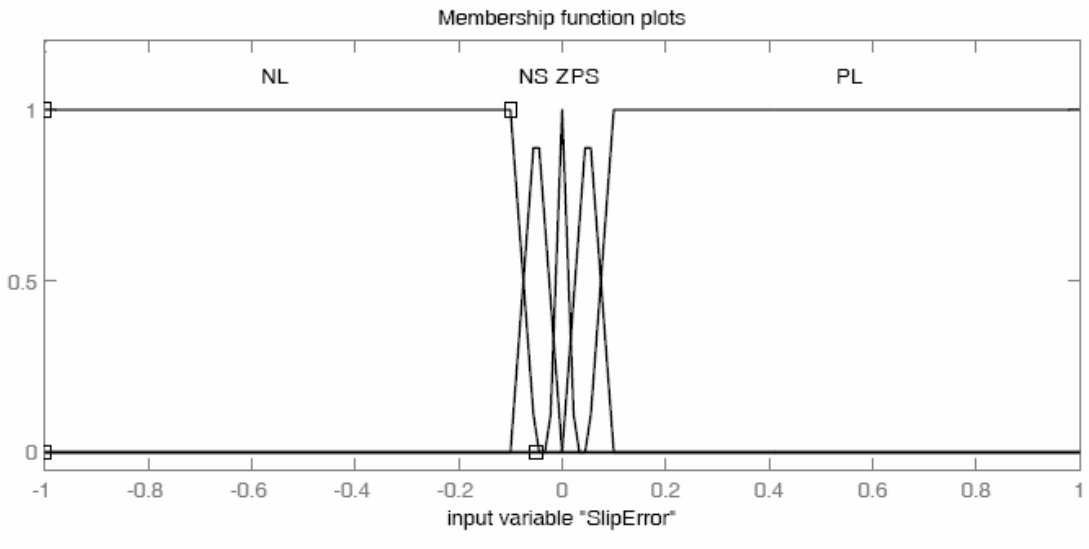

Figure 3.6. Fuzzy set for longitudinal wheel slip error

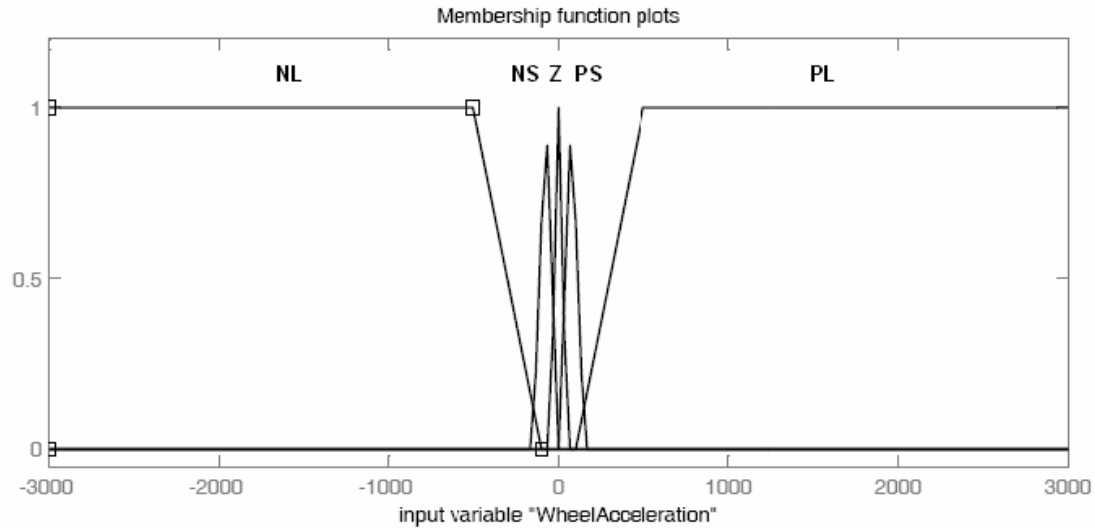

Figure 3.7. Fuzzy set for wheel angular acceleration

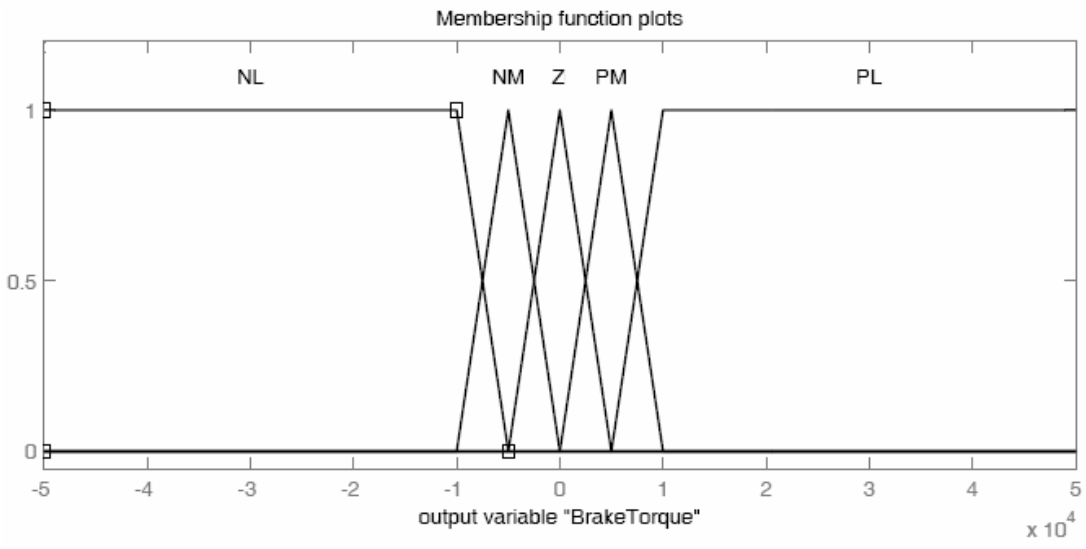

Figure 3.8. Fuzzy set for brake torque change rates

Output fuzzy set was designed to return brake torque change rates between specified limits of -30000 Nm/s and 30000 Nm/s. Because of the centroid method, the domain of the output membership function was extended beyond these limits to attain the necessary values with the condition that the resulting output of the fuzzy logic controller always be in the permissible range.

Table 3.1. Rule table for the low-level fuzzy logic controller

	Wheel Angular Acceleration				
Wheel Slip Error	λ / ω̇	PL	PS	Z	NS	NL
	PL	Z	NM	NL	NL	NL
	PS	Z	Z	NM	NL	NL
	Z	PL	PM	Z	NM	NL
	NS	PL	PM	PL	PL	NL
	NL	PL	PL	PL	PL	NM

The rule table is presented in table 3.1. For a successful design of the fuzzy rule set, it was necessary to observe the plant behavior. For sufficiently large wheel angular acceleration values, the rule base was designed to reduce baking torque at the maximum allowable rate, irrespective of the wheel slip ratio, to reduce the initial wheel slip overshoot insofar as it is possible; on the other hand, the controller was designed to output a gradually decreasing braking torque change rate when angular deceleration drops below a certain limit, to prevent the cycling of the wheel slip observed following the recovery from the initial slippage increase.

Final design of the fuzzy controller was attained following a lengthy trial and error process and an intense study regarding analysis of simulation results. Development stage was explained briefly below to give insight into the design.

The Fuzzy Controller was initially designed to be a Mamdani type single input-single output controller with longitudinal wheel slip error as the only input parameter. It was observed on different road conditions and for different fuzzy set designs that the response tended to have an undesirable oscillatory character for the output of the proposed high-level controller. Extended simulation tests revealed that for different fixed reference slip values, response has a dissimilar character; controller shows a slow, degraded performance in the linear range while in the unstable portion of the μ-slip curve, cycling of the wheel slip is almost unavoidable. In this case, redesign of the fuzzy controller may be required for different road conditions and optimal slip strategies and it should be noted that such a degraded performance is definitely not efficient for reference tracking. Simulations on certain adverse road conditions with low coefficient of friction surfaces showed also that the controller may not able to react properly to prevent the initial slippage increase which is understandable since the single-input controller is certainly not able to recognize the severity of the slippage without slip error rate information or wheel angular acceleration.

In order to improve the closed-loop performance, prevent the undesirable cycling and to avoid excessive slipping in hard braking, fuzzy controller was redesigned to include wheel angular acceleration information as a secondary input and fuzzy rules

were further refined by analysis of the vehicle response against combined braking and turning maneuvers on different surfaces with a wide range of coefficient of friction values.

The final design tracks reference slip signal at any portion of the friction curve with inconsiderable oscillations and controller remains operational even for completely erroneous wheel angular acceleration signals, showing only a limited cycling behavior. Performance of the eventual controller and the early SISO fuzzy logic controller design can be compared with the help of the figures 3.9 and 3.10. Even though the comparison of the two approaches is subject to success of the designs, presented figures provide a general view. Plots clearly illustrate the improved performance of the proposed design for both reference slip values in the linear range of the friction curve (figure 3.9) and around the peak point (figure 3.10). In the unstable portion of the μ-slip curve, amplitude of the oscillations increases even more for single-input controller. Simulations were conducted in MATLAB/Simulink for a vehicle in hard braking on 0.9 nominal coefficient of friction surface.

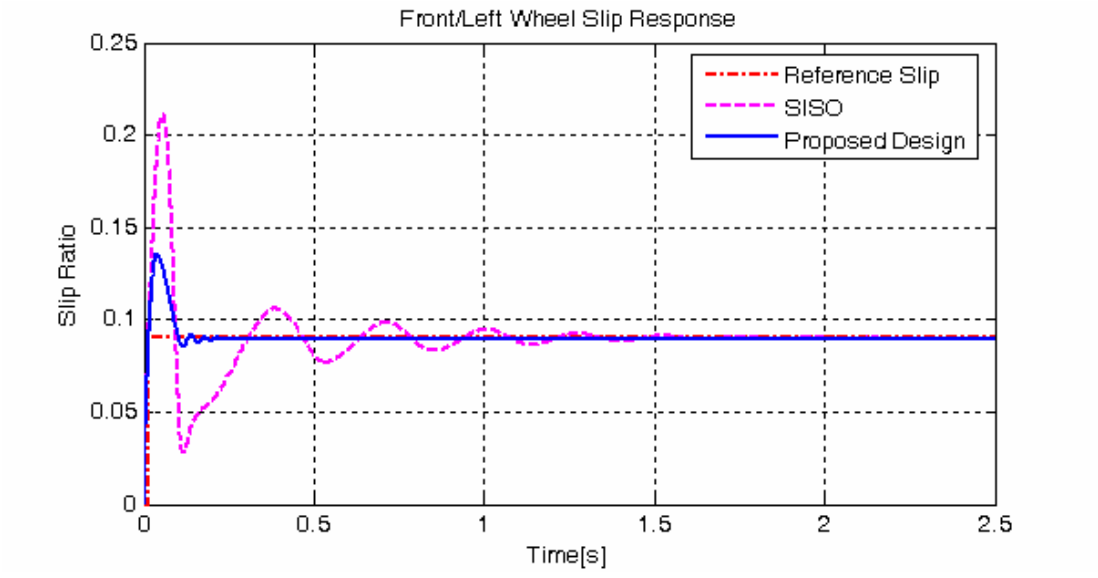

Figure 3.9. Performance comparison for fixed reference slip signal (0.09)

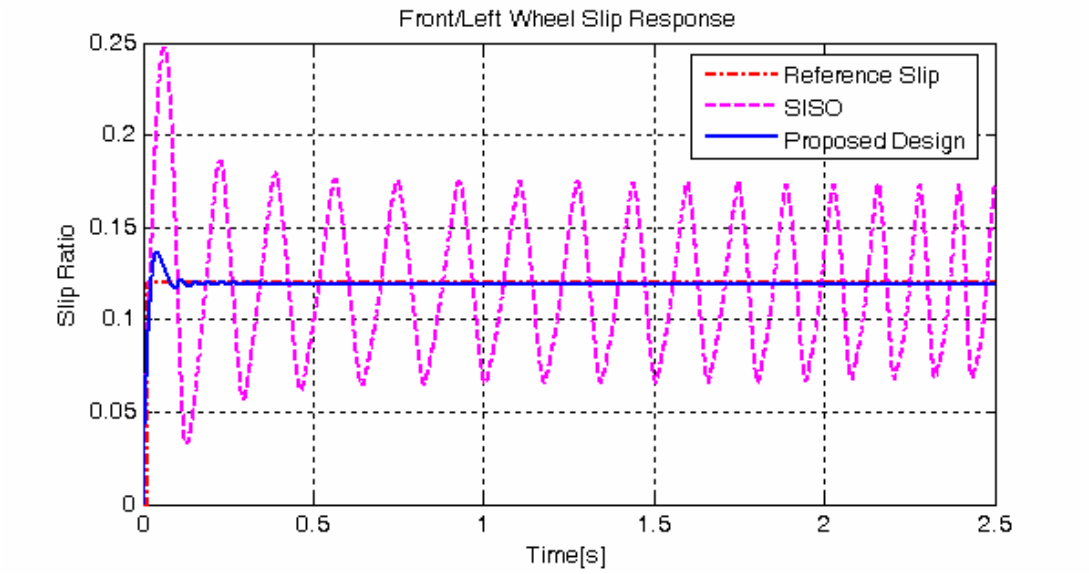

Figure 3.10. Performance comparison for fixed reference slip signal (0.12)

3.2.2. Low-Level PID Controller

PID (proportional-integral-derivative) control is an effective and yet simple control scheme extensively used in industry. More than half of the controllers in industrial applications utilize PID based control methods [32]. Though PID controllers may not ensure optimal control in all cases**,** they are known to provide satisfactory results. The control scheme is applicable to a wide range of systems including complex plants where analytical design methods can not be used. The controller may be formed using only proportional control mode as well or as PI or PD control in the absence of one of the control parameters; however in this study, the controller is designed to include all three terms for enhanced performance. Simulink block diagram of the controller was depicted in figure 3.11.

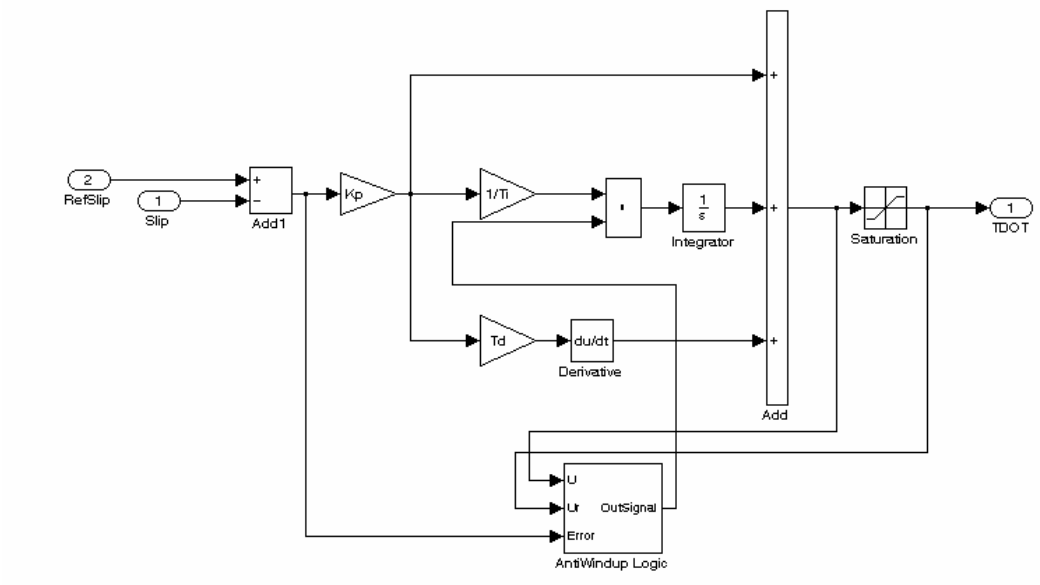

Figure 3.11. Simulink block diagram of the designed PID controller

The controller takes the error between longitudinal wheel slip and the reference slip signal as the only input and attempts to reduce this error through generating a corrective action, limited brake torque change rate, based on the three control parameters. The design of the PID controller was not based on an analytical approach; controller parameters were determined following an intensive simulation study and detailed analysis of results. In the design, it was first desired to minimize the overshoots observed at the initiation of the hard braking and during transition between different surfaces and a small settling time was important for fast recovery from slippage and adaptation; therefore it was decided to have a weighted derivative gain; however integral action was also necessary for a faster response and a satisfactory steady-state performance; for that reason a slight increase of overshoot and oscillations were tolerated.

Integral windup may occur in PID control systems which have limiting constraints over outputs. The problem is basically due to the unnecessary accumulation of the integral term at instances when the control signal is saturated. It may cause excessive overshoots and undesirable transient response since control output, increasing over

the limits without any benefit, also can not be reduced when required, due to the accumulated integral value.

For the low-level PID controller, an additional anti-windup logic was implemented to overcome the problem experienced especially following the initial slippage increase at the start of the ABS operation. The implemented logic block was based on literature [33]. The algorithm simply stops integration at saturation limits according to the sign of the error, the strategy is as below:

'e': 'Reference slip signal' – 'Actual longitudinal wheel slip'
U_{max} & U_{min}: Saturation limits

- When control signal, '*u*', is between the saturation limits: continue integration
- When '*u*' is at U_{max} and '*e*' > 0, stop integration
- When '*u*' is at U_{max} and '*e*' < 0, continue integration
- When '*u*' is at U_{min} and '*e*' < 0, stop integration
- When '*u*' is at U_{min} and '*e*' > 0, continue integration

Contribution of the implemented anti-windup logic to the PID low-level controller can be observed clearly from figure 3.12. The plot is from a MATLAB simulation of the proposed ABS controller for a vehicle in hard braking on a surface with a friction coefficient of 0.5 and presents the behavior of the longitudinal slip of the front/left wheel. The dashed curve shows the significant drawback due to anti-windup. The controller can not recover in time following the initial slippage increase due to accumulated integral action and has certainly a degraded braking performance and lengthened stopping distance.

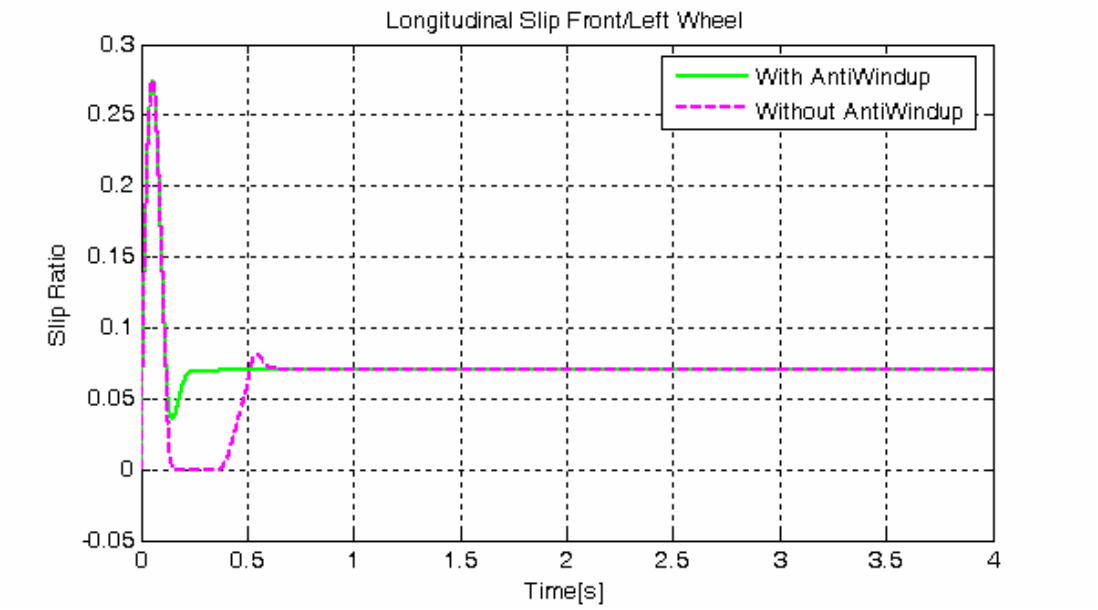

Figure 3.12. Longitudinal wheel slip response with and without anti-windup logic

3.3. MEASUREMENT AND ESTIMATION OF STATES

ABS controller requires longitudinal acceleration information of the vehicle, longitudinal wheel slips and angular acceleration data of wheels as well, for operation. For vehicle acceleration, a longitudinal accelerometer, mounted at center of gravity, is clearly necessary and an estimate of wheel angular acceleration can be obtained through standard rotational wheel speed sensors; however in calculation of wheel slips there exists a considerable uncertainity and in literature the subject is discussed extensively as mentioned before in this text.

In order to calculate longitudinal wheel slip, it is required to know the wheel angular speed and the longitudinal velocity of the tire in the plane of the tire. It is the problem of obtaining longitudinal tire velocity since the former can be readily measured. Various schemes are proposed in literature for wheel slip estimation; most of them ignoring the lateral effects in cornering, focused on estimation of absolute vehicle speed.

The longitudinal tire velocity in the tire plane and thus, wheel slip can be in fact directly calculated through equations presented in chapter 2 (equations: 2.28-2.39). The calculation requires longitudinal and lateral acceleration of the vehicle at center of gravity, yaw rate and steering wheel angle, all of which can be measured directly through sensors of an ESP system. It is thought that the proposed ABS controller can benefit from the sensor hardware of the integrated active safety system and the measured signals are processed through appropriate filtering methods before transmitted to ABS. For design and simulation purposes throughout the study, this direct state calculation method was adopted in this framework, with data obtained from vehicle dynamics modeled in MATLAB/Simulink.

For the purpose of demonstrating the applicability of the controller in the presence of noisy measurements, a Kalman filter estimation method was also developed based on the work performed by Watanabe et al [9]. The scheme estimates absolute vehicle velocity from noisy vehicle longitudinal acceleration data and wheel angular speed. The method incorporates a rule-based strategy which switches the values of covariance matrices during slippage of the wheel from which the measurement is taken. Discrete-time measurement and estimation of the states is appropriate for implementation to MATLAB. The state-space model of the Kalman filter is presented below.

$$\begin{aligned} x(k+1) &= A(k)\cdot x(k) + B(k)\cdot w(k) \\ z(k) &= C(k) + n(k) \end{aligned} \tag{3.1}$$

Where x(k) is the state vector with vehicle longitudinal acceleration and vehicle speed as the states, and z(k) represents the measurements taken from the accelerometer and the data obtained from the rotary wheel sensor signal multiplied by tire radius.

$$x(k)=\begin{bmatrix} a \\ v \end{bmatrix},\quad z(k)=\begin{bmatrix} a_m \\ v_m \end{bmatrix}$$

$$A(k)=\begin{bmatrix} 1 & 0 \\ \tau & 1 \end{bmatrix},\quad B(k)=\begin{bmatrix} \tau & 0 \\ 0.5\cdot\tau^2 & \tau \end{bmatrix},\quad C(k)=\begin{bmatrix} 1 & 0 \\ 0 & 1 \end{bmatrix} \tag{3.2}$$

The variables n(k) and w(k) represent measurement and system noise, covariance matrices of which are defined respectively by R(k) and Q(k). Implemented Kalman filter algorithm is as below:

Time update equations:

$$\begin{aligned} x(k)^- &= A(k)\cdot x(k-1) \\ P(k)^- &= A(k)\cdot P(k-1)\cdot A(k)^T + B(k)\cdot Q(k)\cdot B(k)^T \end{aligned} \tag{3.3}$$

Measurement update equations:

$$\begin{aligned} K(k) &= P(k)^-\cdot C(k)^T\cdot\left[C(k)\cdot P(k)^-\cdot C(k)^T + R(k)\right]^{-1} \\ x(k) &= x(k)^- + K(k)\cdot\left[z(k)-C(k)\cdot x(k)^-\right] \\ P(k) &= P(k)^- - K(k)\cdot C(k)\cdot P(k)^- \end{aligned} \tag{3.4}$$

In implementation, coefficients of noise covariance matrix, R, are adjusted according to a rule base to compensate for the erroneous wheel speed information experienced during slippage of the wheel.

CHAPTER 4

SIMULATIONS

In this chapter, results of the conducted simulations in MATLAB/Simulink environment are presented to show the performance of the designed ABS controller. Simulation tests were carried out for various road conditions including surface transitions. The lateral response of the vehicle is considered an important evaluation parameter for this study; therefore performance of the controller for different steering maneuvers was also tested and presented. For the study, the vehicle data presented in Appendix A was used.

The simulation study includes sequentially, the case without the ABS controller, straight-line test and combined braking and steering case for different road conditions ranging from dry asphalt to icy road. In these simulations, the results for different low-level slip controllers will be compared and discussed for each case. Performance of the ABS was tested for a quantizing controller and for noisy measurement data as well. The results for these cases are also presented briefly in this chapter.

For the study, the simulations were conducted up to the point where the vehicle speed was slowed down to 5 km/h. It is common in literature to discontinue simulation at certain low-speeds [17] because since the longitudinal slip value tends to infinity as the vehicle velocity approaches zero, it becomes difficult to determine and control the slip values. It is also known that even in real applications, numerous ABS controllers do not function for vehicle speeds under 5 km/h, due to the high noise of the wheel speed sensors [34]. A fixed-step solver was used with 1 ms step size for all cases in the simulation study.

4.1. VEHICLE RESPONSE WITHOUT THE CONTROLLER

For a proper assessment of the performance of the designed ABS controller, first, it is required to observe the dynamic response of the vehicle without the controller. Three cases will be examined: simple steering response of the vehicle, braking without steering and combined braking and steering. For each case, simulation tests were performed for three different surface conditions, namely: dry, wet and icy road. The emulated road is thought to be a level surface and the initial speed of the vehicle was chosen to be 90 km/h for dry and wet asphalt conditions and 50 km/h for icy road. In presentation of the results, the emphasis is placed on dry asphalt condition.

4.1.1. CASE I: Steering Response of the Vehicle without Braking

Response of the vehicle was observed for a step steering input and in a j-turn maneuver without any applied driving or braking torque. For the first set of simulations, the surface condition is chosen as dry asphalt road. The road surface is thought to have an evenly distributed coefficient of friction value of 0.9.

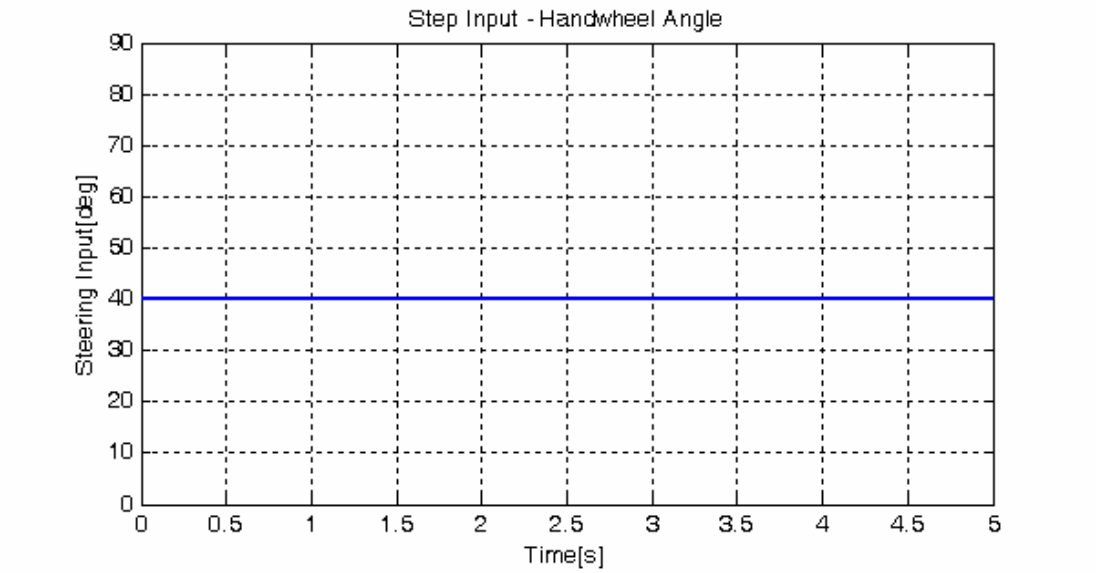

Figure 4.1. 40º Step steering input signal

The presented figures from 4.2 to 4.6 correspond to the case where a step steering handwheel angle input of 40º applied at the start of the simulation. The steering input signal is shown in figure 4.1. The steering ratio is 1:18 as stated in the vehicle data. Note that positive steering input corresponds to a right-hand turn.

In response to the step steer input, the vehicle initially goes through a transient period. Steering input creates front tire cornering forces through the formation of slip angles. However for rear tire side forces to build up, initially a sideslip angle is required to develop at the center of gravity of the vehicle [35]. Generated tire cornering forces result in the development of vehicle yaw motion, lateral acceleration and eventually roll motion of the vehicle. Figures 4.2, 4.3 and 4.4 show respectively yaw rate, vehicle sideslip angle and lateral acceleration plots.

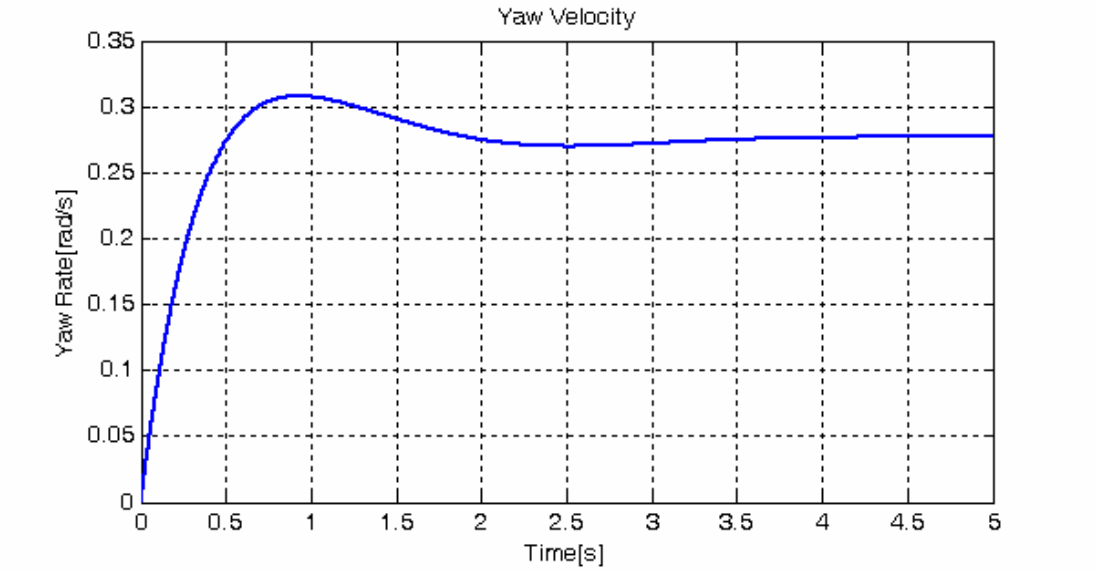

Figure 4.2. Yaw velocity for 40º step steer input on dry asphalt

The yaw rate attains a maximum of 0.31 rad/s approximately and reaches steady-state at about 3.5 seconds as can be seen in figure 4.2. The response curve resembles underdamped second order dynamics. The sideslip angle curve depicted in figure 4.3

reaches its peak value of 4.75º after 1.6 seconds and lateral acceleration behavior has a similar response characteristic as the sideslip angle development. The lateral acceleration reaches a maximum value of 0.71g as shown in figure 4.4.

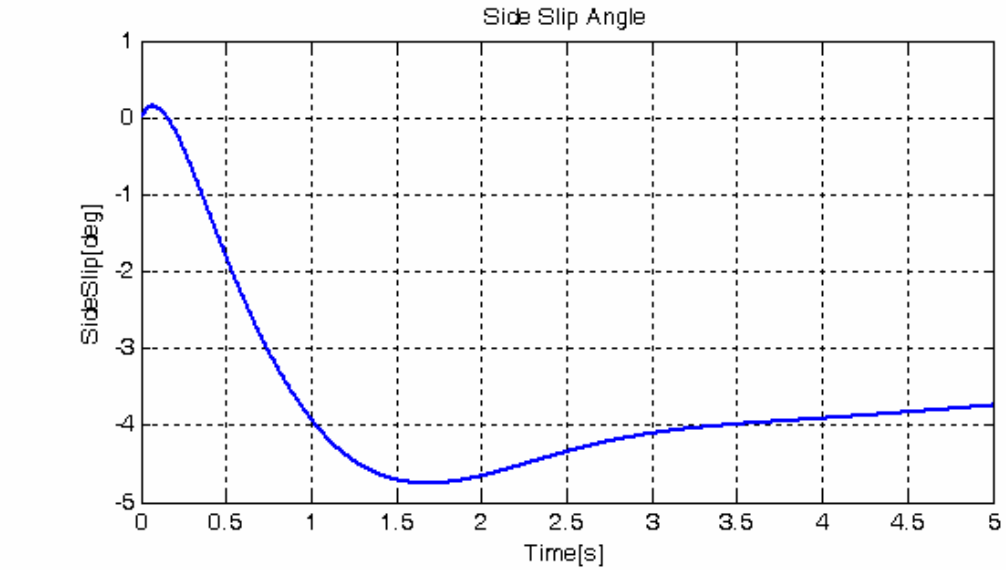

Figure 4.3. Sideslip angle for 40º step steer input on dry asphalt

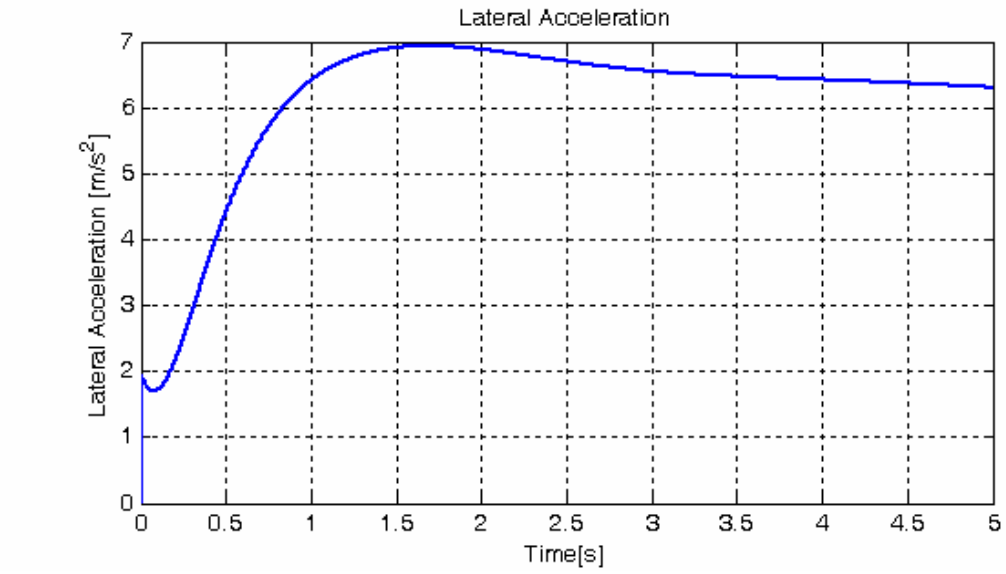

Figure 4.4. Lateral acceleration for 40º step steer input on dry asphalt

It should be here noted that the decreasing trends in the both plots observed after 3 seconds are mainly due to the longitudinal dynamics of the vehicle. The velocity of the vehicle decreases through simulation because of cornering and the effect can be observed in the lateral dynamic response plots. Simulations for a model with constant longitudinal velocity show that yaw, sideslip angle and lateral acceleration curves reach steady-state at approximately 3 seconds.

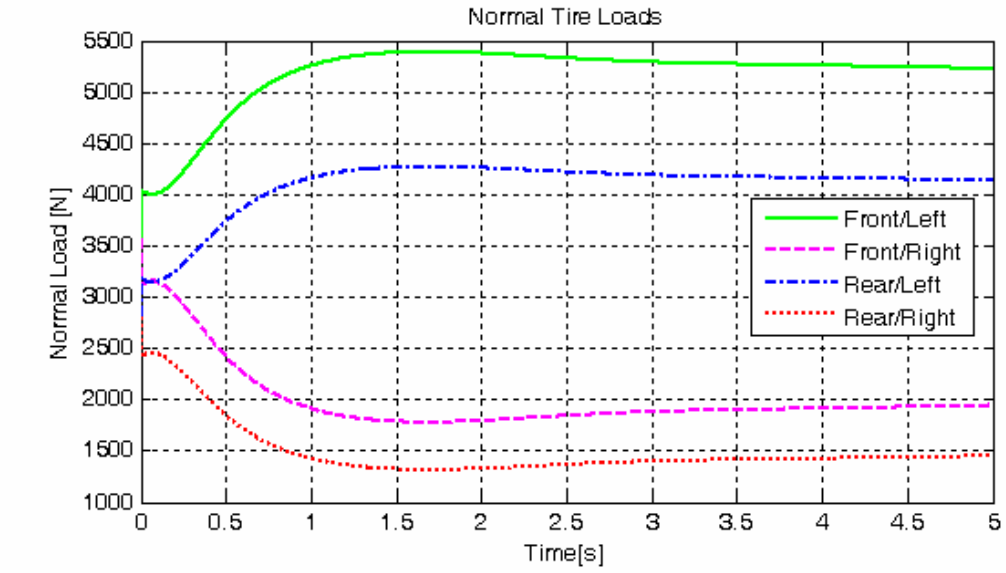

Figure 4.5. Tire normal loading for 40º step steer input on dry asphalt

Figure 4.5 shows the normal loading on the tires. As expected, there is a load transfer from inside wheels to outside wheels. The roll angle development of the vehicle can be examined from figure 4.6. The maximum roll angle value of 2.2º is reasonable for a lateral acceleration of 0.71g.

The next step of simulations was conducted to study the response of the vehicle model to a steering input that simulates a j-turn maneuver on dry asphalt road. The steering input signal is shown in Figure 4.7. The signal is basically a step change of handwheel angle in the amount of 90º and is physically more realistic than the pure

step steer input. Note that this amount of change corresponds to a slip angle of 5º for front tires, at the instant the steering input is applied.

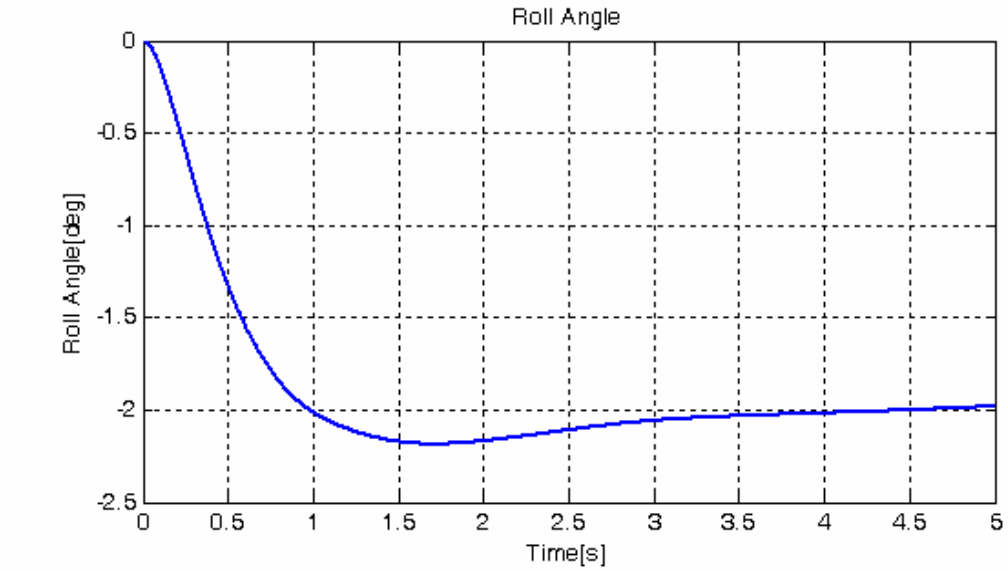

Figure 4.6. Roll angle for 40º step steer input on dry asphalt

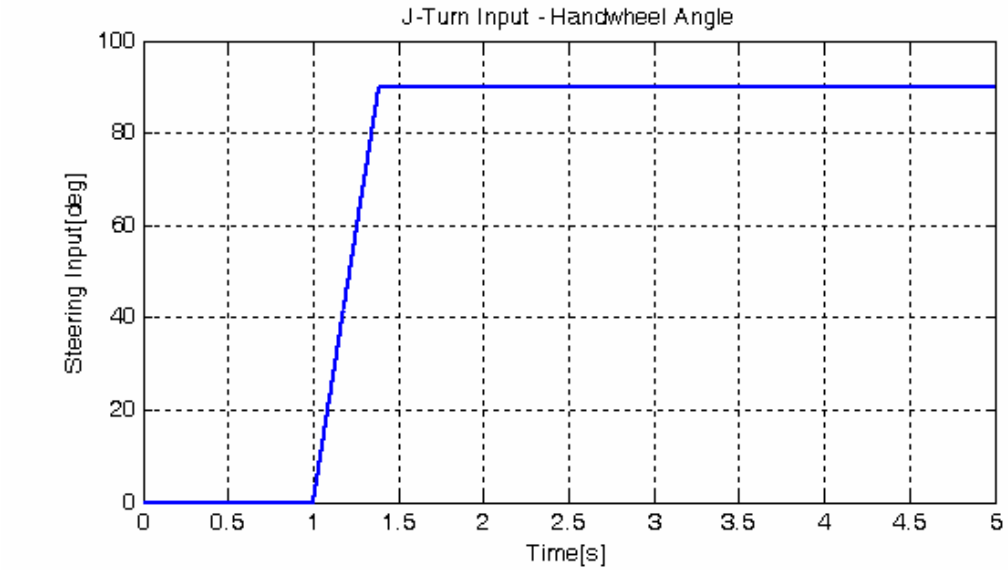

Figure 4.7. J-Turn steering input.

Figures from 4.8 to 4.12 show the response of the vehicle to the steering input signal depicted in figure 4.7. The results indicate a difficult situation for an average driver. The yaw velocity of the vehicle is observed to have damped oscillations with a peak value of 0.515 rad/s before reaching steady state as seen in figure 4.8.

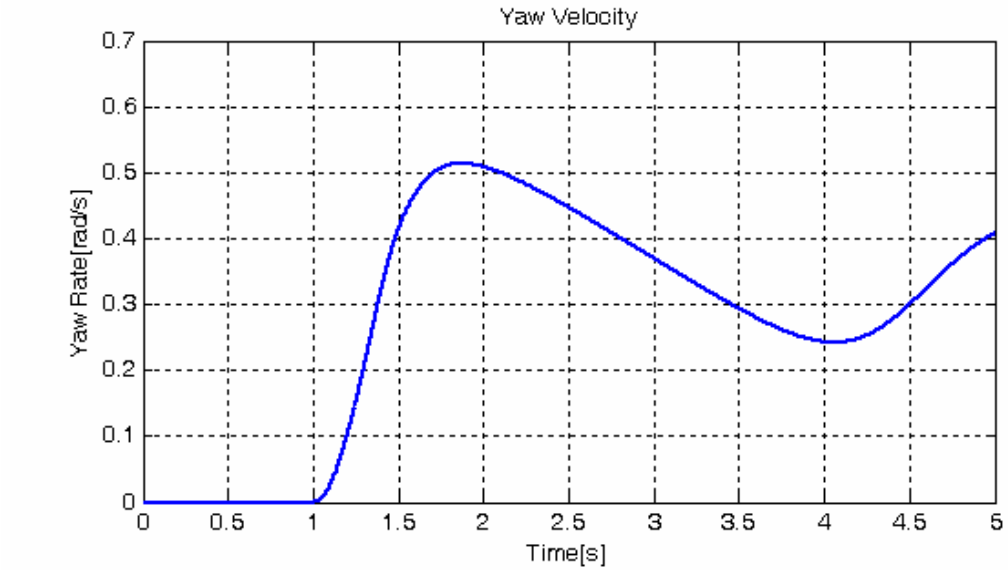

Figure 4.8. Yaw velocity in j-turn maneuver on dry asphalt.

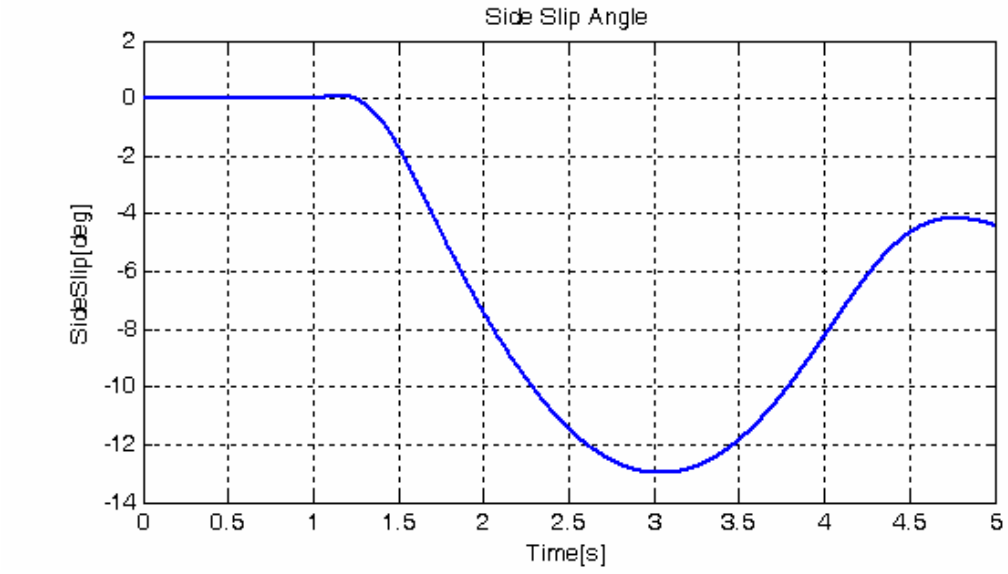

Figure 4.9. Sideslip angle in j-turn maneuver on dry asphalt.

Figure 4.9 shows the sideslip angle curve which has a maximum overshoot of 13º at 3 seconds. This amount of sideslip angle corresponds to a case where the steering loses considerable efficiency and the average driver feels in danger. Lateral acceleration as shown in figure 4.10 reaches 8.5 m/s^2.

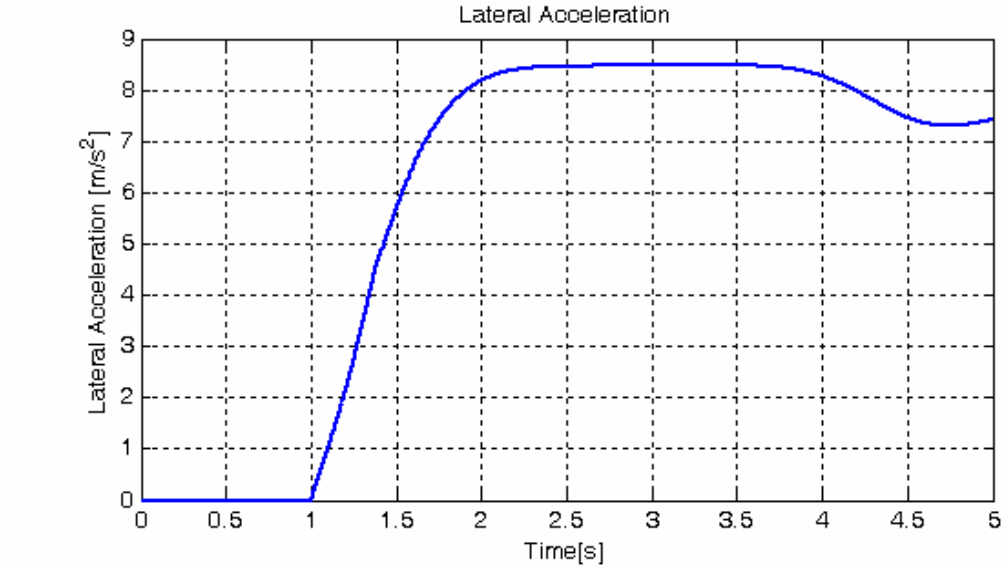

Figure 4.10. Lateral acceleration in j-turn maneuver on dry asphalt

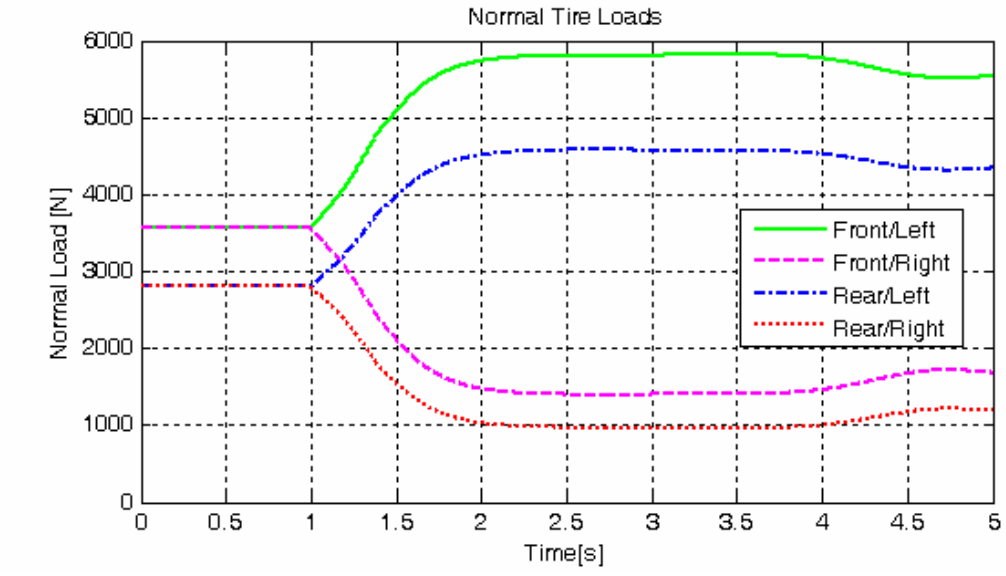

Figure 4.11. Tire normal loading in j-turn maneuver on dry asphalt

Figures 4.11 and 4.12 show respectively tire normal load distribution and roll angle development during the maneuver. The plots indicate that a rollover threat is not to be expected.

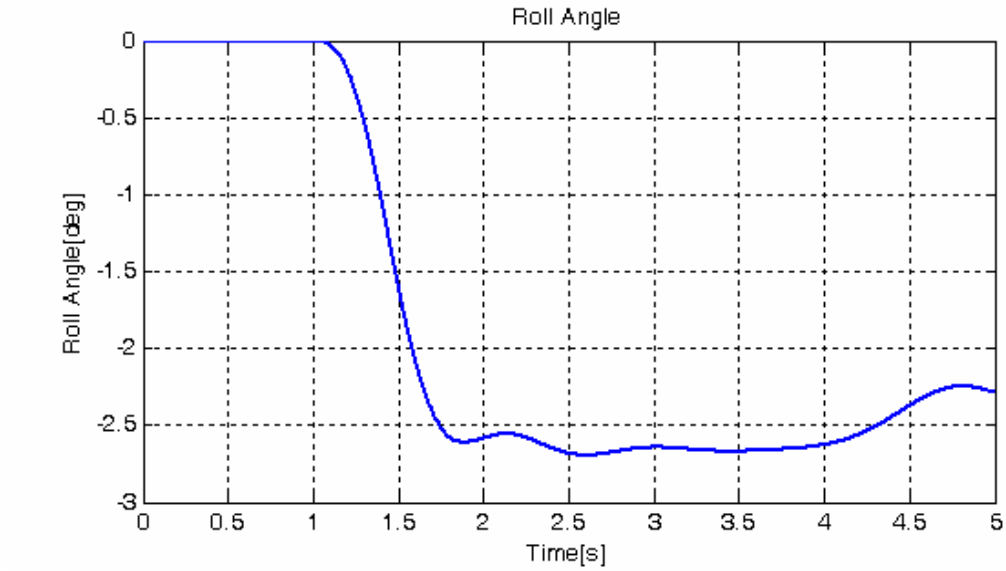

Figure 4.12. Roll angle in j-turn maneuver on dry asphalt

As mentioned before, steering response of the vehicle was also studied for wet and icy road conditions. For these adverse road conditions, lateral performance would be certainly degraded due to limited lateral force generation capability of the tires. Saturation of the tire forces at the limit of adhesion, may cause understeer or oversteer behavior of the vehicle.

For simulations conducted on emulated wet and icy road surfaces, only the 40º step steering wheel angle signal shown in figure 4.1 was applied as the steering input. Figures 4.13, 4.14 and 4.15 present the results of the simulation carried out on wet asphalt road. For this surface condition, the nominal coefficient of friction is chosen to be 0.5. The yaw rate response plot, presented in figure 4.13, shows damped oscillations with a peak value of 0.27 rad/s and the vehicle sideslip angle response shown in figure 4.14 has a maximum overshoot of 6.5º which corresponds to a significant steering inefficiency for this road condition. Lateral acceleration attains

values around 5 m/s^2 which means 30% decrease compared to dry road case. All three plots have essentially the same characteristic of the simulation results on dry asphalt; however quantitatively limited by the reduced lateral side forces due to lower coefficient of friction on tire/road interface.

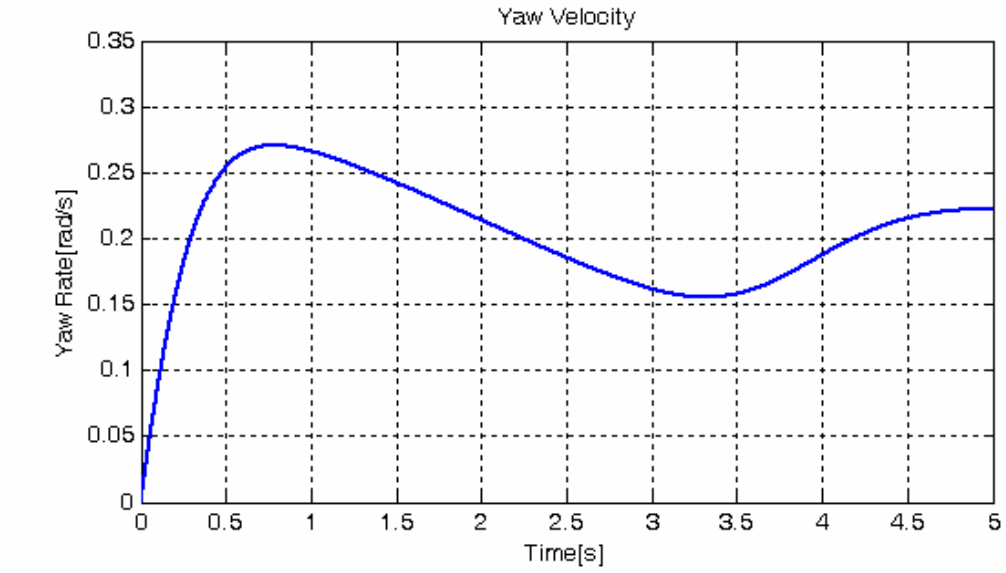

Figure 4.13. Yaw velocity for 40º step steer input on wet asphalt.

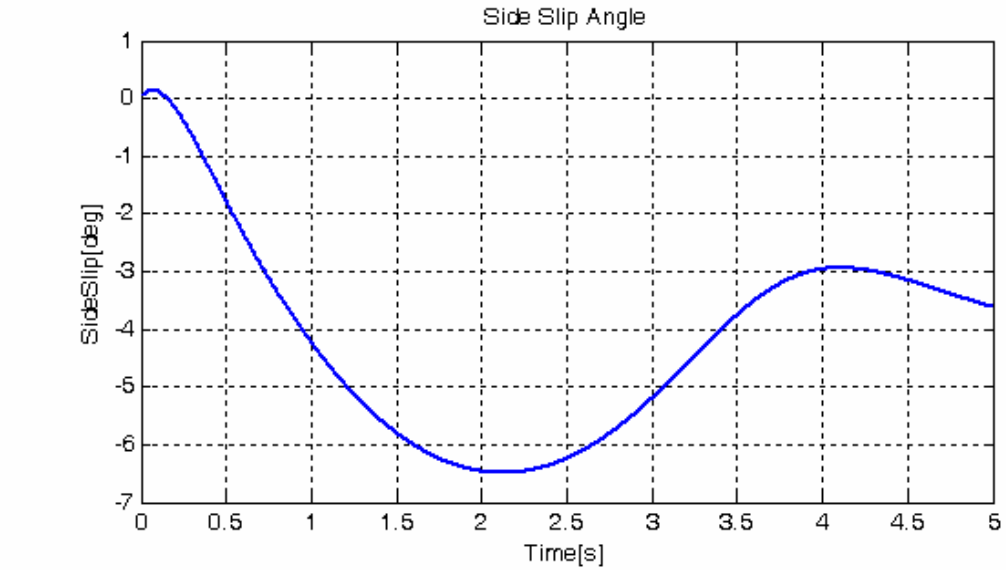

Figure 4.14. Sideslip angle for 40º step steer input on wet asphalt.

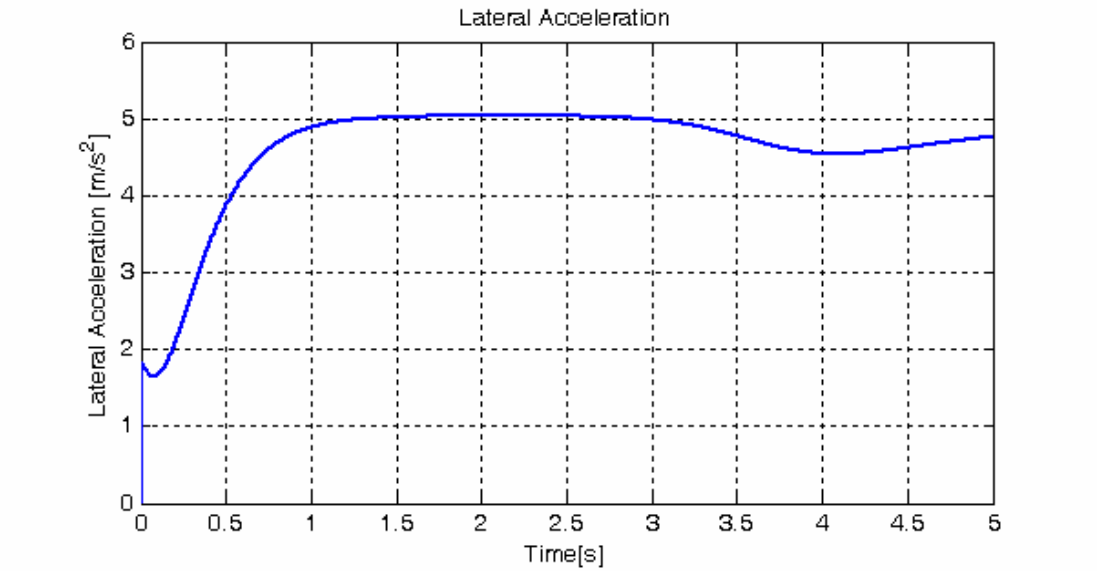

Figure 4.15. Lateral acceleration for 40º step steer input on wet asphalt.

Figures 4.16, 4.17 and 4.18 show results of the vehicle model simulated for an icy road surface represented by a nominal coefficient of friction value of 0.2. For this case, the initial velocity of the vehicle is reduced to 50 km/h.

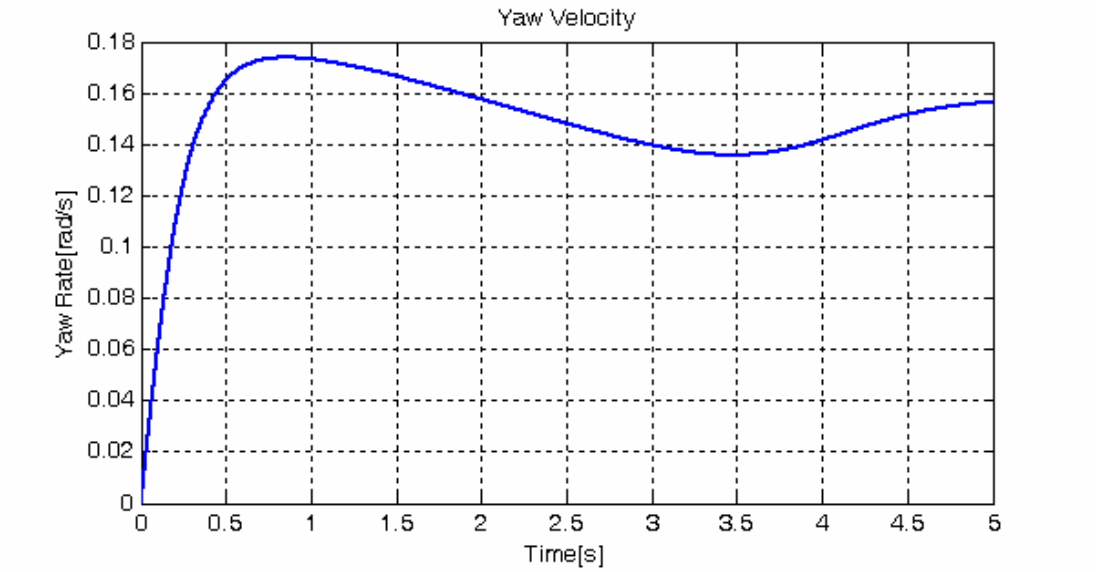

Figure 4.16. Yaw velocity for 40º step steer input on icy road.

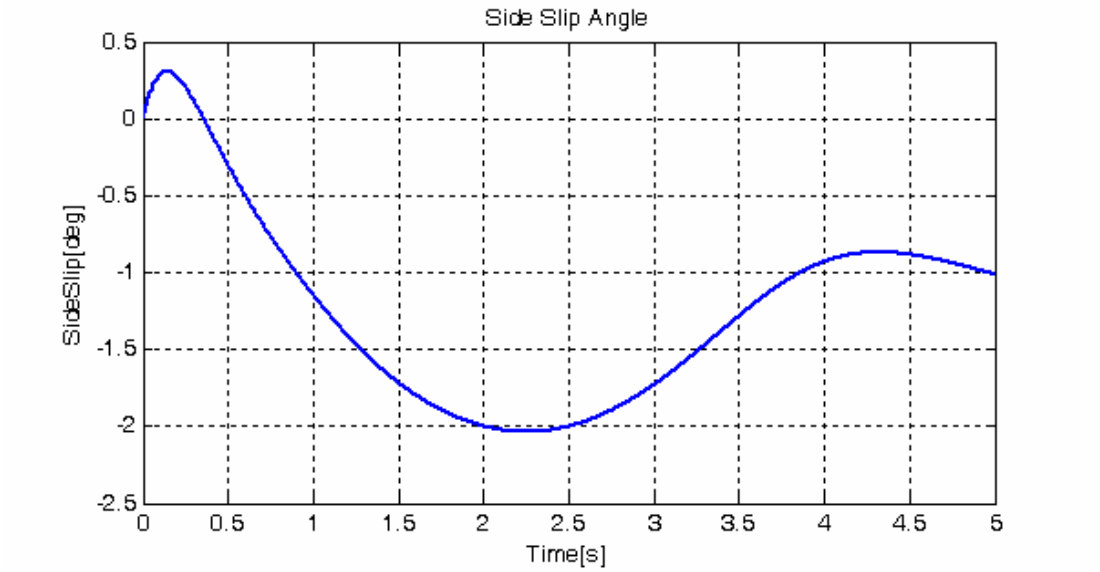

Figure 4.17. Sideslip angle for 40º step steer input on icy road

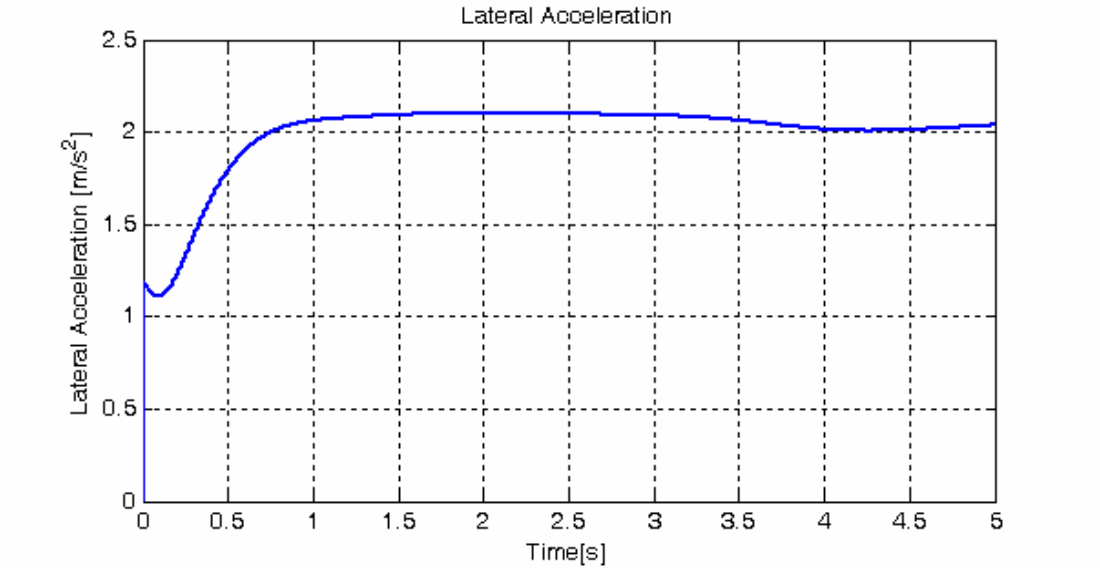

Figure 4.18. Lateral acceleration for 40º step steer input on icy road

Response plots of yaw rate, vehicle sideslip angle and lateral acceleration for icy road resemble simulation results of the wet asphalt case. The oscillatory response curve of yaw rate has a peak of 0.175 rad/s and could not reach steady state during simulation time as seen in figure 4.16. The vehicle sideslip angle plot shown in

figure 4.17, reaches 2º at around 2 seconds. Note that this angle is the physical limit over which vehicles enter into spin for icy road conditions [36]. Lateral acceleration is found to be around 2m/s^2 during the maneuver as shown in figure 4.18.

4.1.2. CASE II: Straight Line Braking

In this part, a straight-line panic braking maneuver was simulated. A total braking torque of 6000 Nm was applied to the vehicle, which was then distributed 70:30 between front and rear axles. In this arrangement, front wheels have 2100 Nm brake torque each and 900 Nm are applied at rear wheels. The initial velocity of the vehicle is 90 km/h for the simulation. Figures 4.19, 4.20 and 4.21 present the results of the simulation conducted on dry asphalt. The distance required for the vehicle to be slowed down to 5 km/h or "stopping distance", as it will be named in this text here after, was found out to be 42.66 m.

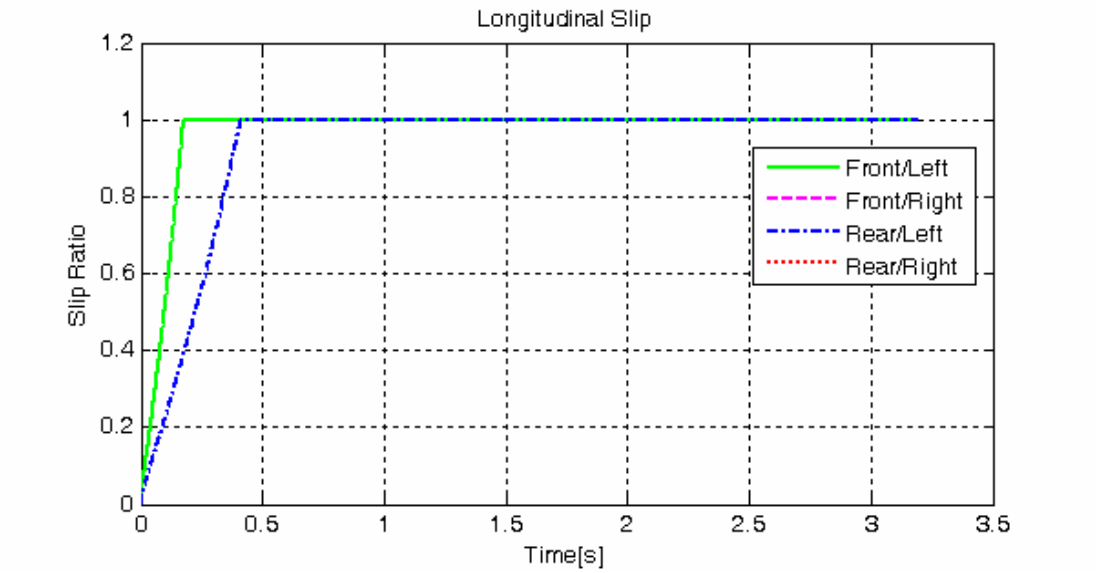

Figure 4.19. Longitudinal wheel slip for hard braking on dry asphalt

Brake lock-up characteristics of the vehicle can be observed from the longitudinal slip vs. time plot shown in figure 4.19. Longitudinal wheel slip ratios of both front

and rear wheels reach 100% slip condition under 0.5 seconds. Front wheels lock before the rear wheels as a result of the purposely arranged bias in the braking torque distribution. It would be unsafe to have a smaller front-rear brake torque ratio, since having the rear wheels lock up first will cause the vehicle to spin out [6]; however note that a high front-to-rear torque distribution proportioning is undesirable as well. In selecting the ratio, maximum braking performance is also considered.

Longitudinal acceleration response is shown in figure 4.20. Acceleration reaches its peak point of 8.94 m/s^2 at about 0.0275 seconds. Discontinuity points of the longitudinal acceleration curve correspond to the instances, the front and rear wheels lock up. The plot clearly illustrates the degraded braking performance due to locked wheels. Figure 4.21 shows the longitudinal tire forces generated during the braking maneuver. The general characteristic of the plot resembles the longitudinal acceleration graph as expected. The braking performance of the vehicle mainly depends on the front wheels which generate approximately 68% of the total braking force for dry road case as seen in the graph.

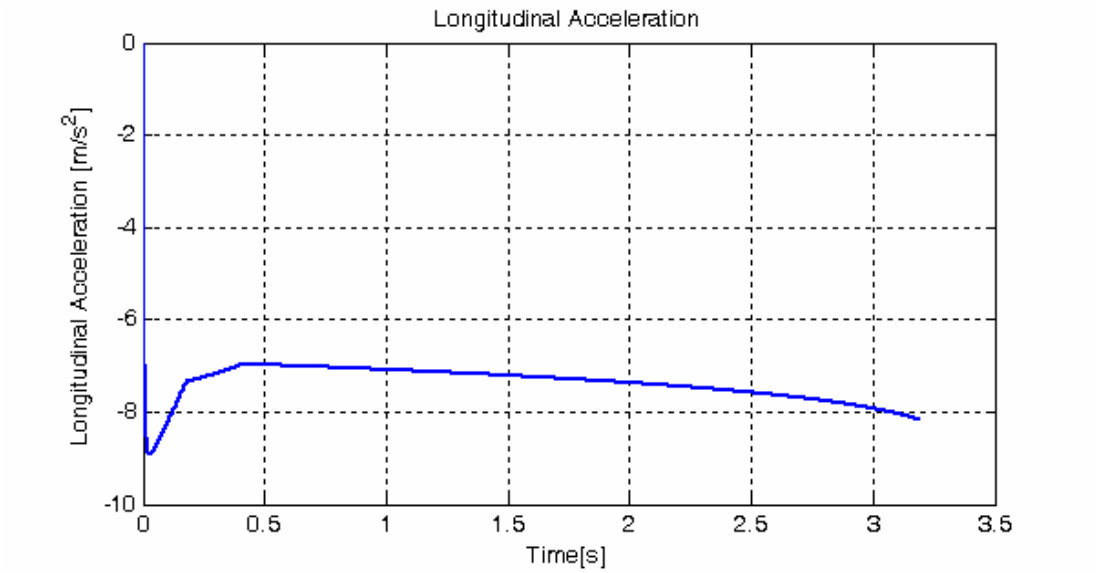

Figure 4.20. Longitudinal acceleration for hard braking on dry asphalt

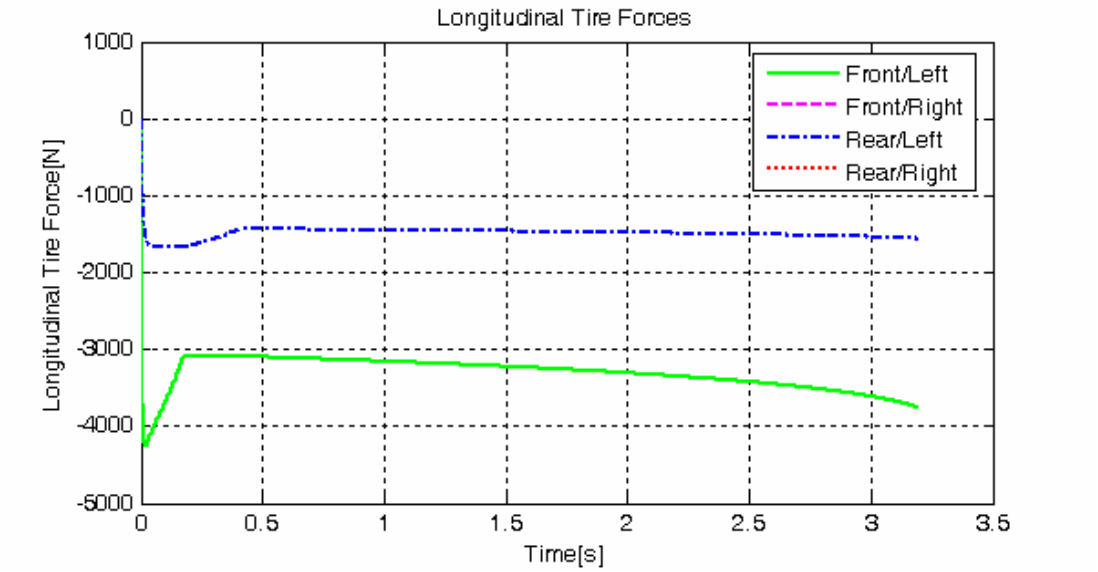

Figure 4.21. Longitudinal tire forces for hard braking on dry asphalt

The model was also simulated for adverse road conditions with 0.5 and 0.2 coefficient of friction surfaces, namely wet asphalt and icy road. Applied brake torques are the same for the two cases. For icy road condition, the initial velocity of the vehicle is reduced to 50 km/h. The response patterns are generally similar to dry asphalt case, therefore presentation of the results are not detailed.

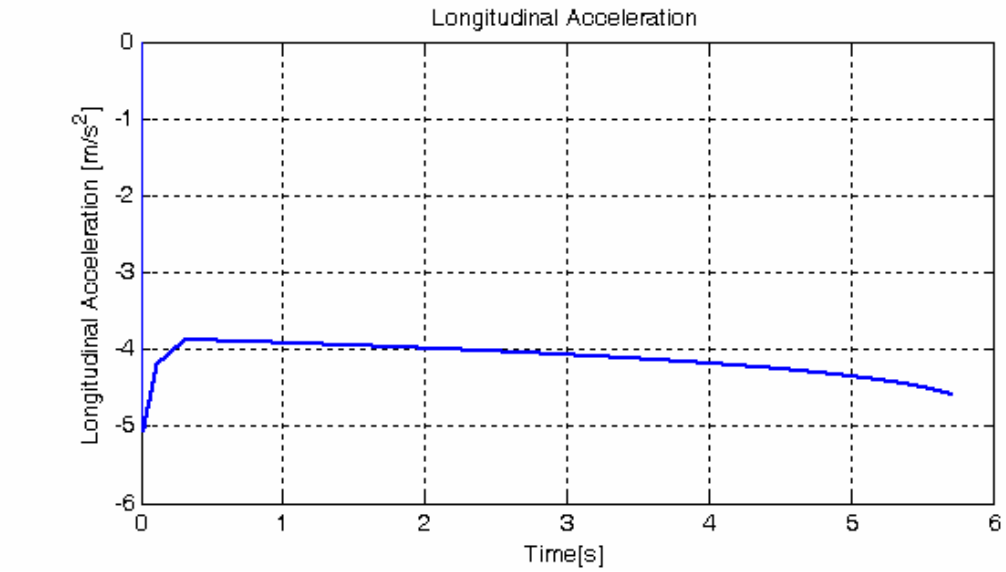

Figure 4.22. Longitudinal acceleration for hard braking on wet asphalt

For wet asphalt, the stopping distance was 77 m, which is almost 35 m ahead of the measurement for the dry road case. The longitudinal acceleration response is shown in figure 4.22. The characteristic of the plot is similar to fig 4.20; however average deceleration is observed to diminish by 45%. When compared with the dry asphalt, both wheels reached 100% slip condition noticeably earlier, rear wheels locking about 0.3 seconds. The front tires generated %62.5 of the total braking torque, a ratio reduced due to the decreased longitudinal deceleration performance.

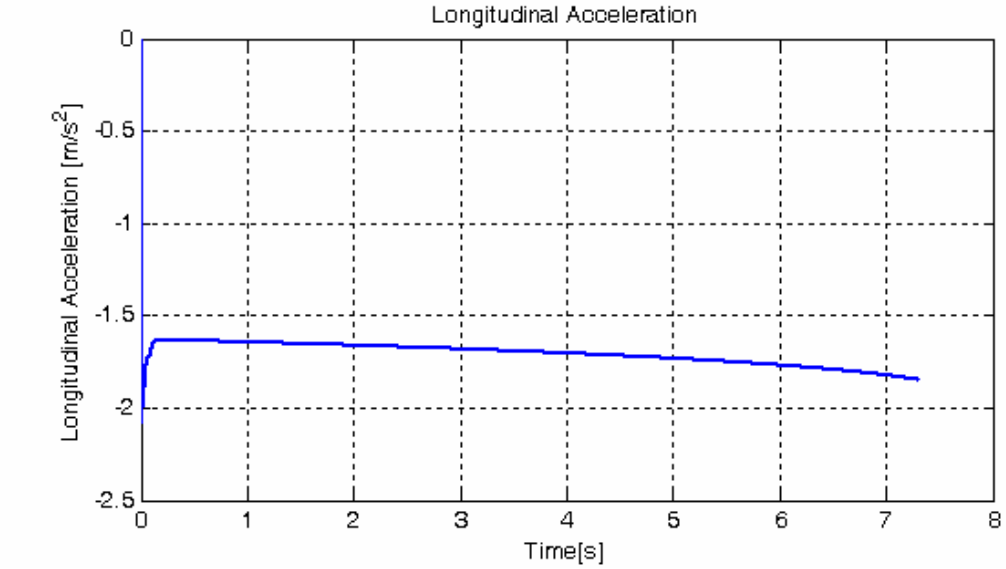

Figure 4.23. Longitudinal acceleration for hard braking on icy road

On icy road, the stopping distance was 56.63 m for the vehicle with the initial speed of 50 km/h. The average longitudinal deceleration was below 1.7 m/s^2 as seen in figure 4.23.

4.1.3. CASE III: Combined Braking and Steering

In this set of simulations, panic braking maneuver with a steering input is simulated. The purpose of this study is to observe the lateral response of a vehicle with locked wheels. As discussed previously, tire side friction coefficient decreases with increasing values of longitudinal tire slip and when 100% slip is attained, the tire is almost not able to produce lateral forces.

6000 Nm total brake torque with 70:30 front-to-rear proportioning was applied to the vehicle as in the straight line case. The steering inputs were the same as in 'Case I', which are shown in figure 4.1 and 4.7. Initial speed was 90 km/h. Only results of the simulation on dry asphalt surface are presented here, since the study showed that results obtained for adverse road conditions do not provide any additional information for the purpose of the work in this part.

Figures 4.24, 4.25 and 4.26 present the results for the step steer input shown in figure 4.1. Longitudinal deceleration performance and brake lock-up characteristic were almost same as in the straight line case; therefore related outputs are not presented here.

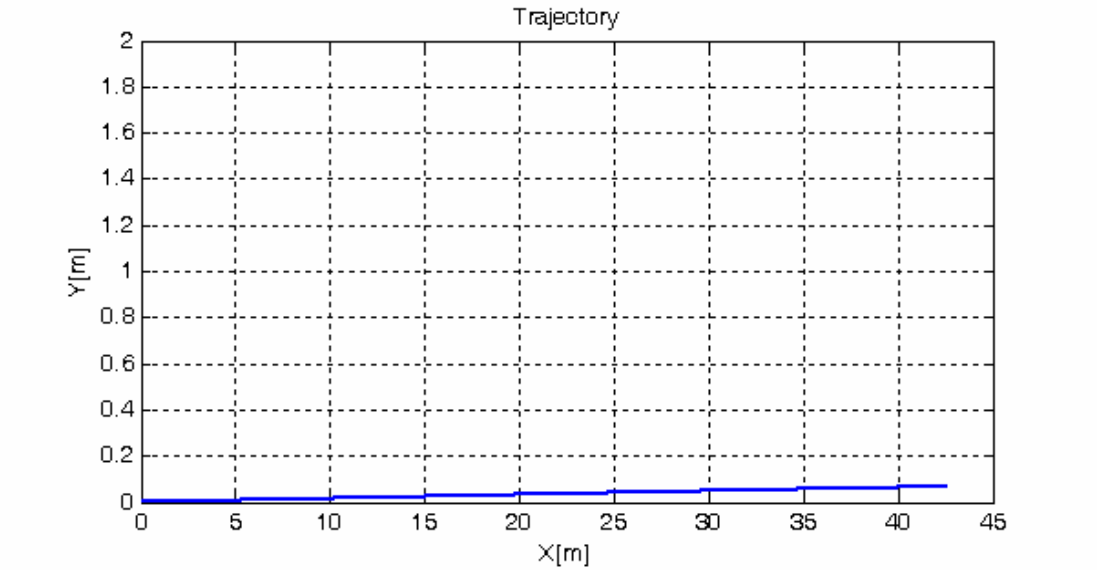

Figure 4.24. Trajectory of the vehicle for 40º step steer input and hard braking

During simulation, vehicle traveled 42.67 m in X direction and deviated only 0.067 m laterally from its straight line path. Figure 4.24 shows the trajectory of the vehicle. Figures 4.25 and 4.26 illustrate the yaw rate response and sideslip angle development of the vehicle.

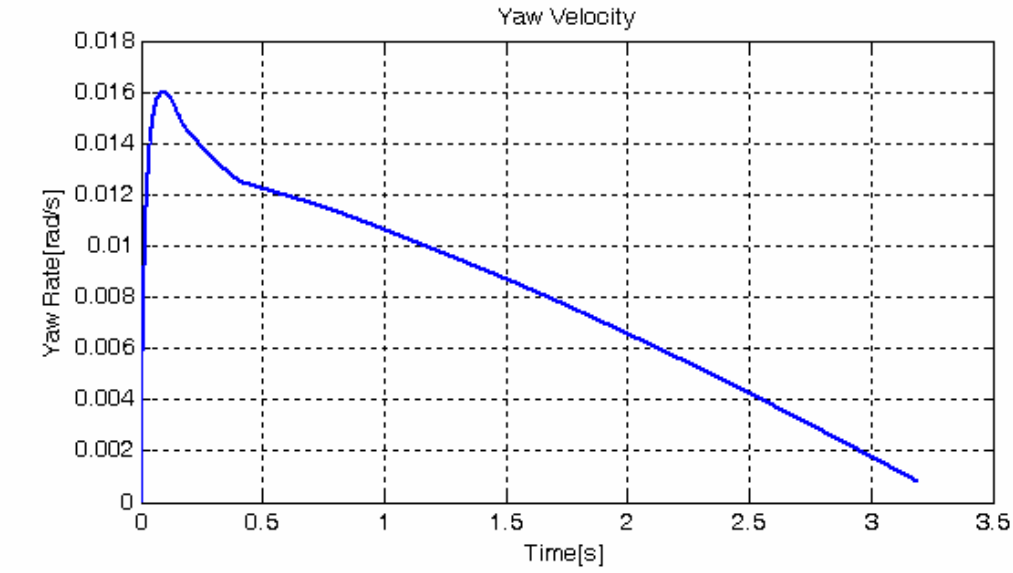

Figure 4.25. Yaw velocity for 40º step steer input and hard braking.

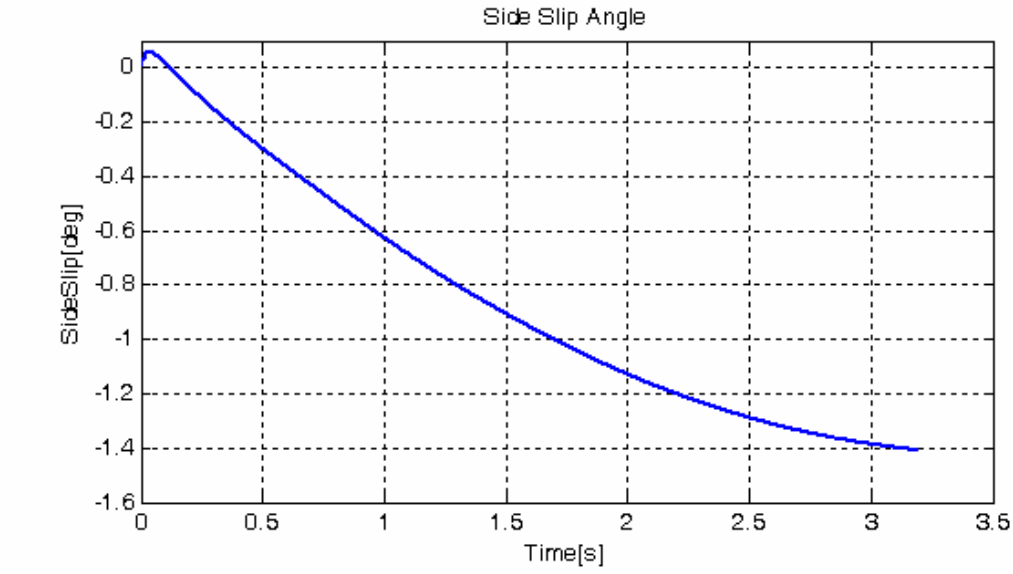

Figure 4.26. Sideslip angle for 40º step steer input and hard braking.

When compared with ‘Case I’, steering response of the vehicle without braking, yaw velocity is observed to attain considerably small values as seen in figure 4.25. Figure 4.26 demonstrates the sideslip angle response of the vehicle. The plot shows that the vehicle was clearly unable to develop the expected sideslip angle and increasing trend of the curve is mainly due to decreasing vehicle speed.

The reason for this poor lateral behavior can be better understood from the response of the vehicle to the j-turn steering input shown in figure 4.7. Results of the simulation are not presented since the vehicle had no lateral response at all and unsurprisingly lateral deviation of the vehicle trajectory was negligible. In the simulation, the j-turn steering input is applied at t =1s, much later than wheels on both axles are locked. In such a case, a vehicle is almost not responsive to steering, and is not expected produce any significant lateral movement. However for the case of step steering input, though the lateral response results were far from the desired level, the vehicle was observed to develop certain yaw rate and sideslip angle because the vehicle began cornering and thus yawing and sideslipping before longitudinal wheel slip values reached 100% slip condition.

4.2. VEHICLE RESPONSE WITH THE CONTROLLER

In this part, performance of the proposed ABS controller was tested and evaluated. The objective of the controller, as expressed in previous chapters, is to retain lateral control of the vehicle under panic braking and if possible, achieve shorter stopping distances. The ABS controller performance will be naturally evaluated from the view of this general objective; however in this effort, it would be proper to approach the controller also as a multi-structure decision unit and assess the contribution of each component separately. The proposed ABS controller basically consists of two sub-controllers: high-level and low-level slip controllers. In this study, independent performance of these sub-controllers will also be discussed in detail.

Simulation study includes straight-line tests and combined braking and cornering maneuvers that simulate emergency driving situations on various road conditions including surface transitions. The results obtained from the uncontrolled vehicle model of the previous section will be reference to the study here. In this part however, in presentation of the results, each case will be explicitly emphasized and examined for different surface conditions since performance and adaptation of the controller for different conditions is essential in any ABS controller study.

4.2.1. CASE I: Straight Line Braking with ABS

A straight-line panic braking maneuver case is studied in this part. It is clear that for this case, driver's aim is to stop the vehicle or reduce the vehicle speed to such a level to avoid a possible accident. In such a situation, naturally, driver expects from a vehicle safety enhancement system to assist in order to achieve the maximum available deceleration; on the other hand, an ABS control system must regulate wheel brake torques to preserve lateral control capability at any instant since the controller can not know the intention of the driver beforehand. It should be underlined that achieving minimum stopping distances is not the primary concern in almost all ABS designs and this study is not an exception. However proposed ABS

controller here is designed to achieve optimal braking efficiency and in this section of the simulation studies, braking performance will be a basic evaluation criterion.

For the simulation, it was assumed that the vehicle was moving at 90 km/h on a level road, when the braking action was initiated. A total braking torque of 6000 Nm was applied to the vehicle, distributed 70:30 between front and rear axles. The case was simulated for three road conditions having even coefficient of friction surfaces of 0.9, 0.5 and 0.2 which simulate namely: dry asphalt, wet asphalt and icy road surfaces.

ABS controller is designed with different low-level slip controller alternatives: fuzzy logic controller and PID controller. Vehicle was simulated for these two cases, and outputs are presented separately. Tracking performance of these sub-controllers will be assessed by comparing the results with the reference slip signal produced by the high-level controller.

4.2.1.1. Dry Asphalt Road Test

Dry asphalt surface provides such a high tire-road traction level that in normal braking conditions, wheel-lock is unlikely. The applied braking torque value of 6000 Nm was selected considering a loaded vehicle on a maximum possible adhesion surface and simulates significantly heavy braking for the chosen vehicle configuration which causes wheel-lock of both front and rear wheels under 0.5 seconds as observed from the results presented in 4.1.2.

Simulation results of the proposed ABS controller for the low-level controller alternatives of fuzzy logic and PID control are presented here sequentially. High level controller structure is the same for the two cases; controller initiation slip threshold values are kept the same for each application.

4.2.1.1.1. Results for Low-Level Fuzzy Logic Controller

Figures from 4.27 to 4.34 present results of the simulation conducted on dry asphalt with the fuzzy logic controller as the low-level controller.

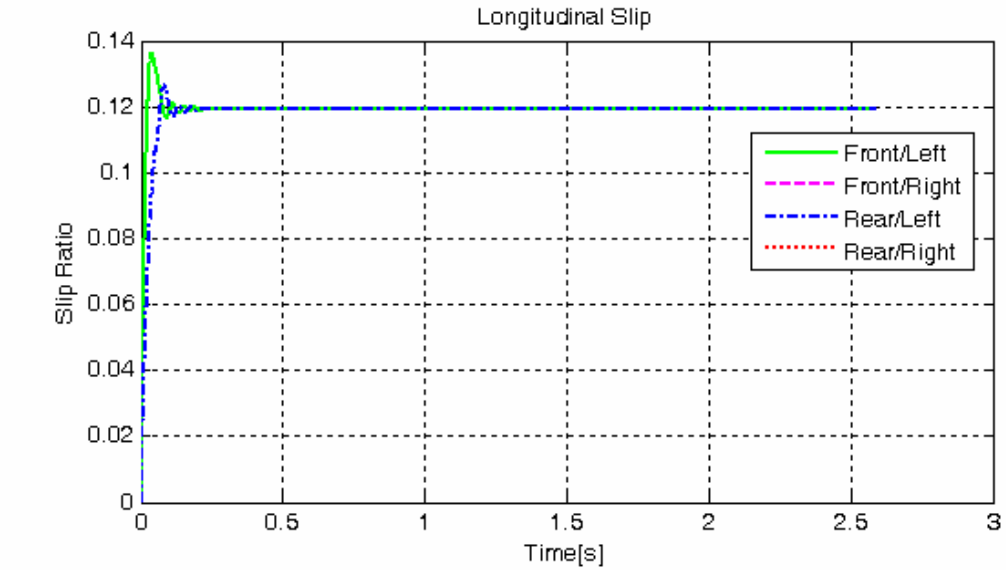

Figure 4.27. Longitudinal wheel slip on dry asphalt road for FLC

Longitudinal slip response values of each wheel can be observed from figure 4.27. Since no steering maneuver is present and ABS initiation slip thresholds are the same for each wheel, right and left tires of each axle attain identical longitudinal slip ratios. ABS controller successfully intervened in time. Wheel slips reach the steady state value of 0.12 very rapidly, after a small overshoot. Definitely the performance of the controller can be more accurately assessed, when the longitudinal slip values are examined together with the reference slip signal information. Figures 4.28 and 4.29 show the superimposed plots of reference signals and longitudinal slip responses of the front/left and rear/left wheels. The low-level fuzzy logic controller tracks the reference slip signals successfully, with only very limited damped cycling. ABS initializes for front/left wheel at t = 0.01 s when corresponding longitudinal slip reaches 0.075. High-level controller outputs 0.1 slip as reference from initialization, until wheel angular acceleration drops below 50 rad/s^2.

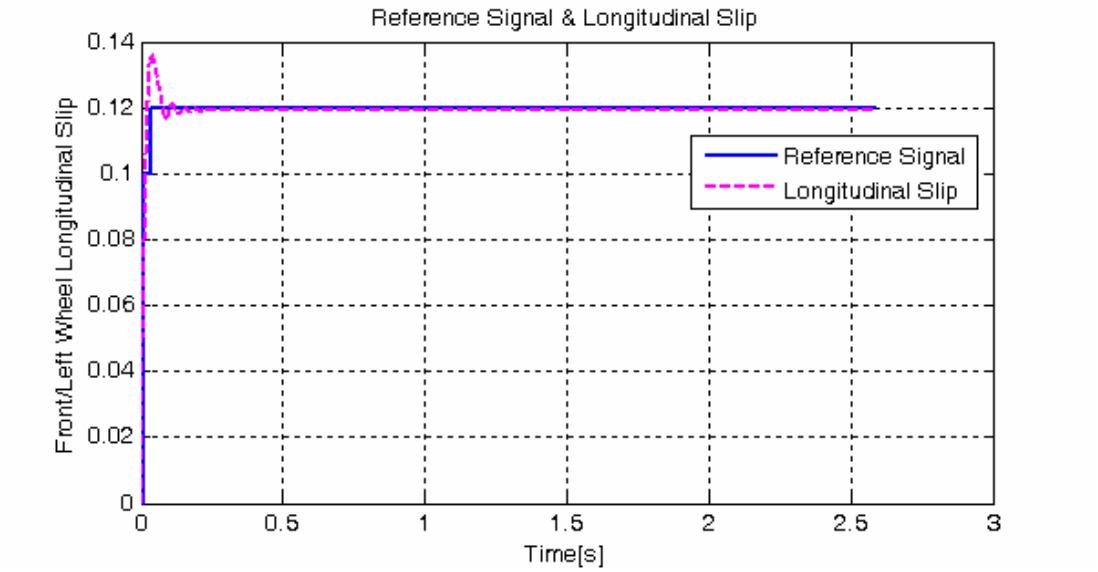

Figure 4.28. Reference slip signal for front/left wheel on dry asphalt for FLC

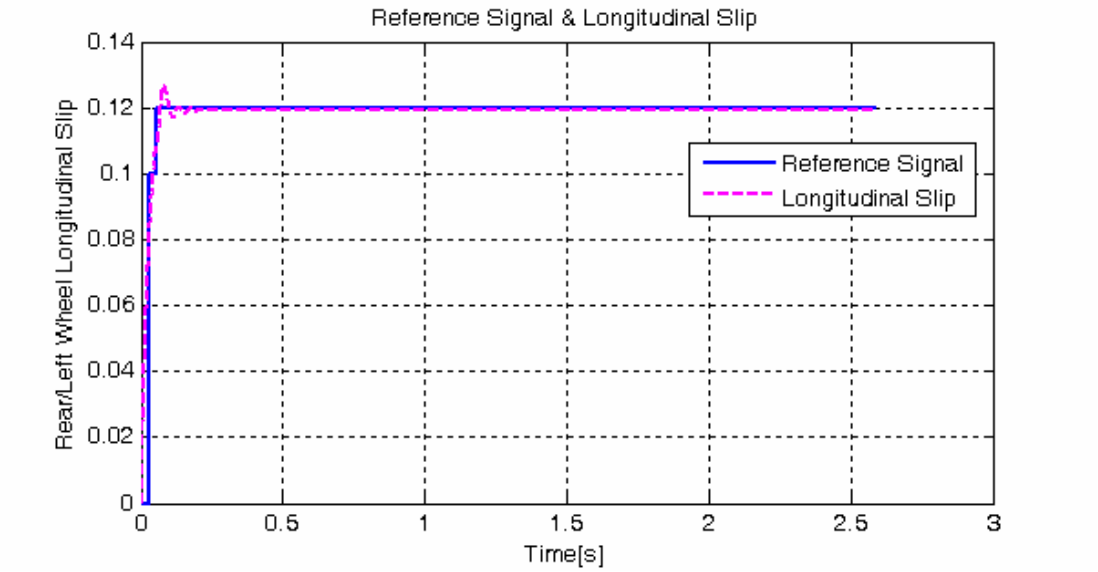

Figure 4.29. Reference slip signal for rear/left wheel on dry asphalt for FLC

Figures 4.30 and 4.31 present wheel angular velocity and angular acceleration response plots. Angular accelerations of both axle wheels, as plotted in figure 4.31, reach steady-state around -26.7 rad/s^2, following minimal damped oscillations.

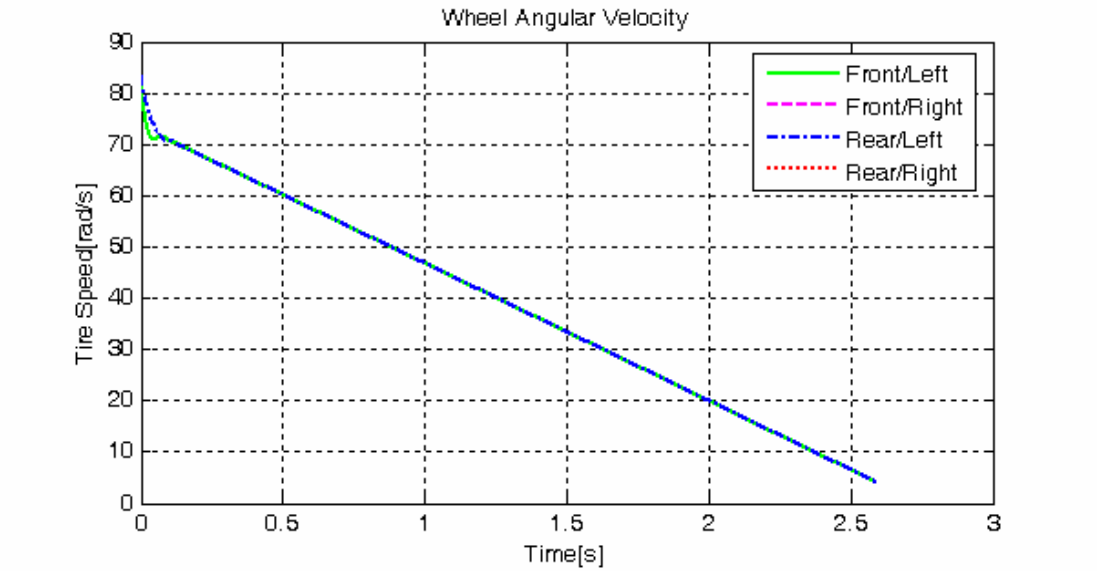

Figure 4.30. Wheel angular velocities for dry asphalt and FLC

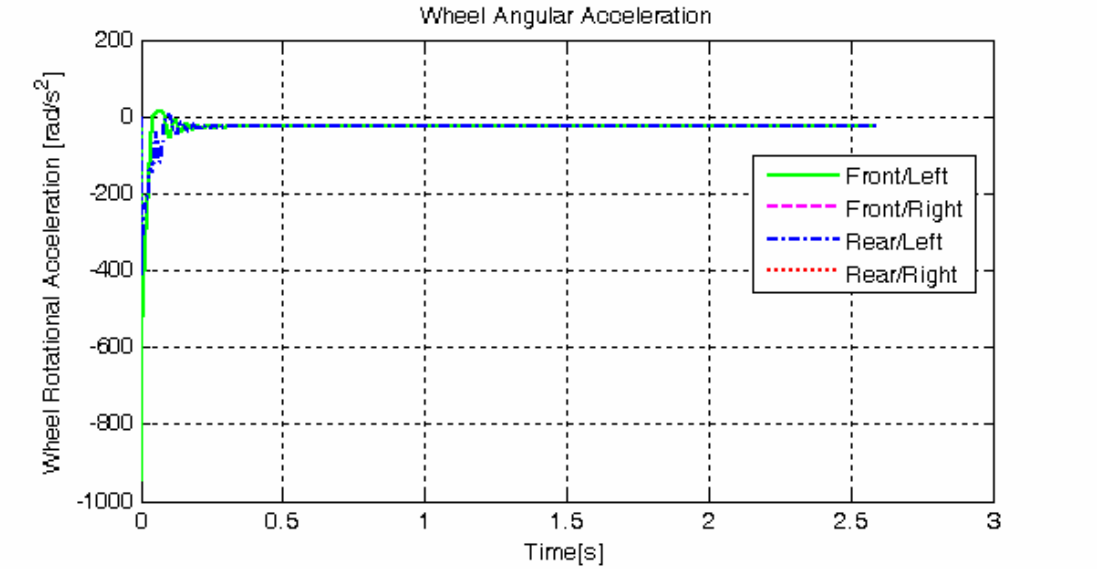

Figure 4.31. Wheel angular accelerations for dry asphalt and FLC

As observed from the graph plotted in figure 4.31, wheel angular deceleration reaches extremely high values instantaneously, at the time the brakes are applied. With the initialization of the ABS, fuzzy logic controller begins to decrease braking torque very quickly due to this elevated angular deceleration level, even though the

longitudinal slip does not even reach the peak point of the μ-slip curve. Steady state values of braking torque are 1347 Nm for front and 546 Nm for rear axle wheels as shown in figure 4.32. Note that the braking torque distribution ratio is close to the initial proportioning of the applied brake moments.

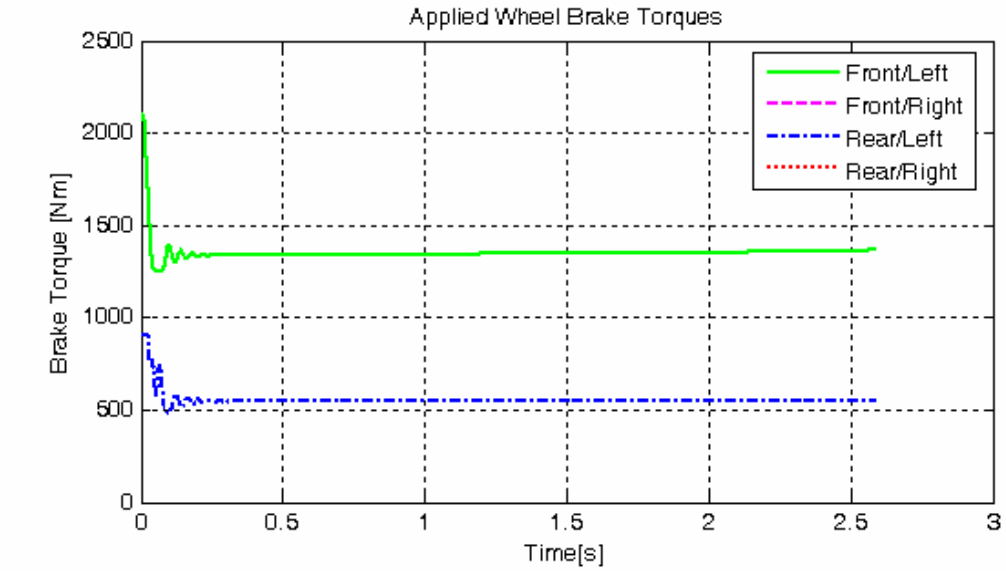

Figure 4.32. Wheel braking torques for dry asphalt and FLC

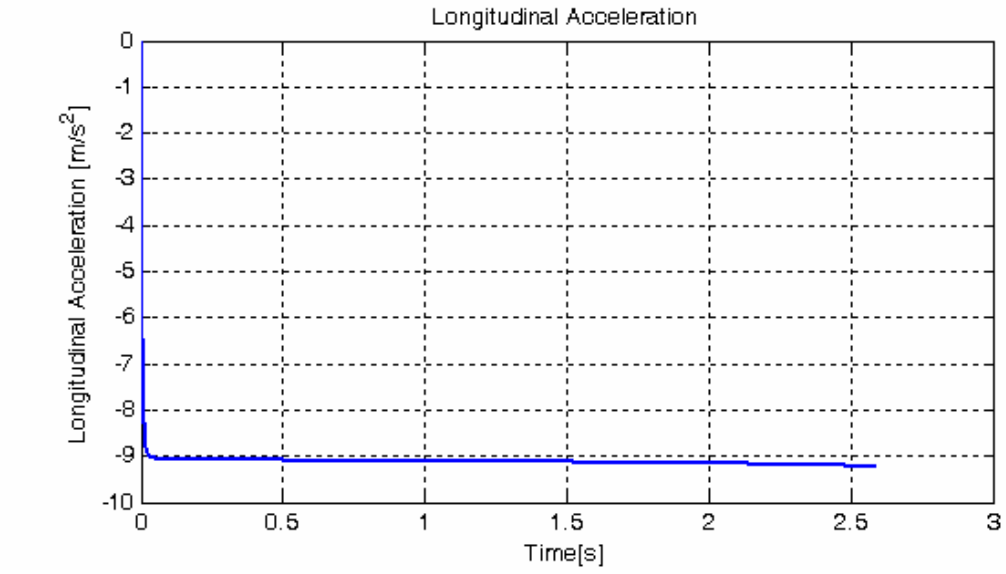

Figure 4.33. Longitudinal acceleration response for dry asphalt and FLC

With the ABS controller activated, vehicle showed a successful braking performance as shown in figure 4.33. Vehicle deceleration was around 9.1 m/s^2 throughout the simulation. Stopping distance was recorded as 34.33 m, which indicates a braking distance improvement over 8 meters compared with the uncontrolled case. Fuzzy reference slip decision logic was designed to set reference slip values that are close to the peak of the μ-slip curve when no steering input is present. This indicates that with a successful tracking performance of the low-level controller, vehicle is expected to achieve minimum stopping distance.

Figure 4.34 illustrates the results of a simulation study conducted to assess the performance of the high-level controller in braking distance improvement. In the study, vehicle was simulated for different fixed reference slip values ranging from 0.05 to 0.25. Unsurprisingly, the locus of points formed from the results of the simulations was found out to be very similar to the μ-slip curve.

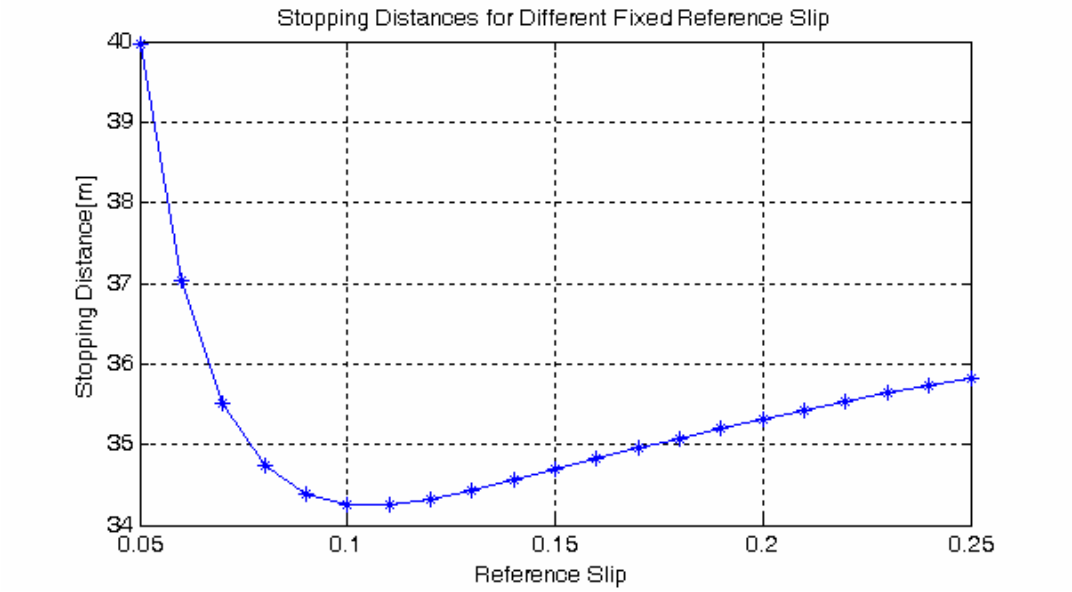

Figure 4.34. Stopping distances for different fixed reference slip values for dry road

As mentioned before, for the reference signal of the proposed high-level controller with surface condition estimator, stopping distance was 34.33 m. Note that, this value is clearly close to the minimum of the curve presented in figure 4.34.

4.2.1.1.2. Results for Low-Level PID Controller

The simulation was conducted again for a controller design incorporating a PID low-level slip controller. Figures from 4.35 to 4.41 are the results for dry asphalt test.

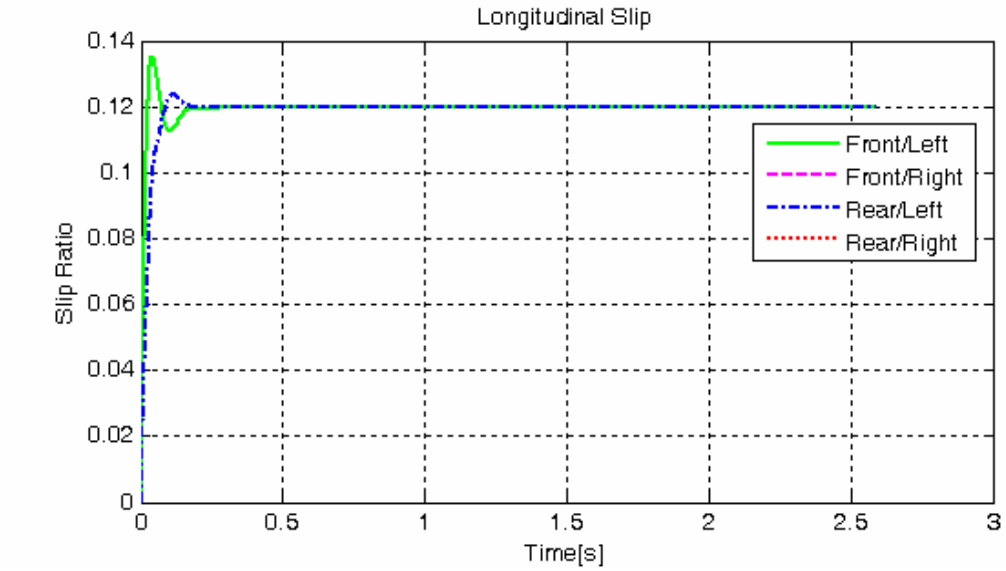

Figure 4.35. Longitudinal wheel slip on dry asphalt for PID

Figure 4.35 shows the longitudinal slip developed at the wheels. The controller was observed to have a successful performance. Overshoot was negligible and the steady-state longitudinal slip was 0.12, the same as in the fuzzy sub-controller case. It should be noted that the response curves showed almost no oscillations, a result which was clearly due to the influence of the weighted derivative action in the design of the PID controller. Response character will be definitely more obvious in the simulation tests conducted on adverse road conditions. Longitudinal slip response curves of the front and rear wheels are illustrated again separately but with reference signals in figures 4.36 and 4.37 for a better judgment of controller performance.

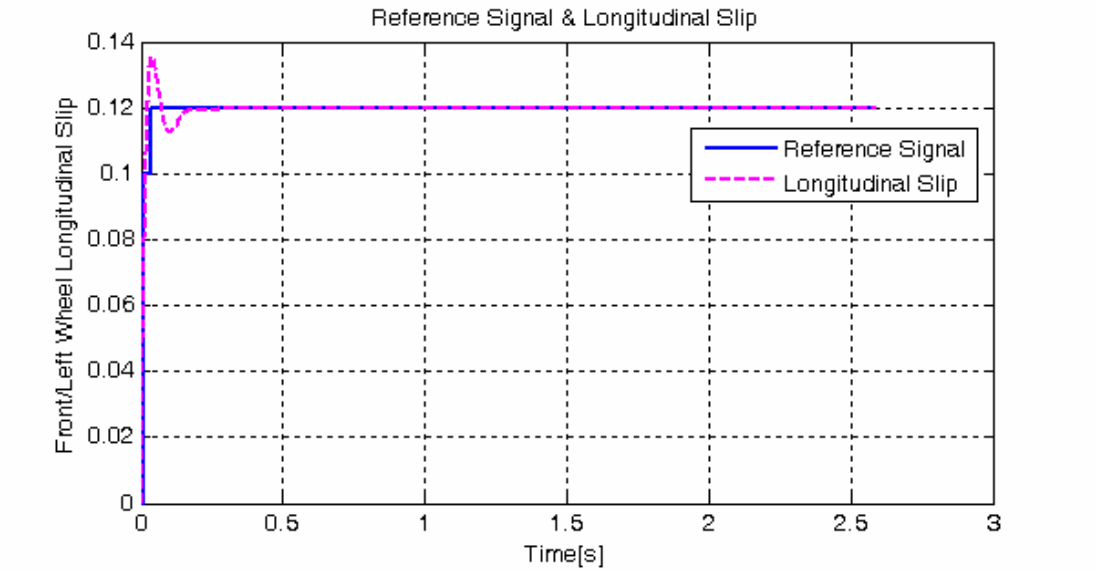

Figure 4.36. Reference slip signal for front/left wheel on dry asphalt for PID

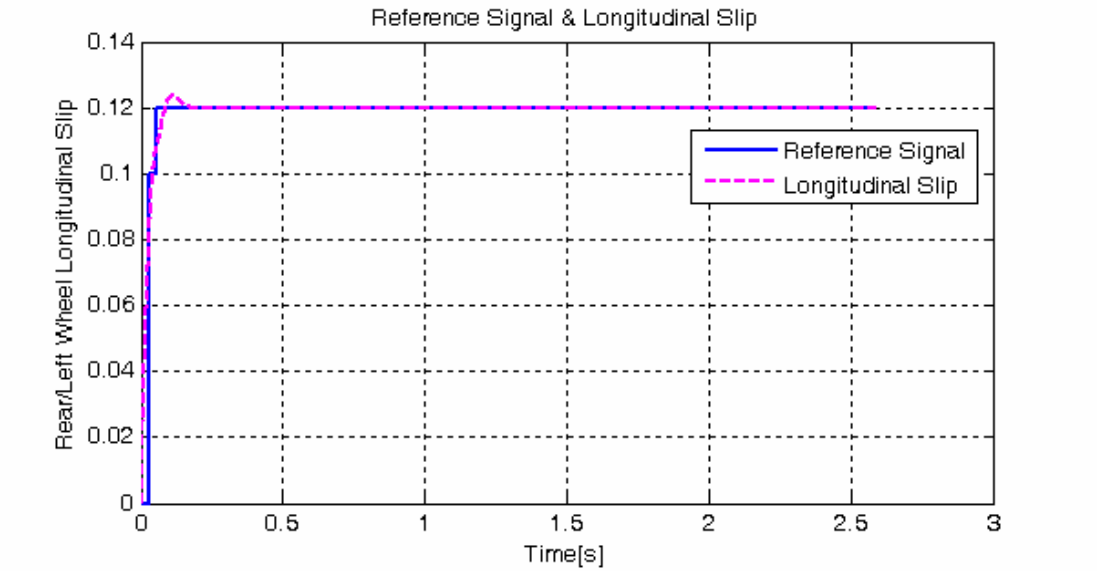

Figure 4.37. Reference slip signal for rear/left wheel on dry asphalt for PID

Figures 4.38 and 4.39 show angular velocity and acceleration plots of the four wheels. The angular velocity response curve presents information parallel to the longitudinal slip plot. Angular accelerations of the wheels of the two axles reach steady state at the same time and unlike the FLC case showed no oscillations.

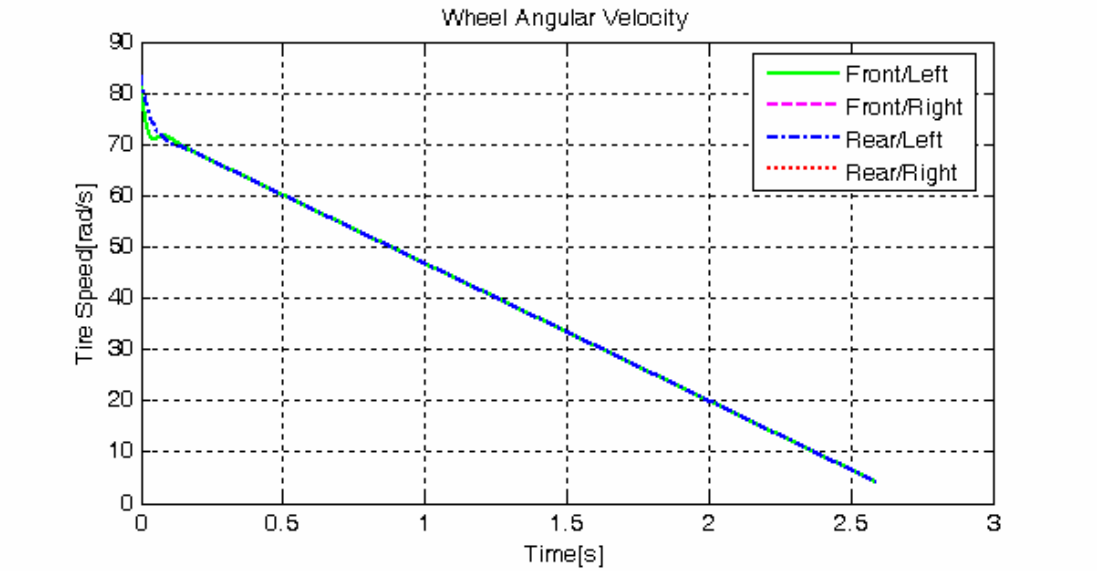

Figure 4.38. Wheel angular velocities for dry asphalt and PID

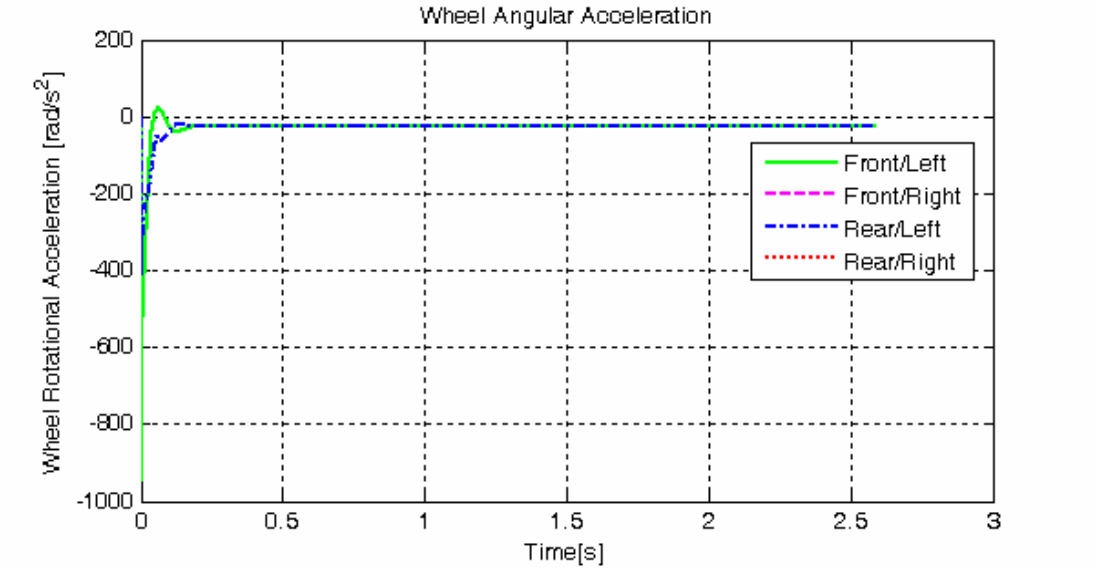

Figure 4.39. Wheel angular accelerations for dry asphalt and PID

Figure 4.40 illustrates the resulting wheel braking torques at four wheels. As expected, the steady-state values are almost the same as in the case of fuzzy controller and pattern resembles angular acceleration response.

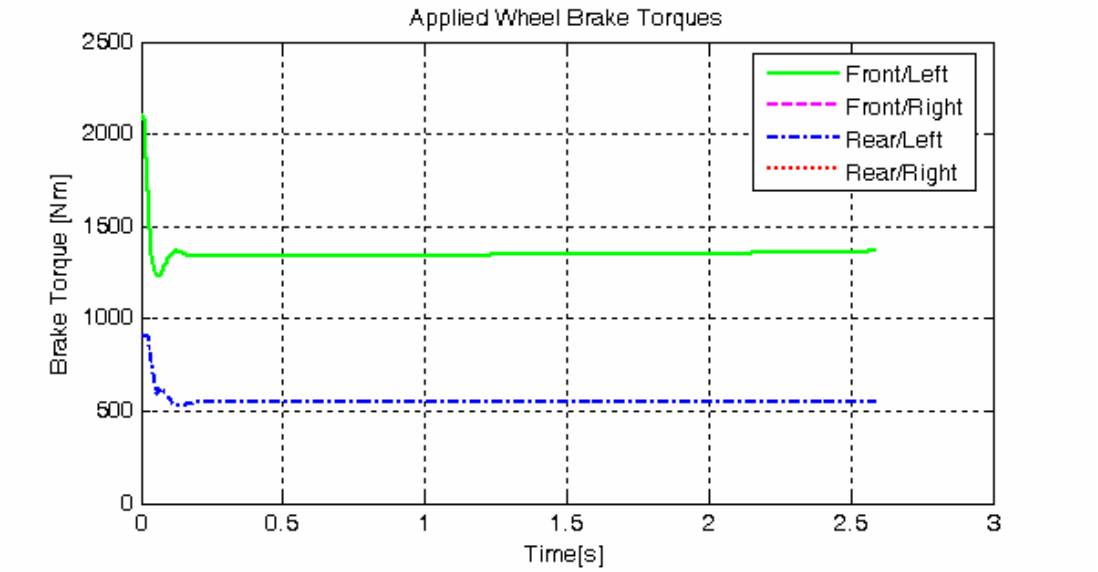

Figure 4.40. Wheel braking torques for dry asphalt and PID

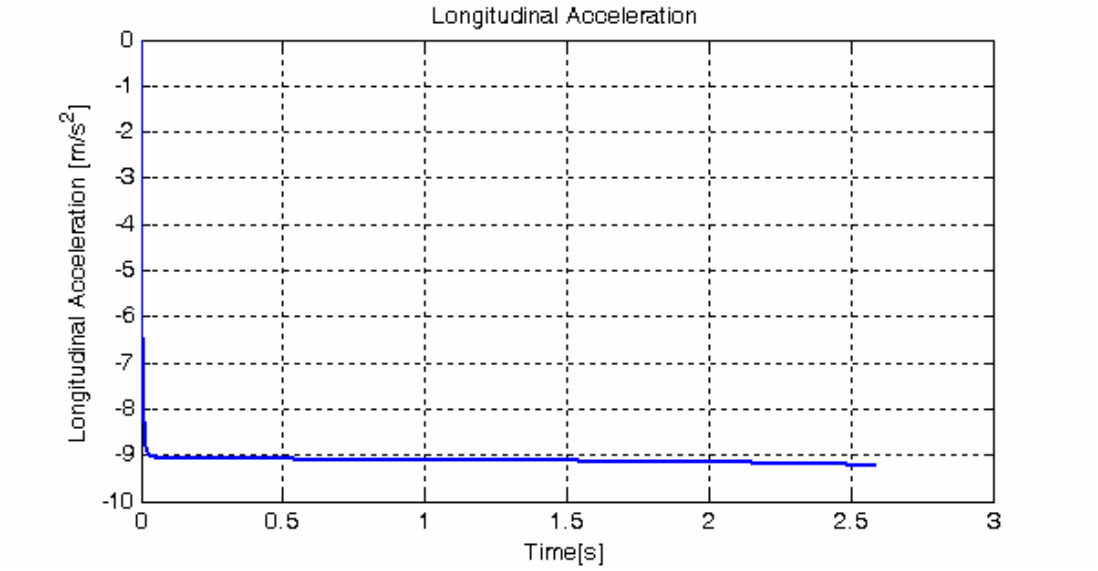

Figure 4.41. Longitudinal acceleration for dry asphalt and PID

Vehicle longitudinal deceleration is shown in figure 4.41. The plot is almost identical to the longitudinal acceleration response depicted in figure 4.33 and naturally, braking performance and the recorded stopping distance is not different than the results found for the fuzzy logic controller case.

4.2.1.2. Wet Asphalt Road Test

Simulations conducted on wet road surface are important in that it is very likely for any driver to come across such a situation in every-day driving and it is possible to examine and assess the response pattern of the controller more clearly in such a condition. As will be seen in results presented in this part, the ABS controller is very successful in preventing the impending lock and maintaining braking torques to track the reference signal for the both choices of low-level controllers. Considering that the most discussions and observations made in the previous part are also valid for this case, the presentation of the results will be put in a briefer form.

4.2.1.2.1. Results for Low-Level Fuzzy Logic Controller

Figures from 4.42 to 4.46 show the results of the ABS controller with the fuzzy logic based low-level controller.

Figure 4.42 presents the longitudinal slips developed at four wheels. The slip ratio at front wheels is observed to make a very sharp increase, reaching over 29% slip, however rapidly returns to the steady-state condition with a small cycling pattern. Comparably at rear wheels, controller had no difficulty as expected, since due to decreased braking deceleration rate, rear wheels, unlike front axle wheels, had more than enough tire loading to cope with the distributed initial braking torque.

The reference signal for the front wheels dispatched by the high level controller can be examined in figure 4.43. After the initiation stage with 10% slip reference output, reference signal takes on the steady-state slip value of 0.07. Reference signal for rear axle wheels is similar and is not presented here.

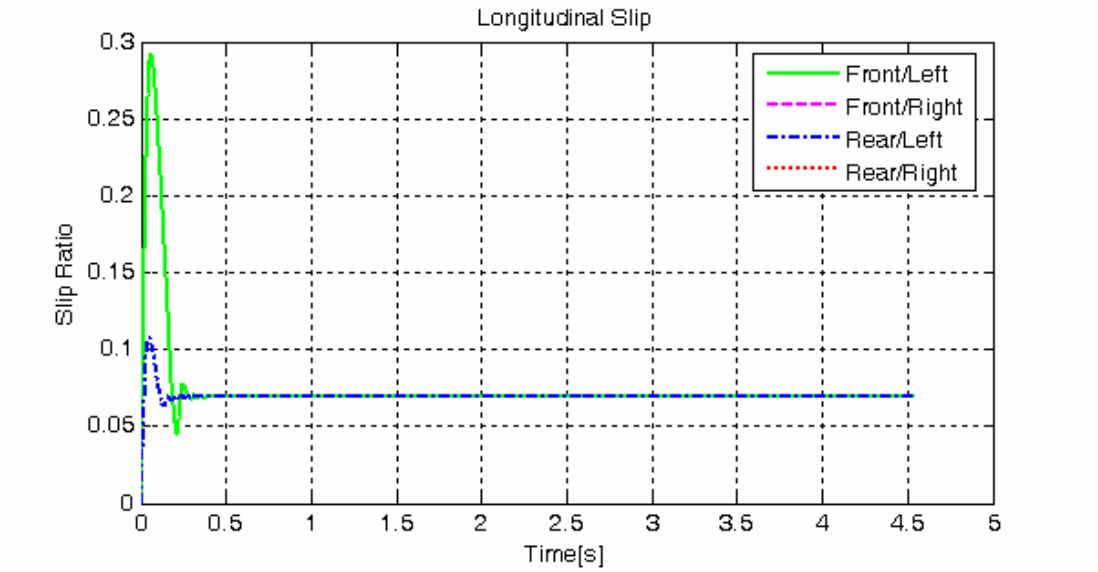

Figure 4.42. Longitudinal wheel slip on wet asphalt for FLC

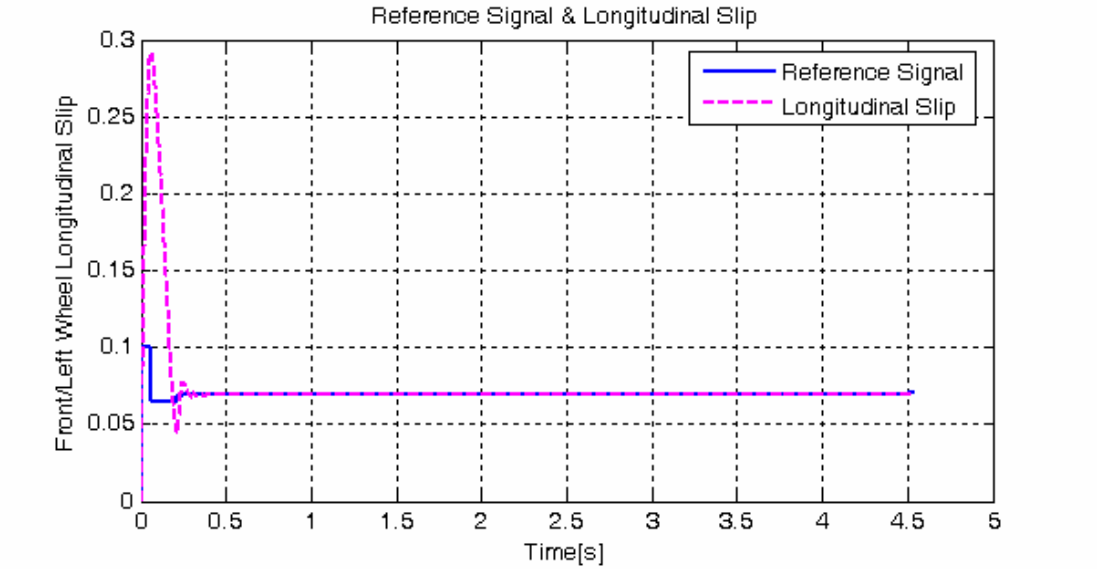

Figure 4.43. Reference slip signal for front/left wheel on wet asphalt for FLC

Figure 4.44 shows the regulation of wheel braking torques due to controller action during the simulation. ABS controllers for each wheel, following initiation, individually tries to decrease the brake torques at the maximum rate possible. Low-

level fuzzy logic controllers evaluate the situation with the wheel rotational acceleration signal and according to this information; they begin to increase the torques. Following a short oscillatory transient response, steady-state is reached.

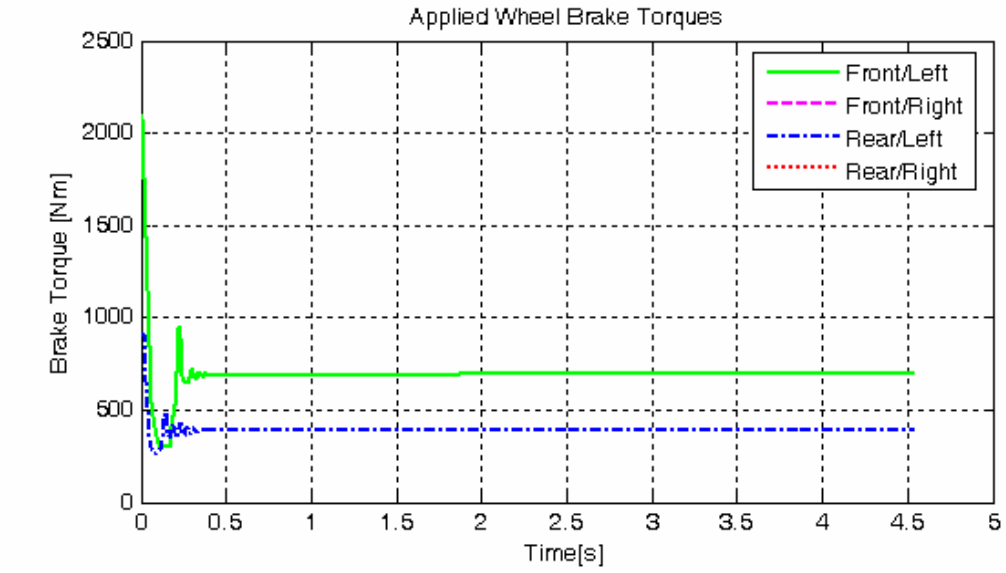

Figure 4.44. Wheel braking torques for wet asphalt and FLC

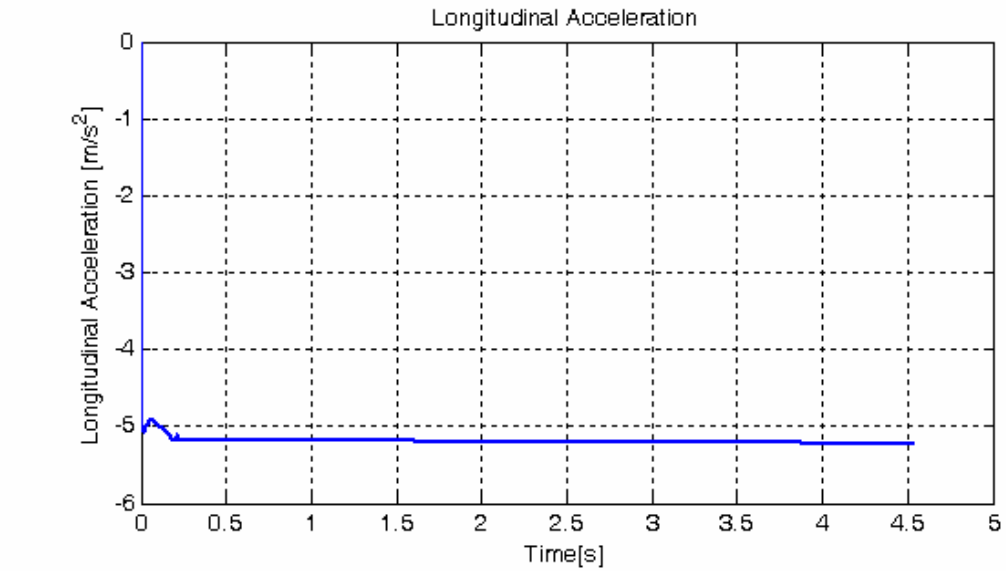

Figure 4.45. Longitudinal acceleration for wet asphalt and FLC

Figure 4.45 illustrates the braking performance of the vehicle. Longitudinal deceleration is about 5.2 m/s^2 during the simulation. Stopping distance was recorded as 60.18 meters which means 17 meters braking distance improvement compared with the uncontrolled case. Simulation with different fixed reference slip values show that the high-level controller and thus, the surface condition estimation was successful in determining the reference slip ratio that provides the maximum braking performance. Figure 4.46 presents the corresponding result. What is not presented here is the successful tracking performance of the controller for each fixed reference signal in the test.

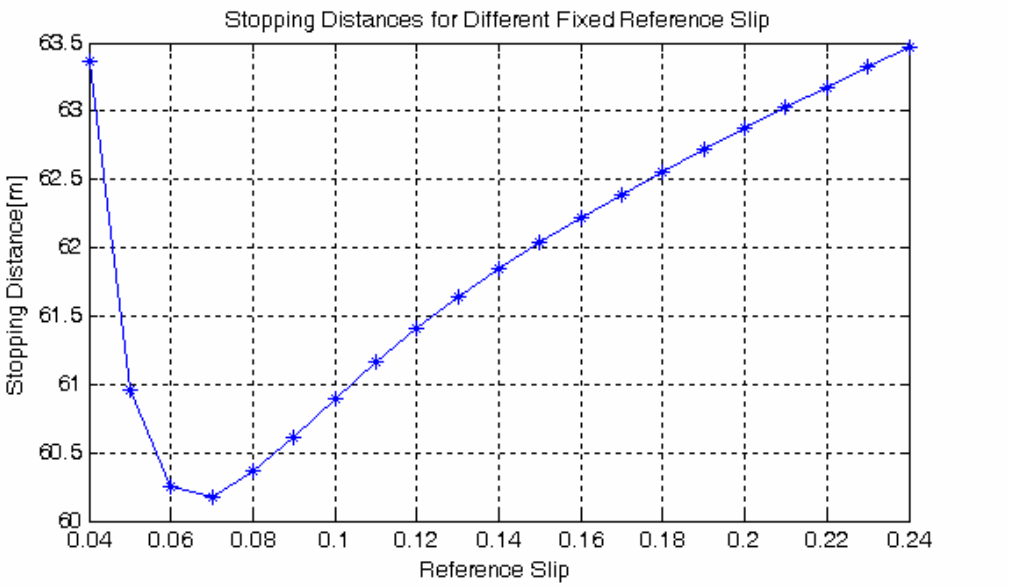

Figure 4.46. Stopping distances for different fixed reference slip values for wet road

4.2.1.2.2. Results for Low-Level PID Controller

ABS controller performance for the low-level PID controller case can be assessed with the help of the figures 4.47 and 4.48 presented as the result of the simulation study.

Figure 4.47 shows the developed longitudinal slips due to braking action. The maximum overshoot of the front wheels is around 0.285 slip, which is slightly better

than the result for the fuzzy logic controller. General trend of the response is however similar for all wheels. It should be noted that the small deviations observed following the initial overshoots in the slip response curves of front and rear axle wheels could be eliminated by decreasing the weight of integrator constant in the design of the PID controller; however the contribution of the integrator term to the steady state performance should not be forgotten. The influence of PID controller design choices to the overall performance will be more obvious in the series of simulation tests for icy road and transitory road surfaces.

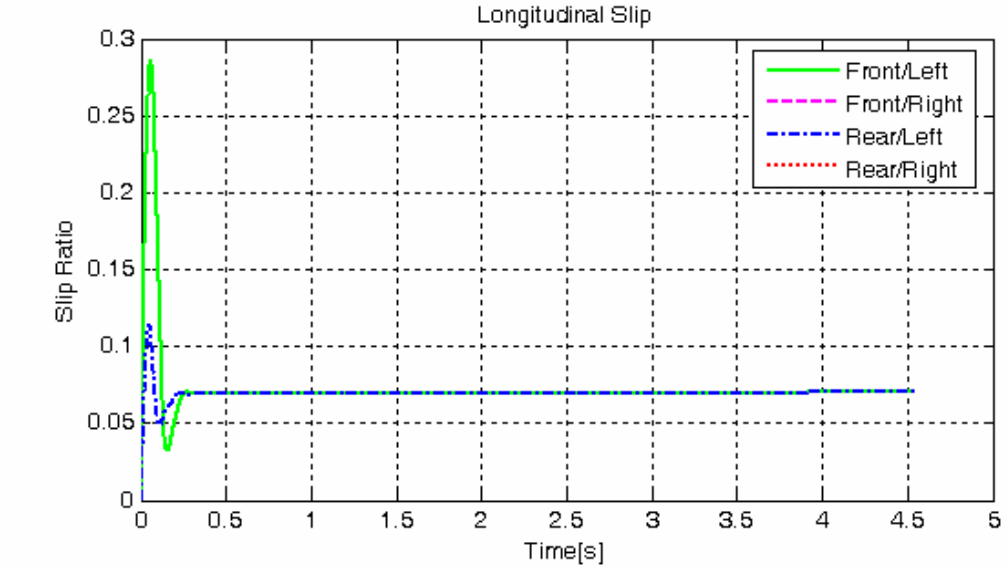

Figure 4.47. Longitudinal wheel slip on wet asphalt road for PID

Figure 4.48 presents the braking torques acting at the wheels during the simulation. The result is in accordance with the longitudinal slip response. Oscillations are not observed unlike the simulation results for the fuzzy logic controller equipped ABS. As expected, the steady-state torque values are found to be approximately same.

Similar longitudinal slip development of the PID controlled system, unsurprisingly, caused a braking performance very similar to the result of the ABS controller with low-level fuzzy logic controller presented in the previous section. The stopping distance was 60.20 meters which is very close to the result of the FLC. Longitudinal

acceleration response plot was almost the same as in the figure 4.45; therefore it is not presented here.

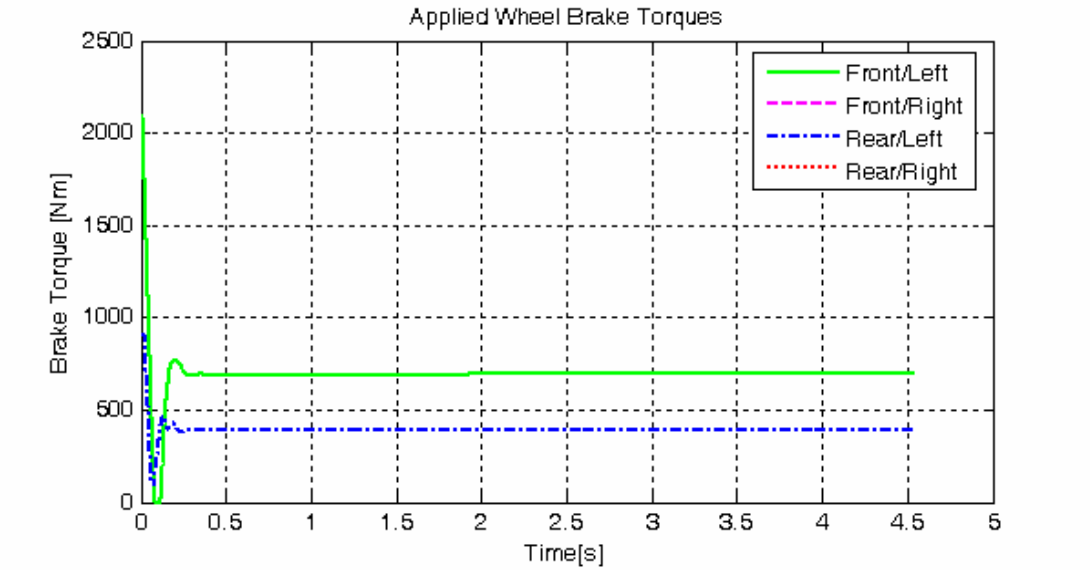

Figure 4.48. Wheel braking torques for wet asphalt for PID

4.2.1.3. Icy Road Test

Compared with the previous road conditions, without doubt, the emulated icy road surface is the most challenging for any ABS algorithm. Due to low coefficient of friction, even a small increase in braking torque may cause a rapid raise of slippage at the corresponding wheel that can be difficult for the controller to compensate. The simulation tests conducted for 0.2 coefficient of friction level constituted an essential part in the design procedure of the ABS controller. The low-level controllers were required to utilize the controller potential effectively to prevent the impending wheel-lock and at the same time provide a satisfactory tracking performance. The high-level controller was expected to set a reference signal that would aim maximum braking performance and take account of the possible tracking errors of the low-level controllers. The initial velocity of the vehicle was reduced to 50 km/h for these simulation tests just as in the previous icy road simulations.

4.2.1.3.1. Results for Low-Level Fuzzy Logic Controller

The performance can be evaluated with the help of figures from 4.49 to 4.54. Figure 4.49 presents longitudinal slip responses of all four wheels. It is observed that longitudinal slip ratio of the front axle wheels increased very rapidly, reaching approximately 72% slippage in 0.07 seconds, which is definitely undesirable; however the controller successfully managed to recover quickly and tracked the reference slip signal which is also presented in figure 4.50.

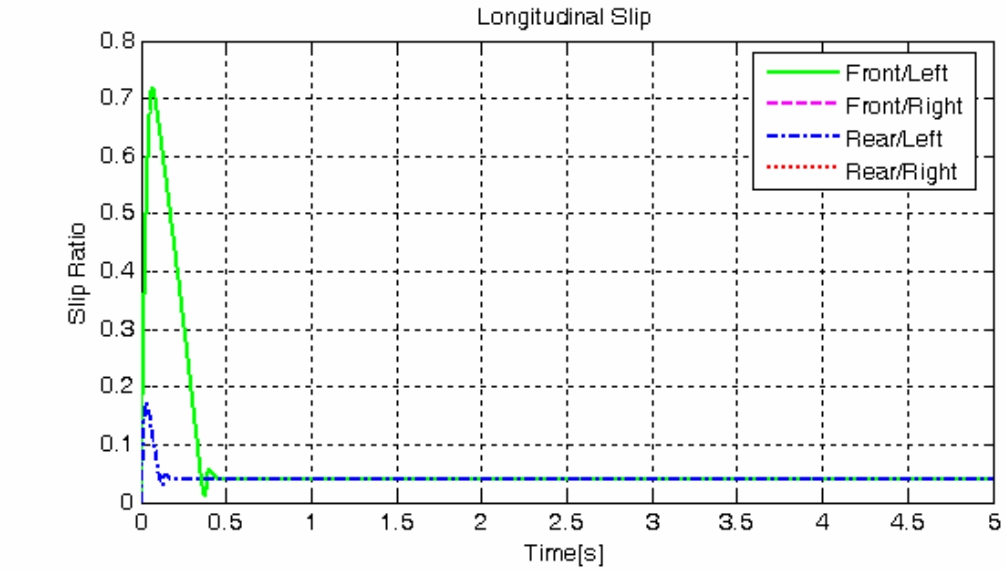

Figure 4.49. Longitudinal wheel slip on icy road for FLC

The elevated slippage at the front axle wheels was actually an expected result due to the limitation of the controller force. The situation will be more clearly understood when evaluated by observing regulation of the brake torques shown in figure 4.51 and the performance of the low-level PID controller in the next part of the study.

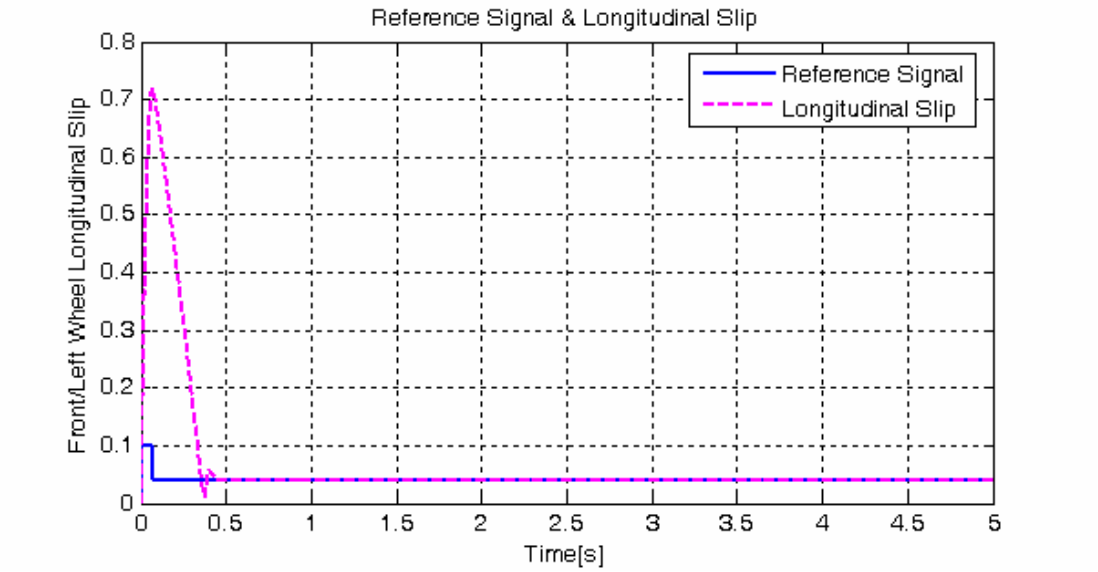

Figure 4.50. Reference slip signal for front/left wheel on icy road for FLC

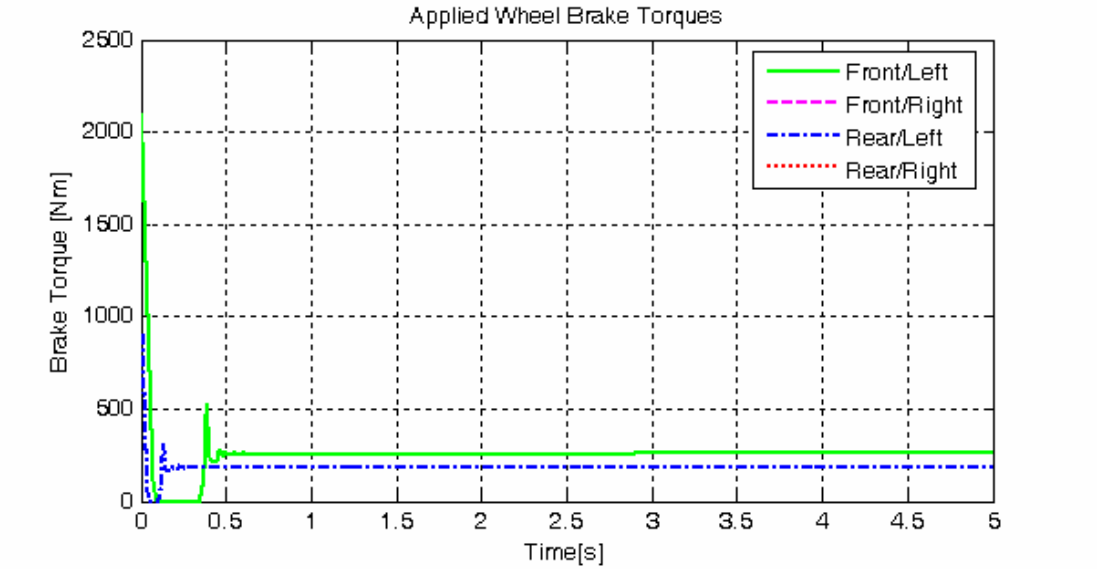

Figure 4.51. Wheel braking torques for icy road and FLC

As seen in figure 4.51, with initiation of ABS, wheel braking torques were very rapidly reduced to the point of zero and hold at that level until the slippage at the corresponding wheel dropped below the reference slip. The steady state values of the braking torques are respectively 256 Nm and 182 Nm for front and rear axle wheels.

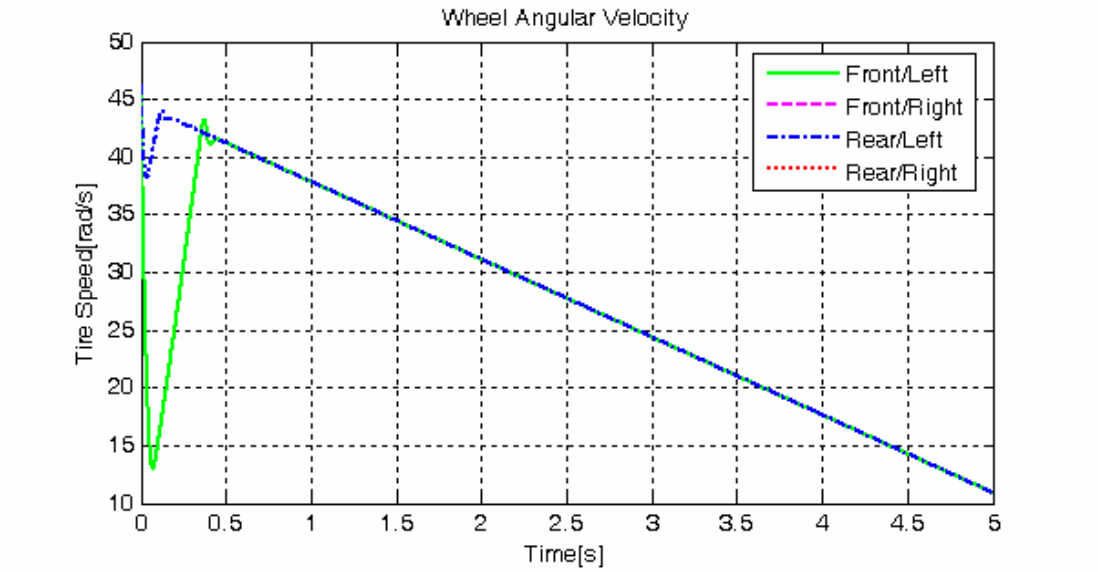

Figure 4.52. Wheel angular velocities for icy road and FLC

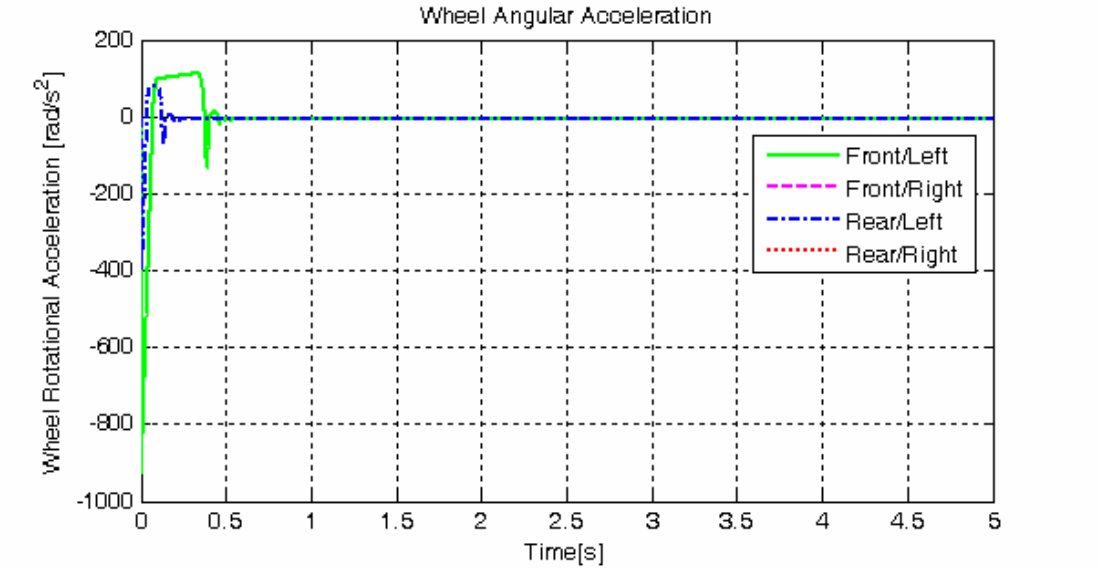

Figure 4.53. Wheel angular accelerations for icy road and FLC

Angular velocities and angular accelerations of the wheels are presented in figures 4.52 and 4.53. Angular velocity response curve is in accordance with the longitudinal slip plot. Angular accelerations of the wheels of the both axle increased to a certain level in parallel with the decrease of the braking torques and kept constant for a time.

When slips were lowered to a level close to the reference signal, accelerations of the wheels began to decrease sharply with the intervention of the controller.

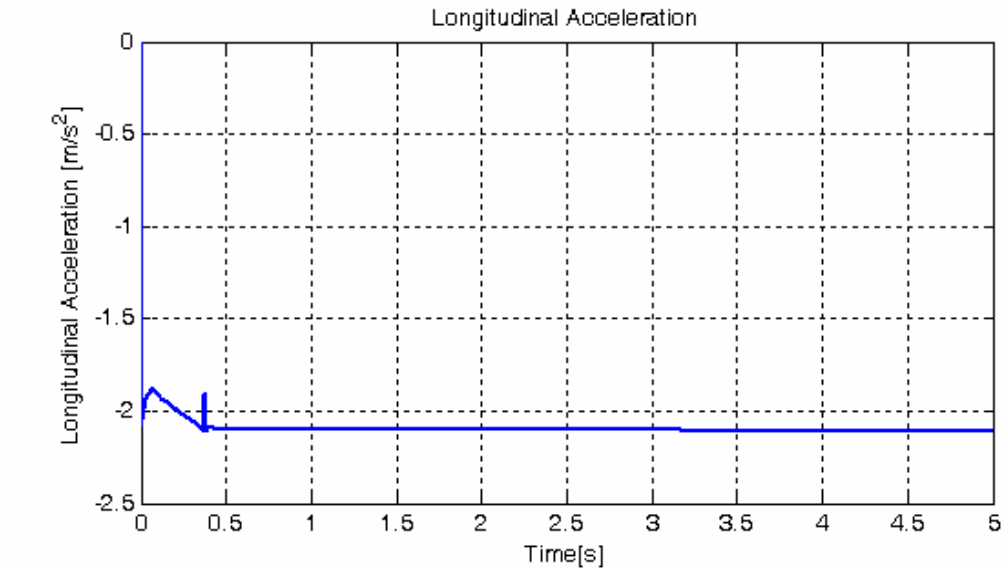

Figure 4.54. Longitudinal acceleration for icy road and FLC

Figure 4.54 shows vehicle deceleration performance. Average vehicle longitudinal deceleration was around 2.1 m/s^2. The deviations observed at about t = 0.07 and 0.38 seconds is in parallel with the overshoots in the longitudinal slip response of front axle wheels. Note that the deviation in the acceleration was not reflected to the reference slip signal of front wheels presented in figure 4.50 for two reasons: elevated wheel acceleration and reference slip saturation. Vehicle stopping distance was recorded as 45.68 meters which means 11 meters braking distance improvement.

4.2.1.3.2. Results for Low-Level PID Controller

Figures from 4.55 to 4.59 present the results of the simulation test conducted on emulated icy road surface. The performance of the ABS with low-level PID controller was similar to the fuzzy controller equipped system.

Figure 4.55 illustrates the longitudinal slip development at wheels. The maximum overshoot of the front axle wheels was found to be approximately 0.69 which is a slight improvement compared to the case of low-level fuzzy controller. It was observed that PID controlled system achieved slightly better results for the initial overshoot of the longitudinal slip for all three road condition cases presented. The reason is mainly due to the design and characteristics of the controllers however it should also be noted that the PID controller output is saturated while the fuzzy logic controller was designed to be between braking torque rate limits.

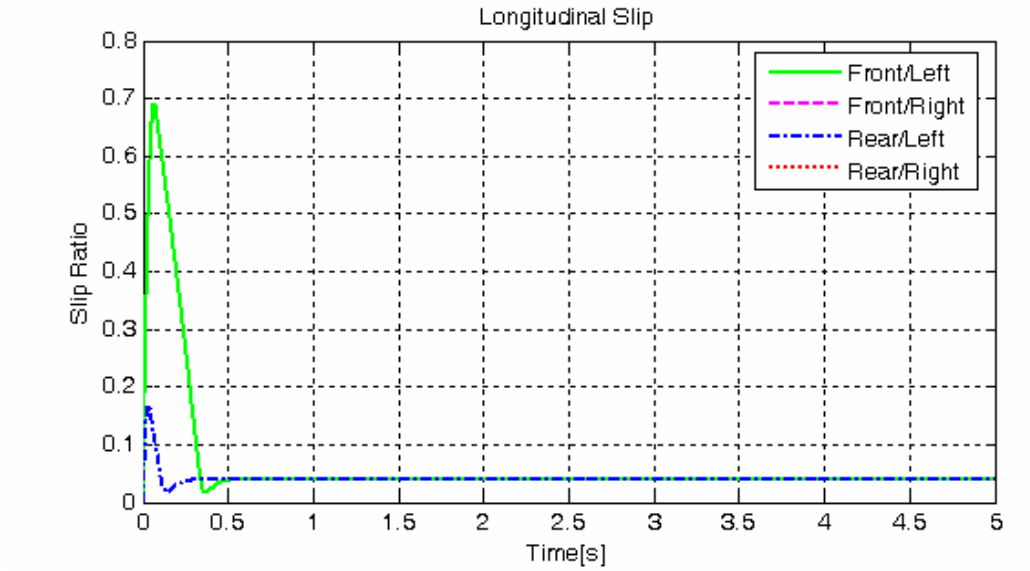

Figure 4.55. Longitudinal wheel slip on icy road for PID

Reference slip signals for both front and rear axle wheels are almost identical to the plot presented in figure 4.50, therefore are not presented here. Wheel angular velocity and angular acceleration response plots are provided in figures 4.56 and 4.57.

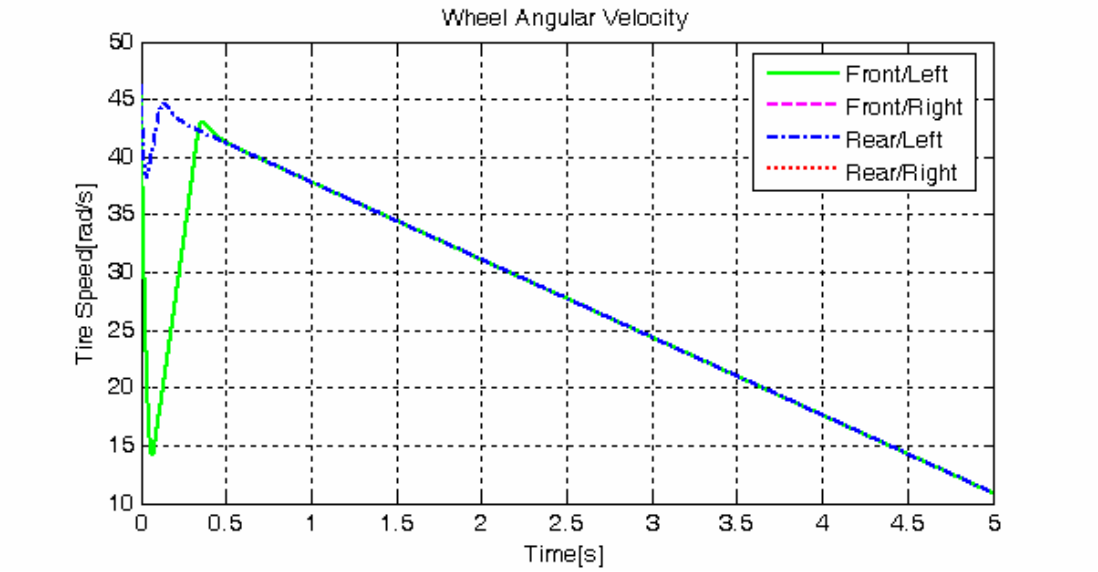

Figure 4.56. Wheel angular velocities for icy road and PID

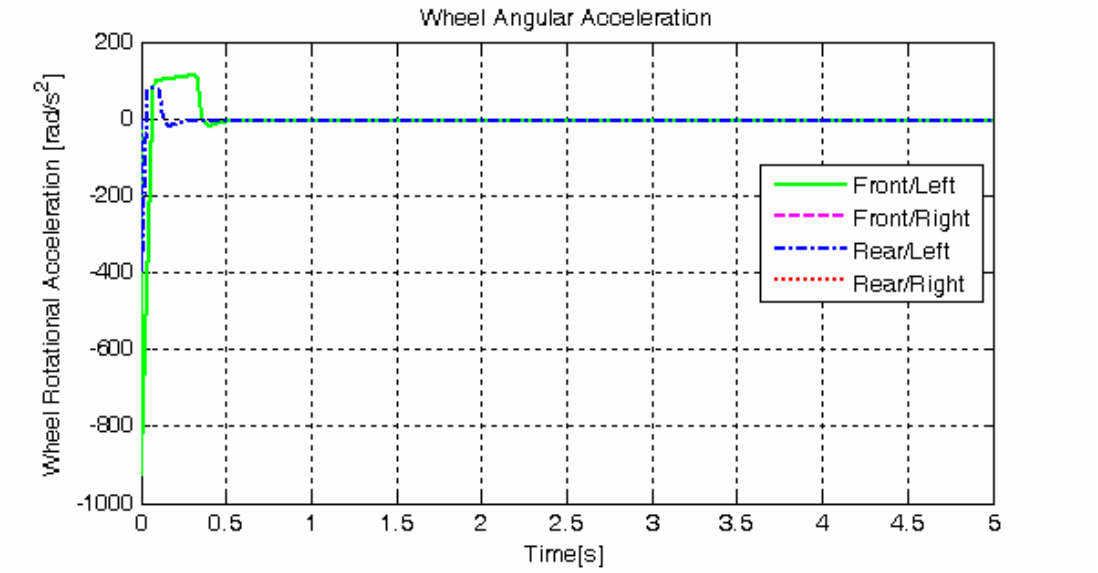

Figure 4.57. Wheel angular accelerations for icy road and PID

Figures 4.58 and 4.59 present respectively, braking torque regulation and vehicle longitudinal deceleration performance. General trend of brake torque development was similar to the fuzzy controlled system; however low-level PID controller showed almost no oscillations and inconsiderable overshoot compared to FLC.

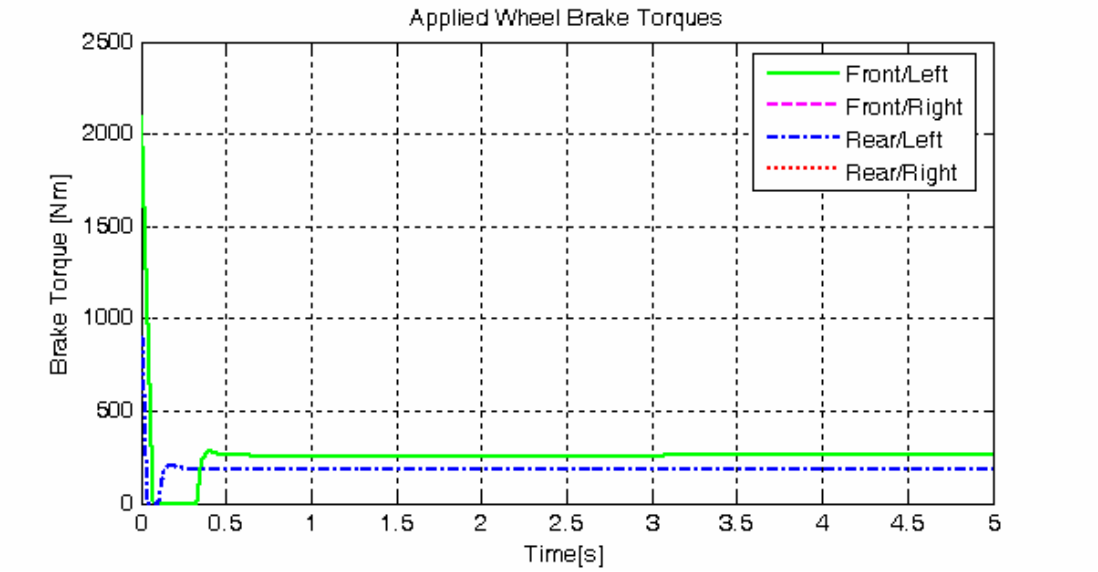

Figure 4.58. Wheel braking torques for icy road and PID

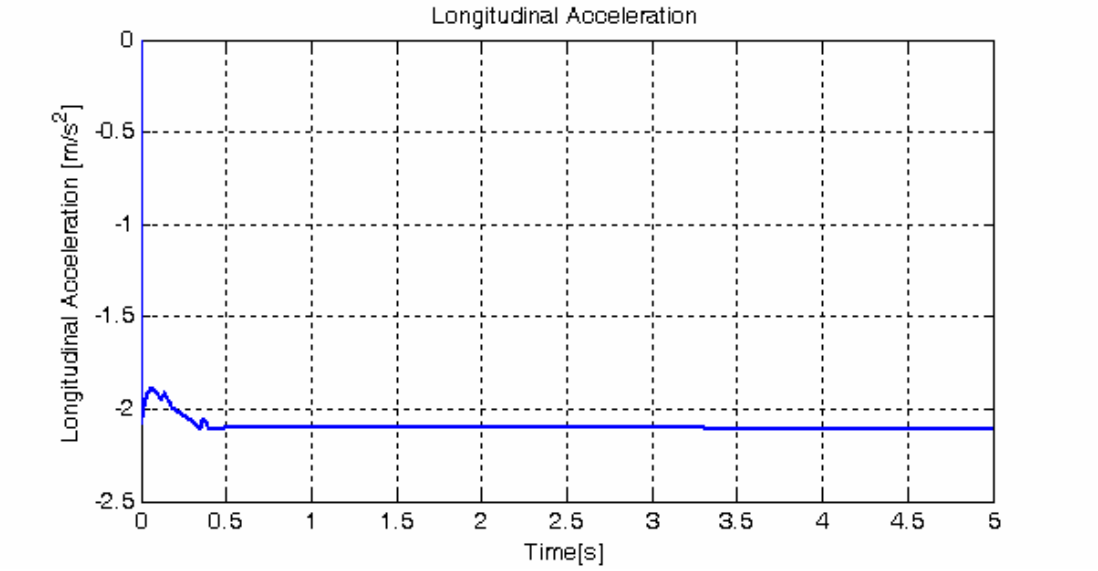

Figure 4.59. Longitudinal acceleration for icy road and PID

Vehicle longitudinal deceleration was around 2.1 m/s^2 throughout the simulation as in the fuzzy controller case and the stopping distance was 45.66.

4.2.1.4. Road Transitions Test

In this part, simulations are conducted for a road condition that has surface friction transitions. In many related studies in literature, such tests are applied to evaluate the reliability and adaptability of the ABS controller. The case is actually very challenging for the controller. High performance is demanded for the surface identifier logic and the low-level controller to achieve the objectives stated previously in this text for the ABS controller.

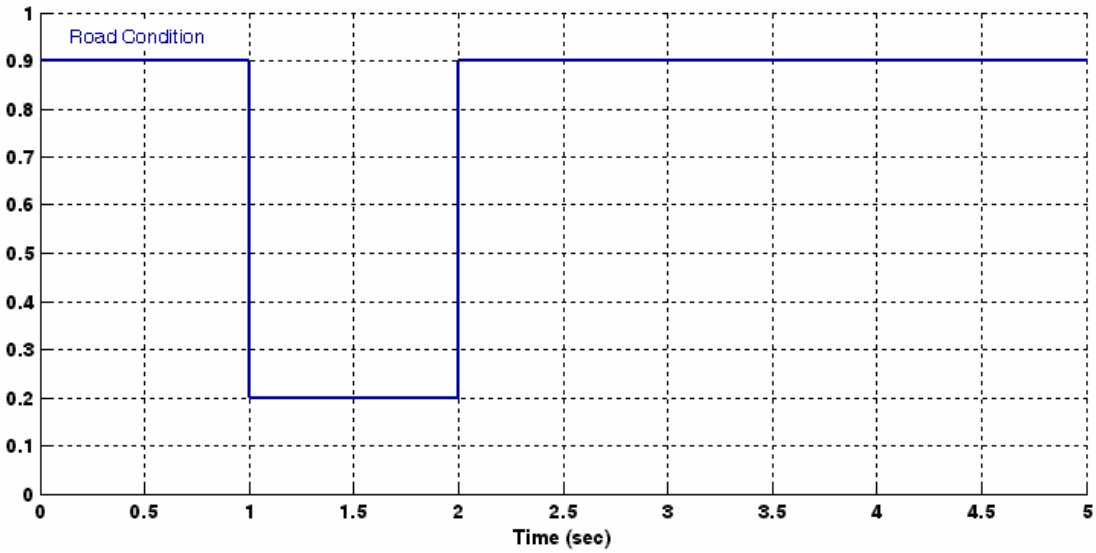

Figure 4.60. Road surface condition for road transitions test

For the test, the road surface is thought to be divided into three segments. Initially the road is emulated as dry asphalt having 0.9 coefficient of friction for the first second of simulation. From 1 to 2 seconds, the road segment is icy road with 0.2 coefficient of friction and changes again to the dry asphalt road for the rest of the simulation time. The changing friction coefficient of the emulated road surface is plotted against time in figure 4.60. The initial velocity of the vehicle is chosen to be 90 km/h, the same as in the previous simulations.

4.2.1.4.1. Results for Low-Level Fuzzy Logic Controller

Simulation results are depicted in figures from 4.61 to 4.65. The ABS controller showed a very successful performance in adapting to changing surfaces. Resulting longitudinal slips at the wheels can be examined in figure 4.61.

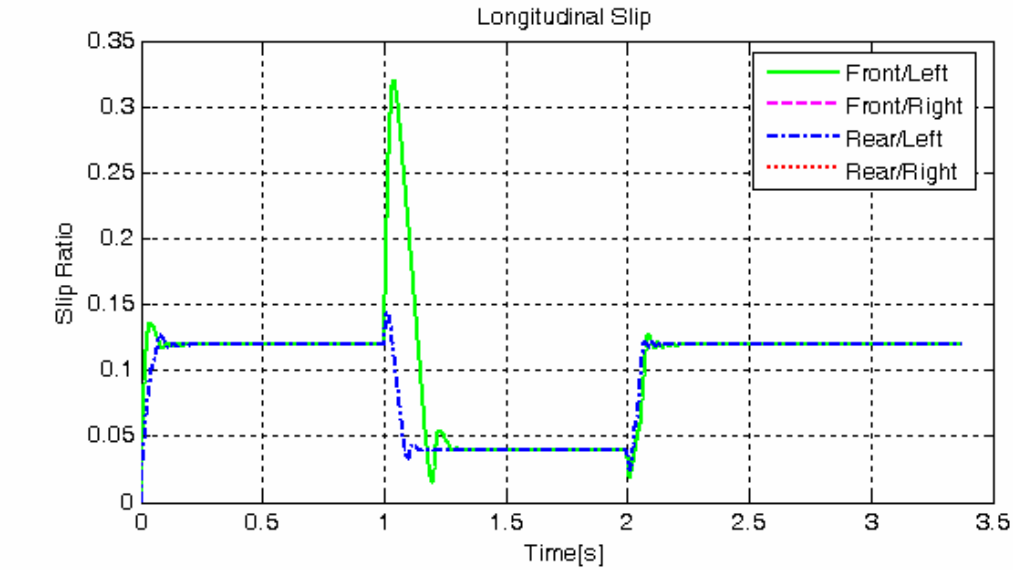

Figure 4.61. Longitudinal wheel slip for changing road conditions for FLC

The performance of the ABS controller for the two low-level controller alternatives was evaluated independently for three different road conditions previously; however here, the controller performance at surface transition points is important. The fuzzy low-level controller reacted to the changing reference signal upon transition from dry to icy road by rapidly decreasing the braking torque at front and rear wheels to zero as can be seen in figure 4.63. Excessive slippage of 32 % is observed for front axle wheels. The fuzzy controller recovered quickly after the overshoot with almost ideal steady-state performance. For the second transition, the situation should be assessed with the reference signal information. The reference slip signal for the front/left wheel, presented in figure 4.62, is alone adequate to reflect the controller performance. For rear wheels the reference signal is similar.

High-level controller detects the surface transition from the provided longitudinal acceleration information and sets the new reference slip signal accordingly. Despite the slightly degraded performance upon transition from icy road back to dry asphalt, the condition identifier logic was successful.

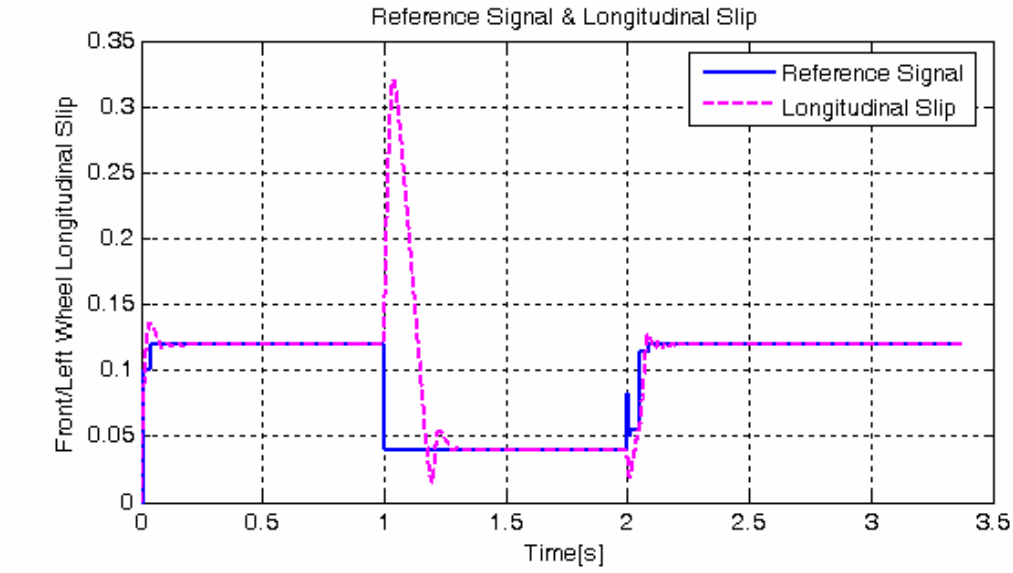

Figure 4.62. Front/left wheel reference slip for changing road conditions for FLC

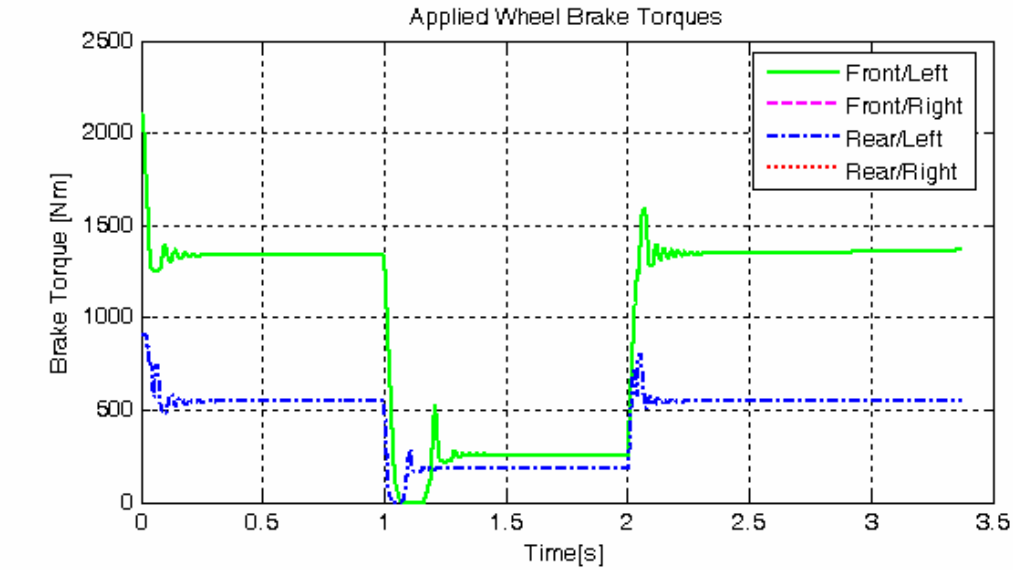

Figure 4.63. Wheel braking torques for changing road conditions for FLC

Figures 4.64 and 4.65 illustrate vehicle longitudinal velocity and acceleration responses. Vehicle speed is observed to be 57.5 km/h while the road surface changes into icy conditions at t = 1 seconds.

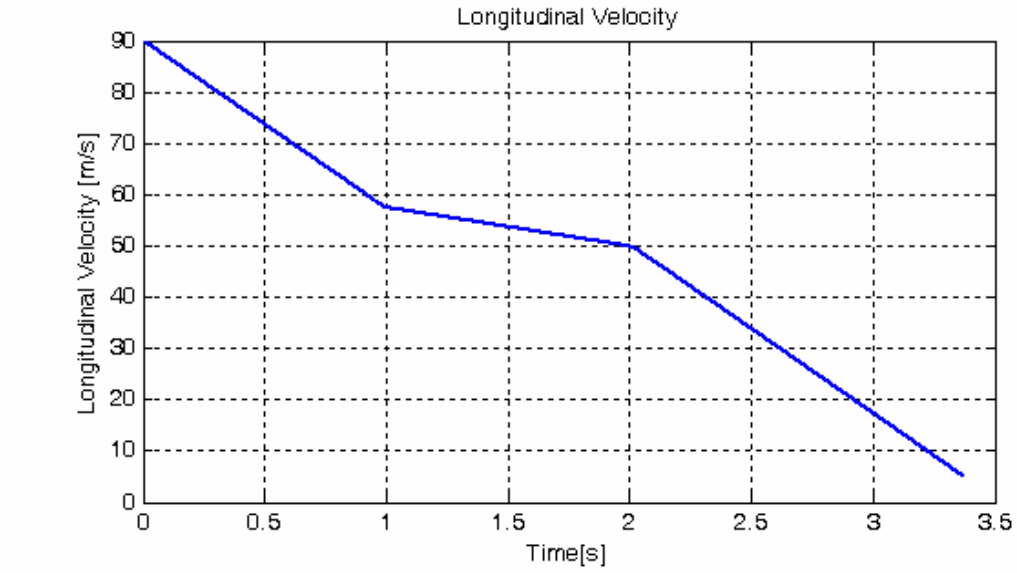

Figure 4.64. Longitudinal velocity for changing road conditions for FLC

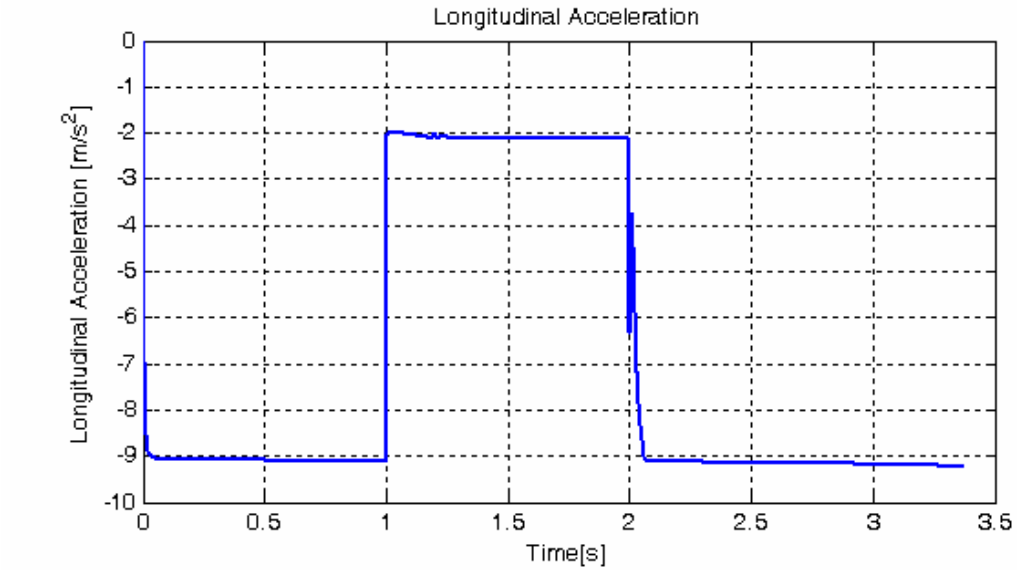

Figure 4.65. Longitudinal acceleration for changing road conditions for FLC

The reason for the degraded performance of the high-level controller at the second transition stage becomes clear in viewing the longitudinal acceleration plot of the vehicle. Upon transition from icy road back to dry asphalt, due to limited braking torque change rates, the low-level controller fails to attain the required brake torque levels and thus, requested reference slip in time. The slip ratio at the front wheels decreases below 0.02 which results degraded braking performance and hence a drop in vehicle deceleration rate. The controller recovers quickly afterwards, however the brief deviation of the vehicle deceleration causes a misinterpretation of surface friction level by the fuzzy logic based surface condition identifier logic.

4.2.1.4.2. Results for Low-Level PID Controller

Simulation results for the low-level PID controller are depicted in figures from 4.66 to 4.69. Longitudinal slip plot can be observed in figure 4.66 below. The tracking performance of the PID controller was comparable to the fuzzy logic controller, although steady-state performance was slightly inferior in comparison, especially upon transition at t = 2 seconds.

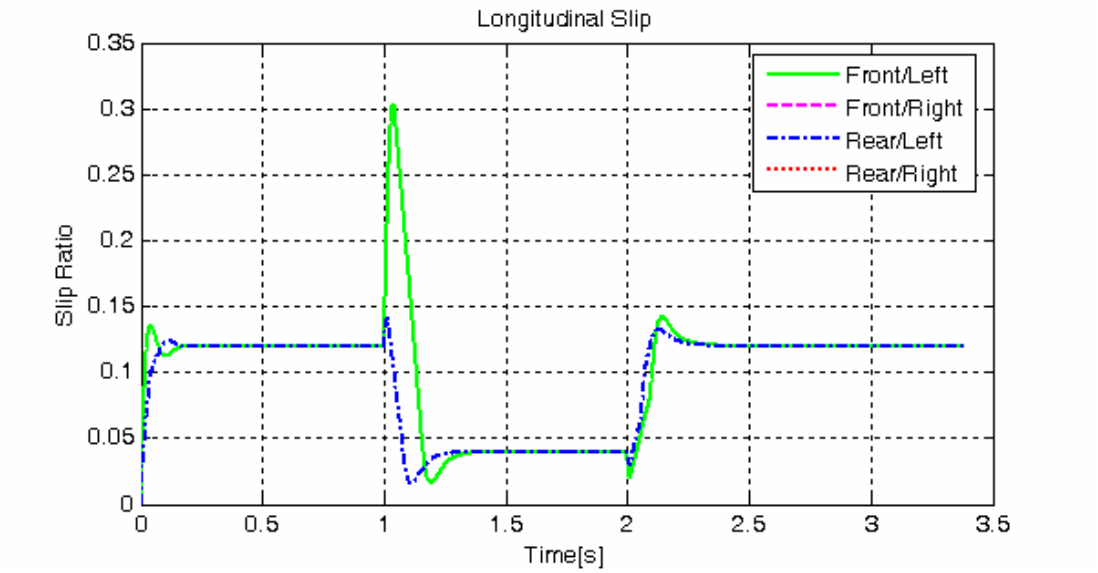

Figure 4.66. Longitudinal wheel slip for changing road conditions for PID

Figures 4.67 shows reference slip signal of the front/left wheel and corresponding longitudinal slip development at the wheel as representative for front axle wheels. The reference signal for rear axle wheels is similar and is not presented.

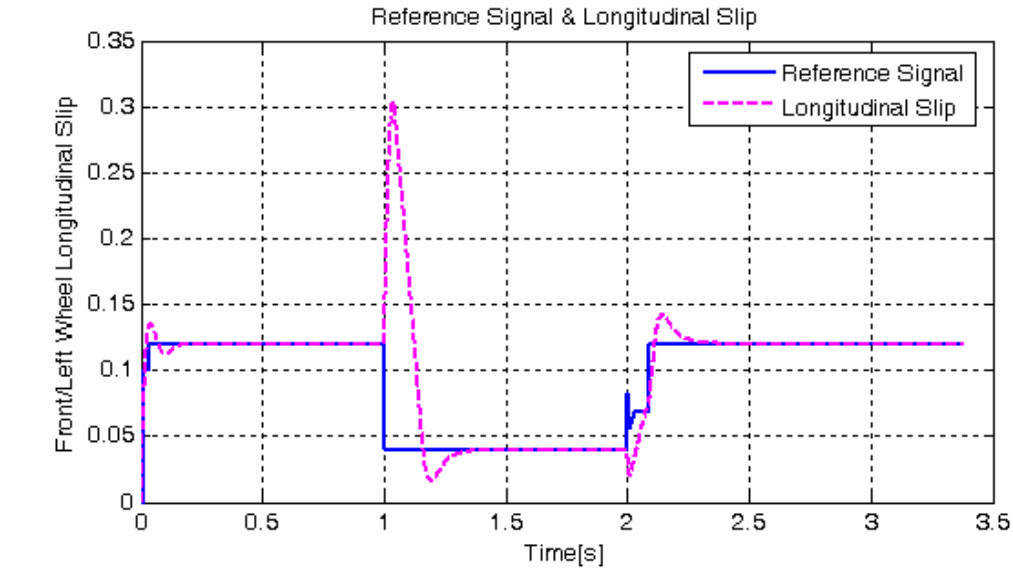

Figure 4.67. Front/left wheel reference slip for changing road conditions for PID

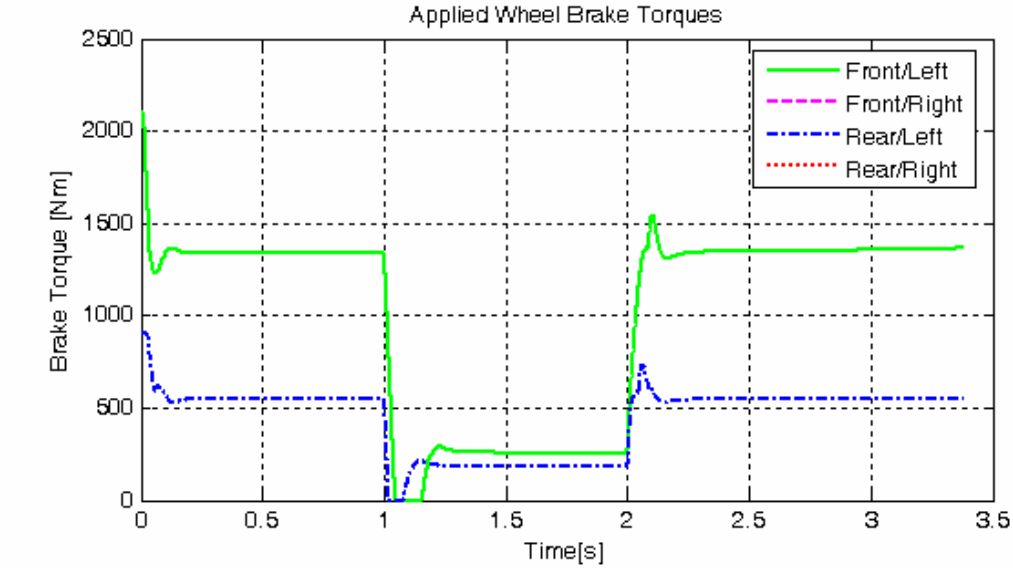

Figure 4.68. Wheel braking torques for changing road conditions for PID

Figure 4.68 illustrates modulation of wheel braking torques. The general trend was similar to the fuzzy controlled case as expected. At the first transition, the low-level controller reduced the braking torque at both wheels to zero at the maximum rate permitted by the actuator. It should be noted that when the braking torque reaches zero, the integrator term for both low-level controllers is saturated at that level to prevent the unnecessary effort and the associated performance failure of the controller and to simulate the actuator realistically.

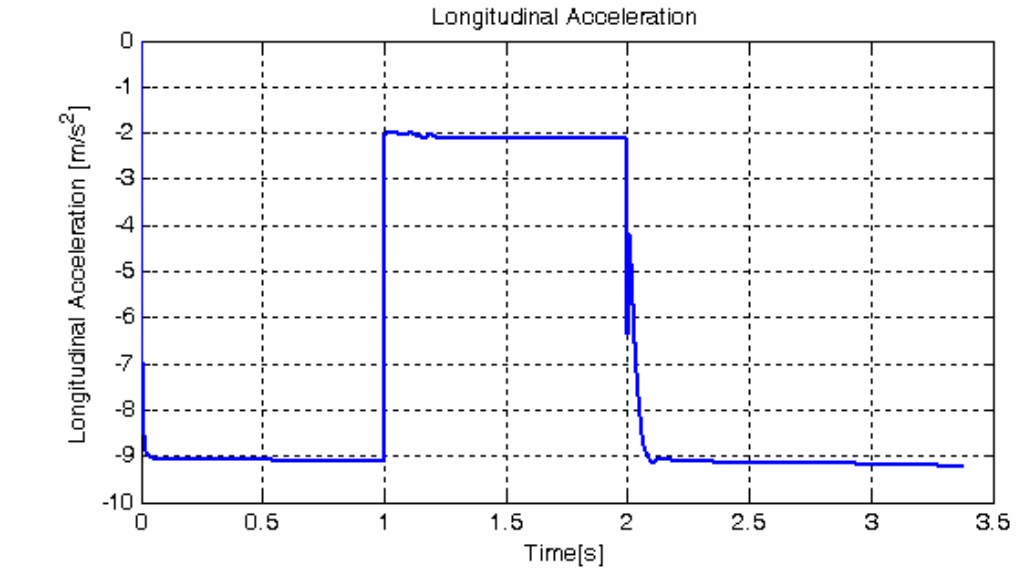

Figure 4.69. Longitudinal acceleration for changing road conditions for PID

Vehicle longitudinal deceleration can be observed in figure 4.69. It is certain that the response plot is identical to the result of the ABS controller incorporating FLC as the low-level controller. The discussion related to the surface condition estimation problem is also here valid. The longitudinal velocity response of the vehicle was not any different from the plot shown in figure 4.64 and hence is not presented.

In the study for road surfaces with varying surface friction levels, simulations were also conducted for a different road surface condition setting; the results are presented in Appendix B.

4.2.2. CASE II: Combined Braking and Steering with ABS

The case is the likely scenario of an emergency braking situation. The driver intends to avoid the collision by steering away from the obstacle while also applying heavy braking at the same time in an attempt to reduce the severity of a possible crash at the least. In such a case, without the ABS controller, the vehicle may not maintain directional control and achieve the intended lateral movement. Previously presented results of the simulation for the uncontrolled case have proved this statement.

ABS controller is expected to preserve directional control by ensuring the development of sufficient lateral tire force at wheels under heavy braking conditions. However it should be not be forgotten that, the lateral response of the vehicle would be certainly degraded due to inevitable, though controlled, slippage of the wheels, thus, the limited tire lateral force margin left and also there exists a compromise between braking performance and handling response. It is difficult to evaluate the performance of the controller here with the results of the part 4.1.1, in which, the response of the vehicle has been observed for only steering input without braking. Although the results have provided a reference to this study, note that the decreasing speed of the vehicle under braking has strong influence over the yaw and sideslipping response and the resulting turning radius.

In presentation of the results in this part, the emphasis will not be over the performance comparison of the low-level controller alternatives since the satisfactory tracking performance has been shown for various road conditions in previous sections and naturally, simulation results for the two controllers are very similar. The general discussion of the simulation study, presented here, will be based on the performance of the fuzzy logic controller. Results of the simulation for PID controller are provided in Appendix C.

4.2.2.1. Dry Asphalt Test

Simulations were carried on for a surface having 0.9 coefficient of friction and different steering inputs: a step steering input applied at t = 0 and a j-turn steering input. Presentation of the results will be for fuzzy logic based low-level controller. Figures from 4.70 to 4.75 depict the results of the simulation conducted for the step steering handwheel angle input of 40º shown in figure 4.1.

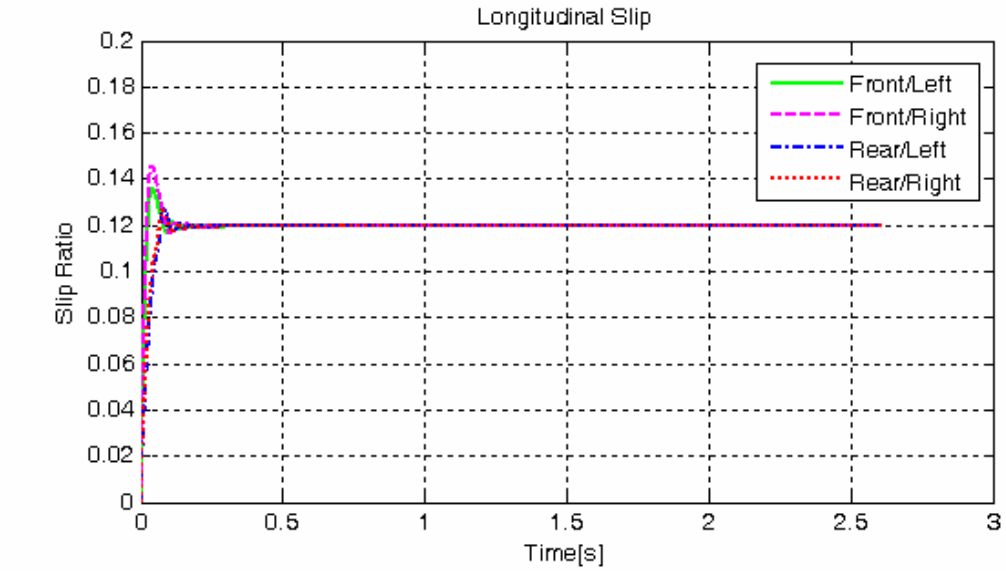

Figure 4.70. Longitudinal wheel slip on dry asphalt for 40º step input for FLC

Figure 4.70 shows longitudinal slip development at the wheels. Effect of lateral load transfer in cornering over wheel slip response is observable; however steady-state wheel slip is 0.12 as in the straight-line case.

Figures 4.71, 4.72 and 4.73 illustrate respectively yaw rate, sideslip angle and lateral acceleration responses. Yaw rate response plot shows the understeer behavior of the vehicle with a reduced yaw rate gain for the same steering input studied previously in the part regarding steering response of the vehicle without braking. Yaw rate decreases in time due to decreasing speed of the vehicle. Sideslip angle development shown in figure 4.72 is similar in trend to the previously studied simulation case of

steering response without braking; however lowered in amplitude like the yaw rate response. After 2 seconds the vehicle slip angle takes positive values because of the decreasing effect of the longitudinal velocity and yaw rate.

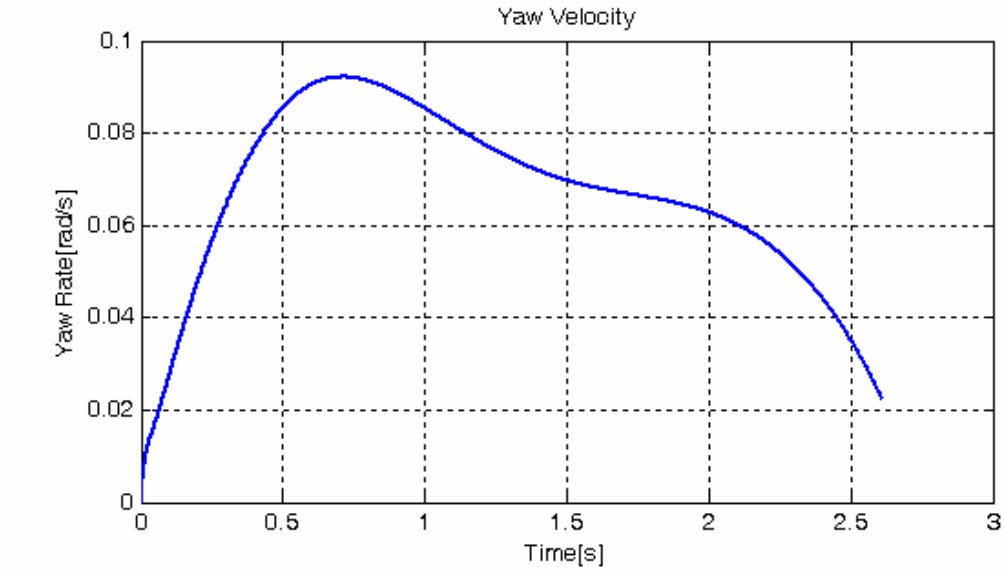

Figure 4.71. Yaw velocity on dry asphalt for 40º step input for FLC

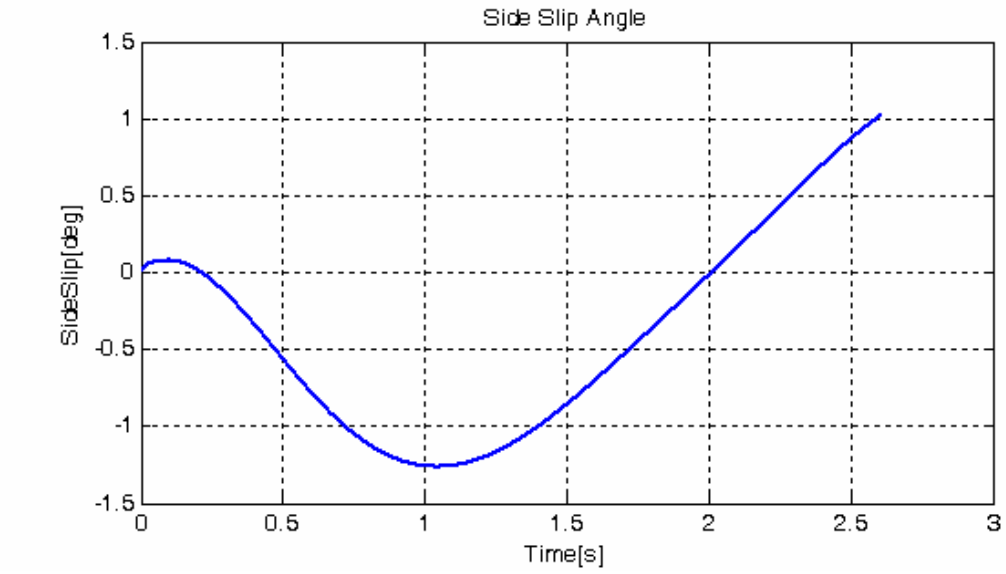

Figure 4.72. Sideslip angle on dry asphalt for 40º step input for FLC

Lateral acceleration of the vehicle is directly related to the developed lateral tire forces. The response graph initially decreases sharply with increase of the longitudinal slips at all wheels; however with the intervention of the ABS controller, the slips are regulated at a certain level, thus allowing lateral tire forces to develop. By this way, lateral acceleration response graph recovers shortly and makes a peak at t = 1 s but decreases slowly in parallel with longitudinal velocity.

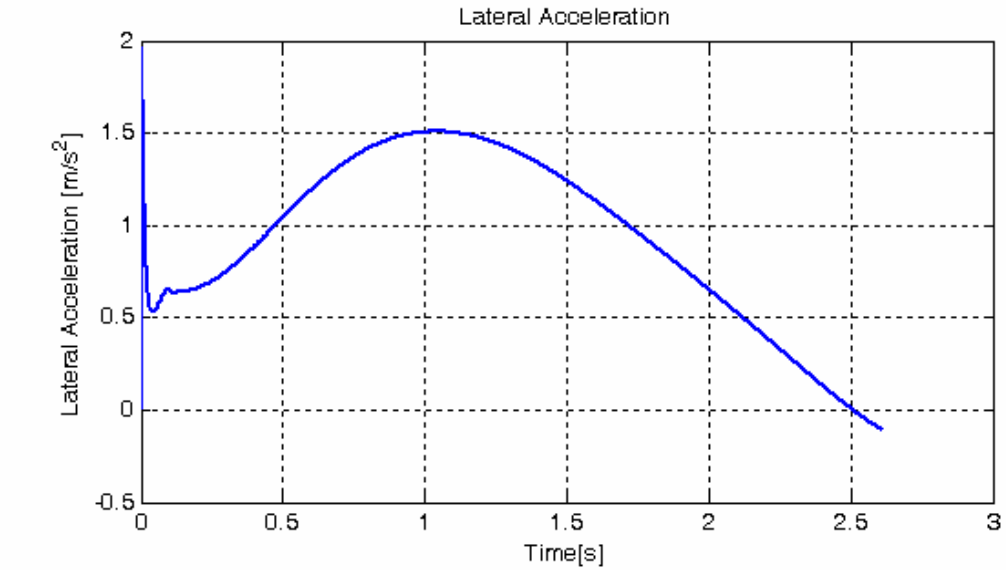

Figure 4.73. Lateral acceleration on dry asphalt for 40º step input for FLC

Figures 4.74 and 4.75 show longitudinal acceleration response and trajectory of the vehicle. The average longitudinal deceleration is slightly reduced by the steering and a small deviation from the average value can be observed at around t = 1s which corresponds to the peak of the lateral acceleration. Lateral movement can be clearly observed from the trajectory of the vehicle. The vehicle advanced 1.8 meters in the lateral direction and 34.52 meters in the longitudinal direction. Note that the stopping distance is comparable to the case of straight-line braking, although the reference signal was not optimized for maximum deceleration this time.

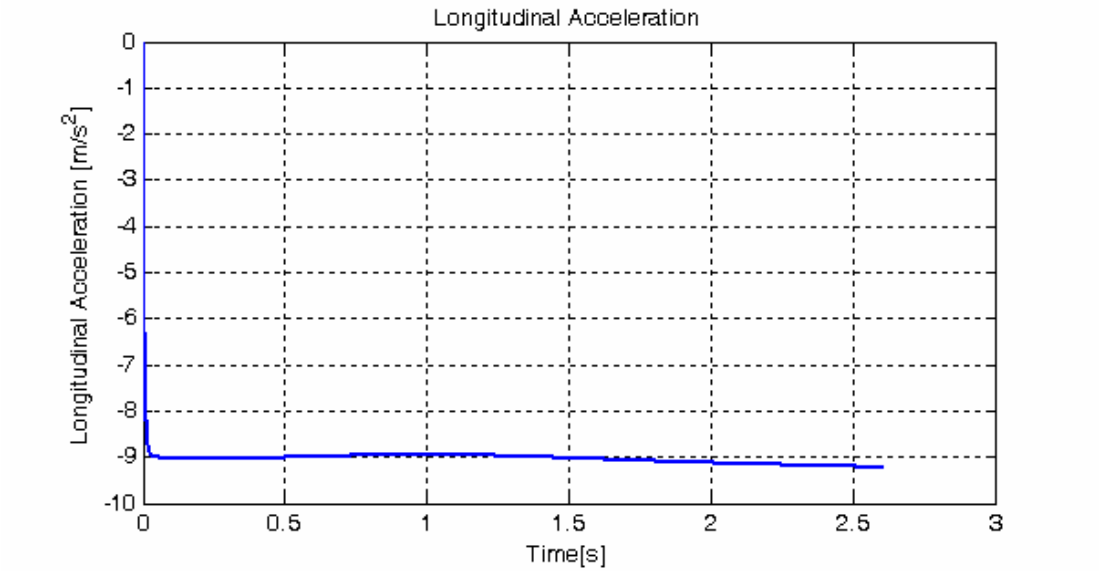

Figure 4.74. Longitudinal acceleration on dry asphalt for 40º step input for FLC

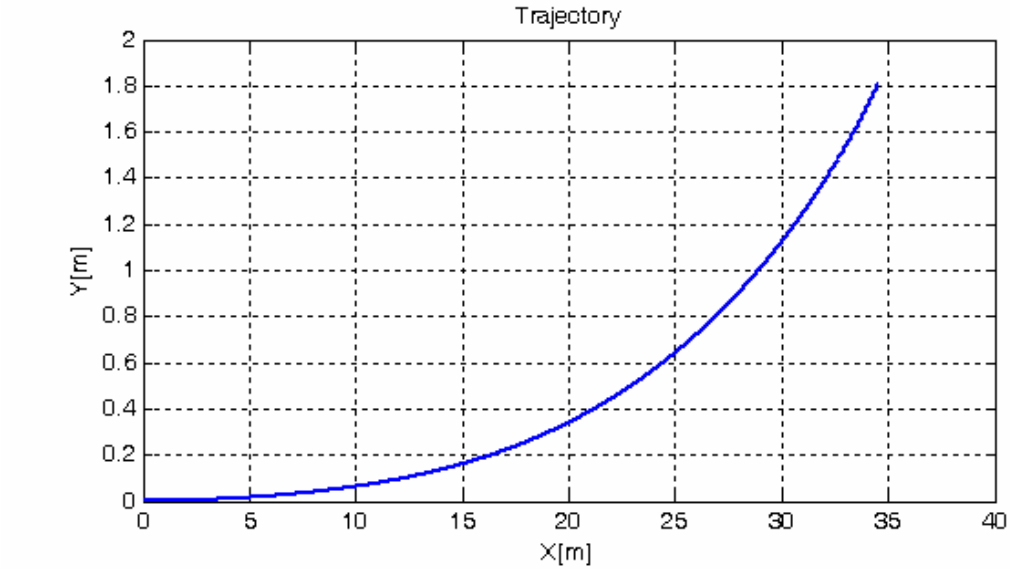

Figure 4.75. Vehicle trajectory on dry asphalt for 40º step input for FLC

From the results, it can be observed that although the ABS controller was successful in maintaining directional control, the steering has lost certain efficiency. At this point, it is desired to see the lateral response of the vehicle for a larger step steering input, since in such a case the driver may respond to the understeer behavior of the

vehicle by applying more steering. For this purpose the step steering input shown in figure 4.76 was applied. 120º degrees handwheel angle corresponds to a slip angle of 6.67º at front wheels. Figures from 4.77 to 4.82 illustrate the results of the simulation.

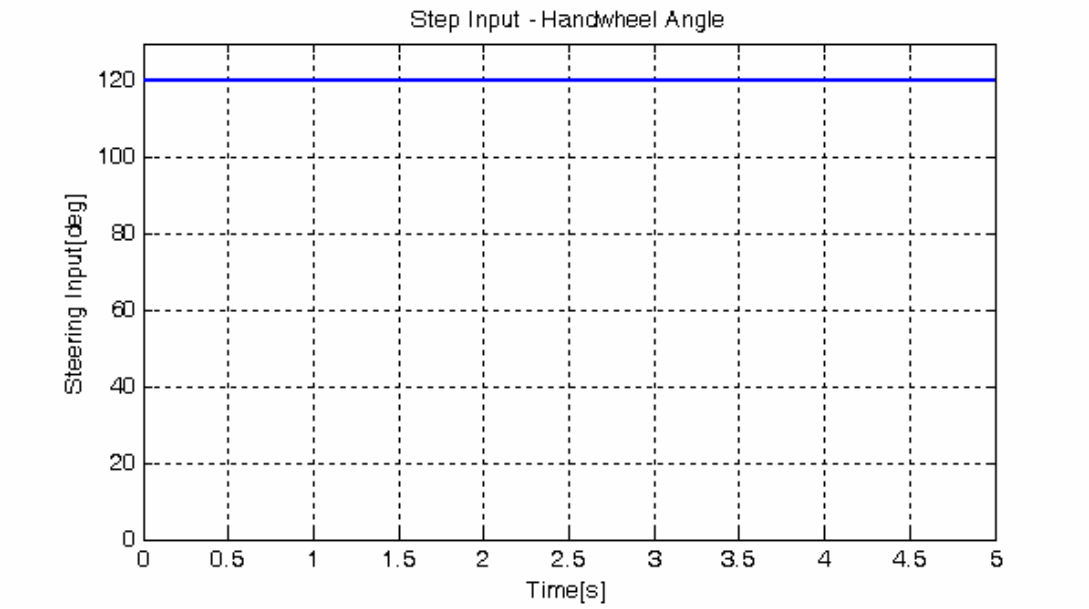

Figure 4.76. 120º Step steering input signal

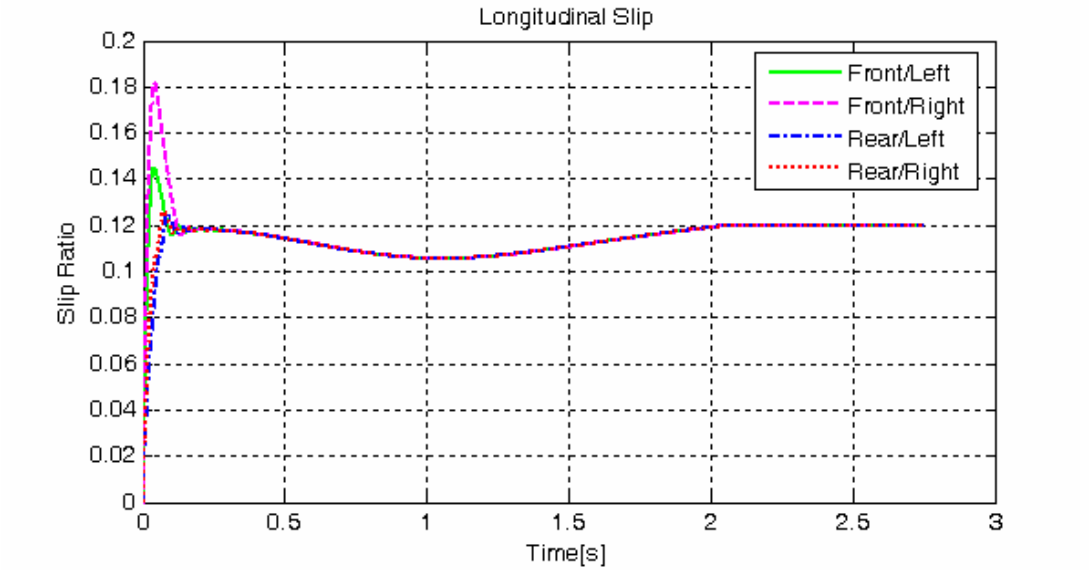

Figure 4.77. Longitudinal wheel slip on dry asphalt for 120º step input for FLC

Figure 4.77 shows longitudinal wheel slip response. Lateral load transfer causes the elevated slippage of the front/right wheel and the noticeable deviation of the slip ratio is a result of a misinterpretation of surface condition of high-level controller due to influence of steering; however it serves to increase lateral movement margin here.

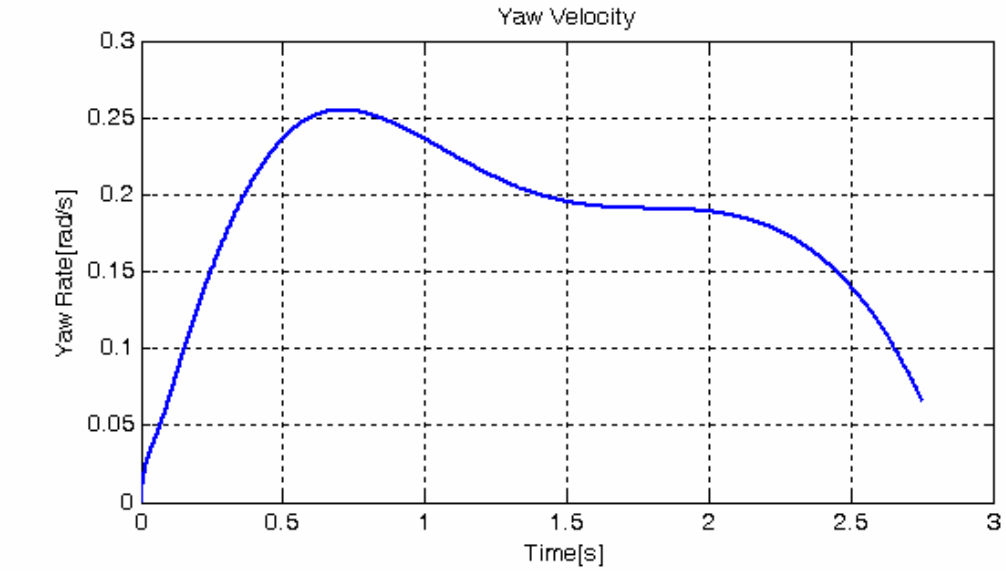

Figure 4.78. Yaw velocity on dry asphalt for 120º step input for FLC

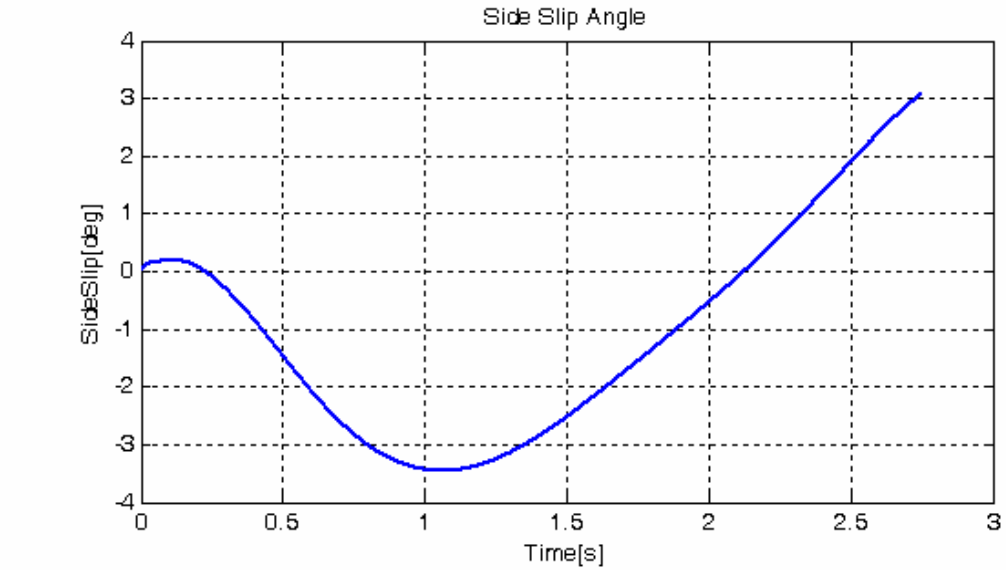

Figure 4.79. Sideslip angle on dry asphalt for 120º step input for FLC

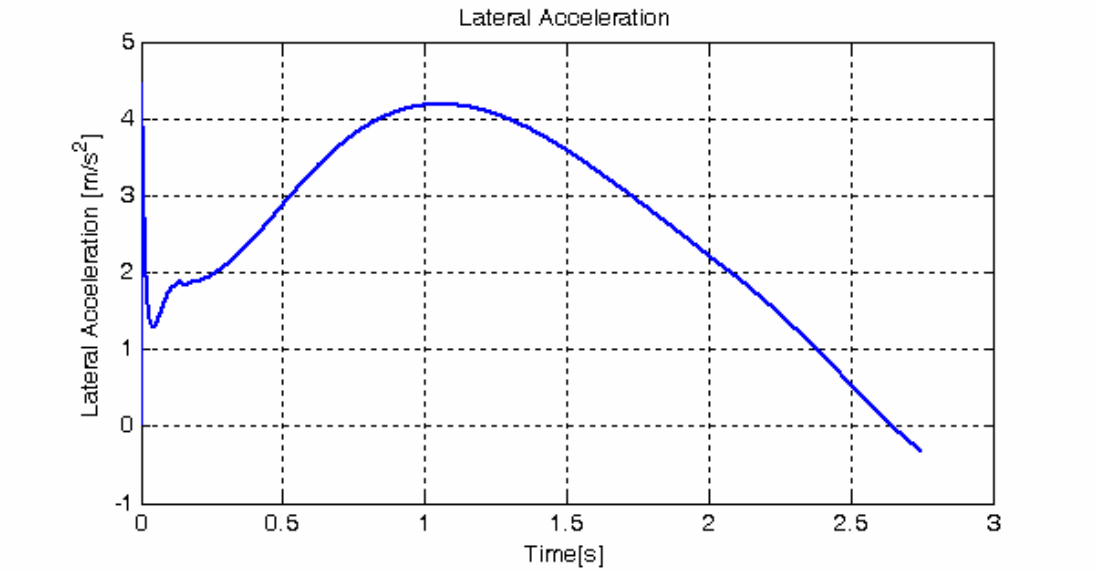

Figure 4.80. Lateral acceleration on dry asphalt for 120º step input for FLC

Figures 4.78, 4.79 and 4.80 illustrate the improved lateral response of the vehicle. ABS controller maintained the lateral stability of the vehicle and provided a greater margin for cornering. The increase in amplitudes observed in all response graphs is almost linear.

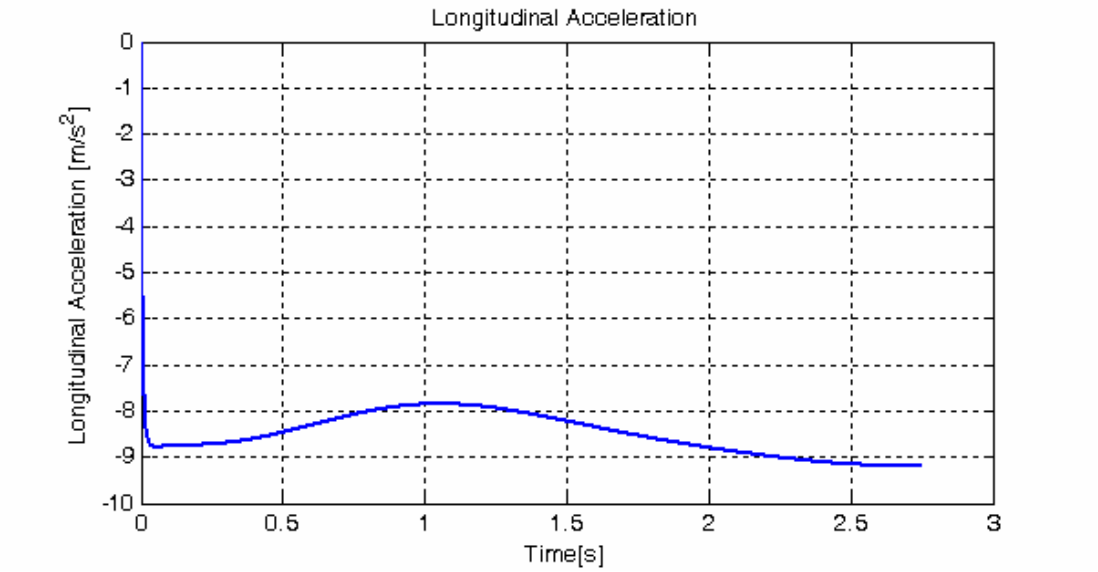

Figure 4.81. Longitudinal acceleration on dry asphalt for 120º step input for FLC

The longitudinal deceleration of the vehicle can be examined in figure 4.81. The plot shows one more time that there is a compromise between deceleration performance and lateral maneuverability. The increase of lateral acceleration caused a decrease in longitudinal deceleration (maximum at t = 1s) and consequently a deviation in reference slip signal and thus in the wheel slip response as observed in figure 4.77.

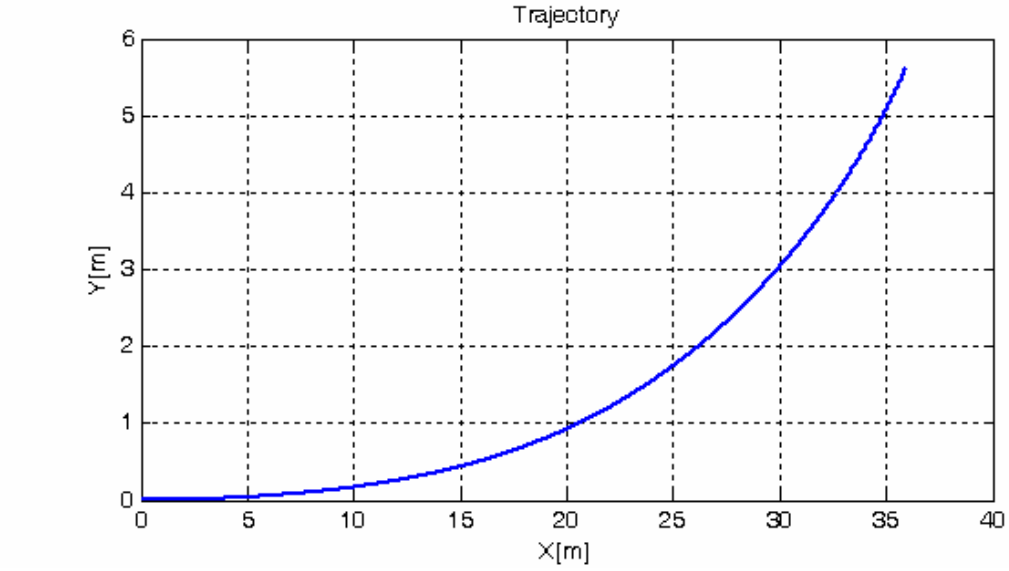

Figure 4.82. Vehicle trajectory on dry asphalt for 120º step input for FLC

The improved lateral response can be clearly seen from the trajectory provided by figure 4.82. The lateral movement at x = 30 m is 3 meters whereas it is 1.15 m in figure 4.75; nevertheless the stopping distance was recorded as 35.95 m which is almost 1.4 meters ahead of the stopping distance obtained in the case of 40º step steering input.

Simulations were also conducted for a vehicle in a j-turn maneuver. The steering input for this case is depicted in figure 4.83. Figures from 4.84 to 4.89 present the results of the simulation.

The input is applied at t = 0.5 s, which corresponds to a time when the longitudinal slips have already reached steady-state; therefore the development of the wheel slips

plotted in 4.84 is almost the same as in the straight-line simulation presented previously in 4.27. The application of the steering input did not have any considerable effect on the reference input hence the slip responses.

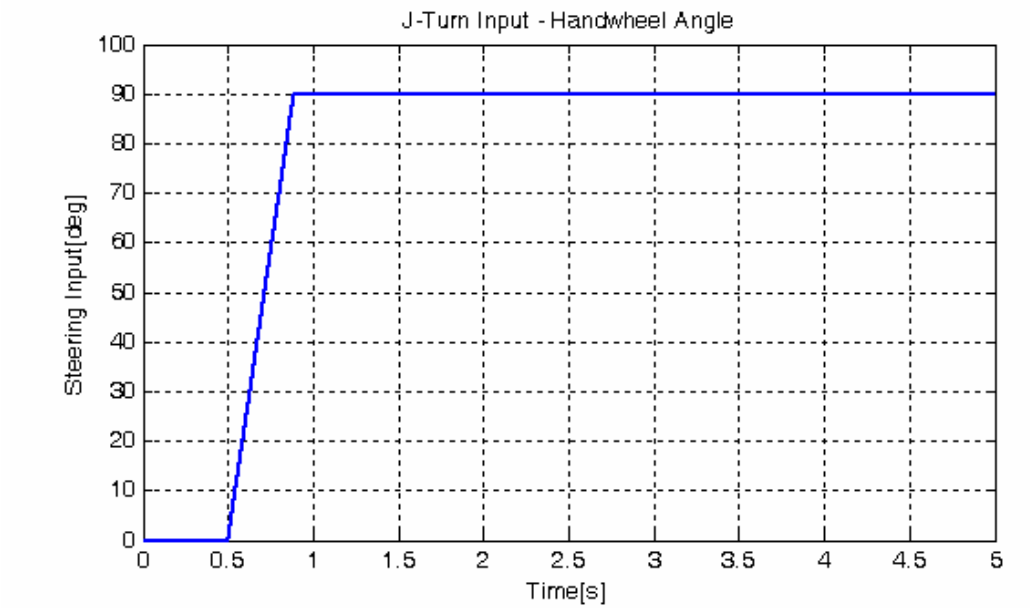

Figure 4.83. J-Turn steering input.

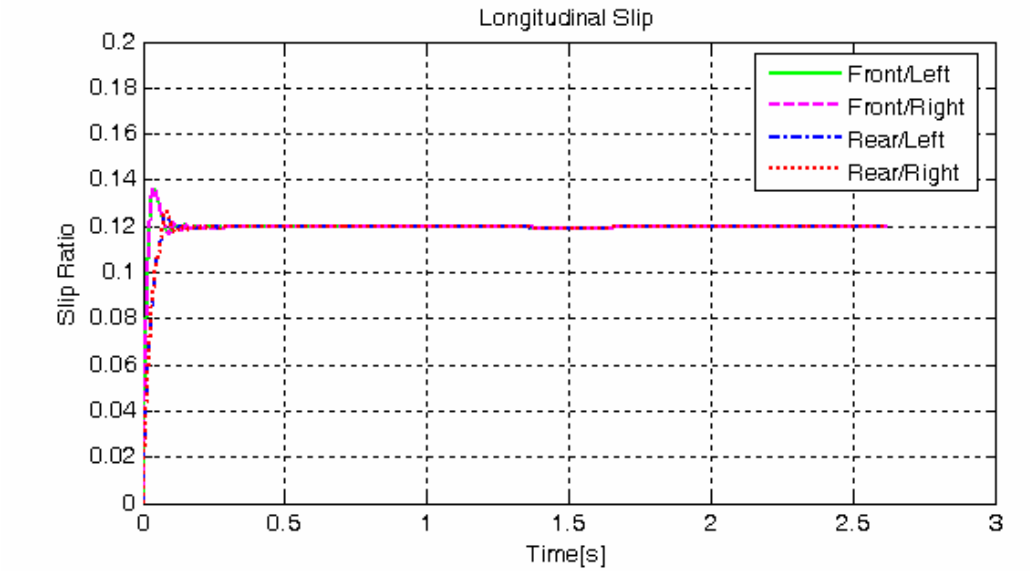

Figure 4.84. Longitudinal wheel slip on dry asphalt for j-turn input for FLC

Figures 4.85, 4.86 and 4.87 present the lateral response of the vehicle. ABS controller successfully maintained the directional control and yaw stability. Vehicle responded rapidly to the steering input at t = 0.5 s by yawing and sideslipping.

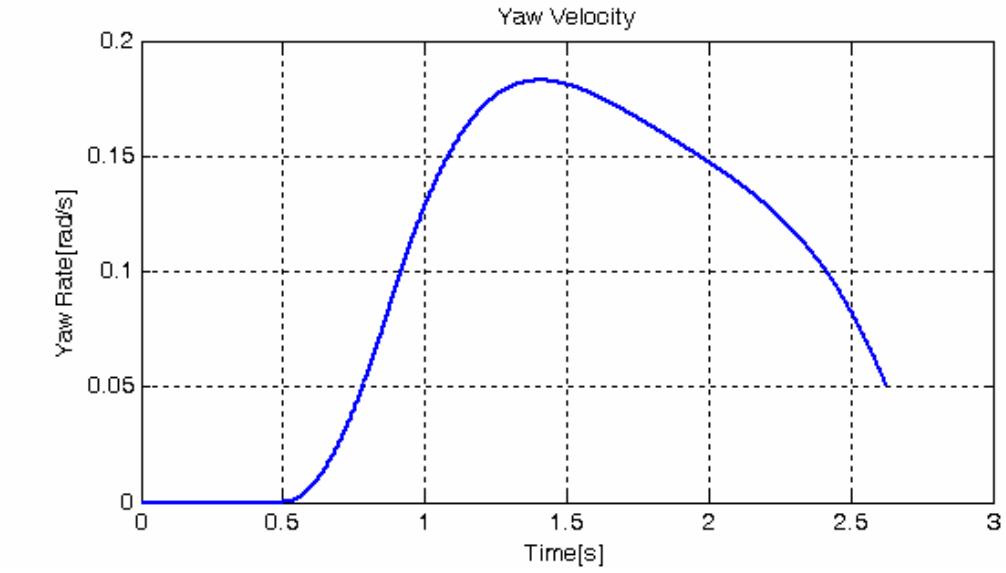

Figure 4.85. Yaw velocity on dry asphalt for j-turn input for FLC

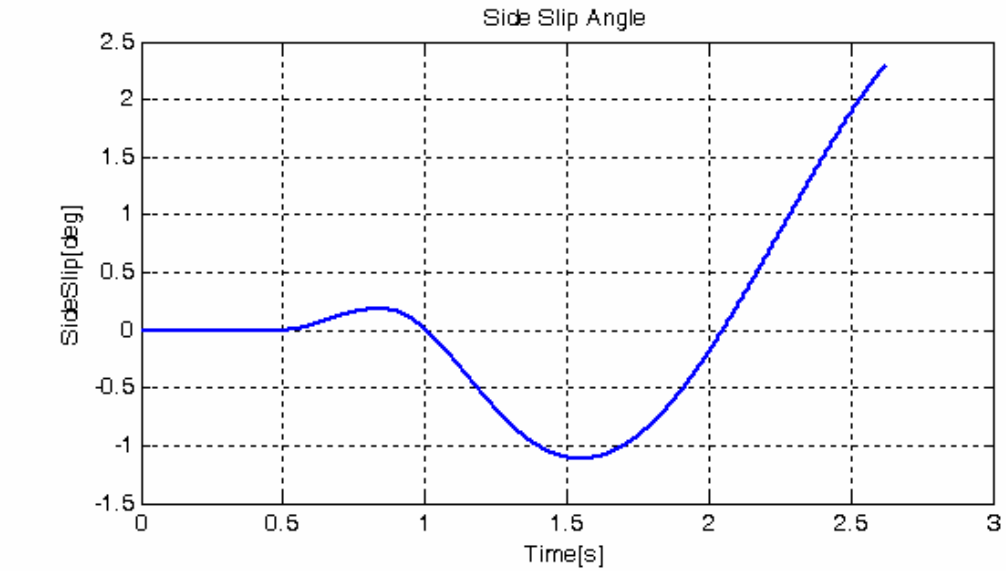

Figure 4.86. Sideslip angle on dry asphalt for j-turn input for FLC

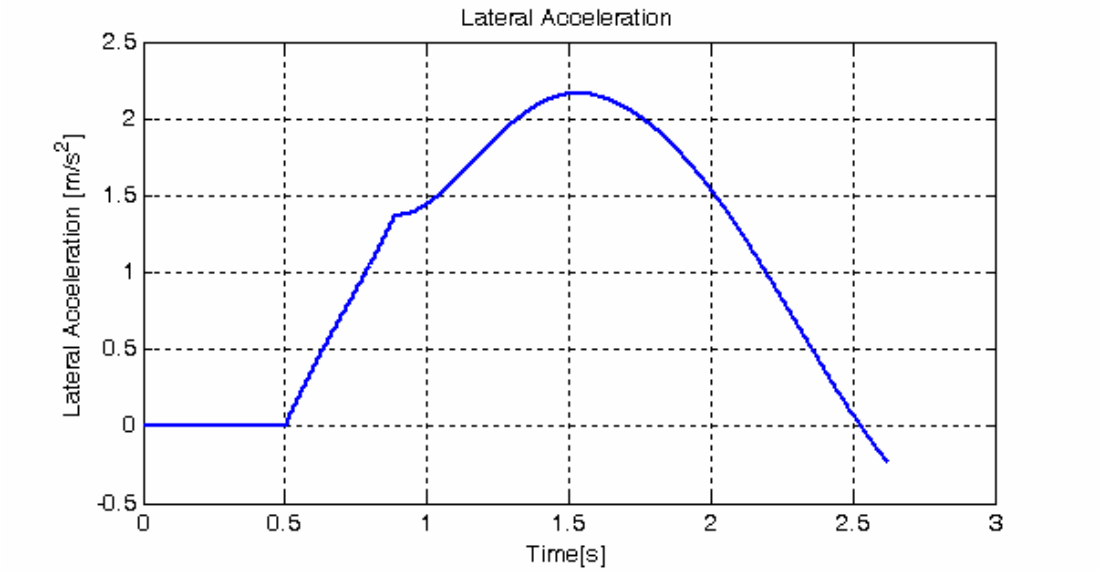

Figure 4.87. Lateral acceleration on dry asphalt for j-turn input for FLC

Figures 4.88 and 4.89 present respectively longitudinal acceleration response and trajectory of the vehicle. A small decrease in vehicle deceleration is noticeable at t = 1.5 s; nevertheless there is not a significant increase in stopping distance (34.61 m).

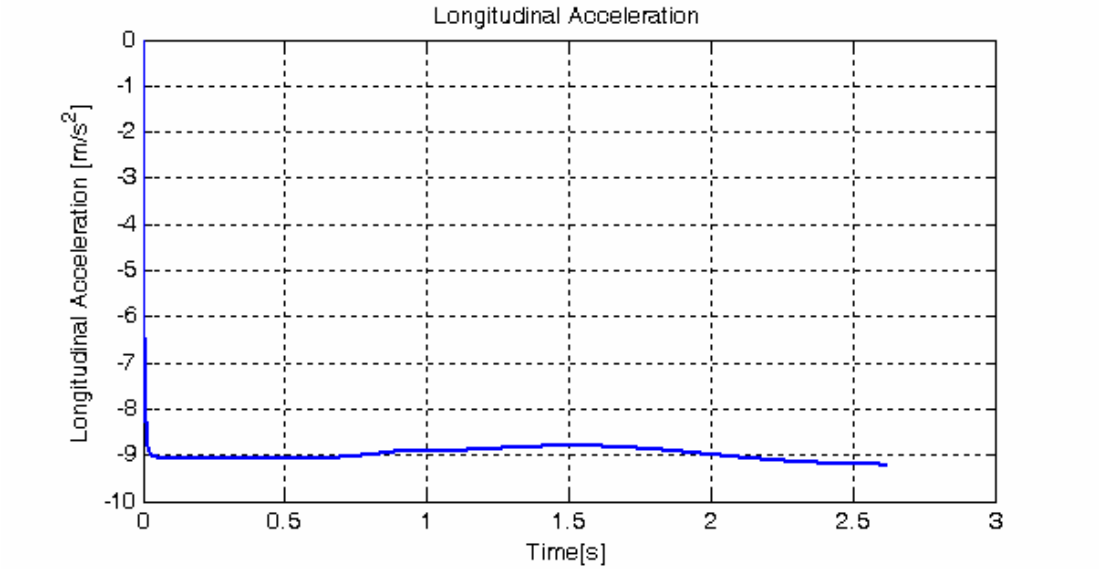

Figure 4.88. Longitudinal acceleration on dry asphalt for j-turn input for FLC

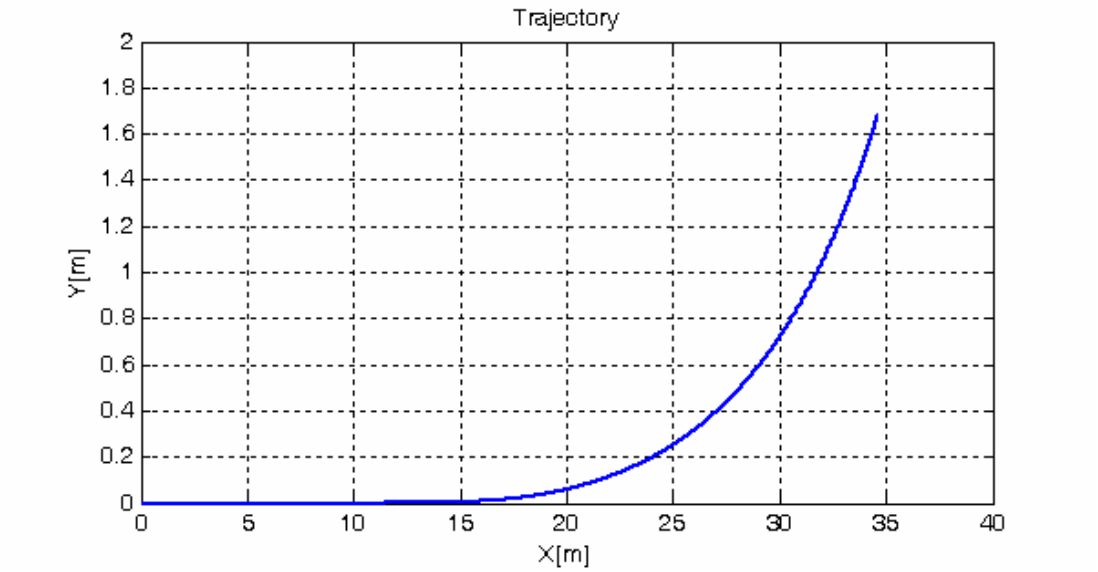

Figure 4.89. Vehicle trajectory on dry asphalt for j-turn input for FLC

4.2.2.2. Wet Asphalt Road Test

Wet asphalt road surface provides lower adhesion for tires, hence, an inferior braking performance and maneuvering capability. Considering surface friction limits and since the general trend of the lateral responses is the same as in dry road test, only the simulation results for the 40º step steering input are presented here in figures from 4.90 to 4.95.

Longitudinal slips are depicted in figure 4.90. The plot is similar to the figure 4.42, however as in the previous cases, the overshoot is slightly increased due to tire loading and lateral effects influence the reference signal which results a discernible deviation of slip ratio curve.

Figures 4.91, 4.92 and 4.93 illustrate the lateral response of the vehicle on wet road with the ABS controller. The plot shows that vehicle, though respectively more responsive to steering input compared to dry asphalt case, drifts toward outside or in other words, shows understeer behavior again. Yaw velocity response shown in

figure 4.91 is very similar to figure 4.71, but yaw rate gain has a higher ratio for the same steering input.

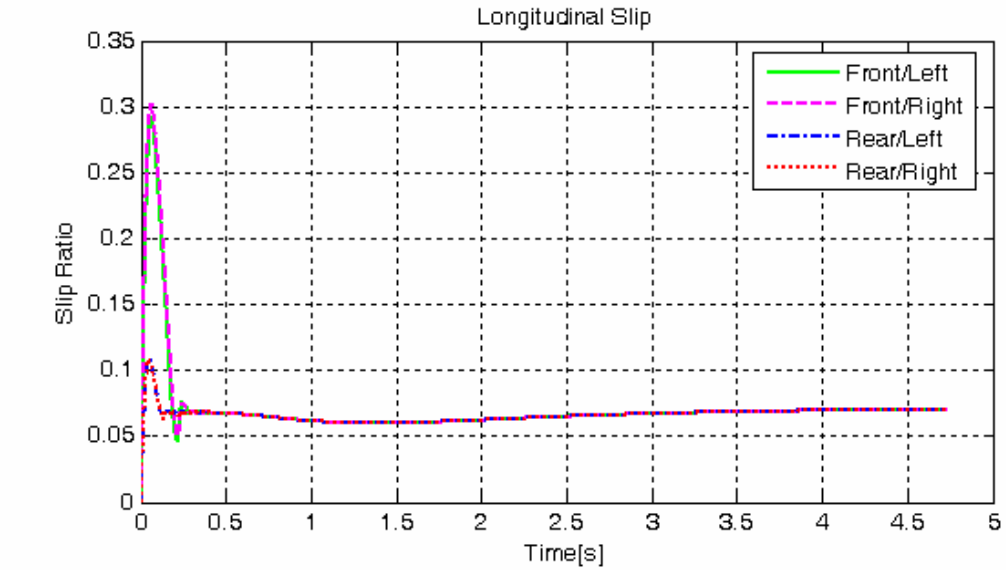

Figure 4.90. Longitudinal wheel slip on wet asphalt for 40º step input for FLC

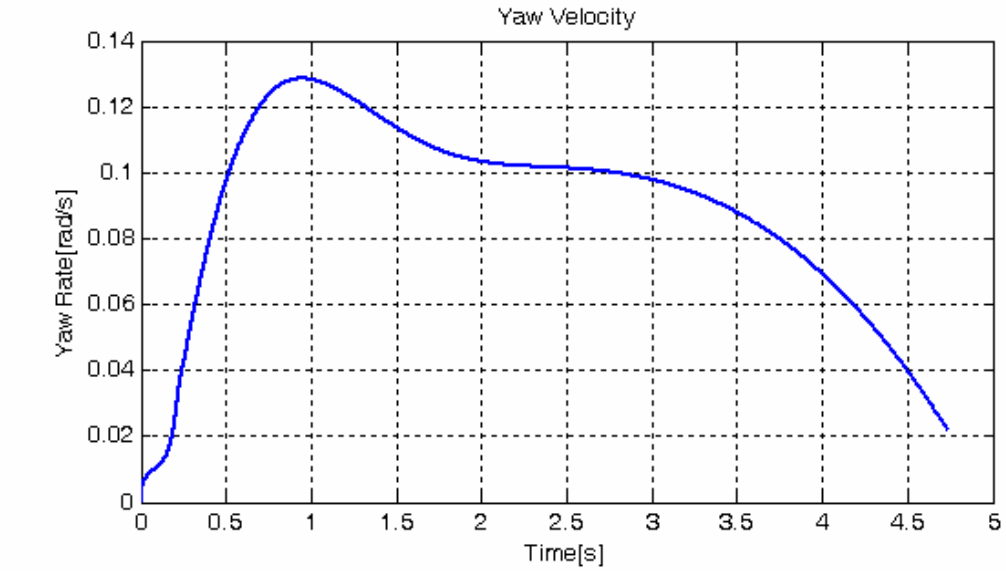

Figure 4.91. Yaw velocity on wet asphalt for 40º step input for FLC

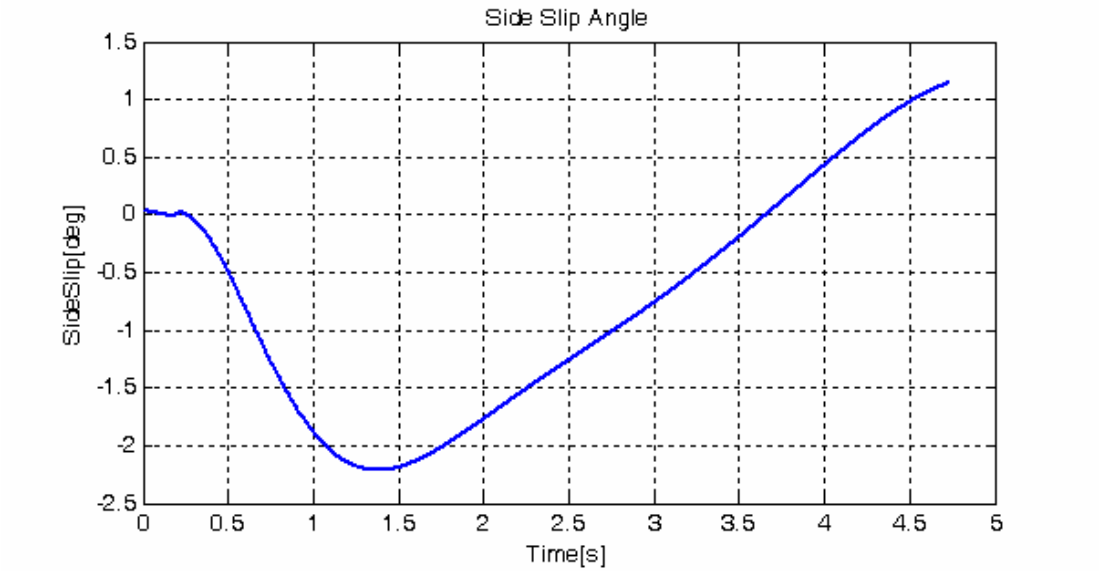

Figure 4.92. Sideslip angle on wet asphalt for 40º step input for FLC

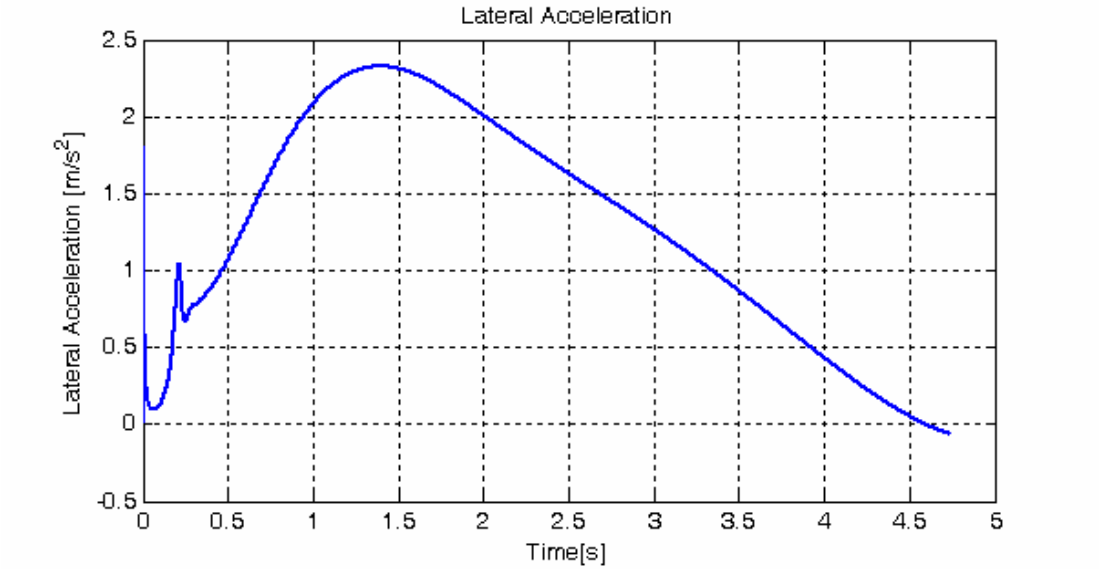

Figure 4.93. Lateral acceleration on wet asphalt for 40º step input for FLC

Vehicle developed considerable sideslipping and lateral acceleration as can be seen in figures 4.92 and 4.93; but the amplitudes of the response graphs decreased in time as is expected from a laterally stable vehicle.

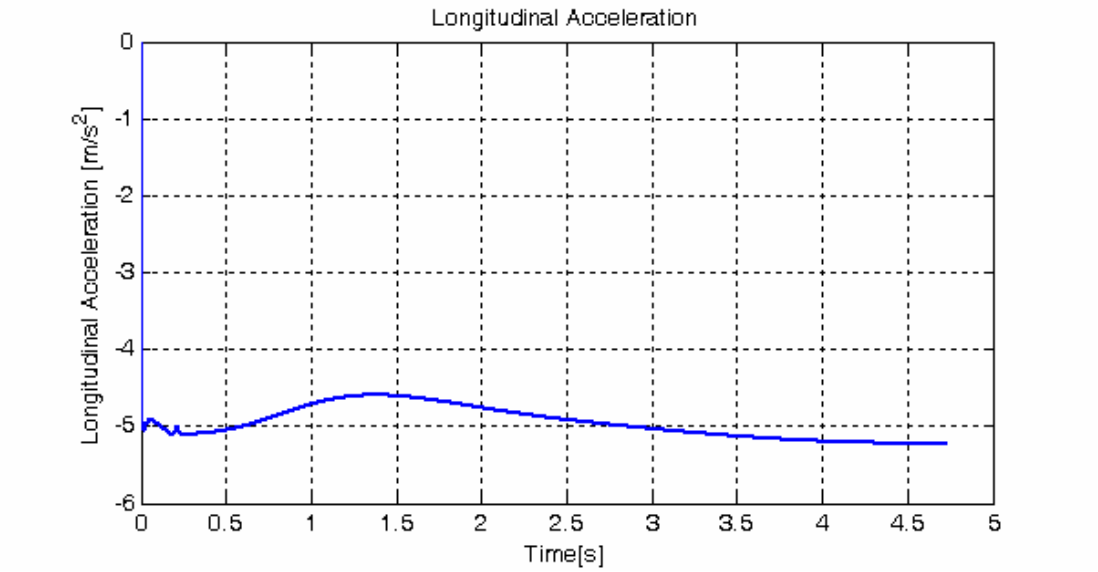

Figure 4.94. Longitudinal acceleration on wet asphalt for 40º step input for FLC

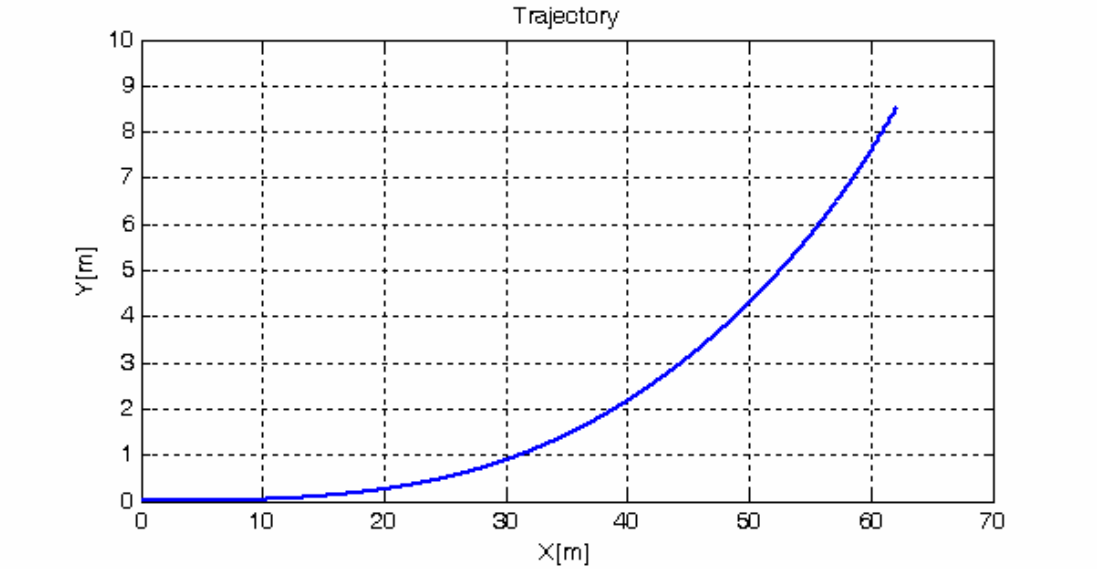

Figure 4.95. Vehicle trajectory on wet asphalt for 40º step input for FLC

The braking efficiency is degraded compared to straight-line case as can be seen in figure 4.94. The distance covered in the longitudinal direction is 62.15 meters which corresponds to almost 2 meters increase due to steering.

4.2.2.3. Icy Road Test

Vehicle response with the ABS controller for 40º step steering input on icy road surface can be examined from figures 4.96 to 4.101.

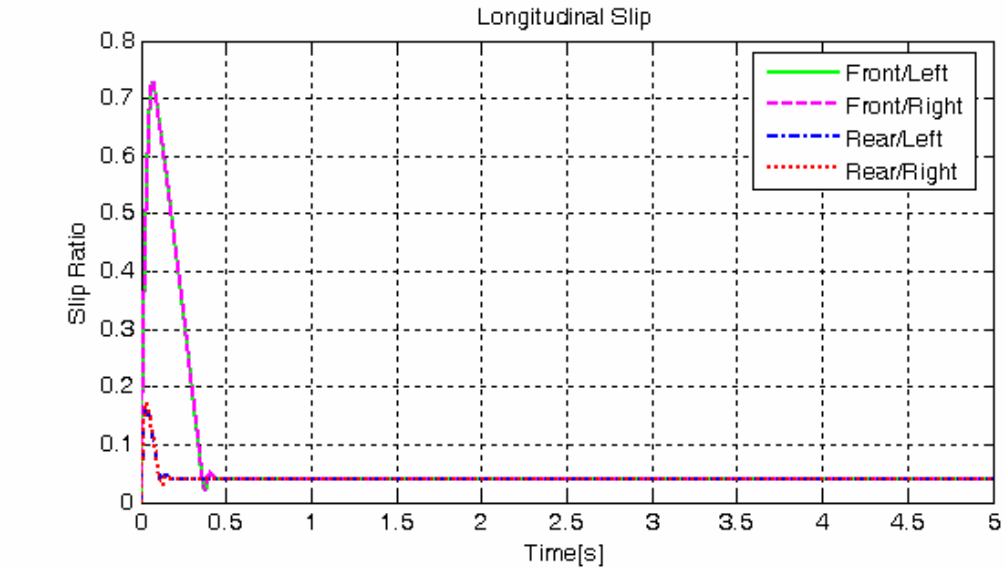

Figure 4.96. Longitudinal wheel slip on icy road for 40º step input for FLC

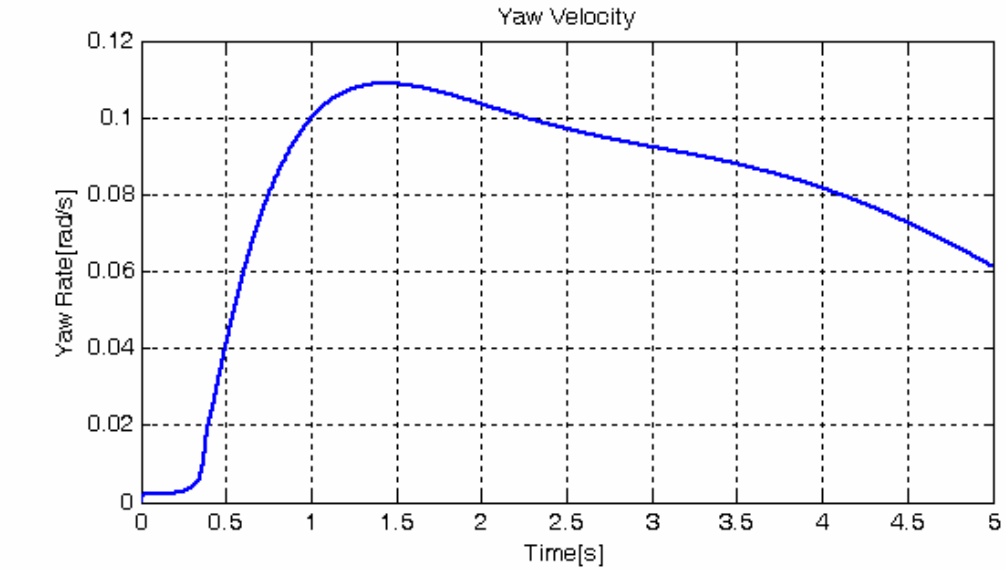

Figure 4.97. Yaw velocity on icy road for 40º step input for FLC

As observed from figure 4.96, longitudinal slips are not affected from the steering and degraded vehicle deceleration plotted in figure 4.100, since reference signal is set constant at the minimum level of 0.04 slip for icy road. Lateral response can be observed from figures 4.97, 4.98 and 4.99.

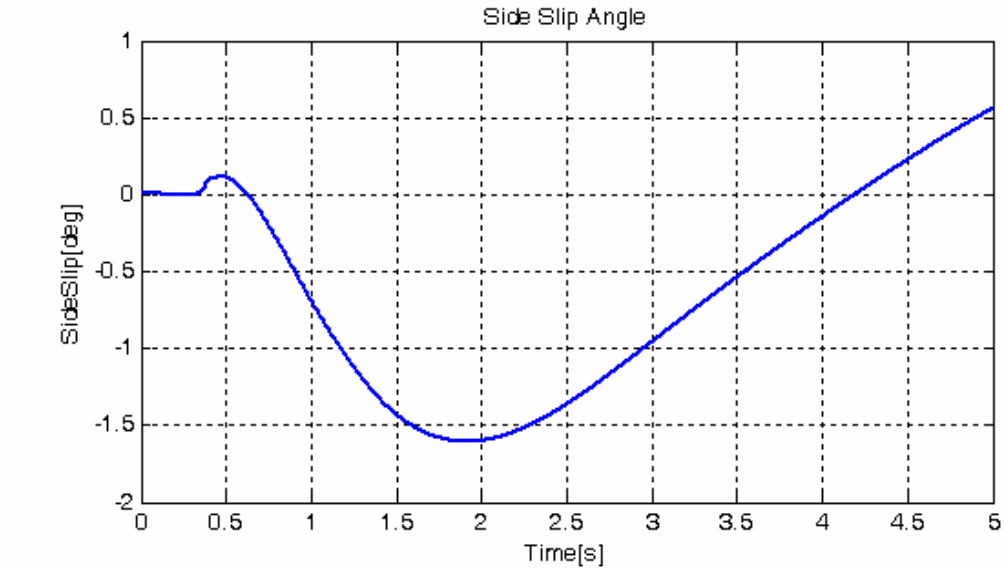

Figure 4.98. Sideslip angle on icy road for 40º step input for FLC

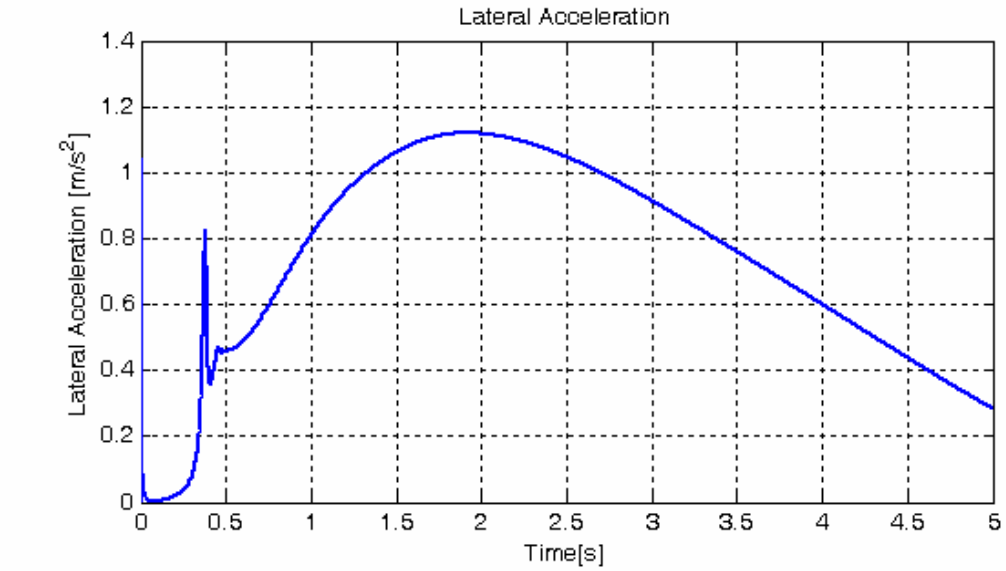

Figure 4.99. Lateral acceleration on icy road for 40º step input for FLC

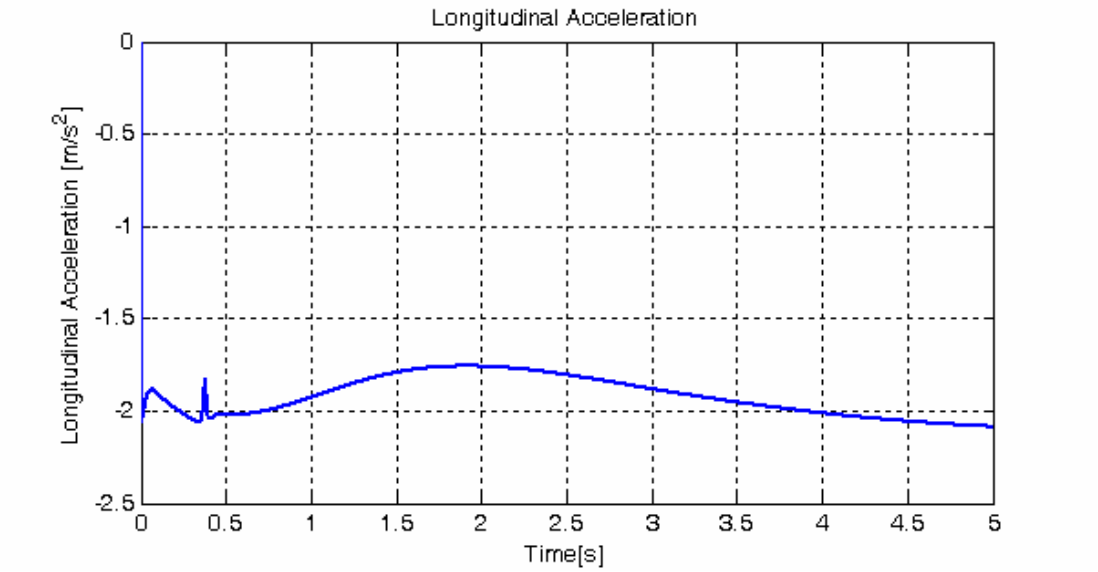

Figure 4.100. Longitudinal acceleration on icy road for 40º step input for FLC

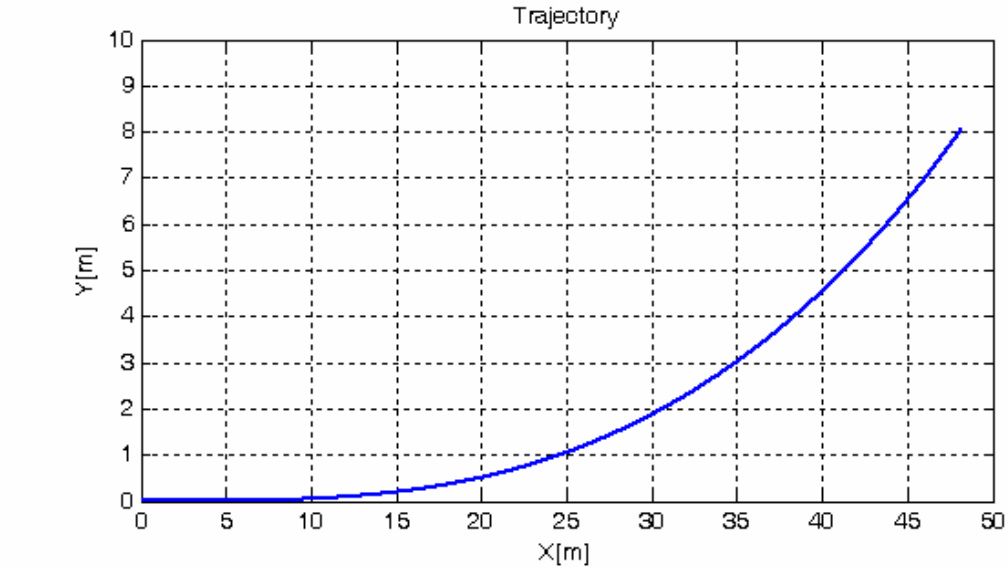

Figure 4.101. Vehicle trajectory on icy road for 40º step input for FLC

Vehicle traveled 48.15 meters in the longitudinal direction and 8 meters in the lateral direction. In evaluating the trajectory curve provided in figure 4.101, it should not be forgotten that the initial speed of the vehicle was 50 km/h at the start of the simulation.

4.3. ABS PERFORMANCE WITH QUANTIZING ACTUATOR

ABS controller was designed for a continuous actuator. The actuator is thought to be able to apply any brake torque change rate that is decided by the low-level controller continuously between certain predetermined maximum and minimum limits; but in application the actuation may have a quantizing nature.

In hydraulic and pneumatic based systems, the pressure in the wheel brake cylinder is mostly maintained through state pulsing of the valves. A popular example is the pulse width modulation (PWM) of the on/off type solenoid valves to control the flow of the fluid to the wheel brake cylinder. A certain pressure building rate can be decided by frequency of the signal and the duty ratio indicative of the valve on/off time; however the resolution of the brake torque changing rate has limits due to many reasons including: valve response times, microcontroller issues and wear concerns.

The current design may show a degraded performance for low resolution quantizing actuators. Although it is not a design objective, it is desired to evaluate the controller with a quantizing actuator to examine wide-range applicability of the design and see the low-level controller limits.

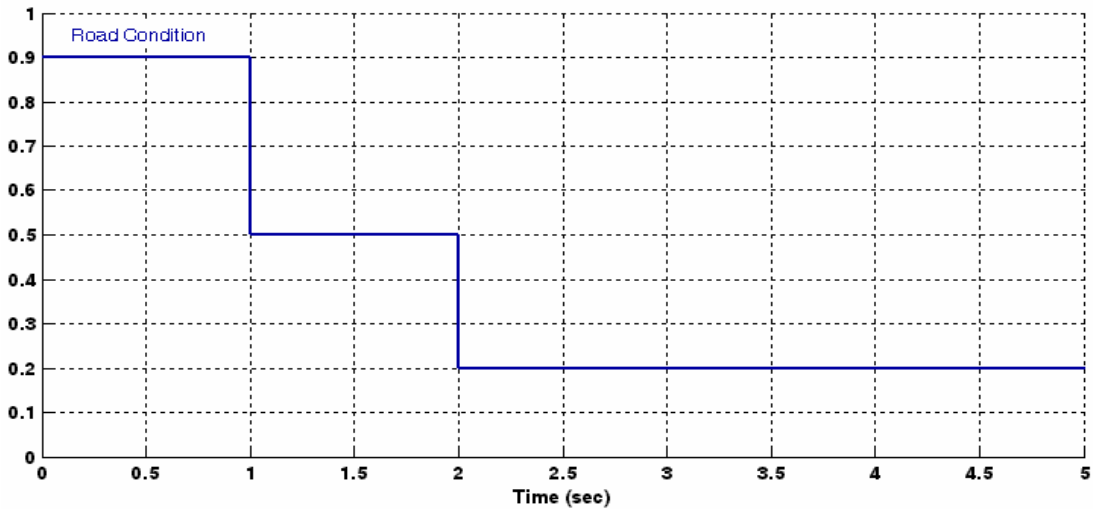

Figure 4.102. Road surface condition

For this purpose, the controller outputs are discretized to 5000 N.m/s increases between the limits -30000 N.m/s and 30000 N.m/s and in this configuration, simulation tests were carried out for the two different low-level controller alternatives. The road surface was chosen to be deliberately a road with changing surface friction levels to challenge the tracking performance of the ABS controller. The changing friction coefficient of the emulated road surface is plotted against time in figure 4.102. The road is initially a dry asphalt surface which changes into wet asphalt conditions at t = 1 s and finally has icy road surface property from t = 2 s until the end of simulation. Initial velocity of the vehicle was 90 km/h and a total braking torque of 6000 Nm was applied with 70:30 front to rear ratio, the same as in the previous simulations. Simulation results for continuous actuator for the same case can be observed in Appendix B.

Figures 4.103, 4.104 and 4.105 present the results of the simulation of ABS with the low-level fuzzy logic controller.

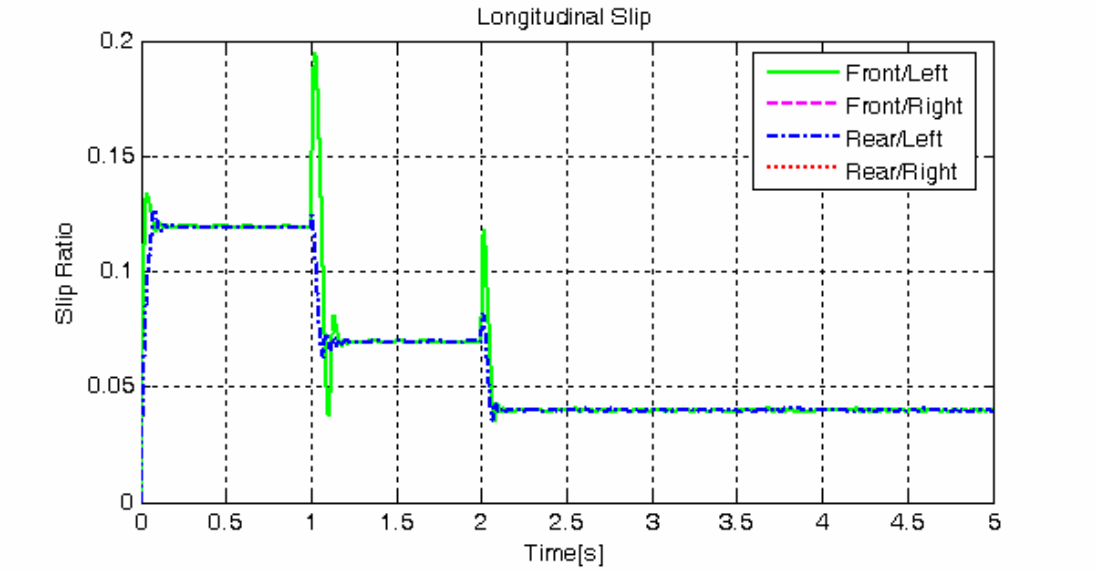

Figure 4.103. Longitudinal wheel slip for quantizing FLC

Longitudinal wheel slip response is shown in figure 4.103, despite the discretized actuator, the controller managed to track the reference slip signal with a performance

very close to continuous actuation. Though barely discernible, steady-state response of the controller is oscillatory. Figure 4.104 illustrates the reference slip signal for the front/left wheel. The signal takes sequentially slip values of 0.12, 0.07 and 0.04 for dry, wet and icy road conditions.

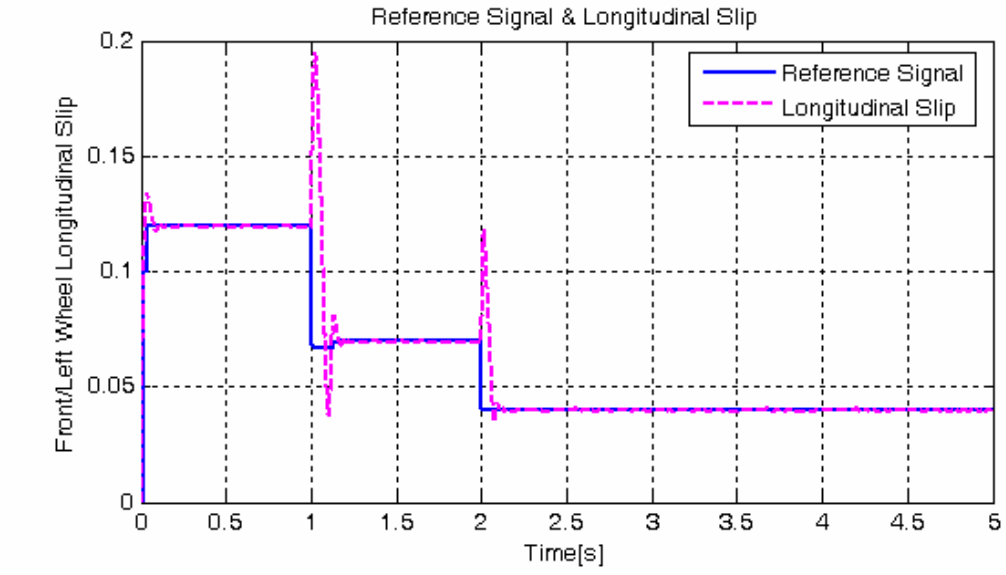

Figure 4.104. Reference slip signal for front/left wheel for quantizing FLC

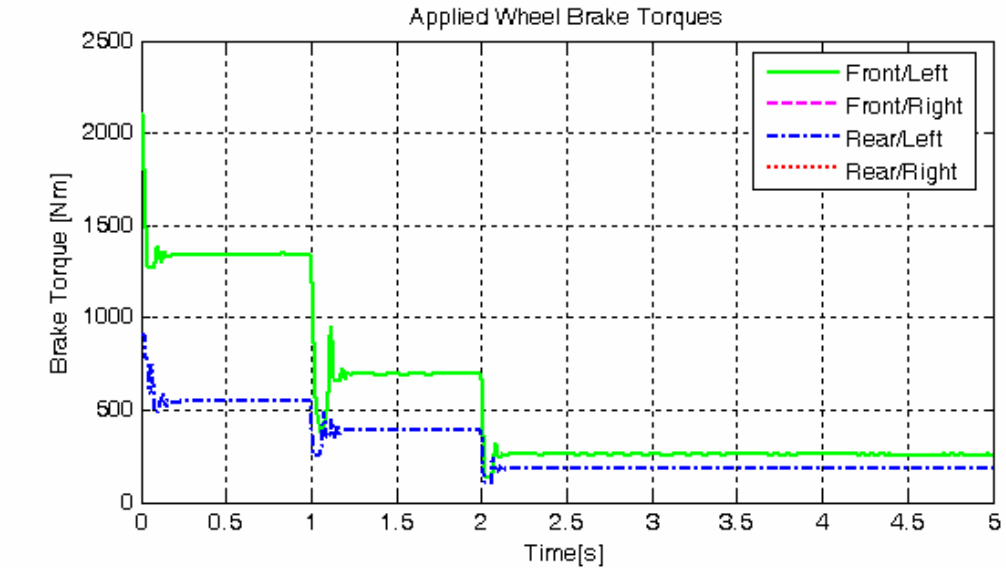

Figure 4.105. Wheel brake torques for quantizing FLC

Figure 4.105 shows the modulation of wheel brake torques. Effect of the discrete brake torque change rate is hardly visible; the general response behavior is preserved.

The performance of the ABS with PID low-level controller for quantizing actuator is illustrated in figures 4.106, 4.107 and 4.108.

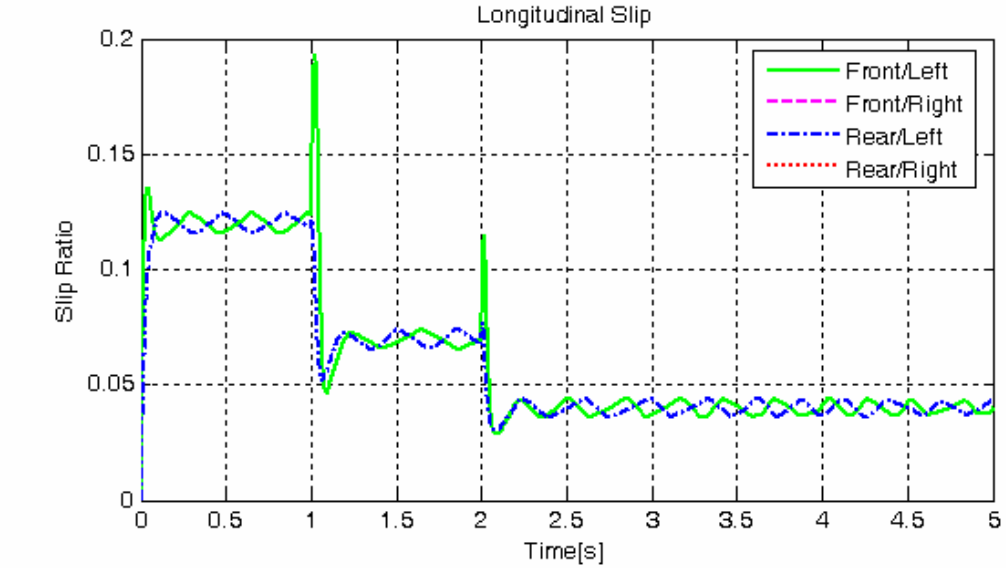

Figure 4.106. Longitudinal wheel slip for quantizing PID

Figure 4.106 presents longitudinal slip development at the wheels. The response has noticeable oscillations around steady-state for each road segment, which is directly the result of the quantization. The behavior resembles the cycling nature of the customary ABS systems. In the case of fuzzy logic controller, the response had also a degraded tracking performance; however the oscillations were not apparent as it is for PID here.

Figure 4.107 provides a superimposed plot of the front/left wheel reference slip signal and longitudinal slip development. The signal is almost identical to the fuzzy controlled system. It is important to note that despite the oscillatory behavior, the

tracking performance of the controller is successful. Figure 4.108 depicts the applied brake torques. The quantized actuation shows its effects on the response.

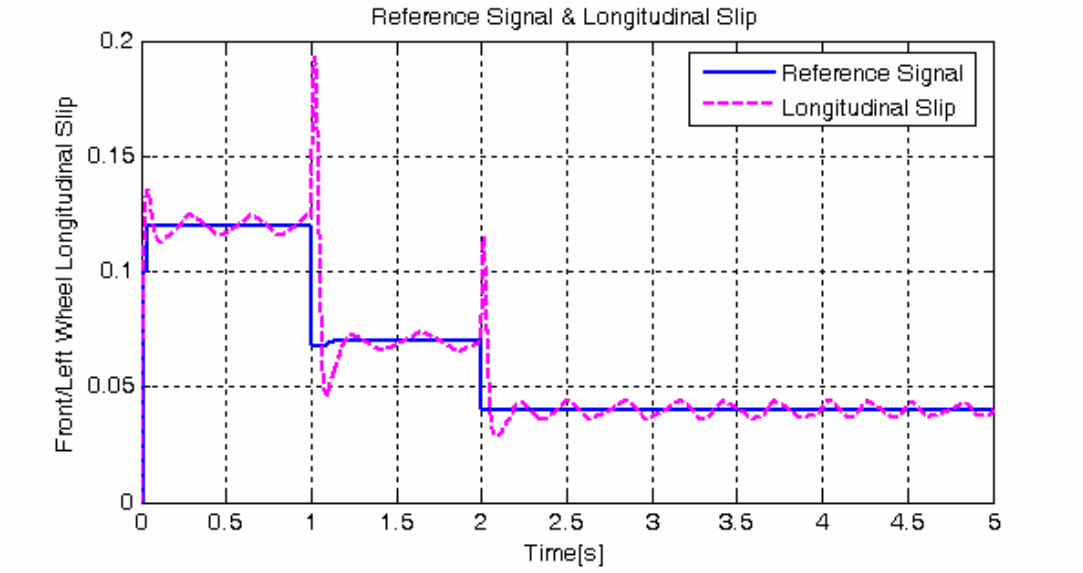

Figure 4.107. Reference slip signal for front/left wheel for quantizing PID

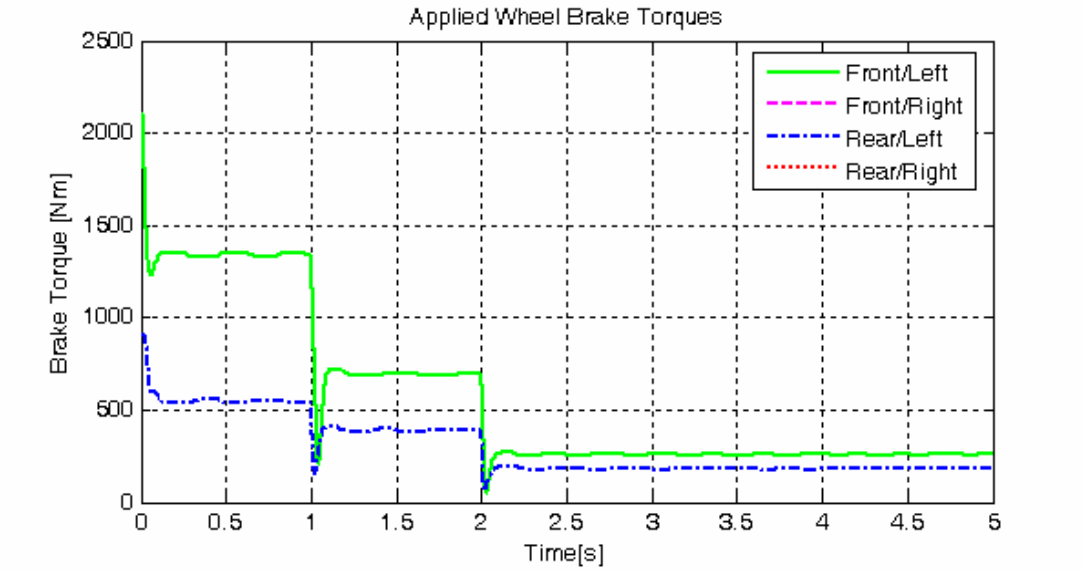

Figure 4.108. Wheel brake torques for quantizing PID

4.4. ABS PERFORMANCE FOR NOISY MEASUREMENTS

In this part, the performance of the ABS controller is tested for noisy measurement data. In application, longitudinal vehicle acceleration, wheel angular acceleration and longitudinal wheel slip data are definitely subject to the sensor noise and uncertainity. In the design, ABS was thought to share the estimated state variables of the Integrated Active Safety System; however at this point it is desired to test the robustness of the proposed controller to noisy data and examine the applicability and flexibility of the design.

The system uses the Kalman filtering method described previously in Chapter 3 to estimate the vehicle speed, which is required for calculation of longitudinal wheel slip. The noise in wheel angular velocity and vehicle acceleration measurement is modeled as normally distributed white noise with zero mean. The longitudinal acceleration signal for the high-level controller is filtered with low-pass 3^{rd} order Bessel filter; however in slip calculation the noisy wheel angular speed measurement is used without any signal processing.

For the study, the road surface represented by figure 4.102 is used which has surface friction transitions sequentially between dry, wet and icy road conditions. The chosen road profile is ideal to observe the vehicle response at the three different road conditions and evaluate the adaptation performance of the controller to changing friction levels. A total braking torque of 6000 Nm with 70:30 front/rear ratio was applied at the start to a vehicle driven in a straight-line with 90 km/h initial velocity. Results for the low-level fuzzy logic and PID controllers are presented below.

Performance of the ABS for the case of fuzzy logic controller can be observed from the figures 4.109 to 4.113. The noisy vehicle acceleration and wheel angular speed signals are the only inputs to the ABS for this study and have noise variances of 0.80 m^2s^{-4} and 0.05 rad^2/s^{-2} respectively. Figures 4.109 and 4.110 show the vehicle longitudinal acceleration signal and wheel angular velocity signal corresponding to the front/left wheel, which are both corrupted with the aforementioned noise.

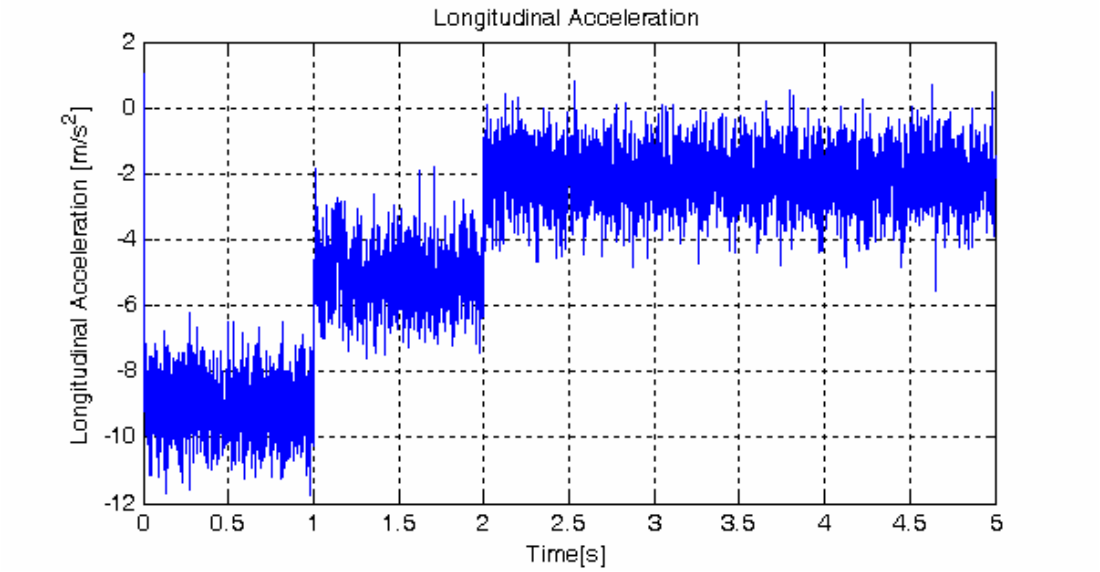

Figure 4.109. Noisy longitudinal acceleration signal for the case of FLC

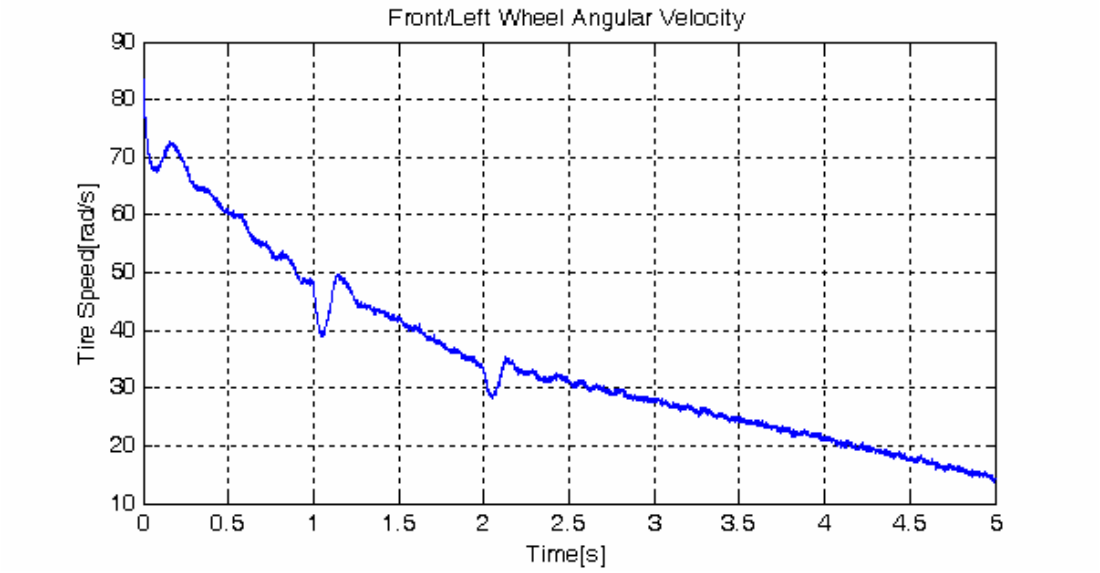

Figure 4.110. Noisy front/left wheel angular speed signal for the case of FLC

Figures 4.111 and 4.112 show the longitudinal wheel slip ratios and reference signal for the front/left wheel. The oscillatory wheel slip response is noticeable; however note that, following the overshoots at the transition points, average slip is very close to the reference slip signal. Despite the degraded performance, the controller is

obviously successful since it manages to limit the cycling in a certain margin. Note also that high-level controller produced a reference signal with ideal slip values for the corresponding surface conditions as in the previous simulations without noise.

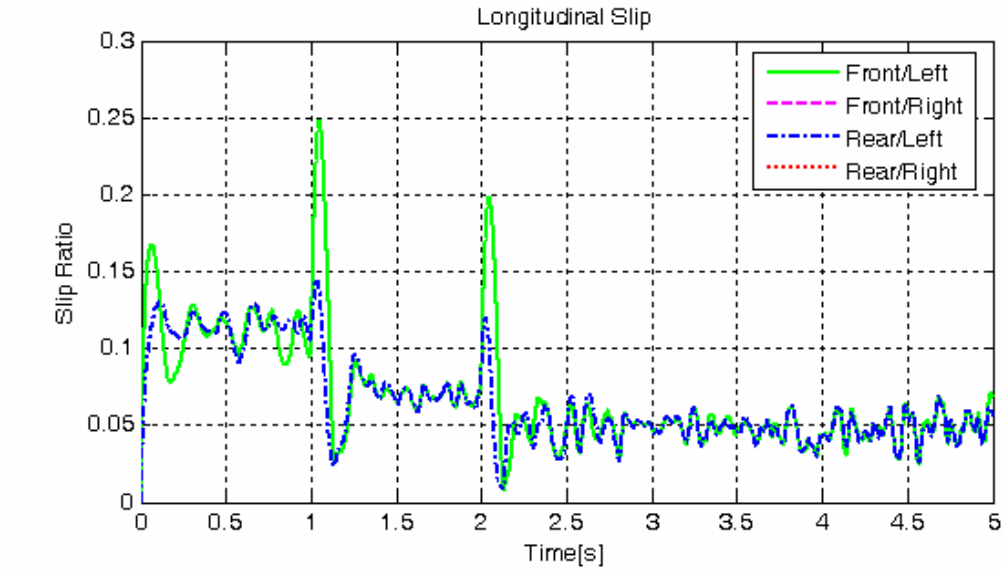

Figure 4.111. Longitudinal wheel slip for noisy measurements for FLC

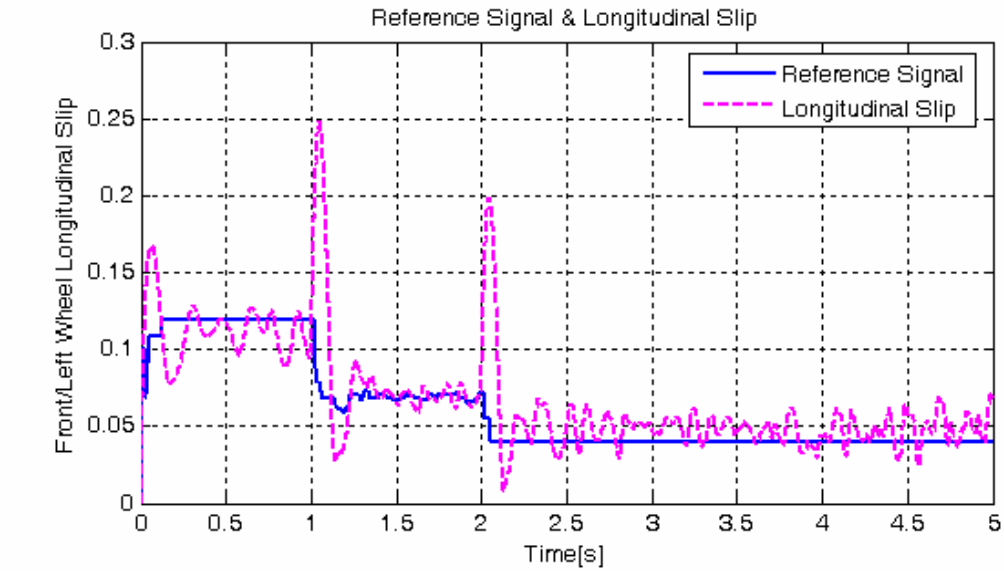

Figure 4.112. Reference slip for front/left wheel for noisy measurements for FLC

It is observed that after 4 seconds, the slip response shows a more oscillatory behavior and grows distant to the reference slip signal. The erroneous trend and increased oscillations are due to the degraded performance of the Kalman estimator at low speeds. It is important to note that however, the general oscillatory character of the longitudinal slip response is not related to the estimation of the vehicle speed but it is mostly due to high-frequency noise in the wheel angular speed signal used in the calculation of wheel slip and angular acceleration signal for the controller.

Figure 4.113 illustrates the regulation of brake torques at the wheels. The high frequency cycling of the wheel brake torques is notable.

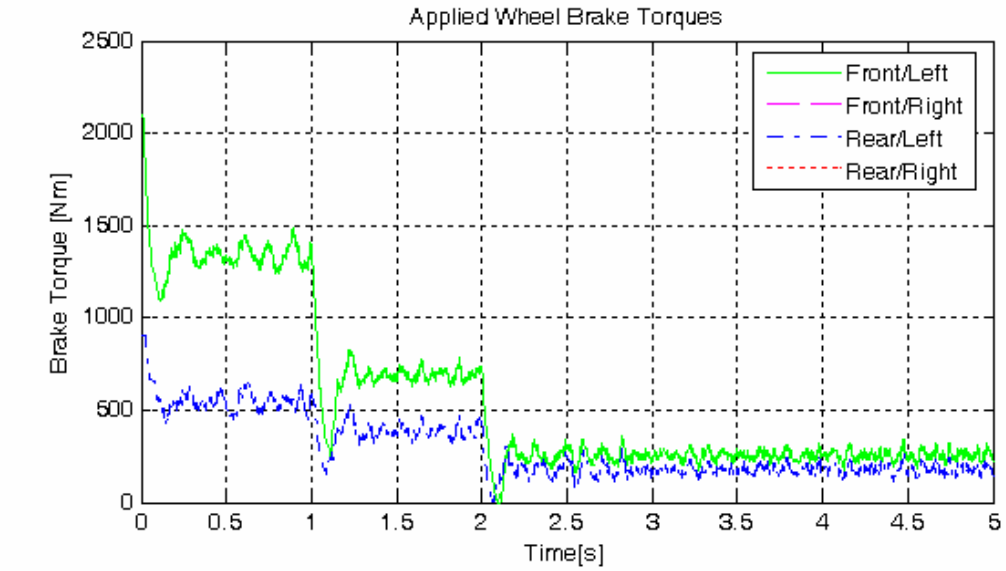

Figure 4.113. Wheel brake torques for noisy measurements for FLC

Figures 4.114, 4.115 and 4.116 are the results of the simulation with the low-level PID controller. Noisy vehicle acceleration and wheel rotational speed signals are not depicted here for this case, since the plots are very similar to figures 4.109 and 4.110. Longitudinal slip and reference slip signal for the front/left wheel presented in figures 4.114 and 4.115 show that PID controller is more successful in the presence of the noise compared to fuzzy logic controller case. The response still has an

oscillatory character; however PID controller provides clearly an improved performance considering the amplitude of oscillations, steady-state response and magnitude of overshoots.

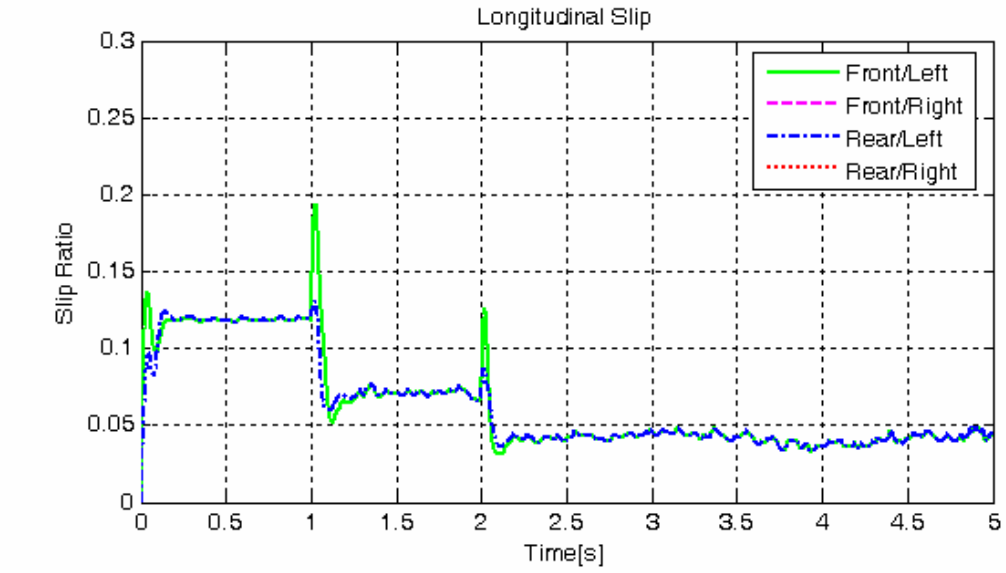

Figure 4.114. Longitudinal wheel slip for noisy measurements for PID

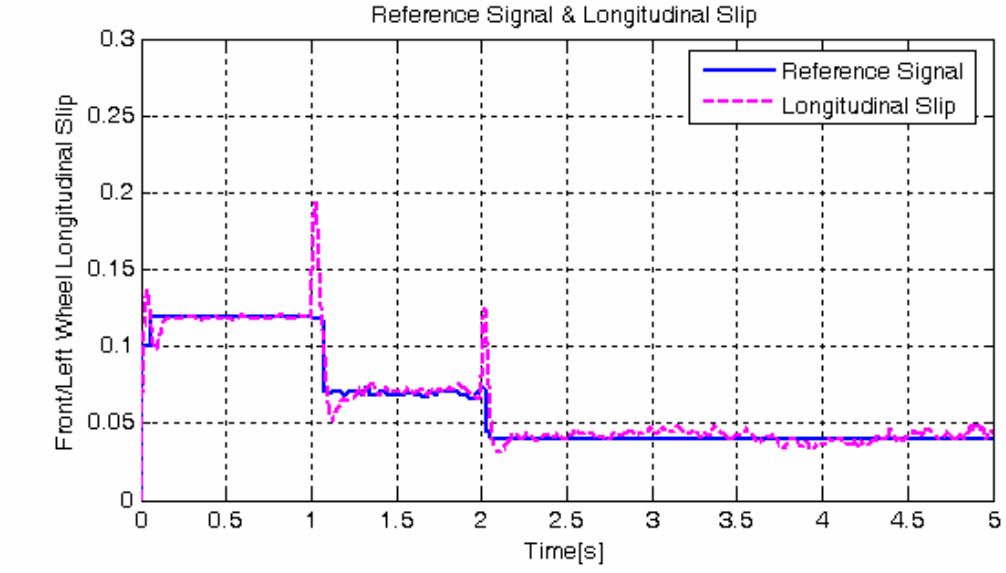

Figure 4.115. Reference slip for front/left wheel for noisy measurements for PID

In the study, in low-speeds, an unexpected characteristic of wheel slip was observed to develop independent of control action, which is probably due to solver issues related to noise, particularly in acceleration data. The implemented Kalman filter algorithm dynamically modifies noise covariance matrices below a certain speed to obtain a more reasonable result; nevertheless the unexpected characteristic is, though barely, still observable after t = 3.5 s in figure 4.115.

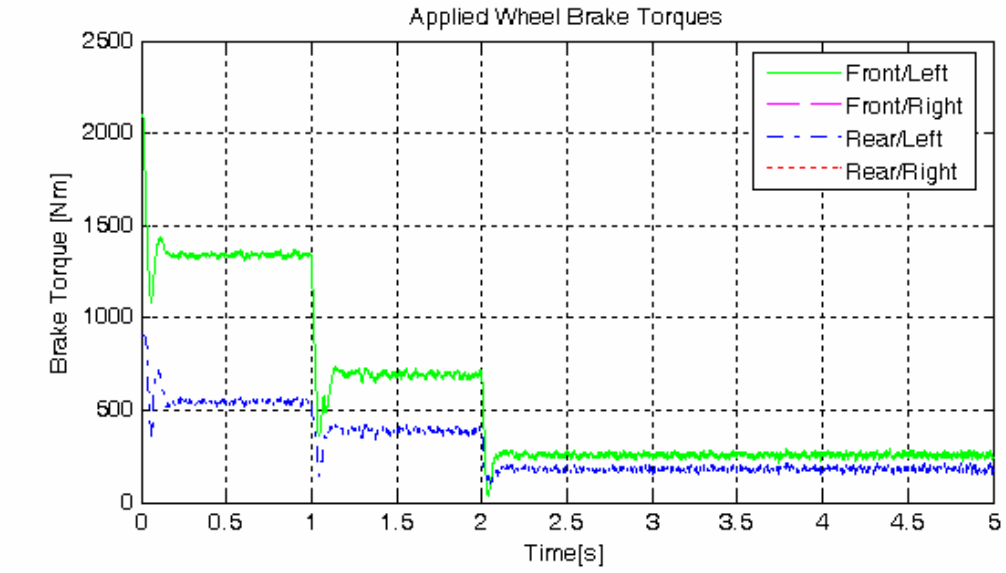

Figure 4.116. Wheel brake torques for noisy measurements for PID

Figure 4.116 shows the wheel brake torques. Despite the enhanced tracking performance of the PID controller, the brake torque regulation has still the undesirable high-frequency response behavior.

CHAPTER 5

INTEGRATION OF ABS WITH AN INTEGRATED ACTIVE SAFETY SYSTEM

Integrated active safety system concept is the last stage of the development of vehicle safety enhancement technologies. It is basically integration of previously developed individual systems under one roof. Despite the usually conflicting objectives of integrated control with flexible marketing strategies of supplier companies, the concept offers promising benefits that can not be overlooked and there are increasing efforts towards systems integration in vehicle active safety applications. Integrated active safety system approach can reduce complexity of the overall system, avoid costly duplication of hardware components and prevent unexpected interactions between subsystems which are mostly due to results of the traditional add-on approach in design. Through achieving control coordination, it is also possible to enhance performance of the previously individually operated systems [37-39].

In this chapter it is intended to present a discussion over integration possibilities for the proposed antilock braking system controller and expected benefits from the coordination of the systems.

Current production ABS is based on a rule-based control strategy which utilizes extensive tables for different brake scenarios [4]. The high level of complexity associated with these systems is undoubtedly a serious issue when further improvement and extensibility are considered. Systems complexity is not only a primary objective of integration but also unsurprisingly a severe limitation for coordination of the systems. The proposed design addresses this by adopting a

subsystem approach and thus decomposing the complicated problem into more manageable subproblems.

The task of the proposed ABS controller is formulated as dynamic reference slip tracking where a high-level subcontroller determines the reference longitudinal wheel slip ratio according to changing road conditions and a low-level subcontroller system attempts to track this signal through modulating brake torque. The structure provides a highly flexible platform for integrated control with other active safety enhancement control systems and in particular with wheel-braking based active yaw stability control. In determination of the reference slip, coordinated decision-making may contribute to achieve a vehicle response along driver demands and the low-level controller can be used directly as a part of a yaw stability control system.

The concept of the adopted hierarchical control structure in the study is actually based on the idea that decisions about the dynamic behavior of the vehicle should be made at a high level considering driver preferences and in a unified manner with different vehicle dynamics control systems. In combined braking and steering maneuvers, coordination of ABS with an active yaw stability control system may result in a vehicle dynamic response closer to the intention of the driver. In current production ABS systems and in literature, directional control is defined as a main objective; however control algorithms work irrespective of the steering input and thus driver request or any other parameter regarding lateral response of the vehicle. A yaw stability controller calculates an ideal yaw rate value representing intended course of the driver for operation and this information can be shared with the high-level controller of the proposed ABS. Reference slip for the wheels may be chosen specifically to generate a brake moment in the direction of the path considering the understeer behavior in ABS operation observed in the presented simulation study. On the other hand, braking force should be maximized as much as possible as well. In such a case, the priority or weighting is decided according to predicted driver intention. A simpler application is to reduce directly reference slip values according to comparison of actual and desired yaw rate to increase the lateral generation capability of the tires at the cost of a lengthened stopping distance. In either case, a

study regarding analysis of driver behavior in emergency braking maneuvers is definitely necessary and precrash systems may be helpful in assessing the situation as well.

Hard braking on split coefficient of friction surfaces, where right and left side of the road has different friction levels, may result in a loss of yaw stability of the vehicle and is definitely an important issue which can be encountered in everyday driving. Interaction of the high-level controller with an active yaw stability controller mentioned above, can help in such a situation. Reference wheel slips are arranged this time to create a corrective yaw moment in the opposite of the turning direction. For this case, considering the objective of shorter stopping distances, it can be preferable to use the method of decreasing reference slip ratio of a single wheel while maximizing braking force from other tires.

The duty of the low-level controller is basically to track the reference slip signal sent by the high-level controller through modulating brake torque at the corresponding wheel. Reference wheel slip assignment method is also appropriate for wheel braking based yaw stability control. Buckholtz [40] uses reference slip assignment for each corner of the vehicle to track a desired yaw rate. The proposed low-level controller can be readily employed for this purpose as well. In the supervision of a coordination logic block or master controller, wheel-braking based active yaw stability control can intervene when it is necessary by simply dispatching reference slip signals directly to the low-level slip controller of each wheel individually. By reference slip tracking, yaw stability control also ensures the prevention of wheel-lock since the low-level controller can maintain wheel slip at every point of the μ-slip curve.

In a unified structure, the low-level controller is positioned as a common lower level module where ABS and active yaw controller, in interaction, determine and assign reference wheel slips as high level functions. Natural extension of this structure is a fully centralized control. Figure 5.1 depicts such an approach. This model requires a specific design for an active yaw controller based on reference slip tracking and a single low-level controller for actuator is not preferable considering failure

management issues in case of failure of the communication link or the low-level controller. A more decentralized control approach can provide redundancy for failsafe operation and is easier to implement. In this configuration, active yaw controller uses the low-level ABS controller only as an explicit function to prevent wheel slippage exceed beyond a certain threshold while it modulates braking torques independently to track desired yaw dynamics. A coordination algorithm constantly monitors longitudinal wheel slip and switches control when a certain slip ratio is reached and wheel slippage is maintained at that point by merely sending the signal as a reference to the low-level controller. In this case, wheel braking torques are directly adjusted by the low-level controller of ABS. The coordination logic may return control to normal operation when the yaw controller demands a wheel braking torque level lower than the torque applied by the low-level ABS controller. For yaw control, it is desirable to limit the wheel slippage to the linear range of the μ-slip curve in which case the reference threshold should be around the peak. A more predictable control is achieved by this way; however a μ estimation algorithm is necessary for this application.

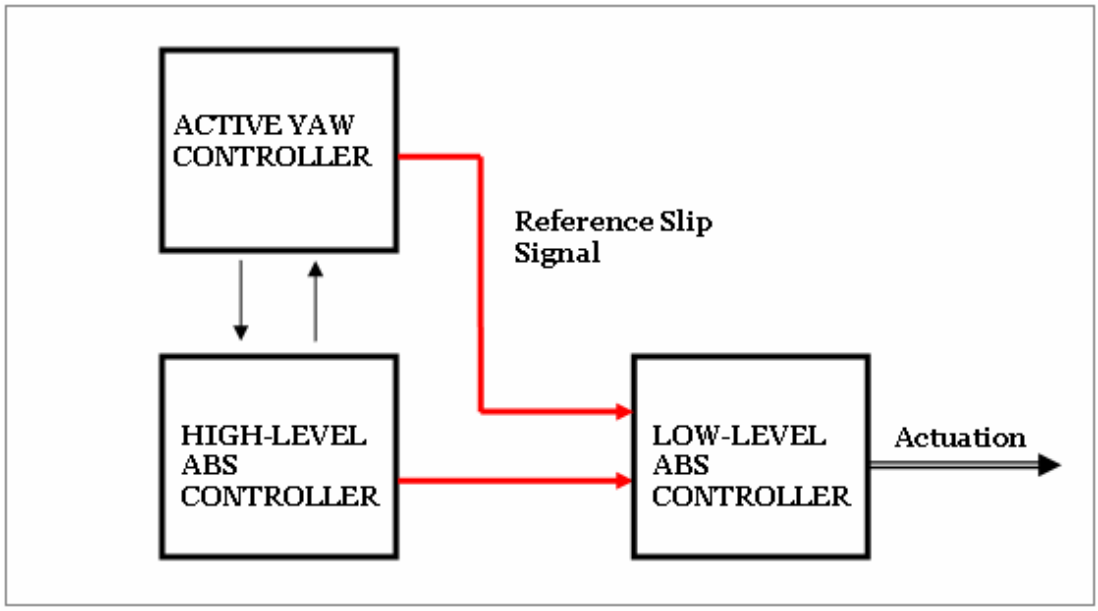

Figure 5.1. Integrated control structure

Sharing of hardware components is without doubt, the first step of integration of vehicle safety enhancement systems. In this study, ABS controller is thought to benefit from the sensors of an integrated system, particularly in the calculation of wheel slip and thus longitudinal velocity in the tire plane. Calculation of wheel slip is a serious issue in ABS design. Conventional ABS works based on only wheel angular speed information and there exists considerable uncertainity in the estimation of wheel slip; however the method of reference slip tracking employed in the design requires an accurate calculation. For this purpose, controller takes longitudinal and lateral acceleration information of the vehicle at center of gravity, yaw rate and steering wheel angle data, all of which can be measured directly through sensors of an integrated active safety system.

CHAPTER 6

CONCLUSIONS

In this thesis work, a design methodology for an antilock braking system (ABS) for road vehicles was developed. In the study, a flexible perspective is adopted both in the controller design approach and presentation of the work considering future integration with an integrated vehicle safety enhancement system controller. The eventual design was realized through extensive simulations on a nonlinear 8 DOF vehicle model constructed in MATLAB/Simulink. The results of the detailed simulation work presented in Chapter 4 show clearly the successful performance of the proposed ABS controller.

In developing the vehicle dynamics model, the intention was to realize an accurate model for proper simulation of emergency braking maneuvers. Although in literature, most researchers do not include steering response analysis in ABS design studies, lateral response in braking maneuvers is important for the objectives of this thesis study and consequently for design procedure and analysis of results. For this purpose, the vehicle model was decided to include longitudinal, lateral, yaw and roll degrees of freedom and effects of lateral and longitudinal weight transfer. Braking system was not modeled to have a more general design approach.

The design approach developed for the ABS controller takes account of more than one aspect. With the adopted hierarchical design of the ABS controller, it is intended to provide a flexible base for integration with ESP. In the supervision of a coordination logic block, wheel-braking based active yaw stability control can intervene when it is necessary by simply dispatching reference slip signals directly to the designed low-level slip controller of each wheel individually or in a more

decentralized control structure, active yaw controller can use the low-level ABS slip controller as an explicit function to prevent the slippage exceed beyond a certain threshold. ABS can also benefit from the integration; in cornering, optimal wheel slip can be calculated with the help of a yaw controller and through analysis of driver reaction. Subsystems of the ABS controller can be readily used as functions in centralized control structure of an integrated active safety system. The arrangement offers an easily expandable structure and is also preferable for diagnostic purposes. From the ABS control view, reference slip tracking has certain advantages over conventional ABS control which adopts limit cycling of longitudinal wheel slip. Maintaining slip at dynamically calculated setpoints adjusted according to surface conditions can provide an improved performance in stopping distances. The conducted simulations indeed showed that it is possible.

The design methodology presented in this study offers both fuzzy logic control and PID control methods for low-level slip controller. Performance of ABS for the two controller alternatives was tested through simulations and results showed that controllers produce almost equivalent results for all the simulated cases. Even in the presence of steering and for changing road surface conditions, slip controllers track the reference signals successfully. In all test cases, by maintaining slip close to the reference signal, a considerable improvement in stopping distances was achieved.

In combined braking and steering simulations, the stability was maintained for all cases, but it was observed that the vehicle exhibited understeer behavior which adversely affects the maneuverability. The simulations showed, however, that it is possible for driver to compensate for the degraded lateral response by applying a larger steering input. In cornering, the adopted high-level controller design indirectly leaves the initiative to the driver since, due to vehicle acceleration based surface condition estimation, reference slip and thus, braking force decreases in proportion to steering intensity but the controller favors principally maneuverability over stopping distances in the presence of steering.

In simulations for adverse road conditions, the vehicle was observed to sustain elevated wheel slippage, reaching slip ratios over 70 % on emulated icy road. This high overshoot of the longitudinal wheel slip was directly related to the limited brake torque change rates since both fuzzy logic and PID slip controllers were designed to reduce brake torques at the maximum permitted rate. It should be also noted that the high slippage observed for front axle wheels on wet and icy road conditions is due to the reduced normal loading on front wheels on slippery surfaces as a result of decreased longitudinal weight transfer. Dynamic brake distribution can reduce the elevated wheel slip considerably and this is a clear contribution of "integration" to the performance of antilock braking system.

ABS controller was designed for a continuous actuator capable of producing wheel braking torques at any rate between predetermined limits; nevertheless the controller was tested for a quantizing actuator as well. Simulation results illustrated the successful performance of the ABS for both slip controllers, even for a road surface with changing levels of coefficient friction.

The proposed ABS controller is thought to benefit from the sensory hardware of the integrated active safety system. This brings certain advantages compared to individually operating ABS controller units. Note that the conventional ABS works based on solely wheel angular speed information. In the simulations, the controller used the signals from the vehicle model calculating necessary input variables through dynamic equations. The performance of the controller was also simulated for noisy signals to show the applicability of the design. For this purpose a Kalman filter was used to estimate longitudinal wheel slip ratios. Simulation results showed that the controller is still functional for both low-level slip controller alternatives though the wheel slip response exhibited oscillations in a limited range.

6.1. FUTURE WORK

As a future study, work on the following items is thought to be important and useful for the improvement of the proposed design and contributory to the methodology presented in this text.

- Hardware in-the-loop simulation (HILS) is definitely advisable for the study.

- Braking system can be modeled for a specific system configuration with transportation delays to realize a more applicable controller design.

- Different control techniques can be used for the low-level controller; sliding mode control (SMC) may be appropriate for the adopted reference slip tracking approach.

- Performance of the ABS controller in coordination with an ESP controller is very important. Such a simulation would be certainly beneficial.

- Pitching motion can be included in the vehicle dynamics model; by this way, effect of road surface irregularities can be taken into account.

REFERENCES

[1] Solyom, S., “Synthesis of a model-based tire slip controller, Thesis, Lund Institute of Technology, 2002.

[2] Limpert, R., ”Brake Design and Safety”, , SAE Publications, Warrandale, PA., 1992.

[3] Kazemi, O., Abdollahpour, R., Sedeh, R.S., Kazemi, H., “An Adaptive Fuzzy Controller for Anti Lock Braking System (ABS)”, 13th Annual (International) Mechanical Engineering Conference, May 2005.

[4] Petersen, I., “Wheel Slip Control in ABS Brakes using Gain Scheduled Optimal Control with Constraints”, Ph.D. Dissertation, Department of Engineering Cybernetics, Norwegian University of Science and Technology, Trondheim, Norway 2003.

[5] “Bosch Automotive Brake Systems”, Stuttgart: Robert Bosch, distributed by SAE, Warrendale, PA., 1995.

[6] Bowman, J.E., Law, E.H. “A feasibility study of an automobile slip control braking system”, SAE Paper 930762, 1993.

[7] Shinomiya, T., Toda, T., et al, “The Sumitomo Electronic Antilock System”, SAE Paper 880320, 1988.

[8] Miyake, K., Yamaki, I., Fujita, T., “Four Wheel Anti-Lock Brake System (ABS) for Four-Wheel Drive Vehicles”, SAE Paper 880322, 1988.

[9] Watanabe, M., Noguchi, N. “A New Algorithm for ABS to Compensate for Road-Disturbance”, SAE Paper 900205, 1990.

[10] Hattwig, P., “Synthesis of ABS Hydraulic Systems”, SAE Paper 930509, 1993.

[11] Naito, T., Takeuchi, H., Kuromitsu, H., Okamoto, K., “Development of Four Solenoid ABS”, SAE Paper 960958, 1996.

[12] Kempf, D., Bonderson, L., Slafer, L., “Real Time Simulation for Application to ABS Development”, SAE Paper 870336, 1987.

[13] Lee, K., Jeon, J., Hwang, D., Kim, Y., “Performance Evaluation of Antilock Brake Controller for Pneumatic Brake Systems” - Industry Applications Conference, 38th IAS Annual Meeting, 2003.

[14] Day, T.D., Roberts, S.,G., “A Simulation Model for Vehicle Braking Systems Fitted with ABS”, SAE Technical Papers 2002-01-0559, 2002.

[15] Madau, D.P., Yuan, F., Davis, L.I., Feldkamp, L.A. “Fuzzy Logic Anti-Lock Brake System for a Limited Range Coefficient of Friction Surface”, Proc. 2nd IEEE Int. Conf. on Fuzzy Systems, Vol.2, pp. 883-888, 1993.

[16] Mauer, G., Gissinger, G., Chamaillard, Y. “Fuzzy Logic Continuous and Quantizing Control of an ABS Braking System”, SAE Paper 940830, 1994.

[17] Layne, J.R., Passino, K.M., Yurkovich, S., “Fuzzy Learning Control for Antiskid Braking Systems”, IEEE Transactions On Control Systems Technology. Vol. 1, No. 2, June 1993.

[18] Yu, F., Feng, J.Z., Li, J., “A Fuzzy Logic Controller Design for Vehicle ABS with a On-Line Optimized Target Wheel Slip Ratio”, International Journal of Automotive Technology, Vol. 3, No. 4, pp. 165-170, 2002.

[19] Mirzaei, M., Moallem, M., Mirzaeian, B., Fahimi, B., “Design of an Optimal Fuzzy Controller for Antilock Braking Systems” Vehicle Power and Propulsion, IEEE Conference, 2005.

[20] Drakunov, S., Özgüner, Ü., Dix, P., Ashrafi, B., “ABS Control Using Optimum Search Via Sliding Modes”, IEEE transaction on control systems technology, Vo1.3 No. 1 March 1995.

[21] Lee, B.R., Sin, K.H., “Slip-Ratio Control of ABS Using Sliding Mode Control”, Science and Technology, KORUS 2000 Proceedings, 2000.

[22] Buckholtz, K.R., “Reference Input Wheel Slip Tracking Using Sliding Mode Control”, SAE Paper 2002-01-0301, 2002.

[23] Wellstead, P.E., Pettit, N. “Analysis and redesign of an antilock brake system controller” IEE Proc. Control Theory Appl., Vol. 144, No. 5, pp. 413-426, 1997.

[24] Watanabe, K., Kobayashi, K., Cheok, K.C., “Absolute Speed Measurement of Automobile from Noisy Acceleration and Erroneous Wheel Speed Information”, SAE Paper 920644, 1992.

[25] Daiss, A., Kiencke, U., “Estimation of Vehicle Speed Fuzzy Estimation in Comparison with Kalman-Filtering”, IEEE 0-7803-2550-8/95, 1995.

[26] Jiang, F., Gao, Z., “An Adaptive Nonlinear Filter Approach to Vehicle Velocity Estimation for ABS” - Proceeding of IEEE CCA/CACSD, Alaska, September, 2000.

[27] Allen, R.W., Rosenthal, T.J., et al, “Steady State and Transient Analysis of Ground Vehicle Handling”, SAE Paper 870495, 1987.

[28] Gillespie, T.,D., ”Fundamentals of Vehicle Dynamics”, SAE Publications, Warrandale, PA., 1992.

[29] Esmailzadeh, E., et al., “Dynamical Modeling and Analysis of a Four Motorized Wheels”, Vehicle System Dynamics, Volume 35, Number 3, March 2001.

[30] Schürr, H., Dittner, A., “A New Anti-Skid Brake System for Disc and Drum Brakes”, SAE Paper 840468, 1984.

[31] Yazicioglu, Y., “Development of a Fuzzy Controlled ABS to Improve Braking Performance and Stability of Automobiles”, M.S. Thesis, METU July 1999.

[32] Ogata, K., “Modern Control Engineering”, 4th Edition, Prentice Hall, 2002.

[33] Packard, A., “ME132 Lecture Notes”, UC Berkeley, Spring 2005.

[34] Hernandez, W., “A survey on optimal signal processing techniques applied to improve the performance of mechanical sensors in automotive applications” Sensors 2007, 7, pp. 84-102, 2002.

[35] Ünlüsoy, Y.S., “ME513 Vehicle Dynamics Lecture Notes”, METU 2006.

[36] Piancastelli, L., Castelli, S., “An ESP Fuzzy Control Algorithm optimized for tyre burst control”

[37] Ünlüsoy, Y.S., Balkan, T., Tekin, G., Şahin, M., Oktay, G., “Integrated Active Safety Systems for Road Vehicles”, Traffic and Road Safety International Congress, Vol. 1, pp. 479-493, Ankara, 17-19 May 2006.

[38] Gordon, T., Howell, M., Brandao, F., " Integrated Control Methodologies for Road vehicles", Vehicle System Dynamics, International Journal of Vehicle Mechanics and Mobility, Vol. 40, Nos. 1–3, pp. 157–190, 2003.

[39] Schilke, N.A., Fruechte, R.D., Boustany, N.M., Karmel, A.M., Repa, B.S., Rillings ,J.H., "Integrated Vehicle Control", Vehicular Technology Conference, 1989 IEEE 39th, Vol.2, pp. 868-877, May 1989.

[40] Buckholtz, K.R., "Use of Fuzzy Logic in Wheel Slip Assignment – Part I: Yaw Rate Control", SAE Paper, 2002-01-1221, 2002.

APPENDIX A

VEHICLE DATA

Table A.1. Vehicle parameters*

M	1300 kg	I_w	2.1 kg m2
M_s	1170 kg	I_{zz}	2500 kg m2
a	1.1 m	I_{xxs}	750 kg m2
b	1.4 m	K_R	0.55
h	0.5 m	K_Φ	45000 Nm/rad
h*	0.2 m	C_Φ	2600 Nm/rad/s
R	0.3 m	K_{rf}	-0.1 rad/rad
T	1.4 m	K_{rr}	0.1 rad/rad
Sr	1:18		

Table A.2. Allen tire model parameters [27] – P185/70 R 13

A0, A1, A2, A3, A4	1068, 11.3, 2442.73, 0.31, -1877	T_w	7.3 in
B1, B3, B4	-0.000169, 1.04, 1.69x10-8	T_p	24 psi
C1, C2, C3, C4	1, 0.34, 0.57, 0.32	CS/FZ	17.91
F_{ZT}	980 lbs	Ka	0.05

*Vehicle parameters are modified from the set of data used in the work of Esmailzadeh,E [29]

APPENDIX B

SIMULATION FOR A ROAD SURFACE WITH CHANGING FRICTION LEVELS

This part is the continuation of the simulation study presented in "4.2.1.4. Road Transitions Test". Figures from B.2 to B.9 present simulation results conducted for the road surface condition plotted (nominal friction coefficient, μ, against time) in B.1, sequentially for fuzzy logic and PID low level controller choices. Initially vehicle velocity is 90 km/h.

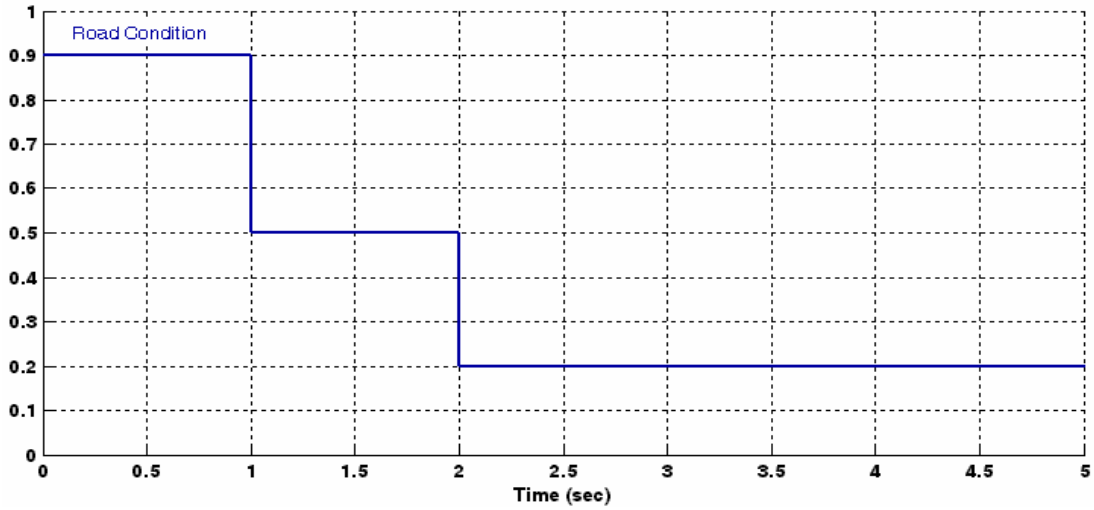

Figure B.1. Road surface condition

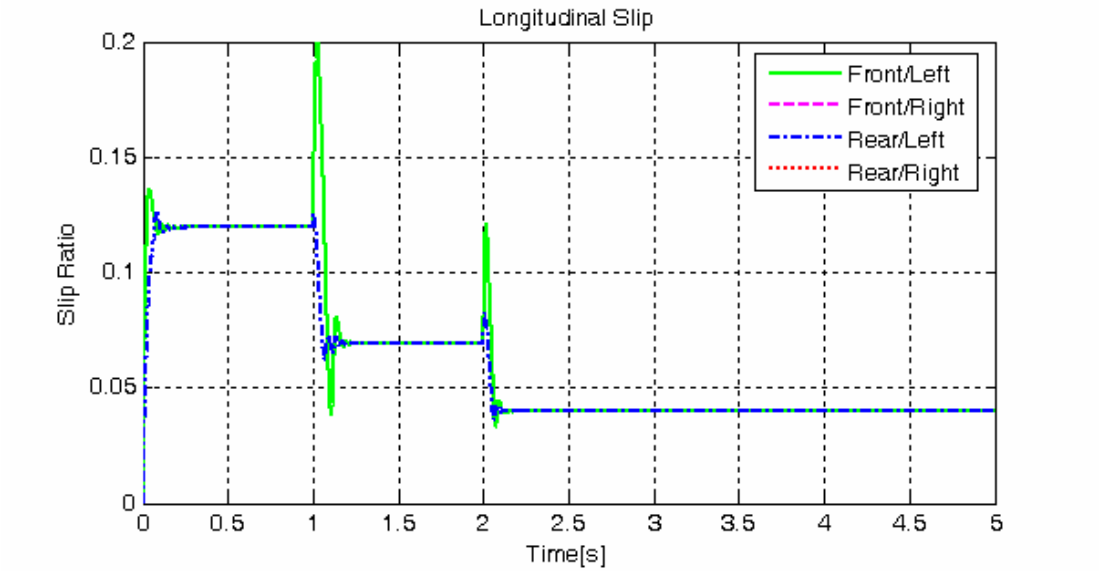

Figure B.2. Longitudinal wheel slip for changing road conditions for FLC

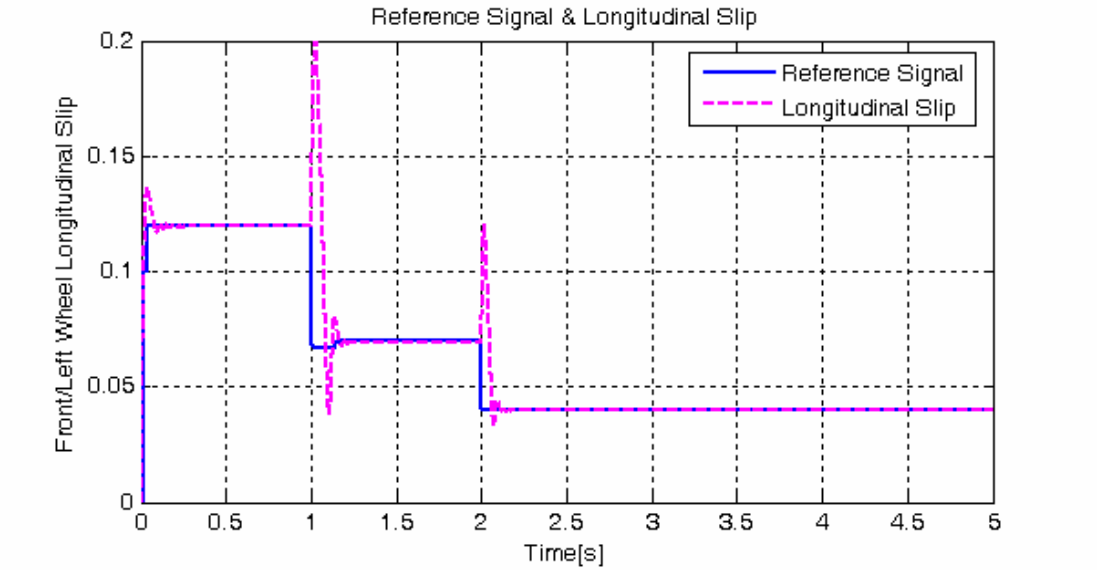

Figure B.3. Front/left wheel reference slip for changing road conditions for FLC

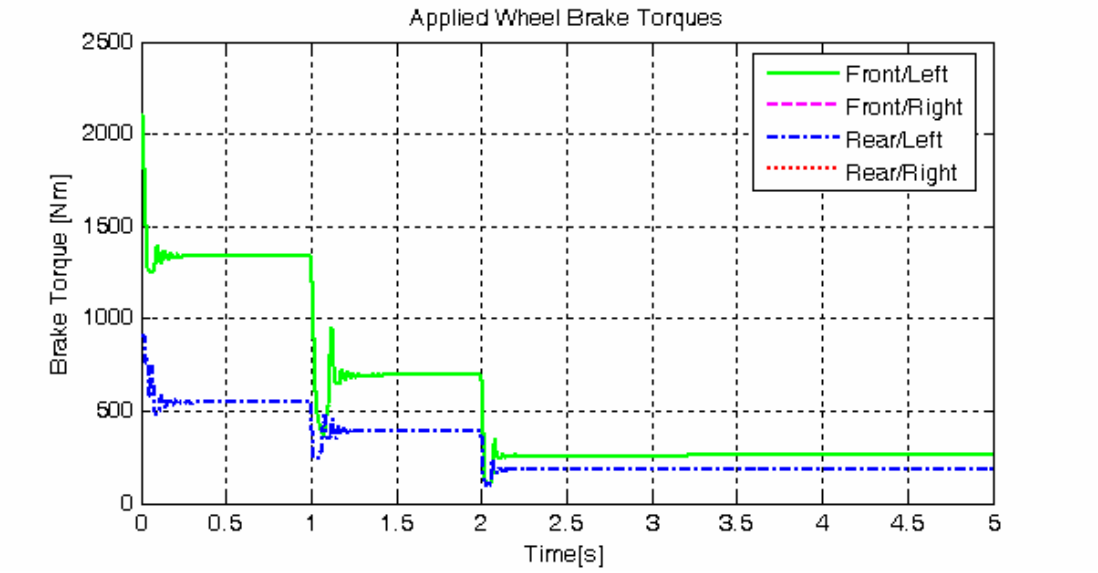

Figure B.4. Wheel braking torques for changing road conditions for FLC

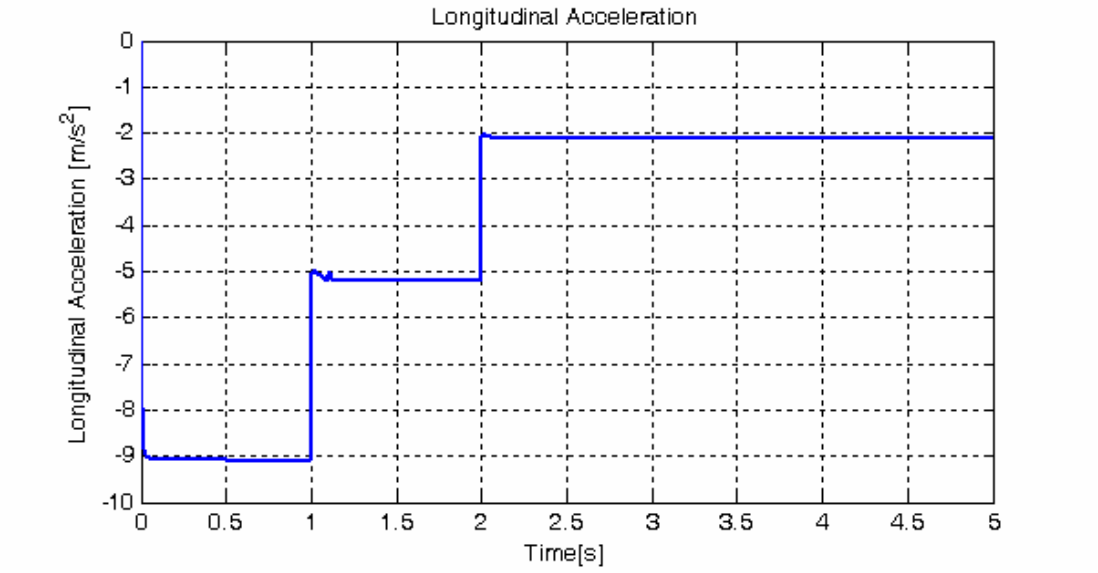

Figure B.5. Longitudinal acceleration for changing road conditions for FLC

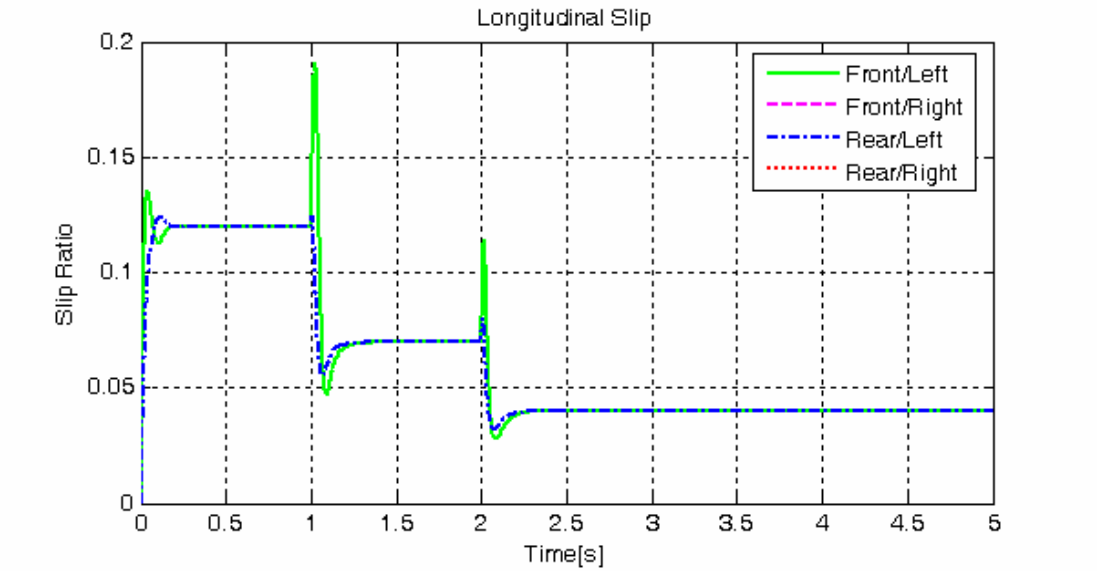

Figure B.6. Longitudinal wheel slip for changing road conditions for PID

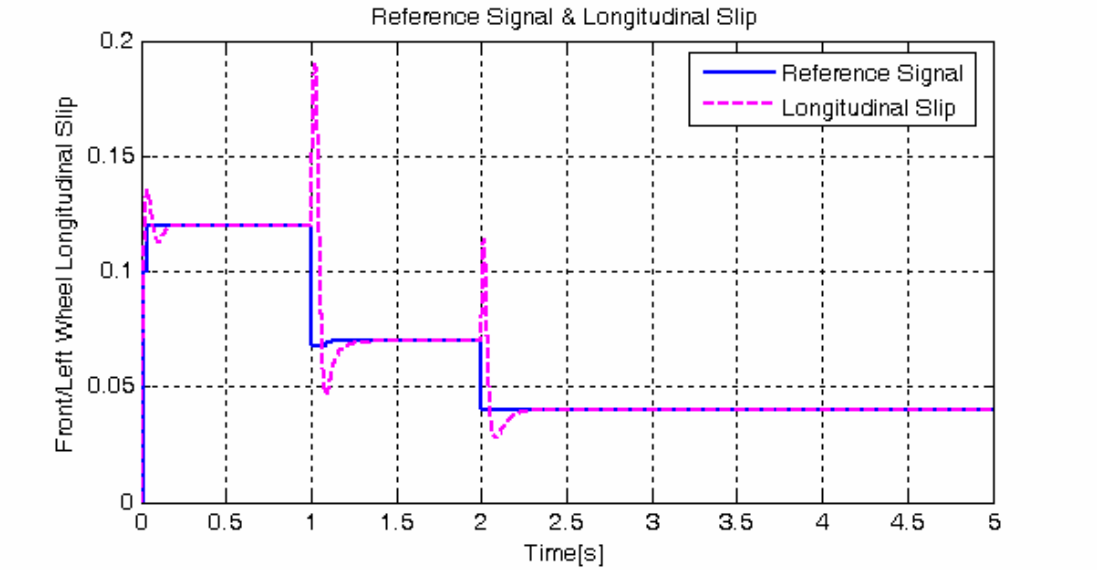

Figure B.7. Front/left wheel reference slip for changing road conditions for PID

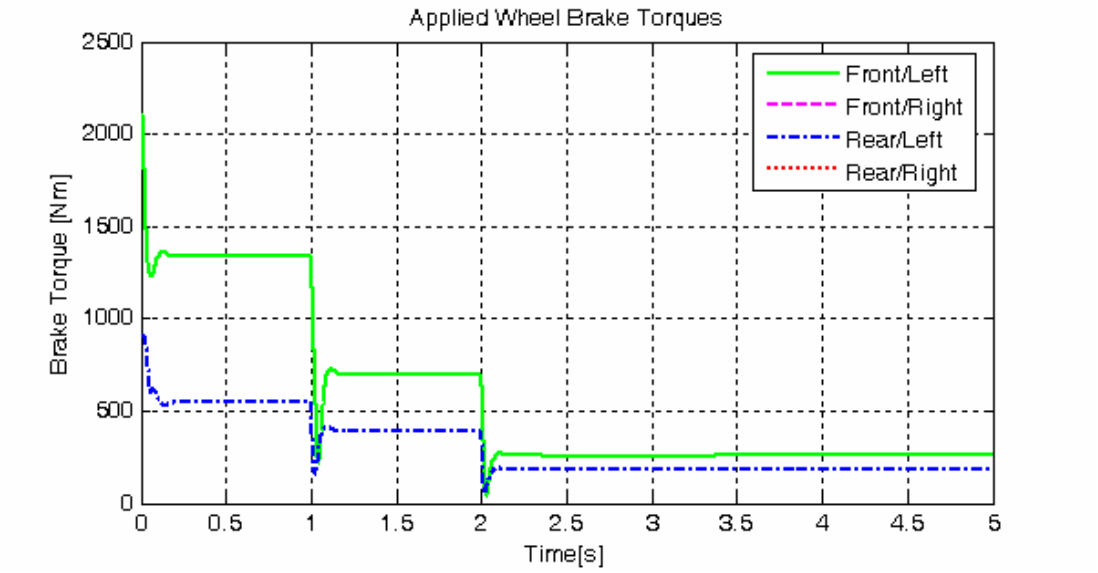

Figure B.8. Wheel braking torques for changing road conditions for PID

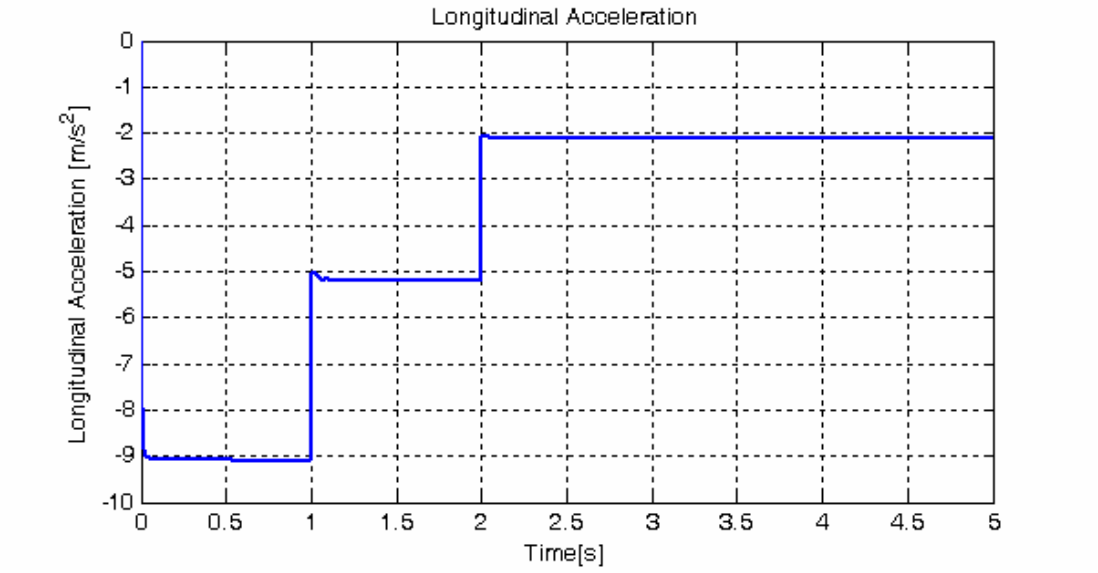

Figure B.9. Longitudinal acceleration for changing road conditions for PID

APPENDIX C

COMBINED BRAKING AND STEERING SIMULATIONS FOR LOW-LEVEL PID CONTROLLER

C.1. Dry Asphalt Road Test

Figures from C.1 to C.6 present the results of the simulation conducted for the step steering handwheel angle input of 40º shown in figure 4.1.

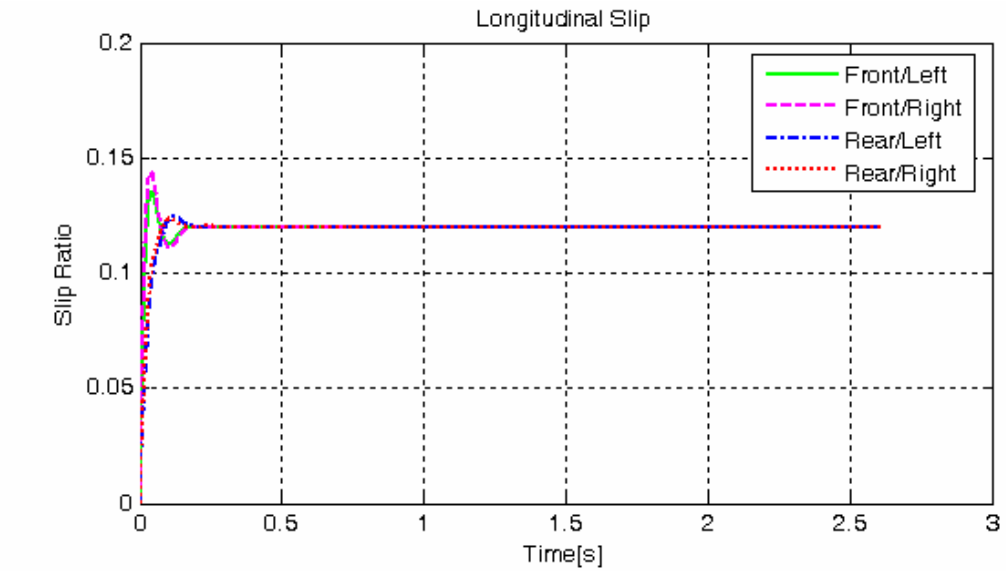

Figure C.1. Longitudinal wheel slip on dry asphalt for 40º step input for PID

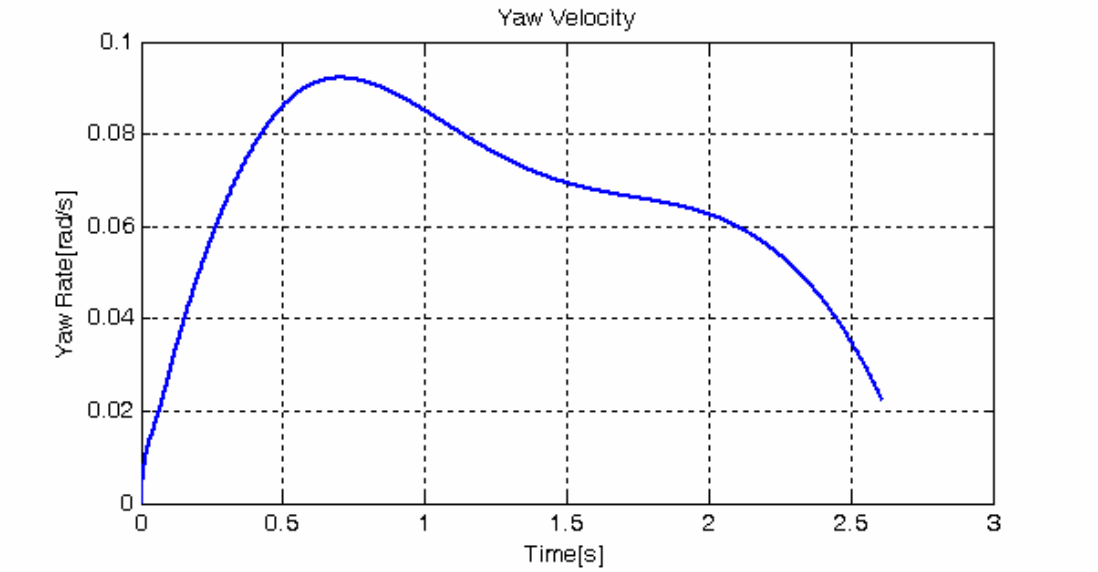

Figure C.2. Yaw velocity on dry asphalt for 40º step input for PID

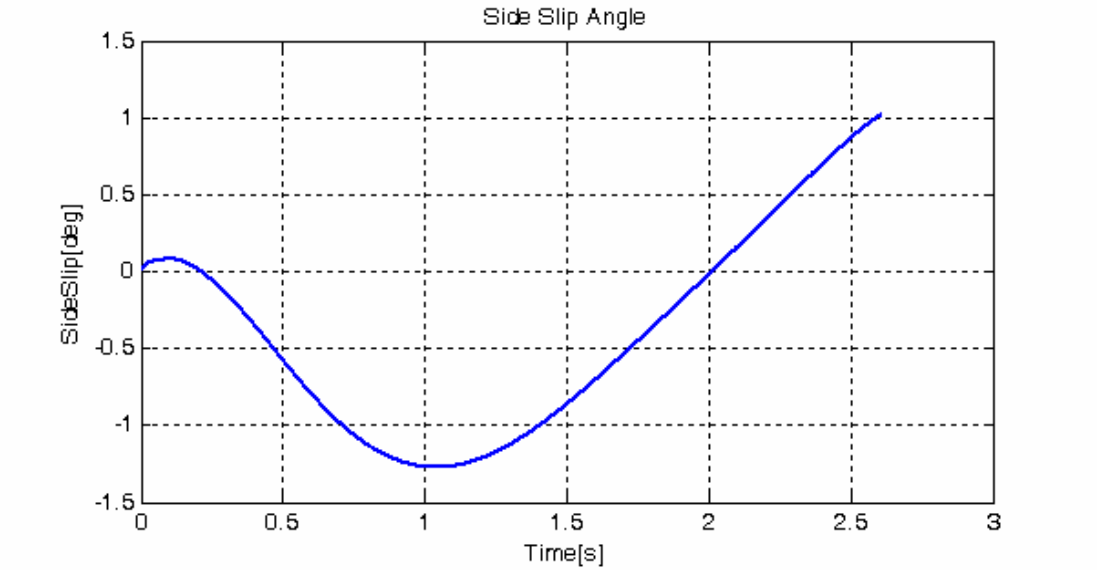

Figure C.3. Sideslip angle on dry asphalt for 40º step input for PID

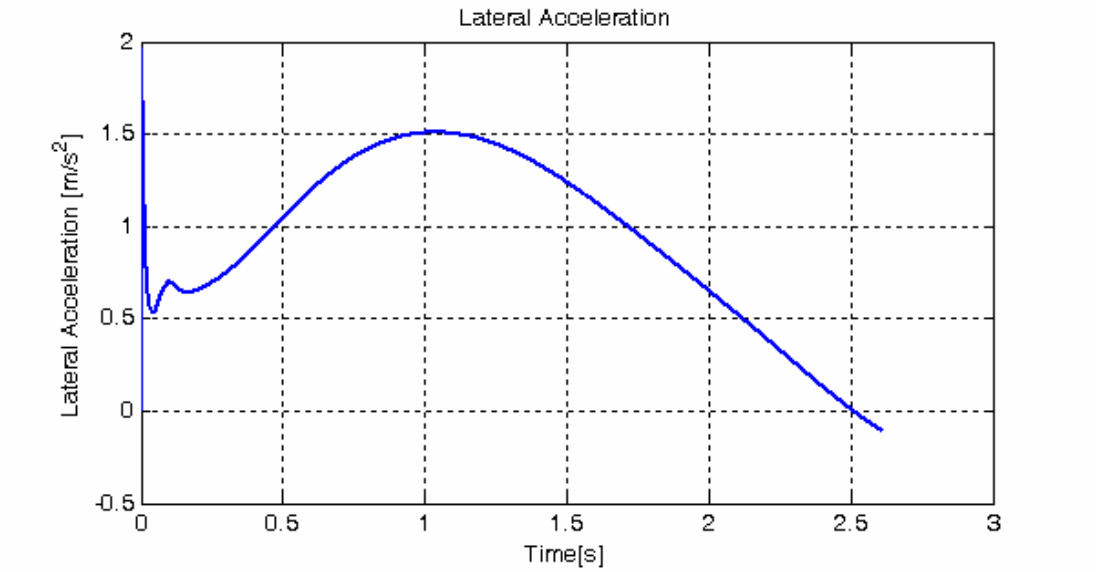

Figure C.4. Lateral acceleration on dry asphalt for 40º step input for PID

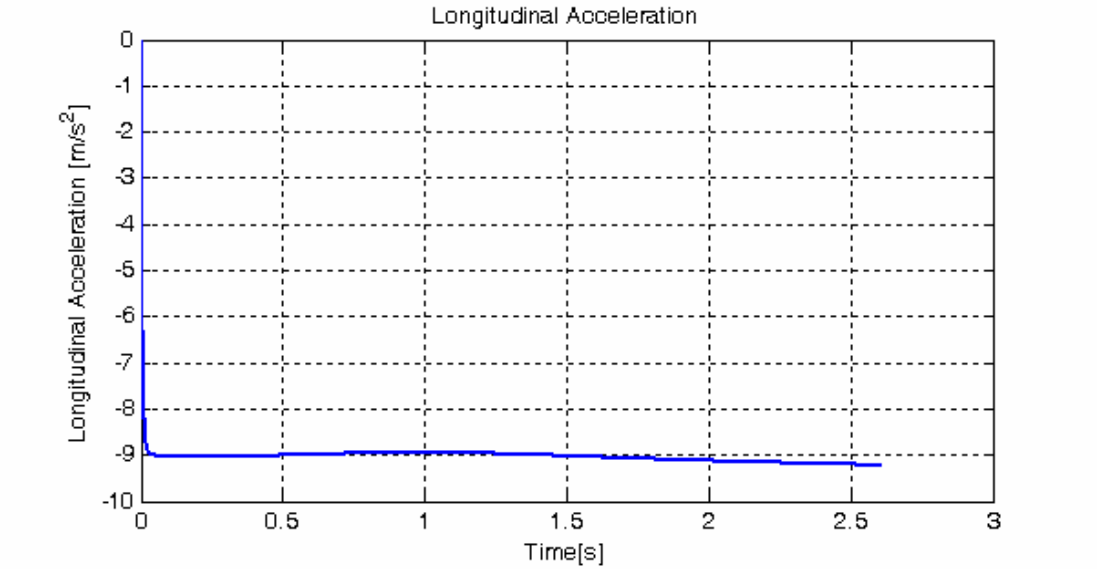

Figure C.5. Longitudinal acceleration on dry asphalt for 40º step input for PID

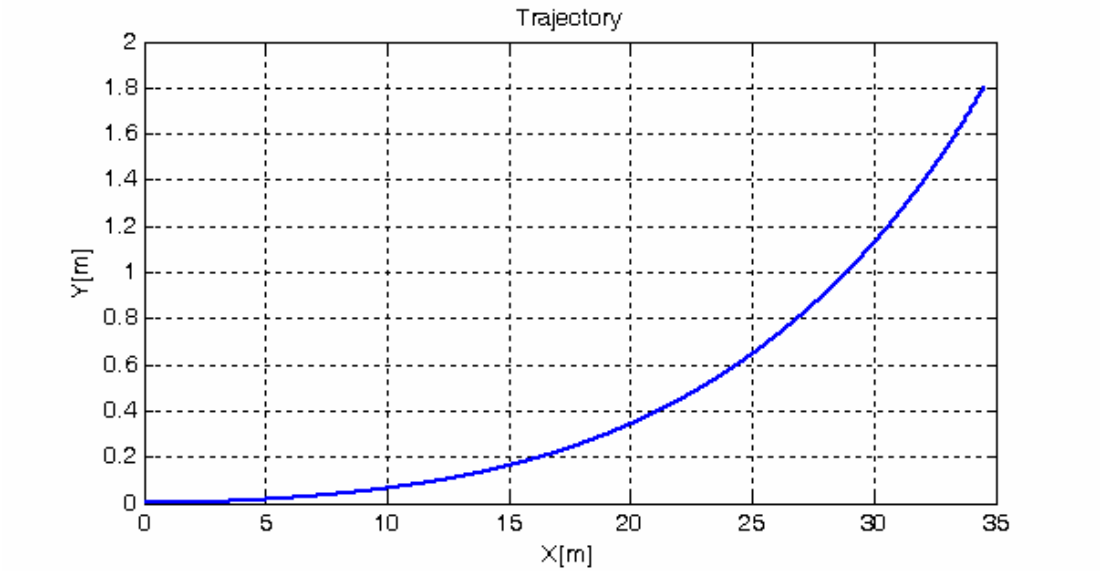

Figure C.6. Vehicle trajectory on dry asphalt for 40º step input for PID

Figures from C.7 to C.12 illustrate the results of the simulation for the step steering handwheel angle input of 120º shown in figure 4.76.

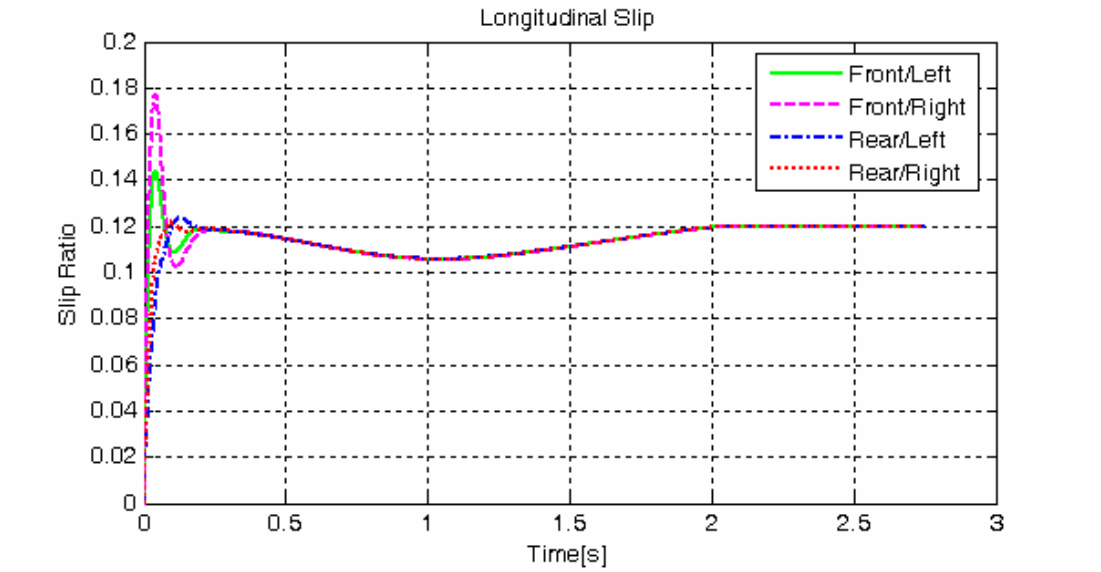

Figure C.7. Longitudinal wheel slip on dry asphalt for 120º step input for PID

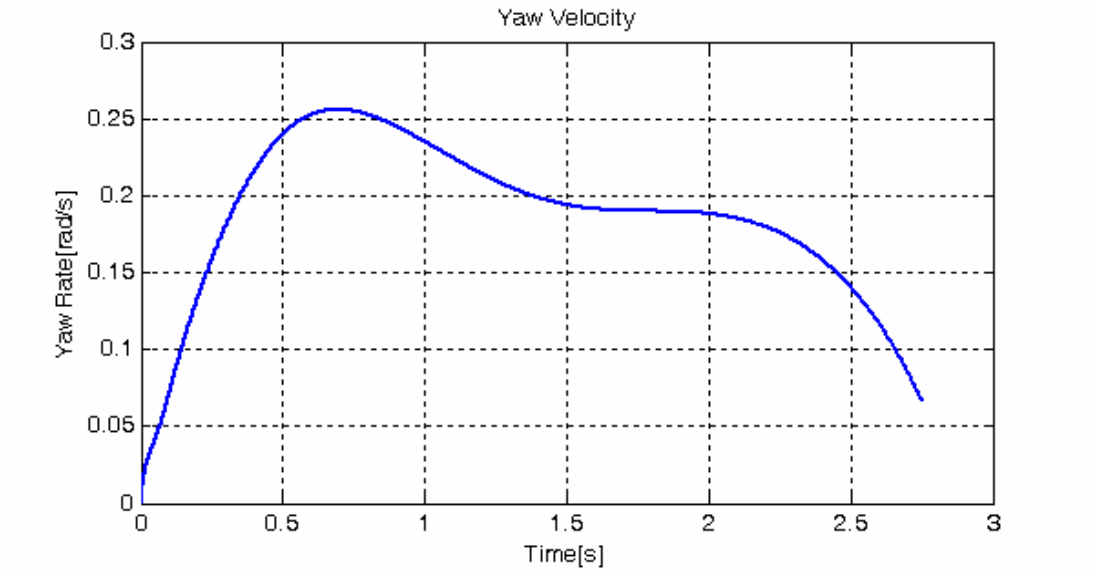

Figure C.8. Yaw velocity on dry asphalt for 120º step input for PID

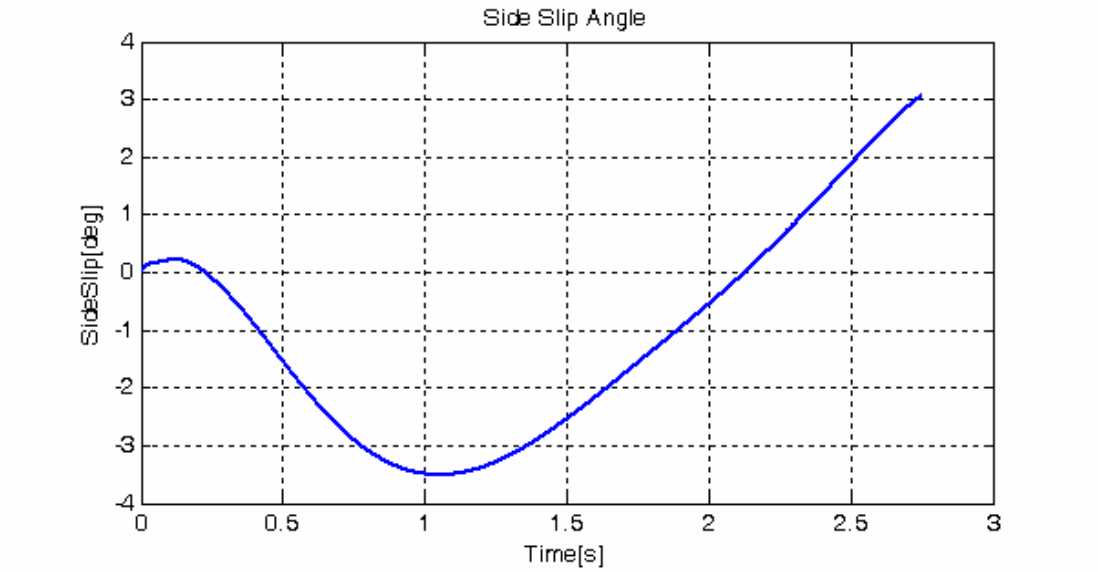

Figure C.9. Sideslip angle on dry asphalt for 120º step input for PID

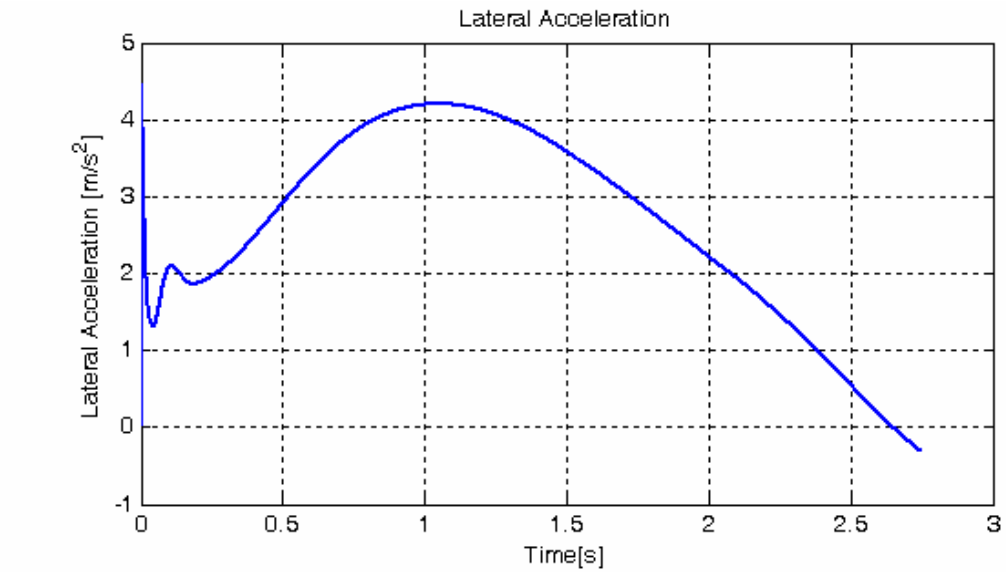

Figure C.10. Lateral acceleration on dry asphalt for 120º step input for PID

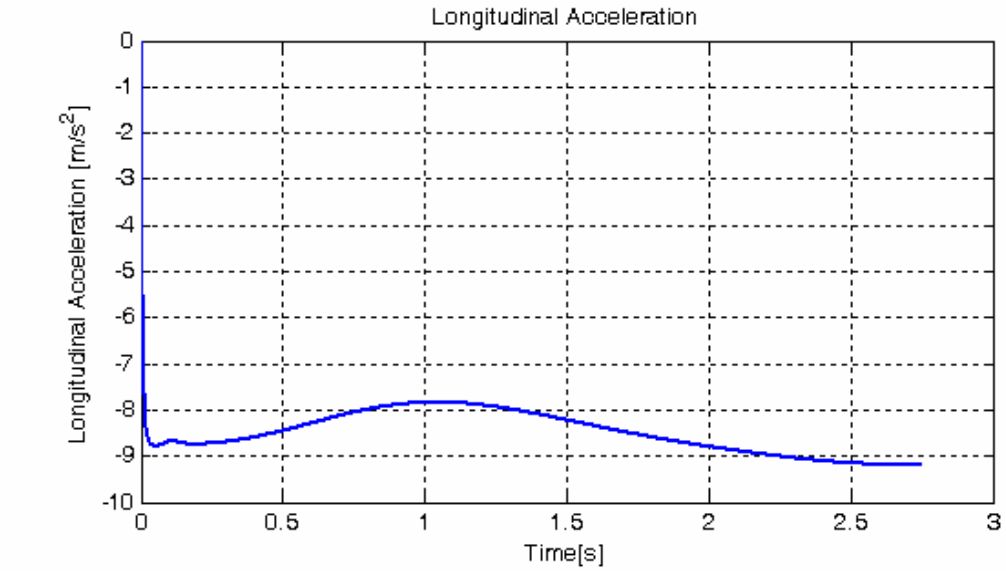

Figure C.11. Longitudinal acceleration on dry asphalt for 120º step input for PID

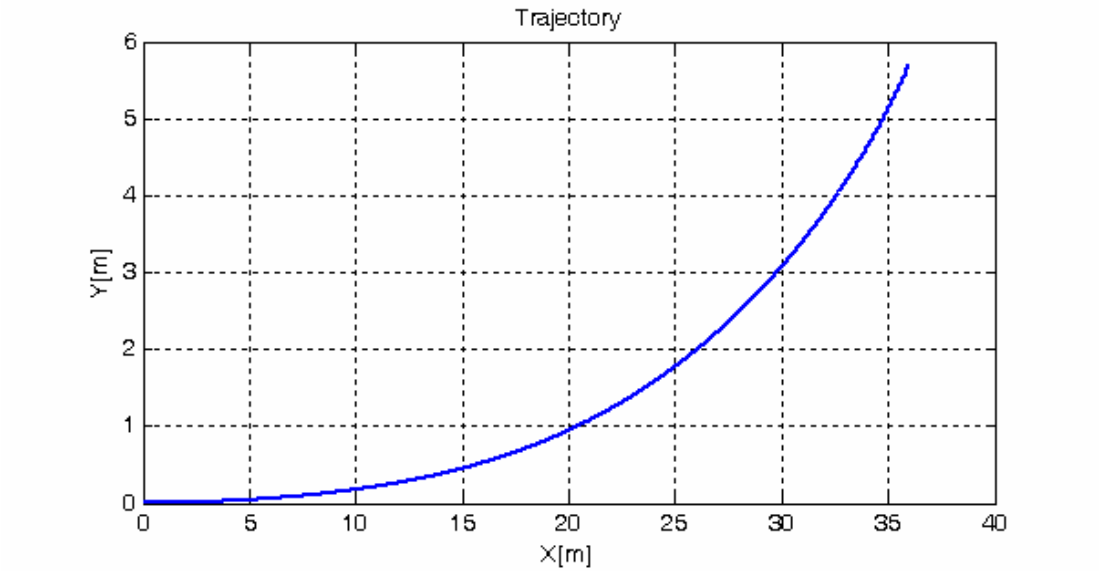

Figure C.12. Vehicle trajectory on dry asphalt for 120º step input for PID

Simulation results for the j-turn steering input depicted in figure 4.83 are provided in figures C.13 to C.18.

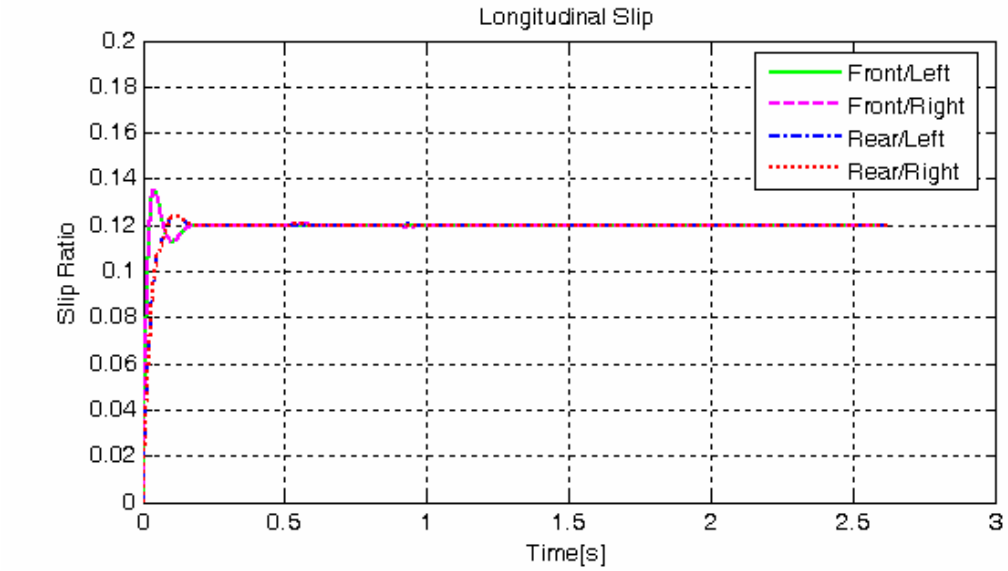

Figure C.13. Longitudinal wheel slip on dry asphalt for j-turn input for PID

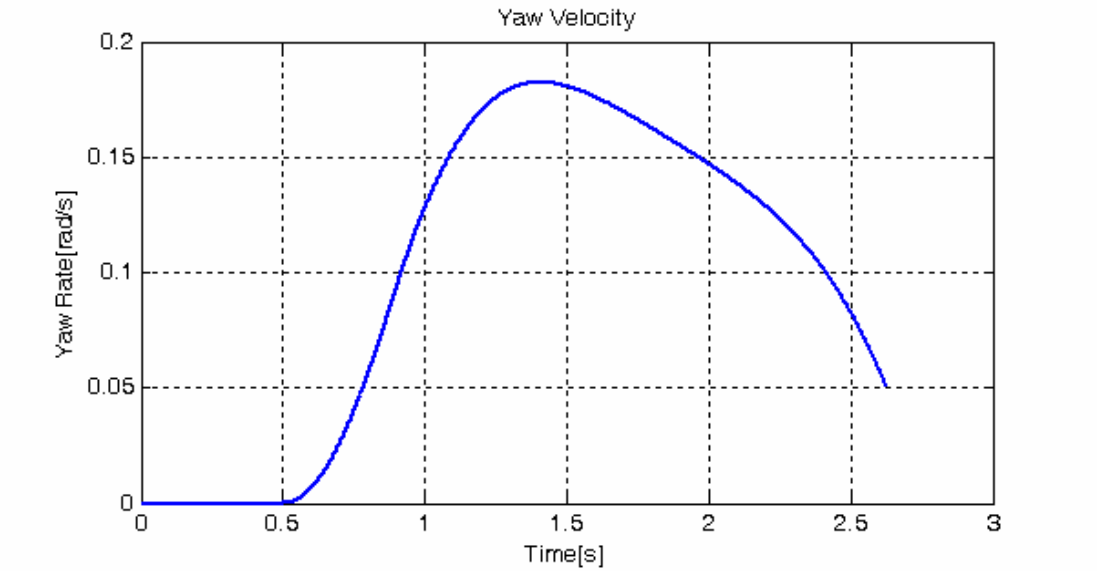

Figure C.14. Yaw velocity on dry asphalt for j-turn input for PID

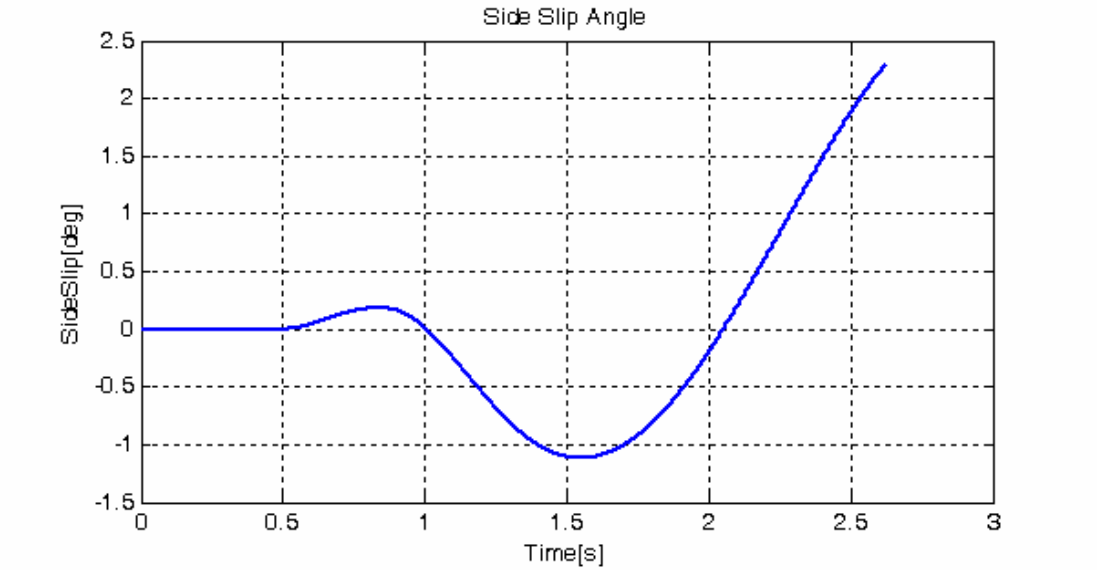

Figure C.15. Sideslip angle on dry asphalt for j-turn input for PID

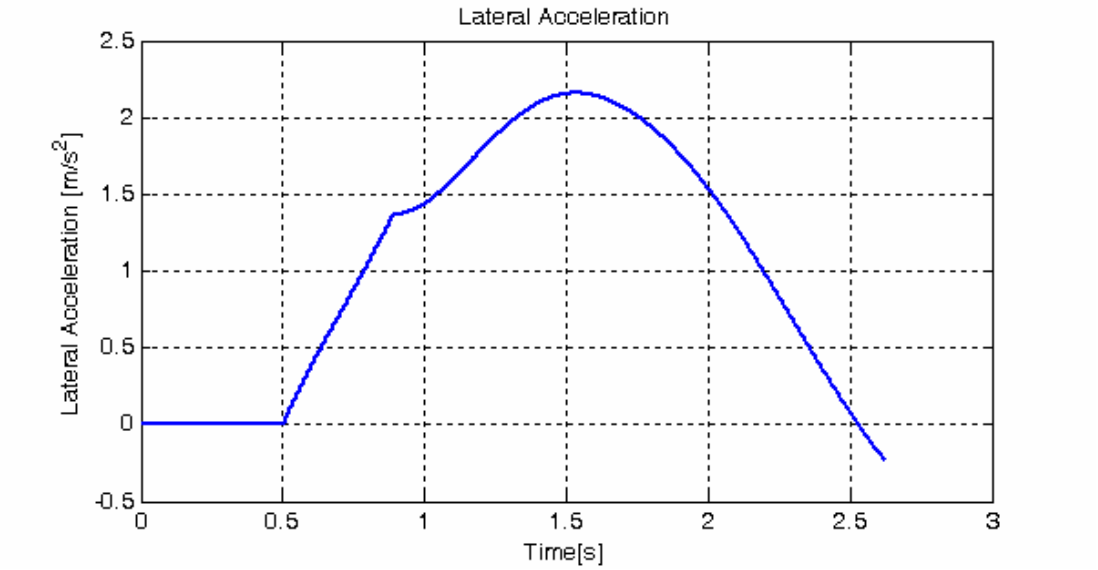

Figure C.16. Lateral acceleration on dry asphalt for j-turn input for PID

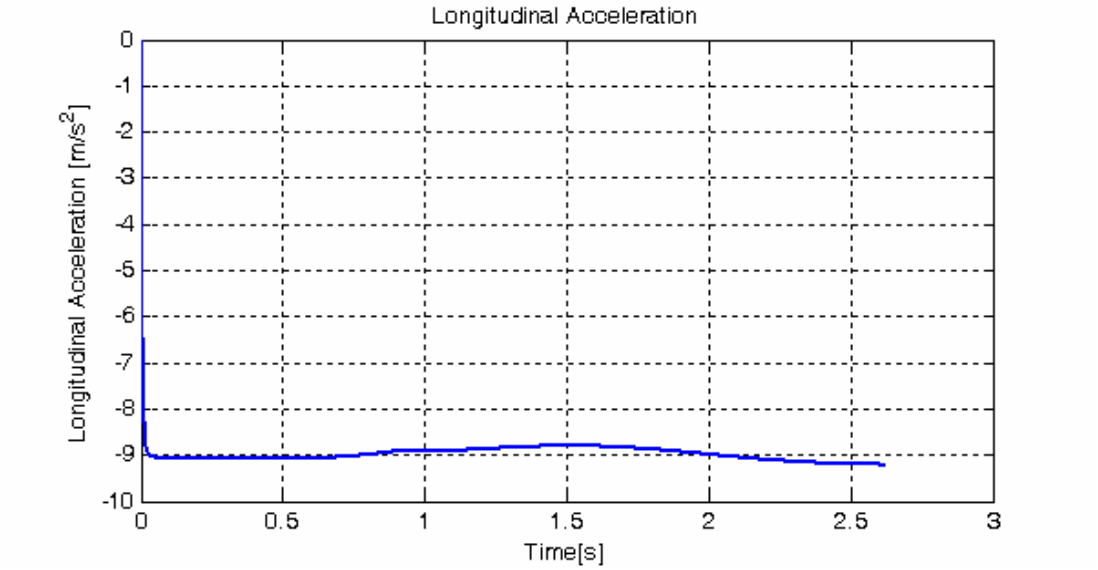

Figure C.17. Longitudinal acceleration on dry asphalt for j-turn input for PID

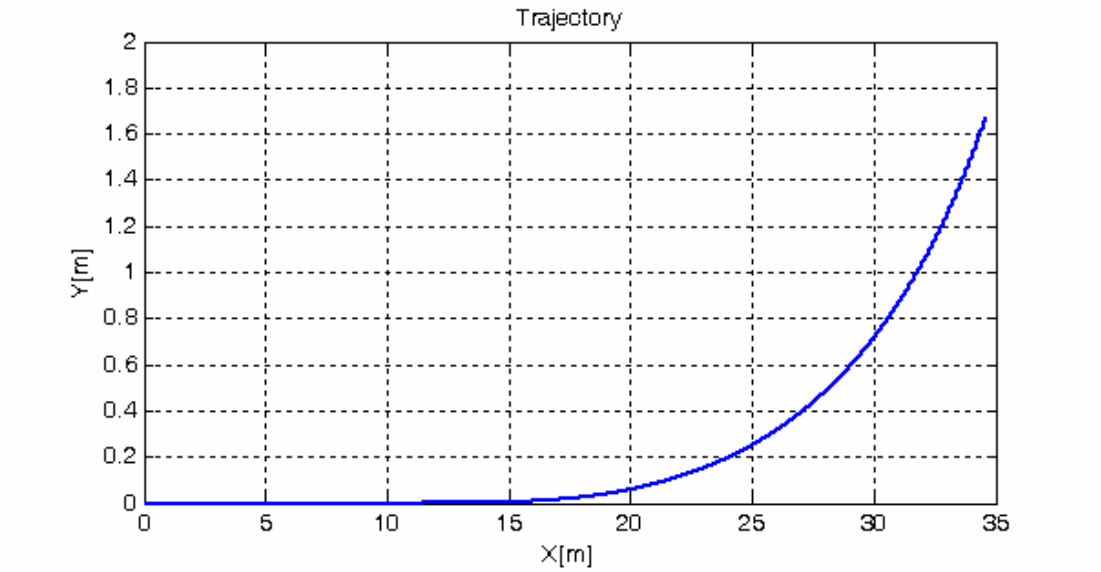

Figure C.18. Vehicle trajectory on dry asphalt for j-turn input for PID

C.2. Wet Asphalt Road Test

Simulation results for the 40º step steering input on emulated wet asphalt road surface are presented here in figures from C.19 to C.24.

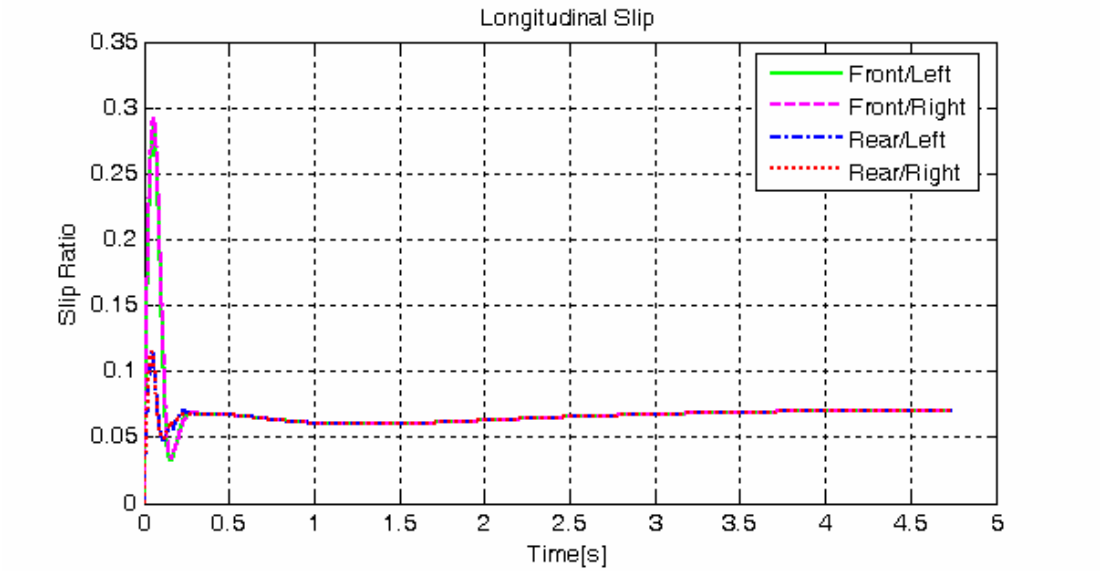

Figure C.19. Longitudinal wheel slip on wet asphalt for 40º step input for PID

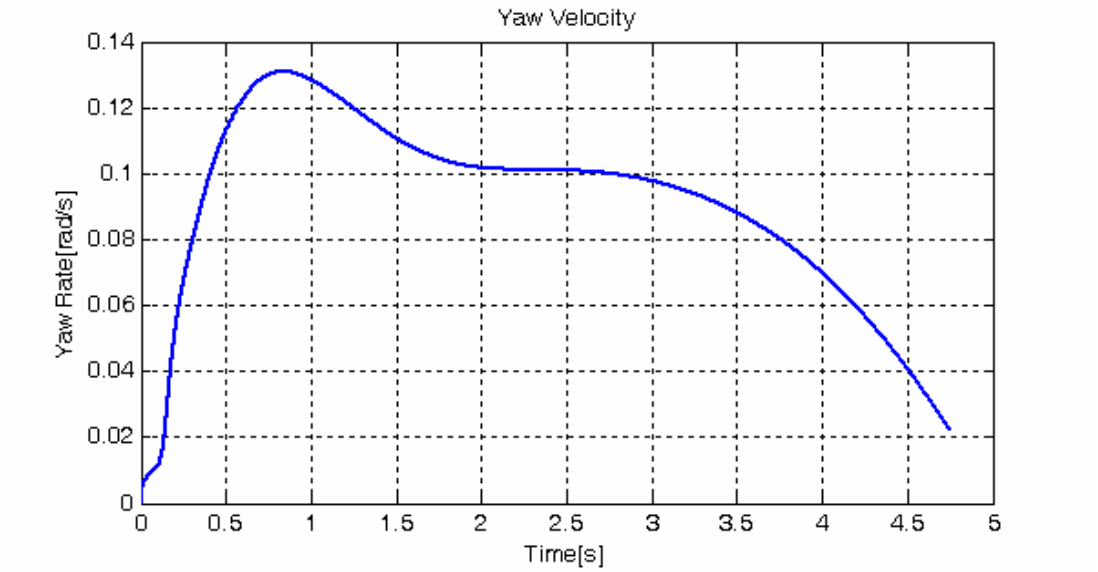

Figure C.20. Yaw velocity on wet asphalt for 40º step input for PID

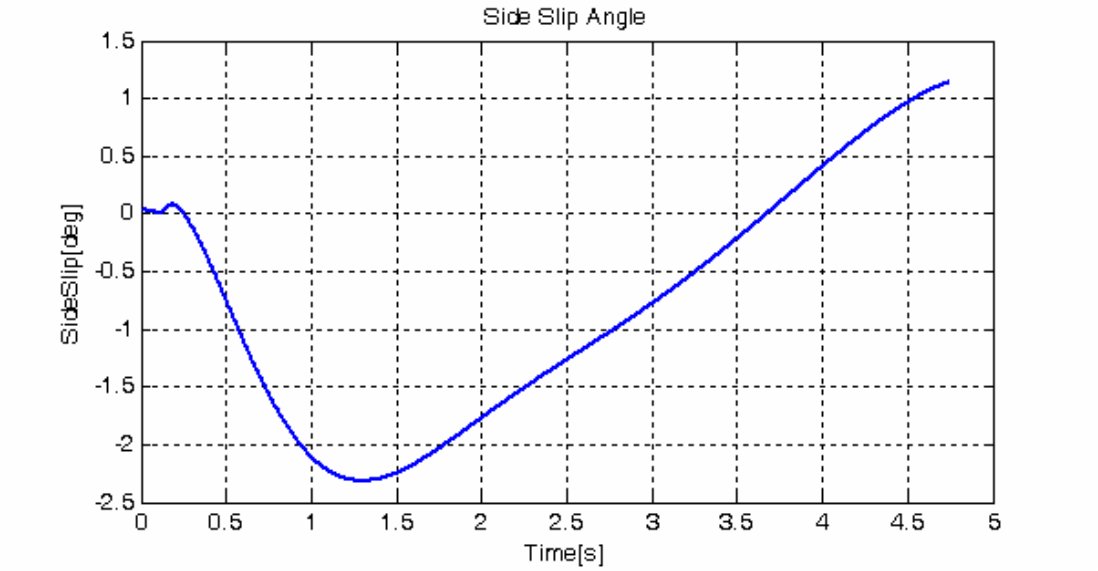

Figure C.21. Sideslip angle on wet asphalt for 40º step input for PID

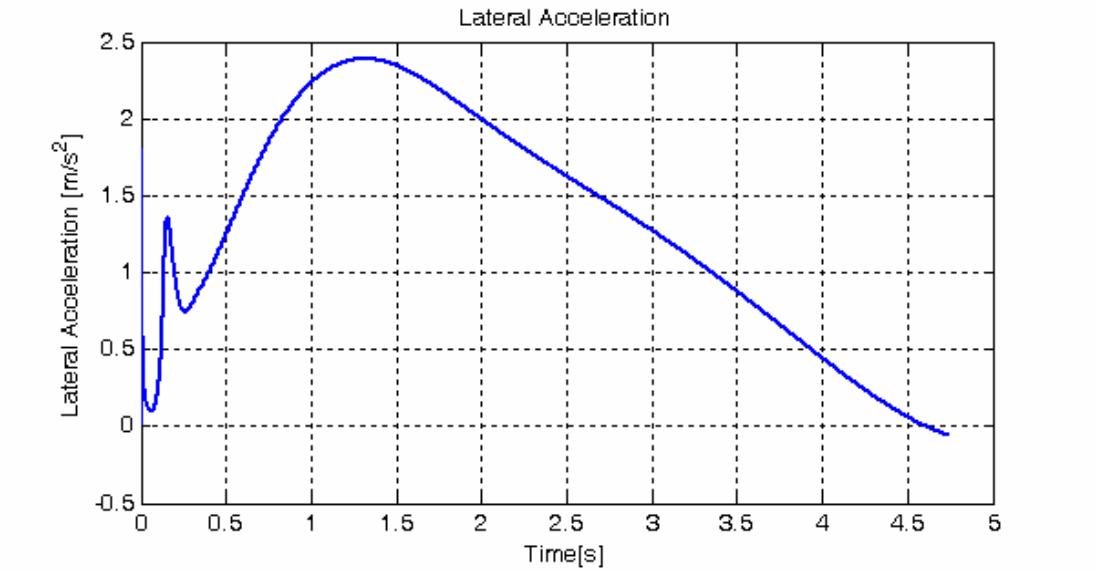

Figure C.22. Lateral acceleration on wet asphalt for 40º step input for PID

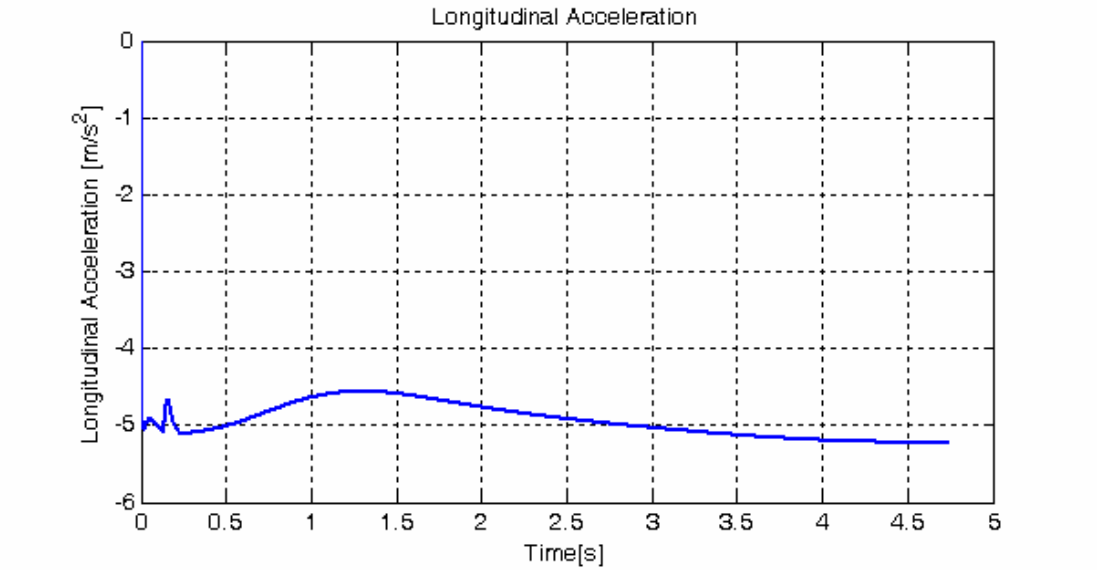

Figure C.23. Longitudinal acceleration on wet asphalt for 40º step input for PID

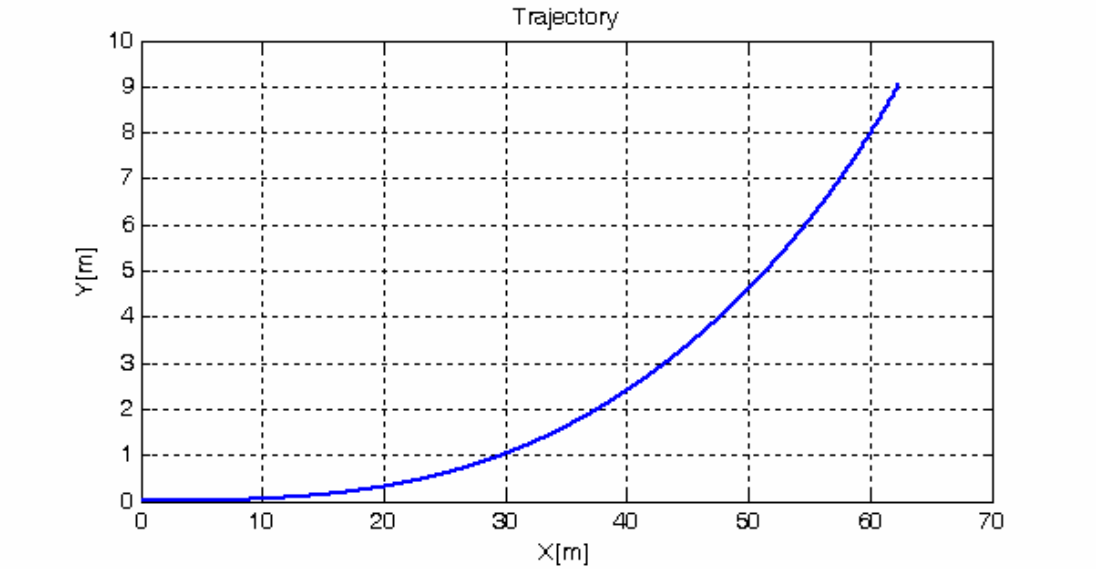

Figure C.24. Vehicle trajectory on wet asphalt for 40º step input for PID

C.3. Icy Road Test

Simulation results for the 40º step steering input on emulated icy road surface are illustrated in figures from C.25 to C.30.

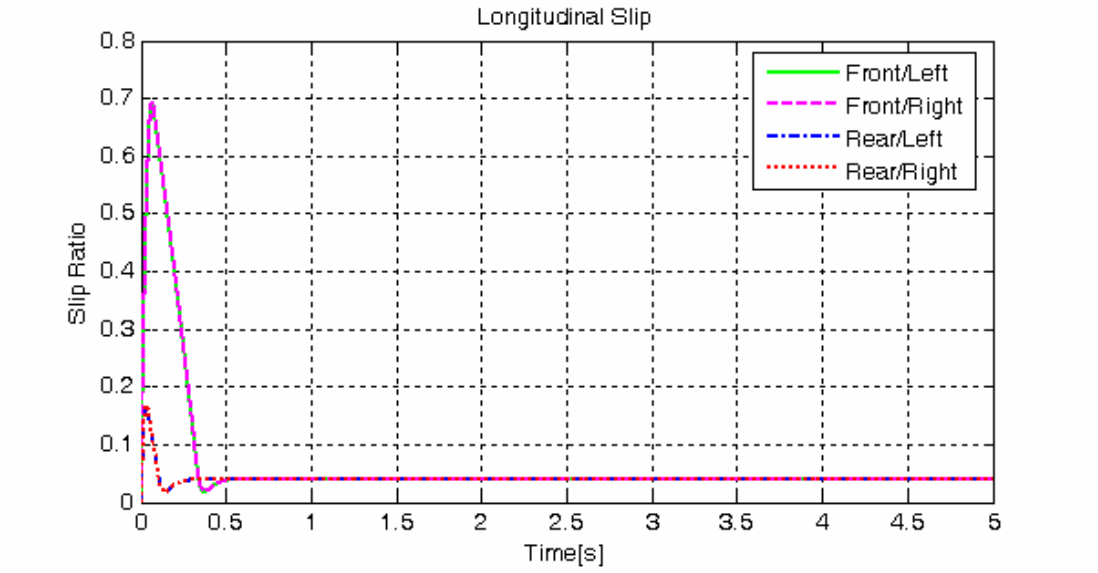

Figure C.25. Longitudinal wheel slip on icy road for 40º step input for PID

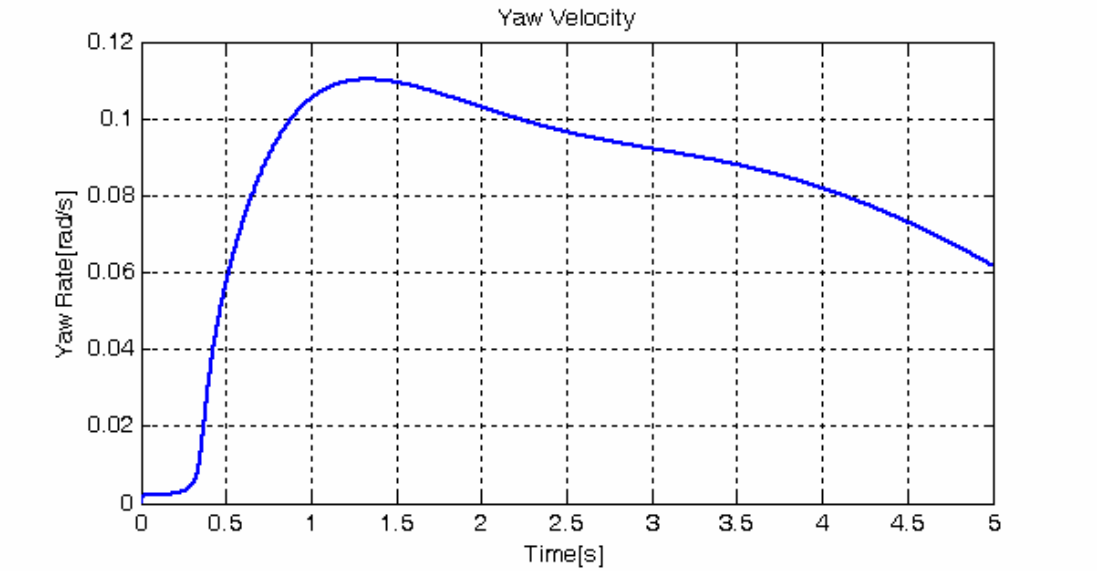

Figure C.26. Yaw velocity on icy road for 40º step input for PID

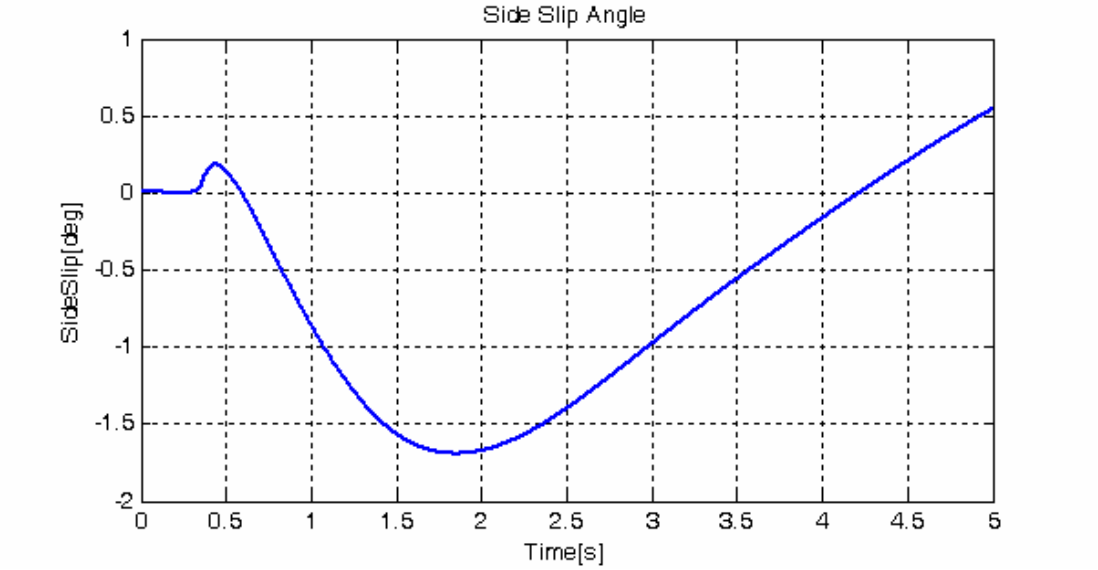

Figure C.27. Sideslip angle on icy road for 40º step input for PID

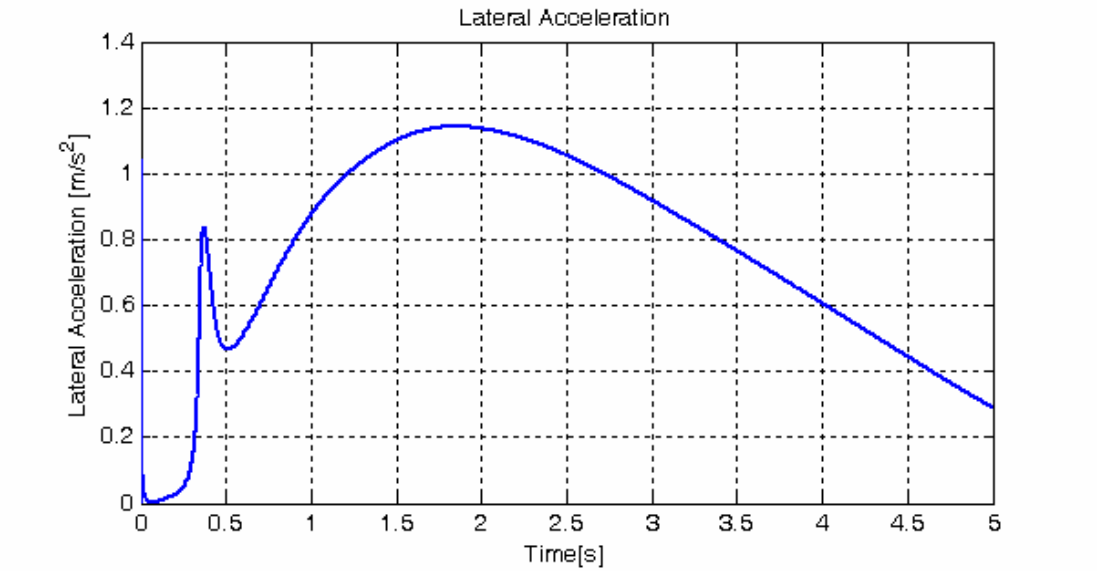

Figure C.28. Lateral acceleration on icy road for 40º step input for PID

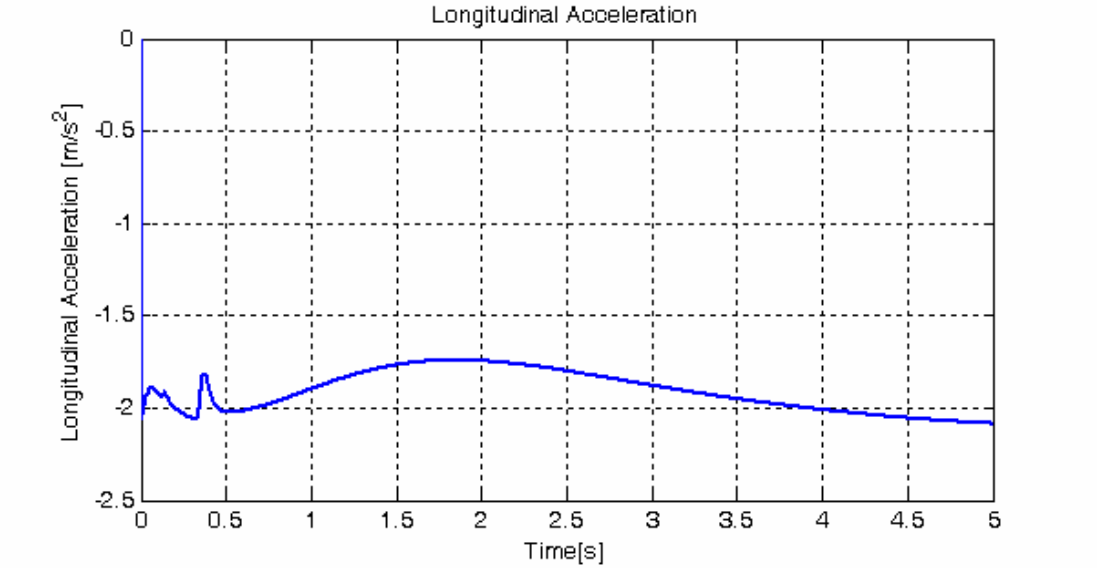

Figure C.29. Longitudinal acceleration on icy road for 40º step input for PID

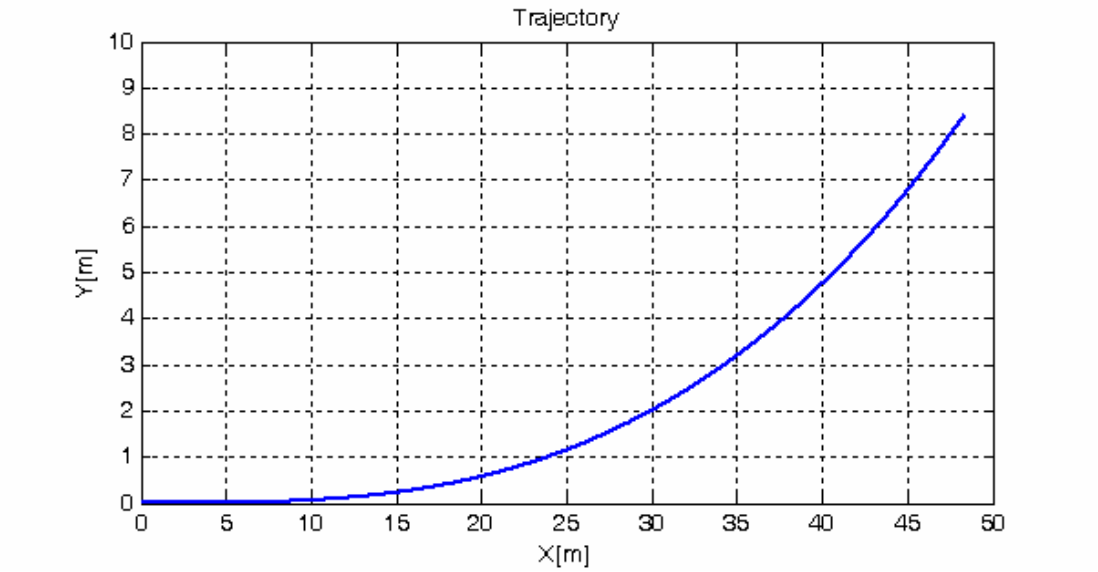

Figure C.30. Vehicle trajectory on icy road for 40º step input for PID